A Review of the State of the Practice of Earthquake Analysis of Jacket Structures

Joint Industry Project

by
PMB Engineering, Inc.
San Francisco, CA 94111

December 1993

Contents

ILLUSTRATIONS

Figure

Section 1
Introduction

1.1 STUDY OBJECTIVES

The objective of this study was to compile information describing the current state-of-the-practice for earthquake analysis of offshore structures. As a result of the current activity with respect to regulations and assessment requirements for existing structures, and the limited amount of new construction in areas where earthquake loadings dominate, the information is focused towards the analysis of existing structures in support of reassessment. Aspects of design for earthquake loadings are not addressed.

1.2 DOCUMENT OVERVIEW

The document includes seven sections. Sections 2 and 3 present general issues and background towards earthquake analysis. Section 4 provides details relative to linear and nonlinear modeling of platforms. Sections 5, 6 and 7 present details of procedures for response spectrum, pushover and time domain analysis, respectively.

An independent report has been written by Professor C. Allin Cornell on the topic of "Seismic Risk Analysis of Jacket Structures." This report is included as Appendix A.

Section 2
Earthquake Design and Requalification Philosophy

2.1 EVOLUTION OF OFFSHORE EARTHQUAKE DESIGN PRACTICE

Present seismic design practice for offshore platforms focuses on two primary objectives:

1. To provide sufficient strength and stiffness to ensure no significant structural damage for earthquakes with a reasonable likelihood of occurrence during the life of the structure

2. To provide reserve strength and/or ductility to prevent collapse during rare intense earthquakes.

These requirements are typically designated as the Strength (SLE) and Ductility (DLE) Level Earthquake conditions, respectively.

Owners and regulators generally set criteria for the SLE requirement to balance initial cost of fabrication against losses associated with earthquake damage to achieve an economic optimum. Such losses could include interruption of cash flow, repair costs and increased maintenance costs. The DLE requirement provides safety against structural collapse with its associated catastrophic consequences to human life, environmental pollution and capital investment.

The current design guidelines provided in API RP 2A [1993] represent years of development most of which took place during the mid to late 1970's and early 1980's. The current recommended practice for seismic design, which has been essentially unchanged since the 15th edition in 1984, provides a series of guidelines for jacket framing and detailing which have been determined through analyses to provide adequate ductility and resistance to extreme earthquake loading. In situations where a jacket configuration does not meet the API guidelines or where the site conditions or earthquake hazards warrant special analysis, the recommended practice dictates that analyses be performed to demonstrate adequate ductility of the structure.

2.2 SEISMIC REASSESSMENT

The criteria used for seismic design of offshore structures have changed significantly over the last 30 years. This change has resulted from 1) improved understanding of regional seismicity, site effects and corresponding surface ground motions, and 2) increased experience relative to efficient structural framing arrangements and detailing which provide greater ductility thereby improving structural response under extreme earthquake loading.

In the 1960's very little was known about seismicity in offshore California. Large earthquakes that have occurred since that time (e.g., 1979 San Fernando earthquake M = 6.8)

have caused substantial damage to buildings, freeways and bridges and have prompted investigators to increase study into the regional seismic environment. Investigation has identified new faults, improved the definition of potential earthquake magnitudes generated by known faults and refined the definition of site ground motion intensity resulting from postulated earthquakes. As a result, the current definition of site seismicity is generally more severe than that established previously.

The API RP 2A [1993] is generally recognized as the standard for seismic design of fixed based platforms. Many revisions have been made to these recommendations regarding seismic criteria, design and analysis methods since its first issue. California platforms installed prior to RP 2A guidelines were typically designed based on the Uniform Building Code or other simplistic criteria which, by today's standards, would be considered inadequate.

Consequently, older platforms in seismic regions may have three areas of deficiency:

1. Inadequate ground motions for original design
2. Structural framing which is not arranged or detailed for ductile behavior
3. Reduced capacity resulting from damage, corrosion or fatigue degradation

2.3 DESIGN VERSUS REQUALIFICATION ISSUES

The seismic reassessment process involves many of the same procedures associated with the design of new platforms. However, due to significant differences regarding economically feasible options for new design versus reassessment of an existing platform, each process requires a different philosophy. Existing platforms may be evaluated for SLE conditions. However, if a platform does not conform to these requirements it is not likely that strengthening, or other remedial measures, put in place to achieve this level of performance, will be cost effective. Reassessment methodology concentrates therefore on failure prevention and thus requires procedures similar to that of DLE analyses.

The reassessment of existing platforms is a relatively new process and has not yet been standardized in the U.S. as design is. This lack of standardization creates some difficulty in establishing performance requirements which must be developed on a case by case basis depending upon the risks (i.e., hazards, exposures and consequences) associated with the future operations of the platform.

The objectives of a platform reassessment are:

1. To ensure that the hazard to personnel and risk of pollution do not exceed levels which are deemed acceptable by the public

2. To develop a cost effective plan for safe and reliable continued operation of the platform.

Section 3
Summary of Analytical Requirements for Performance Assessments

Accurate analysis of the potential risks to a facility from earthquakes requires a multi-disciplinary approach comprising seismology, geology, soils mechanics, structural mechanics, and economic factors. Basic technical steps are listed below:

1. Characterization of seismotectonic environment and seismic activity in the region affecting the site.

2. Evaluation of the seismic exposure of the site, including source to site attenuation and local site effects.

3. Characterization of site ground motion, typically by scaled historical earthquake time history records, synthetic records, and/or response spectra.

4. Evaluation of structural response.

Accurate analysis also requires knowledge of the variabilities of characteristic values, the uncertainties in the analysis procedures and how output from one step will be used in subsequent steps.

The return period adopted for strength requirement ground motions is generally higher than for storm waves. There are three principal reasons for this. Firstly, seismic loads imposed on a structure are highly dependent on the stiffness and energy dissipation characteristics of the structural system, including the piling and supporting soils, and so uncertainties in soil properties result directly in similar uncertainties in loads. Secondly, the uncertainty in the estimation of ground motions is higher than for wave heights. Thirdly, at the 100 year recurrence level, the sensitivity to increase in return period is greater for ground motion intensity than it is for wave heights.

In the case of the strength requirement, a platform is typically characterized as a linear elastic system with five percent viscous damping. Damping comes in small parts from the welded steel structure, hydrodynamic damping and rattling of the conductors in their guides; and in a larger part from the nonlinearity of the near field soils supporting the piling. Higher values of damping are not precluded, but we believe this would only be likely with unusual soil conditions, such as relatively soft or weak layers.

In the case of the ductility requirement, full advantage should be taken of the softening and inelastic energy absorption capacity of the jacket, piling, supporting near field soils, and free field soil column. Several cautions are pertinent, however:

- Soils properties are often established so as to provide a conservative estimate of piling capacity. Use of lower bound near-field soil properties in a seismic analysis

may lead to unconservative results since they limit transmission of the ground shaking into the piling. Similarly, increases in soil stiffness from strain rate effects may increase the transmission of ground shaking to the piling.

- The site ground motion must be defined for a point consistent with the point of input for the structural analysis. If the structural analysis includes a model of the free field soil column (to include the benefits of soil energy absorption and phase lag in the ground motion input along the length of the pile shaft), then seabed free field motion records would be inappropriate; records should instead be provided for a point below the pile tips. If the site soil is relatively uniform and stiff, modeling the free field soil column may not be necessary. However, the piling tends to be driven laterally by the near surface soils but vertically by deeper soils further down the pile shaft. This needs to be recognized in the generation of input ground motion criteria. Further comments on near-field modeling are given in Section 4.2.4.

- Inelastic deformation may lead to secondary P-δ effects which must be included in the analysis.

- Characterization of the site ground motion should include consideration of the duration of shaking. Successive strong pulses in a ground motion record may lead to progressive collapse as the structure stiffness reduces.

- Components in the jacket must be appropriately detailed to tolerate the inelasticity. Provision of redundant load paths and strong ductile joints, and avoidance of low diameter/thickness ratios and slenderness ratios are desirable to ensure structure components will meet ductility demands without brittle failures.

There are several alternative procedures which can be used to perform most earthquake analysis for either new design or reassessment of offshore structures. The wide variety of platform types, earthquake loading and performance requirements makes it impossible to identify a specific procedure which is most appropriate for all applications. In most situations it is likely that several alternative analytical procedures could be used to obtain the same final conclusion. The characterization of platform response under earthquake loading is very complex, in particular for extreme earthquakes, so the objective of the analyst should be to identify an analytical procedure which provides a sound basis of understanding structural performance in support of whatever the decision is that must be made (e.g., member sizing for new design, remedial measures for existing platforms).

The particular objectives of the analysis should be clearly specified and used to determine the most effective analytical approach. The selection of the appropriate method is generally based on the following factors:

- The expected level of response (i.e., linear or nonlinear)
- The basis of performance criteria (e.g., member and joint utilization against allowable stresses)
- The specific areas of the platform being investigated (i.e., deck, jacket, foundation)
- The way in which ground motions are defined (e.g., uniform hazard spectra or recorded ground motion accelerograms)
- The modeling, software and hardware requirements associated with the analytical method

3.1 FACTORS AFFECTING ANALYTICAL METHOD

3.1.1 Expected Level of Response

New Design. The approach as applied to design is straightforward in that it is required that structural response under Strength Level Earthquake (SLE) conditions will be elastic and that response under Ductility Level Earthquake (DLE) conditions will likely be inelastic. Analysis in support of design under SLE conditions is therefore typically based on response spectrum or modal superposition methods, both of which utilize a constant stiffness matrix.

Most structures which are designed for regions where the earthquake loading controls most or all of the design will experience some degree of inelastic response under extreme, ductility level, earthquake conditions. The API guidelines provide a basis for platform configuration and component sizing which has demonstrated adequate reserve strength and ductility for certain levels of extreme earthquake loading. The API guidelines do not require that any explicit ductility analyses be performed if the design of the platform conforms to the specified guidelines. If explicit ductility analyses are required, the API guidelines recommend that a time history analysis method be used and that the structure demonstrate survivability.

Reassessment. The API is currently developing recommendations for assessment of existing platforms including requirements for platforms subjected to hurricanes, storms, earthquakes and ice loading. These recommendations will likely focus on demonstration of adequate ductility for platforms in earthquake dominated regions. The focus towards ductility, or

demonstrated survivability, under extreme earthquake conditions is based on the objective of prevention of loss of life and pollution. Assessing an existing platform for strength level earthquake loading will provide useful information to support a cost/benefit analysis of the alternative remedial measures. However, it is not likely that the new provisions within the API will include a requirement for strength level analysis since the results of such analysis affect only economic decisions, rather than those of life safety and pollution.

The analytical requirements for reassessment therefore become very similar to those associated with the DLE requirements of the API (API RP2A (1993) Sections 2.3.6d and C2.3.6d). It is expected that most existing platforms located in earthquake dominant regions will exhibit some inelastic response under extreme earthquake loading. Most analyses will therefore require a nonlinear method. In some instances where significant reduction in loading of the platform has occurred (e.g., offloaded facilities) it may be possible to verify adequate response using a linear analysis approach.

3.1.2 Performance Criteria Basis

New Design. The are two level of performance criteria for new design as recommended by the API RP2A, viz., strength and ductility. Strength requirements may dictate framing arrangements, member sizes, joint can requirements and pile penetration. Performance of structural members is assessed using utilization formula based on the material allowable stress. Performance of piling is assessed based on pile capacity information with an appropriate factor of safety. The analytical method used for new design must therefore provide the appropriate member force and stress information to determine maximum utilization. All but the pushover analysis method provides such information. Time domain analyses can be used to calculate member utilization for components modeled as linear components, however, this will involve more effort than is required for response spectra analyses due to the volume of information which must be handled.

Ductility requirements are based on demonstrating that the platform can sustain extreme earthquake loading without collapse. In situations where earthquake loading does not control the structural design or where the ratio of ductility to strength level loading is small, it may be possible to demonstrate that a structure can sustain extreme loading with limited or no nonlinear behavior. In these situations the DLE analysis can be performed using SLE analysis methods.

In situations where the DLE loading will induce significant nonlinear behavior the analysis should address critical issues such as load redistribution, degradation in strength and stiffness of structural elements and soils and large deformation effects. A time history analysis utilizing a model with a coupled soil/pile/structure representation is the preferred method.

Reassessment. The performance criteria for reassessment is essentially identical to that of the DLE requirement for new design.

3.1.3 Coupled and Uncoupled Analysis

Any number of analyses may be performed to analyze the primary components of a platform for earthquake loading. These components include secondary structures (i.e., drilling masts, flare booms), deck structure(s), jacket and piling. For example, separate analyses are typically performed to design the deck and jacket structures. However, for all conditions, a global analysis of the complete structural system must be performed in which all components must be represented to some extent.

Uncoupled analyses utilize models in which some components are represented with simplified or equivalent modeling so that their response is defined with a level of accuracy which is adequate in terms of the effects on the primary components being modeled. For example, an analysis of a jacket may be based on a model which includes the deck structure represented as a simple box with appropriate weight, mass and stiffness so that the global dynamic behavior and jacket member forces are accurately determined. This approach would not be appropriate if the dynamic response of the deck (i.e., local modes) were to contribute to the forces delivered to the jacket. This approach would also fail if inelastic behavior were to occur within the deck which would change its dynamic behavior.

Uncoupled analyses are necessary when elements of the systems cannot be adequately defined. Secondary topsides structures, for example, may not be fully defined during the jacket and deck design. However, a representation of their estimated mass should be included in any analysis of the jacket and these structures should probably be represented in terms of estimated dynamic behavior (i.e., mass and stiffness) in any dynamic analysis of the deck structures.

The modeling and assumptions required for uncoupled analyses should have a conservative basis. Uncoupled methods are therefore convenient for components whose design is controlled by other conditions.

Coupled analyses utilize models in which the components are represented with a degree of detail adequate to capture the complete interaction between the components. The important aspects of this interaction are dynamic response and nonlinear behavior.

In some instances, such as for specific deck components (communications mast, drilling rig, etc.) deck floor response spectra can be developed from the global analysis of the jacket and used as the basis for seismic analysis of the specific deck component.

3.1.4 Definition of Ground Motions

Ground motions are defined either in terms of a response spectrum or accelerogram (i.e., ground acceleration versus time). Linear response spectrum and nonlinear pushover analysis are performed on the basis of a ground motion spectrum. Time history analyses require the definition of a ground accelerogram. The definition of a ground accelerogram requires that several additional issues be addressed. This includes the selection of records representative of motions expected at the site, record scaling, number of records required to envelop the probable motions at the site and the use of natural and synthetic records.

3.2 METHODS

The analytical methods which are commonly used fall into the following categories;

Linear Response	Nonlinear Response
Response Spectra	Monotonic Pushover
Mode Superposition	Time Domain
Time Domain	

Within each of these basic analysis types there exist several variations. The analytical strategy which is selected will then dictate the requirements of the model and computer software to be used. In some instances, the modeling and software requirements may dictate which method is selected.

Similar analytical methods are used for design of new platforms and assessment of existing platforms. Most of the differences come from the characterization of the structure (i.e., nominal versus expected yield material strengths) and the measurement of performance (i.e., member utilization versus platform stability). These differences affect the way in which an analysis procedure is applied to a given problem. However, they do not affect the basic mechanics of how the analysis is executed.

Each type of analysis can be used as part of the process for either new design or assessment of existing structures. However, the information provided by each is significantly different which thus dictates the applicability and usefulness of each method. The applicability of a particular method is dependant upon the specific aspects of the problem (i.e., structural configuration, foundation characteristics, site seismicity) which therefore requires that the analyst understand the advantages and disadvantages of each method and its suitability to the specific problem. In most instances, a combination of analytical methods will yield the greatest understanding of the structural response. However, this may require an impractical

level of resources. The analyst must therefore evaluate the mix of methods to be applied to the problem in terms of the value of the information provided and the level of effort required to complete the analysis.

Section 4
General Modeling Issues

4.1 LINEAR MODELING

4.1.1 Element Types

The type of element adopted to represent a member depends on developing the correct stiffness characteristics representative of its structural behavior. The modeling of various components is given in the following sections.

In general, linear beam elements with axial and bending stiffness are used for most of the jacket. Truss bars have only axial stiffness and, although this may reduce the number of degrees of freedom in a model somewhat, bending effects for both stiffness and code checking are missing.

4.1.2 Jackets

Jacket members. Jacket members are mostly modeled by three-dimensional beam elements since bending moments can be of importance in many members in the jacket. This will be particularly true for several levels above the piles, where the pile bending moments are transferred into truss action in the jacket, and in the higher jacket elevations where the bending results from portal frame action in the unbraced bay below the deck. Since axial loads in the legs reduce the lateral stiffness significantly (p-δ effect) the leg elements should have the ability to generate geometric stiffness from user-supplied or program-generated axial forces.

It is normal practice to use a single element to represent a member between its connections with other members. In this modeling there are no independent displacements at the center of the member and so local vibrations in the member are not modeled well, especially if element masses are simply the translational masses, lumped at the nodes. Some braces are, however, long enough that significant lateral vibrations can occur. If this is the case, either of the following can be used:

1. One or more extra nodes can be added between the ends of the member, dividing it into two or more elements.

2. The member can be checked after the jacket analysis is complete for local vibrations caused by transverse motions of the ends.

Further comments on local vibrations are given in Section 5.1.2

Joints. Because joints are generally somewhat stiffer than the members that frame into them, joints are usually treated as rigid connections to the more flexible members

themselves. In some framing systems adding joint flexibility can significantly change the distribution of force among the members. The critical sections for the members themselves are also at the face of the joints, providing another reason for including joints explicitly in the model, since structural analysis software can often determine member forces at the junction between the flexible member and the rigid joint.

Joint Cans and Stubs. Joint cans and stubs affect both the stiffness and strength of members. The stiffness effects are sometimes accounted for by adjusting the member properties,but strength still needs to be checked with the actual section properties. Cans and stubs are often modeled explicitly.

Secondary Structural Components. There are a number of secondary structural components that need to be accounted for, but which would overwhelm the model with unnecessary and time-consuming complexity. One example is the horizontal bracing scheme to support conductors horizontally, which may have considerable complexity. Global loadings from earthquakes seldom design these bracing systems, so equivalent members that represent their total contributions to jacket stiffness and mass are generally adequate. Both structural and added mass should of course be included in the equivalent members. However, this may not be the case for some existing structures for which seismic reassessment is done if it is suspected that the conductor support system may have framing that could be in the seismic load path.

Conductors. Conductors generally contribute two items to the dynamic analysis. The first is considerable mass, both structural and hydrodynamic. The second is considerable geometric (p-δ) stiffness, since the jacket provides the stiffness that resists the toppling of the conductors. Their horizontal stiffness is generally unimportant relative to the jacket and so, in principal, they could be lumped into one single vertical string at their center of mass in plan. To provide more accurate distribution of the lateral forces from the conductors onto the horizontal bracing, the conductors are generally lumped into a number of vertical strings, far less however than the actual number present. The details of the horizontal bracing will dictate the number of lumped equivalent conductors. Care should be taken to model the total structural and hydrodynamic masses correctly in the equivalent elements, since these represent significant proportions of the total, and are particularly important in loads generated in the horizontal bracing.

Appurtenances. Appurtenances such as boat landings and barge bumpers and cathodic protection may contribute some mass and perhaps locally stiffness to the jacket, but their design is seldom governed by earthquake loading. They should be modeled as equivalent members with correct total mass and approximately correct stiffness, if appropriate.

4.1.3 Deck Structures

Main Deck Structure. Many times the design of the deck is done by a different consultant than the one who designs the jacket. In such cases, the deck structure is usually represented in a lumped mass fashion in the jacket analysis. Displacement or acceleration history at the nodes at the jacket/deck interface are then used to perform the explicit analysis of the deck structure. Because this is not considered the optimum analytical approach, at least one analysis of the complete deck/jacket structure should be performed. Similar to the jacket all primary structural members should be included in the model with mass appropriately lumped at the nodes. If members are long or if there is some general concern about local modes, then intermediate nodes with appropriate mass should be included in the deck model.

Secondary Structural Components. Various items such as cranes, flare booms, and drilling rigs may be attached to the deck. In addition to adding mass and dead load, the flexibility of these items can affect the motion of the whole platform especially in the neighborhood of these components. It is desirable, therefore, that these items be modeled at least as equivalent members with correct stiffness and mass.

In general, explicit inclusion of deck secondary structures into the overall model is prohibitive due to the large number of degrees of freedom and number of modes that would have to be extracted to capture that response. Typically, specific nodes are included at the various points of interest and deck response spectra are generated. These spectra reflect the dynamic effects at these locations accounting for the global response of the structure (deck/jacket/foundation) and interaction between the secondary and primary systems.

Upon obtaining such spectra, a response spectrum analysis of the specific secondary structure can be "independently" performed using the spectra as the input ("forcing function").

Equipment Loads. Deck equipment contributes importantly to the mass and dead load on the structure. However, it is generally very stiff relative to the rest of the structure, so its stiffness need not be modeled explicitly. The mass and dead load from each piece of equipment can therefore be lumped at the appropriate position, and attached rigidly to the deck model.

After determining the accelerations of these items from the dynamic analysis, the required strength of the deck attachments can be determined from gravity plus mass times acceleration. Alternatively, a deck floor response spectrum approach can be used.

4.1.4 Linear Modeling of Foundations

Since most offshore structures have piled foundations, the focus in this discussion will be on pile modeling. In modeling earthquake response of offshore structures, the foundation system plays an important role. For strong motion earthquakes, a significant amount of energy dissipation takes place through the hysteretic and radiation damping behavior of the foundation system. Cyclic degradation of the soil leads to loss of stiffness and capacity of the foundation which alters the dynamic characteristics and ultimate strength of the structure. High strain rates associated with earthquake loading are accompanied by an increase in soil stiffness and resistance. Radiation damping has been shown to be important for stiff soils and the vertical response of the structure.

All of the above-mentioned aspects of pile-soil behavior are nonlinear in nature, and may be of importance even at rather small deformations. The effects of these nonlinearities must generally be accounted for even in linear structural analysis. This can be done by including equivalent linear properties of the soil pile system in linear elements. These equivalent linear properties should reflect best linear estimates of the stiffness, damping and mass of the foundations. The nonlinear stiffness is represented by an average or secant stiffness, while the damping should include representation of the energy absorbed each cycle by hysteretic and radiation damping effects. It should be noted however that, even with well designed equivalent linear foundations, a linear analysis is not capable of modeling some important aspects of soil-pile behavior, such as accumulation of plastic displacements at the pile top, and changes in soil properties with time from cyclic degradation.

In a linear analysis program, the soil-pile system is often modeled using an equivalent segment of a free standing pile that is fixed at the base and connected to the offshore structure at the pile top. The properties of the free-standing pile, such as the length, moment of inertia, area and Young's modulus, are adjusted to give an equivalent stiffness approximating that of the actual pile-soil system evaluated at the anticipated level of pile response.

The equivalent stiffness of a single pile at a given load level can be conveniently determined using a nonlinear pile analysis computer program. In such an analysis, the anticipated load level is applied at the pile top and the corresponding displacement is evaluated using the computer program. The relationship between the applied load and the corresponding displacement expresses the equivalent linear pile stiffness at this particular load level. If the actual pile load obtained from the linear structural analysis program is different from the load used to evaluate the pile stiffness, this process should be repeated iteratively until the actual pile loads match those used to evaluate the equivalent pile stiffness.

Alternatively, using computer programs that allow the user to specify a set of stiffness constants at the boundaries, the same objective can be achieved by specifying the pile head stiffness matrix directly at the interface between the pile and the structure.

4.1.5 Mass

Lumped Versus Continuous Mass. There are two ways to model the mass from a member that has mass distributed along its length. The first, known as the consistent mass method, is more mathematically rigorous but is not necessarily more accurate, and results in a full mass matrix for each element. In the second procedure the translational mass from half the member is simply lumped at the nodes at each end, resulting in terms only on the diagonal of the element mass matrix.

Added Mass. Transverse hydrodynamic (added) mass for well-submerged tubulars is approximately equal to the mass of water displaced by the members. In the axial direction, the added mass is of the order of magnitude of a the mass of a sphere of the diameter of the cylinder, which is small compared to transverse added masses and is normally neglected, particularly since it has usually already been accounted for by the member into which it frames.

Other bodies have added masses dependent on their shapes. For instance, a thin plate has virtually no added mass in directions in its plane, but has a large added mass (of the order of magnitude of a sphere circumscribing the plate) perpendicular to it. Added masses can be found for many shapes in Det norske Veritas (1977).

Because of the sensitivity of individual members to direction, the added mass of the whole platform varies somewhat with direction.

Added masses change and become frequency-dependent as the body approaches within a few diameters of the free surface. This is generally a negligible effect for surface piercing members that extend several diameters below the surface. For any element with axes and hence added masses oriented at an angle to the global axes, when the mass matrix is transformed to global coordinate axes it becomes a full matrix, requiring that the full structure mass matrix be stored. If the program uses lumped masses, only the diagonal of the mass matrix is usually stored, and the off-diagonal terms are lost. This is usually not a problem when most other primary members are oriented along the global axes. It is also unimportant when the structure is fairly regular, as a jacket usually is. In this case the lost terms arising from one diagonal brace at a joint, for instance, would have been canceled out anyway by terms from another diagonal brace in the same plane, meeting at that joint.

Entrapped Fluid Mass. Fluid enclosed by a structural member or group of members or conductor can be lumped at the adjacent nodes, just like mass from the member itself, provided it is constrained to move with the member. It will act equally in the axial and transverse directions, since it is a true mass, accelerating with the body that encloses it.

If the enclosed fluid can slosh around in the body, and the mass of the fluid is significant relative to other masses in the region, this should be modeled as a dynamic element with mass and stiffness.

4.1.6 Damping

Sources of Damping. There are three principal sources of damping.

1. From the steel
2. From the soil
3. From the water

For a linear analysis, the structure will be required to develop stresses below yield, and so damping in the steel is quite small. Damping ratios of less than 1% of critical are generally thought to be appropriate.

Hydrodynamic damping from drag forces depends on the level of excitation, but is generally of the same order as that from the steel. In time history analyses, this could be modeled explicitly.

At design levels of excitation, significant amounts of energy are absorbed by the soil in hysteresis effects and radiation damping (elastic waves radiating from the piles). This is the major contributor to the total damping.

API RP2A (1993) recommends a damping of 5% to cover all effects, unless other substantiating data is available to replace this value.

Derivation of Mass- and Stiffness-Proportional Damping Coefficients. The damping ratio can be used directly in either the response spectrum method or time history by modal analysis. If the direct integration time history method is used, natural vibration modes are not employed and damping must be specified as a damping matrix **C** that acts directly on the nodal velocities. One commonly used method is to use Rayleigh damping, described below.

The damping matrix **C** is assumed to be constructed from the stiffness and mass matrices, **K** and **M** from the relationship:

$$\mathbf{C} = a_m\mathbf{M} + a_k\mathbf{K}$$

It can be shown that, for any mode with natural period T sec, the damping ratio associated with the mass- and stiffness-proportional damping, a_m and a_k, is given by:

$$\xi = a_m T/4\pi + a_k \pi/T$$

It is therefore possible to set the damping ratio ξ to any desired values ξ_1, ξ_2 at any two modes with periods T_1 and T_2, by choosing values of a_m and a_k from the two following equations:

$$\xi_1 = a_m T_1/4\pi + a_k \pi/T_1$$

$$\xi_2 = a_m T_2/4\pi + a_k \pi/T_2$$

The damping associated with a_m increases linearly with modal period and that from a_k decreases asymptotically to zero, so the resultant from both has a minimum between the two modes and increases with increased or decreased periods.

Example: Assume the first three periods of the platform are 2.1 sec and 2.0 sec in the horizontal directions, and 1.5 torsionally. The next modes have periods of say 0.8 sec, 0.7 sec. It would be appropriate to set the damping to the desired value (5%) at a period of 2.05 sec, ignore the torsional mode, and then again use 5% at 0.75 sec. The resulting damping ratio is shown in Figure 4-1 as a function of modal period. As the modal periods decrease below 0.5 sec there is an apparent excess of damping, but these modes usually contribute little to the forces in any primary members.

4.1.7 Static Loads

Gravity. Gravity loads should be applied over the members at the points at which they occur. Gravity-loaded beams should have nodal loads including both rotational (fixed end moments) and translational forces derived from the distributed loads. If these local member forces are then included in the member forces after the dynamic analysis, accurate member force distributions along the members can be obtained.

Buoyancy. Buoyancy can be handled in one of two ways.

1. The simplest is to use the net submerged density (weight - buoyancy) for all nonflooded elements. These should be applied as distributed loads, generating nodal forces and moments as follows:

   - The axial forces applied to each element node are not strictly correct, since the axial components of these are derived from non-existent forces
   - Member geometric stiffnesses (p-δ) are correct
   - The member axial forces computed are not strictly correct since the applied axial nodal forces were not correct
   - Code checks are correctly performed

2. The alternative is to apply the gravity and buoyancy forces to the element at the correct locations and in the correct directions. On tubulars, this will include transverse forces resulting from the difference in pressure around the circumference, and end forces from the surrounding hydrostatic pressure times the area of the cross section based on the outer diameter. In this case:

   - The axial forces applied to each element node are strictly correct, since they are derived from actual hydrostatic forces.
   - The member axial forces computed are strictly correct since the applied axial nodal forces were correct.
   - Member geometric stiffnesses (p-δ) have to be corrected by using an effective axial load determined by reducing the true axial load p by a force equal to the local hydrostatic pressure times the area of the cross section based on the outer diameter.
   - Code checks are correctly performed only if the axial forces are reduced by the same force defined in the previous paragraph.

   The advantage in the latter formulation, which is somewhat more difficult to conceptualize, is that the same formulation can be used with floating bodies.

Example:

A weightless tubular stretches from above mean water line to the mudline and is attached to the seafloor by a pin.

There are no axial forces anywhere in the tubular since there is no axial force at the top, and there is no way that the horizontal hydrostatic pressure along its length can develop vertical loads.

Nevertheless there is considerable (p-δ) stiffness keeping it from falling over, and this is derived from the effective axial force that varies from a large tension value at the bottom where the hydrostatic force is high, to zero at the top.

This axial force is exactly what would have been computed from the net submerged density concept. Using the submerged density method, forces from the net buoyancy act upward at each node, developing axial forces that increase from a maximum at the mudline to zero at the top.

4.1.8 Corrosion

The environment of the ocean is continually eroding passive anodes and unprotected steel unless protection is provided by cathodic protection, coatings etc. Corrosion can be accounted for by a uniform reduction in the wall thickness of members.

4.2 NONLINEAR MODELING

This section addresses the details of nonlinear modeling that are different from those presented for linear analysis in Section 4.1.

Important items to consider include the following: yield strength, ultimate strength, post-yield behavior, buckling, load reversal, hysteretic behavior, energy absorption, damage, and failure.

4.2.1 Structural Element Types

The type of element adopted to represent a member depends on the actual expected behavior of the member under extreme loading conditions. The key to adequate modeling of nonlinear members is developing the correct load-deformation (stiffness and strength)

characteristics. The major difference between linear and nonlinear modeling is the incorporation of the strength limits of the modeled components.

Conventional nonlinear elements include lumped- and distributed-plasticity beam-columns, struts, nonlinear truss bars, damaged members, near-field soil elements, gap-friction elements, and shim elements.

Nonlinear Beam-Column Element. Structural components which develop significant bending and are expected to exhibit inelastic response (e.g. substructure legs and piling) should be modeled with nonlinear beam column elements . These nonlinear elements reflect the elastic-plastic relationship for beam-columns that fail by yielding in tension or compression in combination with torsion and flexure. These members yield before buckling because of their relatively low slenderness ratio. A graphic representation of a bending moment/axial force interaction relationship of a nonlinear beam-column is shown in Figure 4-2. An important aspect of this element response is that, initially, as the member yields and develops a plastic hinge, the flexural and axial resistance of the member increase slowly or remain approximately constant as shown in Fig 4-2. With increased deformation, this may then be followed by a reduction in capacity, and eventually by failure of the member, at which point the member can carry no more load at all. This pattern of response represents the fundamental difference between the beam-column response and that of the strut which, when the critical axial (i.e., buckling) load is reached, relieves axial load rather suddenly (Fig. 4-3).

Nonlinearities are frequently modeled by lumping them at discrete hinges at the ends, or at the ends and mid-point of the member. The moment-rotation relationship of these discrete hinges depends on the length of the yielding region in the actual member, adjacent to each hinge modeled. This, in turn, depends on the distribution of bending moments along the member, which depends on the type of deformation the member is experiencing. This deformation might, for instance, be (1) like a cantilever, (2) in double curvature bending, as in a column restrained by heavy beams, or (3) constant moment bending. Thus for a given member section, the moment/rotation curve for the hinges depends on the type of bending deformation occurring. Care must be taken not to confuse the moment-rotation relationship of the discrete hinges with the moment curvature relationship of the section itself.

For damaged beam-column members, unsymmetric failure surfaces can be generated and used in place of the symmetric failure surface options in the program.

Buckling Strut Element. Members which are expected to display significant axial load reversal due to the cyclic nature of seismic loading are represented using a strut element. These nonlinear elements are used to represent the slender braces that fail in compression

by buckling. The strut element is an axial member (i.e, single degree of freedom at each end) which does not develop flexural forces. This element type is typically found to provide accurate representation of diagonal braces, which carry minimal flexural forces. A graphic representation of the force-deformation relationship of the strut is shown in Figure 4-3.

Marshall [1977] suggested the following expression for the lower bound resistance of a brace as it is compressed beyond its buckling load:

$$\frac{f}{f_{lim}} = \frac{\Delta_{lim}}{\Delta}$$

where

f = axial stress

f_{lim} = axial stress at buckling

Δ = axial deformation

Δ_{lim} = axial deformation at buckling

To include the effect of slenderness, an exponent was included on the right hand side expression that depends on the slenderness ratio.

The buckling strength can be estimated from data provided in, for instance, Galambos, 1988 or AISC (current edition).

Based on various experimental results, it appears that the post-buckling hysteretic loop tends to be less pinched as the slenderness ratio decreases; consequently, it develops a larger energy absorption capability.

In tension, the typical assumption is made that the member behaves in an elastic-perfectly plastic manner.

In addition to yielding and buckling, the element may also be allowed to fail. The failure of the element may be governed by the following equation:

$$\left(\frac{E_f}{E_{cf}}\right) + \left(\frac{E_s}{E_{cs}}\right) = 1.0$$

E_f = cumulative flexural energy at plastic hinges

E_{cf} = ultimate flexural energy

E_s = cumulative inelastic strength energy

E_{cs} = ultimate inelastic strength energy

The ultimate energy terms are calculated as follows:

$$E_{cf} = 4 M_p \theta_{hinge}$$

$$= 4 M_p \left(\theta_{cr} - \theta'_y\right) \left(L_p + L_n\right)$$

where

θ_{cr} = critical curvature

θ'_y = M_p/EI

L_p = length of plastic hinge

L_n = additional finite hinge length to account for additional hinge rotation observed in test results

M_p = plastic moment capacity of section

and

$$E_{cs} = \left(P_y + 0.005 E_{SH} A\right) \left(0.01 L + \Delta_{joint}\right)$$

where

P_y = tensile yield load

E_{SH} = strain hardening modulus (0 0.01 E)

A = cross-sectional area

L = member length

Δ_{joint} =joint distortion at failure (= 5% of the diameter of the chord)

Once the failure criterion is reached during the analysis, a percentage reduction in the ordinate of the load-deformation curve can be applied at each subsequent time step. As a result, the element fails progressively but gradually. When the force envelope drops to less than 1 percent, say, of its original value, the failure of the element is assumed to be achieved and the stiffness of the element is no longer included in the model.

Note that these equations described the actual moment/axial force interactions that are used to define failure, and are converted to an axial failure force to be used in the strut element.

As was mentioned above, the strut element is an axial member, and thus cannot account for the effect of flexural member behavior. This aspect of the response of the strut element complicates the modeling for dynamic analysis. As the structure responds to the ground motion oscillatory displacements, velocities and accelerations occur throughout the entire platform. These oscillations result in accelerations transverse to the member which, in the actual structure, induce shear and flexural response within the members. Due to the lack of flexural response within the strut element, the transverse accelerations and resulting member end moments must be approximated prior to the execution of the analyses so that the critical buckling forces can be reduced. An algorithm used to modify the buckling force, P_{lim}, is defined as follows:

$$\left(\frac{1}{1 - P_{lim}/P_{cr}}\right)\frac{3}{4}\frac{M}{M_p} = \cos\left(\frac{\pi}{2}\cdot\frac{P_{lim}}{P_{ult}}\right)$$

where

M = moment due to applied lateral loads

P_{cr} = Euler load for pin-ended case

P_{ult} = ultimate strength of centrally loaded column with fixed ends

P_{lim} = buckling force

P_{ult} = ultimate strength of centrally loaded column with fixed ends

M_p = plastic moment

Yielding Truss Bars. Yielding truss bars are elements that only carry axial load, which are assumed to yield in both tension and compression, and generally behave in an elastic-perfectly plastic manner.

4.2.2 Jackets

Jacket Members. The primary element types used for offshore nonlinear analysis are
(1) those that represent members under bending and axial loads (legs and piles)
(2) those primarily loaded axially (vertical diagonal bracing)
(3) soils.

Expected Failure Mode. Potential failure modes for offshore structures can be categorized into three areas: foundation failure, jacket failure, and deck failure. Foundation failures would be characterized by plunging and/or pulling out of piles, or by double-hinging the piles below the mudline. Jacket failures would be characterized by buckling and yielding of diagonal braces, followed by double-hinging of the legs in those bays. Deck failures would be characterized by double-hinging of the deck legs in a portal frame, or a failure similar to that discussed for the jacket. Note also that a combined failure mode is possible, namely, one set of hinges forming in the deck legs, and the second set of hinges (completing the collapse mechanism) forming in the piles at or below the mudline.

Struts vs. Beam-Columns. Both of these element types are very important for modeling nonlinear behavior in offshore structures. Beam-columns capture the important characteristics of legs and piles, namely their ability to carry axial and bending loads, the interaction between them, and the effects of large displacements. Most current algorithms for such elements, however, do not incorporate buckling, as most beam-column type members have relatively low slenderness ratios, and will yield before buckling. Struts, on the other hand, appropriately model the buckling and yielding behavior of members primarily loaded axially. Unfortunately, the effects of lateral loads and end bending moments are usually only approximated in strut formulations, and thus have the potential for being somewhat inaccurate at the local level.

Cyclic Degradation. Cyclic degradation is the phenomenon of member strength reduction due to cyclic loading that yields the member. The importance of cyclic degradation is measured by three quantities: percentage strength reduction, increase in damping, and energy absorption. Legs and piles tend to have little, if any, cyclic degradation, and therefore tend to provide more energy absorption. Diagonal bracing, on the other hand, tends to have a good deal more cyclic degradation, due to the loss of strength after the member has buckled. Because of this, buckled braces will tend to have less energy absorption than legs and piles.

Hysteresis. Hysteresis is the behavior of the stress-strain relationship of a yielded material under cyclic loading, as shown in Fig. 4-13. It contributes to total system damping by energy absorption (the area enclosed in a hysteretic loop is a measure of the energy absorbed).

Damage. Damage can occur during installation or operation. During installation it can result from dropped objects and piling operations. During operation ship impact and dropped objects can cause damage. Damaged members should be represented by modification to the normal properties of the members.

Jacket Joints. For linear analysis, because joints are generally somewhat stiffer than the members that frame into them, joints are usually treated as rigid connections to the more flexible members themselves. In nonlinear analysis, where members are allowed to yield, buckle, hinge, and fail, joint modelling becomes a more important issue, especially in terms of strength.

Modeling of joints for nonlinear analysis can be accomplished in two ways:

1. Actual representation of joint cans and stubs with nonlinear beam-column elements

2. Incorporating the strength and stiffness characteristics of the joint into the model by adjusting the member properties of those elements framing into the joints in question.

Option 1 requires more nodes and elements, and longer analysis run times. Option 2 requires more detailed calculations and assumptions concerning the behavior of the joint and framing members. Potential differences in the local behavior of the two options may have an affect on the global performance of the model.

Joint Capacity and Stiffness. Joint capacity is a function of the outer diameter, the wall thickness, the angle between chord and brace, and welding details, and is usually estimated

from curves based on non-dimensional ratios between these quantities. The amount of test data for joints is small compared to that available for member capacities and actual joint geometries in offshore platforms do not usually have corresponding test cases, so data must be interpolated or extrapolated. API gives lower bound strength equations for design, but no recommendations for actual ultimate strengths.

Compressive failure is a crushing or a punching-type, whereas a tensile failure will be a pulling out (ovalization) of the can. Good design would have members buckling or yielding prior to joint failure. If the joint is not explicitly modeled, member properties should be adjusted to reflect limiting strengths of the joint.

Secondary Structural Components. This subsection reviews the validation of linear modeling assumptions used to represent secondary components in nonlinear analysis.

In general, secondary structural components are of only minor interest in nonlinear analysis. For most cases, if these components are included, they can be modeled as linear elements. Care must be taken, however, to ensure that these members do not attract large amounts of load due to failure of surrounding primary members, and artificially support the structure.

A case where secondary framing is important from a modeling standpoint is when significant damage has occurred to surrounding primary framing. If alternate load paths through secondary framing are utilized, nonlinear modeling would be prudent for analysis of extreme loading conditions.

4.2.3 Deck Structures

Deck Members. The majority of primary deck members typically consist of deck girders and beams, and deck legs (portal frames). These members are best modeled with nonlinear beam columns. If diagonal bracing is included in the framing, these elements can be modeled as axial struts.

Deck Joints. Typical joint arrangements in offshore deck structures consist of the following:

1. Diagonal tubulars framing into tubular legs
2. Diagonal tubulars framing into wide flange sections
3. Wide flange sections (beams, bracing) framing into tubular legs
4. Wide flange sections framing into other wide flange sections

There is very little information available regarding the nonlinear response of these joint configurations. It is preferable to detail connections so that the full strength of the member can be attained. When reassessing existing structures, conservative estimates for joint strength should be used.

Deck Secondary Structural Components. Usually, deck secondary structural components are a concern in terms of their weight, mass, and location on the deck. Some components, though, such as drill rigs, quarters, and flare booms, are in actuality individual structures that may require modeling if the situation dictates. Selection of appropriate modeling elements follow the same basic guidelines as for jackets and decks. For members loaded primarily in bending, use beam-column elements; for members loaded primarily axially, use struts or truss bars.

4.2.4 Nonlinear Modeling of Foundations

Foundation Model. The motion of the soil/pile system can be divided into two parts:

1. The motion of the soil that occurs without the presence of the structure. This is the free-field or far-field soil motion.

2. The motion of the piles relative to the soil. This is the near-field effect.

The mathematical model of the pile/soil system consists of two or three of the following sets of elements, as shown in Figure 4-11:

1. Pile elements, modeled by a number of nonlinear beam-columns.

2. A far-field soil model representing the free-field motion of the soil column, vertically and horizontally. The motions of the far-field is unaffected by the pile motions. Depending on the stiffness of the soils, and the properties provided to the engineer for near-field elements, this model may not be needed. See comments below on the data provided by this model.

3. Near-field elements that connect the piles to the soil, vertically and horizontally. The strength and stiffness of these elements depends on the state of the far-field soil and the relative motion of the pile and far-field soil. For instance in loose sands, liquefaction of the soil near the surface may reduce its near field strength and stiffness to zero.

Pile Modeling. In a nonlinear earthquake response analysis, piles are modeled explicitly using nonlinear beam column elements. For lateral pile loading and piles that are

relatively flexible compared to the soil in the axial direction (most offshore piles are flexible in the axial direction due to their length), most of the soil resistance is mobilized at the upper segments of the pile. To accurately represent the soil resistance in this zone, spacing between the pile nodes should be smallest at the pile top, with the spacing/diameter ratio of 2 to 3, and increase with depth to reach an S/D ratio of 6 to 10 at the pile tip.

For strong motion earthquakes, large bending moments combined with high axial loads at the top segments of the pile lead to the formation of plastic hinges which are adequately modeled using nonlinear beam-column elements. If earthquake loading continues to increase on the structure, a second hinge will be formed down the pile which then forms a mechanism. High bending moments at the pile top could be accentuated by gapping between the soil and pile at the top few feet of the pile which results in a cantilever-like unsupported length of the pile.

Soil-Pile Interaction of Single Piles. The near-field soils adjacent to the piles are represented using nonlinear elements reflecting the lateral bearing (p-y), skin friction (t-z), and end bearing (q-z) force deformation characteristics of the interaction between the soil and piles as shown in Fig 4-5. The algorithm should model both hysteretic and radiation damping effects within the soil/pile interface. Radiation damping is damping that results from elastic waves generated by the pile/soil interface, that flow radially out from the piles, into the surrounding soil. These elements are distributed along the length of each pile and represent the forces generated at the interface between the soil and pile for a variable tributary length of pile (see Figure 4-5). A graphic representation of a typical force-deformation relationship is shown in Figure 4-4. The soil profile and the location of the soil springs are specified by the user. There should be at least one soil spring representing each soil layer. The behavior of the soil springs is completely defined by the following items; the backbone curves, the hysteretic behavior, cyclic degradation effects, strain rate effects and modeling of damping.

- **Backbone Curves.** Backbone curves are the load deflection curves of individual soil springs during initial loading. Only translational load deflection curves are typically included in pile analysis while rotational load deflection relationships are neglected. Backbone curves are usually called t-z in the vertical direction, p-y in the horizontal direction and q-z for the pile tip. Several empirical methods were developed to establish the backbone curves, e.g. (API 1993) and (PMB 1989).

- **Hysteretic Behavior.** Hysteretic behavior of soil elements during cyclic loading is a set of rules that define the load deflection curves during unloading and reloading. During unloading, the backbone curve is still the basis for the pile-soil load deflection behavior, however, the backbone curve is modified during unloading and subsequent reloading according to the hysteretic behavior rules. A

typical backbone curve and the hysteretic loops developed during unloading and reloading is shown in Figure 4-6. Correct modeling of the hysteretic behavior of the soil elements is very important in earthquake analysis since the shape and size of the hysteretic loops determine the amount of energy dissipated through the foundations during cyclic loading. Hysteretic behavior also affects the amount of plastic deformation accumulated in the soil elements which in turn affects the load distribution in the offshore structure.

Another aspect of hysteretic behavior is the correct modeling of gapping in the lateral direction. During severe storms, the top few feet of the piles separate from the soil due to large lateral deflections thus developing a gap between the pile and surrounding soil. In the lateral direction, gapping increases pile stresses as the top few feet of the piles are laterally unsupported and act as a cantilever. Axially, the ultimate capacity of the pile decreases due to loss of soil support from the top few feet.

- **Cyclic Degradation.** Similar to fatigue in metals, under repetitive cyclic loading, soil degrades and loses capacity and stiffness. Cyclic degradation occurs both in the axial and lateral directions and should be accounted for in pile analysis. Loss of stiffness alters the natural period of the structure which affects the dynamic characteristics of the offshore structure. In addition, loss of stiffness accelerates the accumulation of plastic displacements of the foundations which affects the stresses in the structure.

  Several empirical models have been developed to account for cyclic degradation of piles, e.g. (Matlock and Foo 1979) and (Karlsrud and Haugen 1985). The cyclic degradation model developed by Karlsrud and Haugen involves establishing a failure interaction diagram that gives the number of load cycles to failure, applied at a particular load level, versus various load combinations as shown in Figure 4-7. In this figure, Q_c is the cyclic stress amplitude, Q_{av} is the mean stress, and Q^1_{uz} is the current reference static capacity as determined by the initial static tests. The number of cycles in each test is shown in parentheses, and contour lines for 10, 100 and 1000 cycles are given. Failure interaction diagrams similar to the one shown in Figure 4-7 can be developed from laboratory cyclic load tests on soil samples and applied to the individual discrete soil elements along the pile shaft. The number of cycles to failure depends on both the mean load and the cyclic load component.

  Figure 4-12 shows typical degrading strength during multiple loading cycles.

Figure 4-8 is obtained from a nonlinear seismic analysis of a platform offshore California and shows the total axial pile load versus the axial pile capacity throughout the earthquake excitation. Notice that, in this case, the axial pile capacity degradation of about 30% at the end of the earthquake shaking.

- **Strain Rate Effects.** The rate of load application affects the load deflection behavior of the pile. At higher strain rates, the stiffness and capacity of the soil-pile system increases. The strain rate effects are usually taken into account by specifying a standard, or static, rate of loading, usually the rate of loading at which the soil samples are loaded in laboratory tests. The actual rate of loading is then compared to the static loading rate and the increase in static resistance is evaluated as a function of the ratio between the dynamic (actual) rate of loading and the static reference rate of loading. Several empirical formulae are used to evaluate the dynamic soil resistance such as the logarithmic formula or a power law formula.

  Strain rate effects are important for both axial and lateral loading. For cohesive soils, an increase in the rate of loading of about 1000 times results in about a 30% increase in the soil resistance. There is very little data available regarding the strain rate effects in cohesionless soils.

- **Foundation Damping.** Foundation damping stems from two sources; hysteretic damping and radiation damping. Hysteretic damping results from the dissipation of energy due to soil inelasticity and is accounted for directly by modeling the hysteretic behavior of the soils as discussed previously. Radiation damping results from the energy dissipated associated with propagating elastic waves in the soil.

  At large strains, foundation hysteretic damping is the main source of foundation damping and is much larger than radiation damping. However, at small strains, radiation damping is an important source of damping and should be accounted for. Radiation damping mainly depends on the shear modulus of the soil which is a function of the strain level. The soil shear modulus decreases as the soil strain increases. Radiation damping is typically frequency dependent and could be evaluated theoretically based on continuum mechanics. However, for time domain analysis of offshore structures, radiation damping can be approximated by a frequency independent coefficient (O'Rourke and Dobry 1979). It has been shown to be most important for stiff soils and high frequency axial loading.

Group Effects. Group effects characterize the behavior of a pile group versus the behavior of a single pile. The capacity and stiffness of a pile group is different from the sum of the capacities and stiffnesses of the individual piles.

As a pile displaces, the soil around it also displaces and if there are other piles in the affected zone of the soil, they will also displace. Accordingly, a pile can displace with no loads applied to it due to its presence in the proximity of another loaded pile. For static and low frequency loading typical of offshore structures, this behavior causes an increase in the flexibility of individual piles and a decrease in the pile group stiffness. For an earthquake analysis, it is important to consider such effects which alter the dynamic characteristics of the structure.

In the axial direction, the pile group capacity may decrease or increase depending on the soil type, and the number and type of piles in the group. Pile group capacity should be examined for each case individually (Poulos and Davis 1980).

The stiffness of a pile group can be evaluated using the interaction factors approach developed by Poulos and Davis. An interaction factor between two piles gives the displacement of one pile due to a unit displacement imposed at the other pile. Interaction factors were developed for static (Poulos and Davis 1980) and dynamic (Kaynia and Kausel 1980) loading. Static interaction factors mainly depend on the spacing to diameter ratio and the relative rigidity of the pile to the soil. In addition to these parameters, dynamic interaction factors depend also on frequency of vibration. The interaction factors referred to above were evaluated based on the principles of linear continuum mechanics and should be used only in a linear analysis. Figure 4-9 shows typical static interaction factors developed by Poulos and Davis. Nonlinear group effects were considered by O'Neill and Ghazzaly, 1977.

Free-Field Soil Motions The seismologist normally provides to the engineer an earthquake record that represents expected ground motions of the appropriate return period. These ground motions may have been estimated from ground motions in the area or more likely from ground motions recorded at locations that have similar seismic conditions. They may represent an estimate of the motions deep underground, at bed rock, or they may represent estimated motions at the surface. Depending on the soil conditions these soil motions may be rather different.

In deep alluvium there may be considerable modification of the magnitude and frequency content of the motion near the surface when compared with motions deep below the surface. Magnitudes of motion may increased several times, and dominant periods tend to increase. It may therefore be important to ascertain whether these ground motion records represent surface or bedrock motions.

The free-field motion of the soil column may be of importance for two quite separate reasons:

1. The change in stress and pore pressure in the soil from the earthquake motions changes its character, and hence affects the stiffness and strength of the near-field elements that couple the piles to the soil.

2. The changing displacements in the soil over the depth of the piles induces stresses in the piles and reactions between the piles and the soil, as the piles are forced to try to accommodate to the displaced shape of the soil column.

Various computer programs are available that can model the free-field motion of the soil. These frequently use an iterative approach by linearizing the soil stiffness properties, and determining effective damping based on the energy absorbed by hysteretic effects, and then determining soil motions from a dynamic analysis of the earthquake with this linear soil model.

For deposits consisting of soft saturated soils, such as are frequently found offshore, it has been found that to obtain meaningful results, it is necessary to utilize a nonlinear stress-strain model that can incorporate degradation of modulus with time, due to increase in pore pressure or remolding.

The input motion to such programs may be at bedrock or at the surface. By the process just outlined, the motion at any elevation can be found, along with the associated soil conditions at any level, to be used for the near-field elements. A program of this type will also indicate whether liquefaction of loose sands will occur and over what depths.

If the difference in motion of the free-field soil between the top and the bottom of the piles is small relative to the expected motions of the piles, the far field model need be used no further, except for the information it has provided on soil strength for near-field elements. Essentially this means that the displacements of the soil ends of the near-field elements are all the same, the far-field soil moving as a rigid body. Otherwise the far field soil motions should be used in the dynamic modeling of the superstructure/pile/soil system. This means that the soil ends of the near field elements all have different histories of motion. This decision can be made after a preliminary analysis has been performed with the far-field motions the same from point to point, i.e., the soil mass to which the near-field elements are attached, moves as a rigid body.

4.2.5 Components of Damping in Nonlinear Analysis

The contribution of damping from hysteretic behavior becomes dominant for structures with significant inelastic response as is typically the case for DLE conditions. The effect of the various contributions is shown for one example in Figure 4-10 which shows deck displacement time histories for three analysis:

- All sources (soil hysteresis, Rayleigh (5%) and relative velocity)
- Hysteresis and Rayleigh (5%)
- Hysteresis

In this example, hysteretic behavior was limited to the soils. This component of damping would increase if brace buckling were allowed to occur. The comparison is also affected by the relatively high value of Rayleigh damping which was used. A value of 2% is more appropriate for analysis where other sources are modeled explicitly. If these adjustments are made, the response for the three cases is identical.

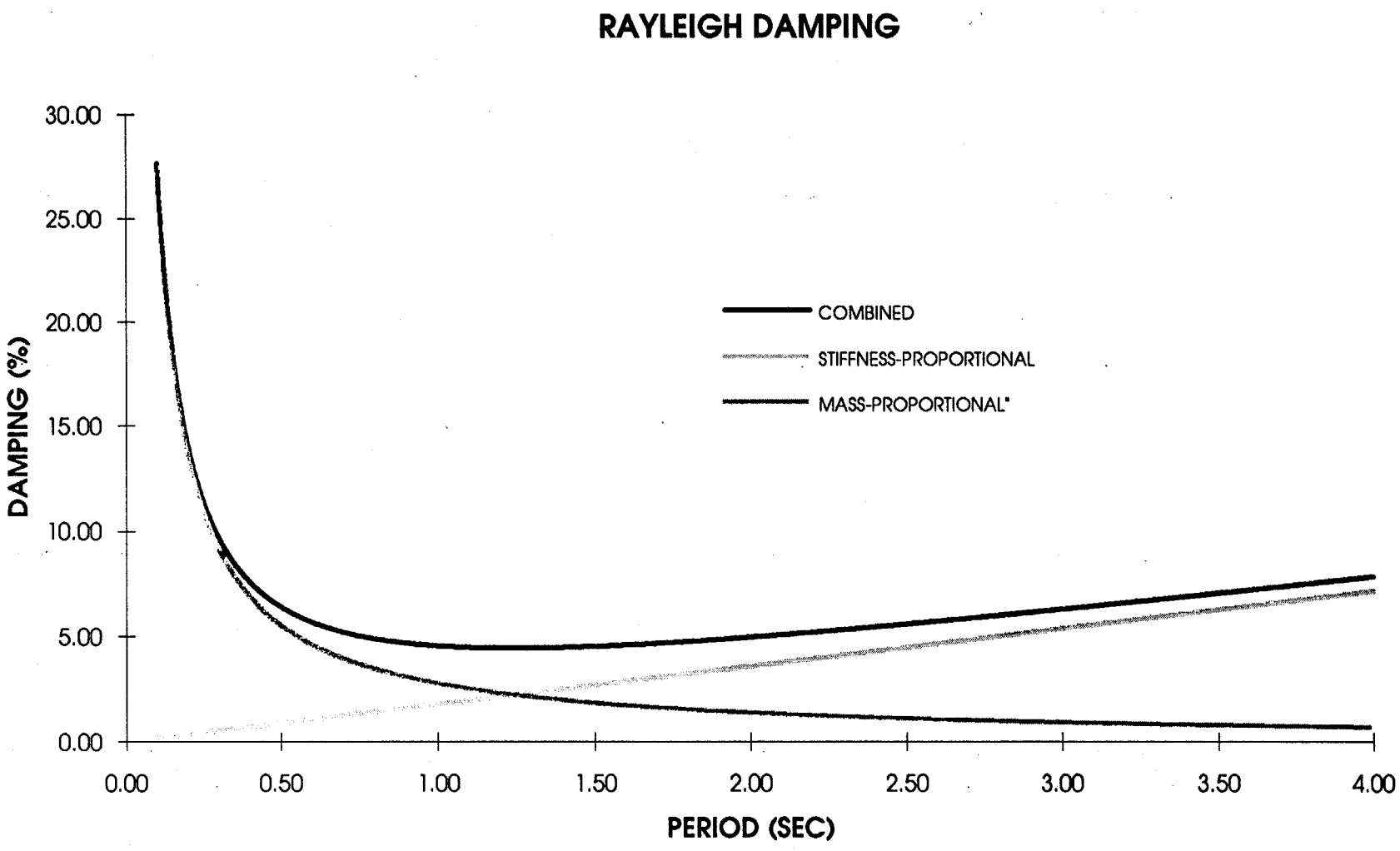

RAYLEIGH DAMPING

FIGURE 4-1

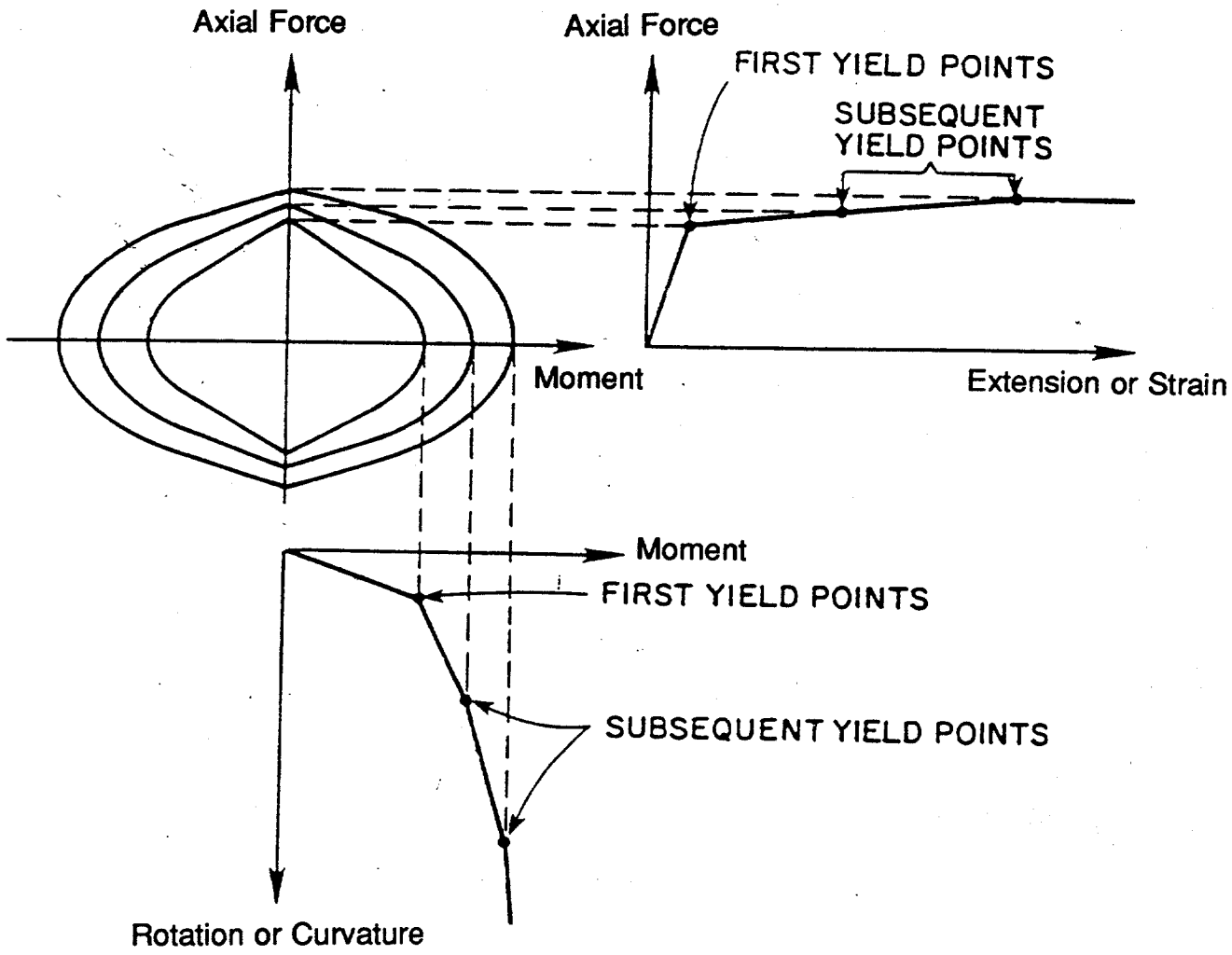

Two-dimensional
Interaction Curve

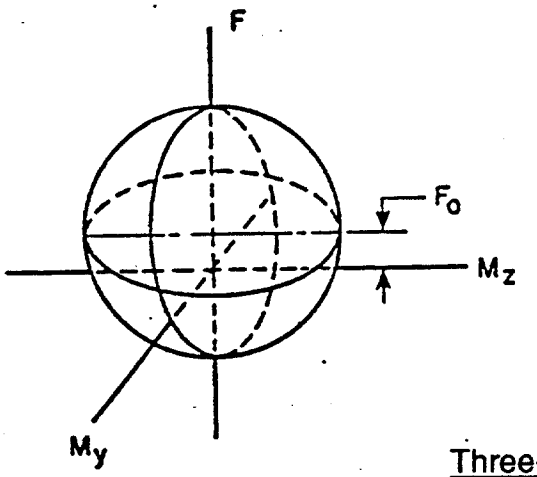

$$\phi = \left(\frac{M_y}{M_{yu}}\right)^2 + \left(\frac{M_z}{M_{zu}}\right)^2 + \left(\frac{T}{T_u}\right)^2 + \left(\frac{F-F_o}{F_u}\right)^2 = 1$$

INTERACTION SURFACE

Three-dimensional
Interaction Curve

FIGURE 4-2 BEAM-COLUMN MOMENT/AXIAL FORCE INTERACTION

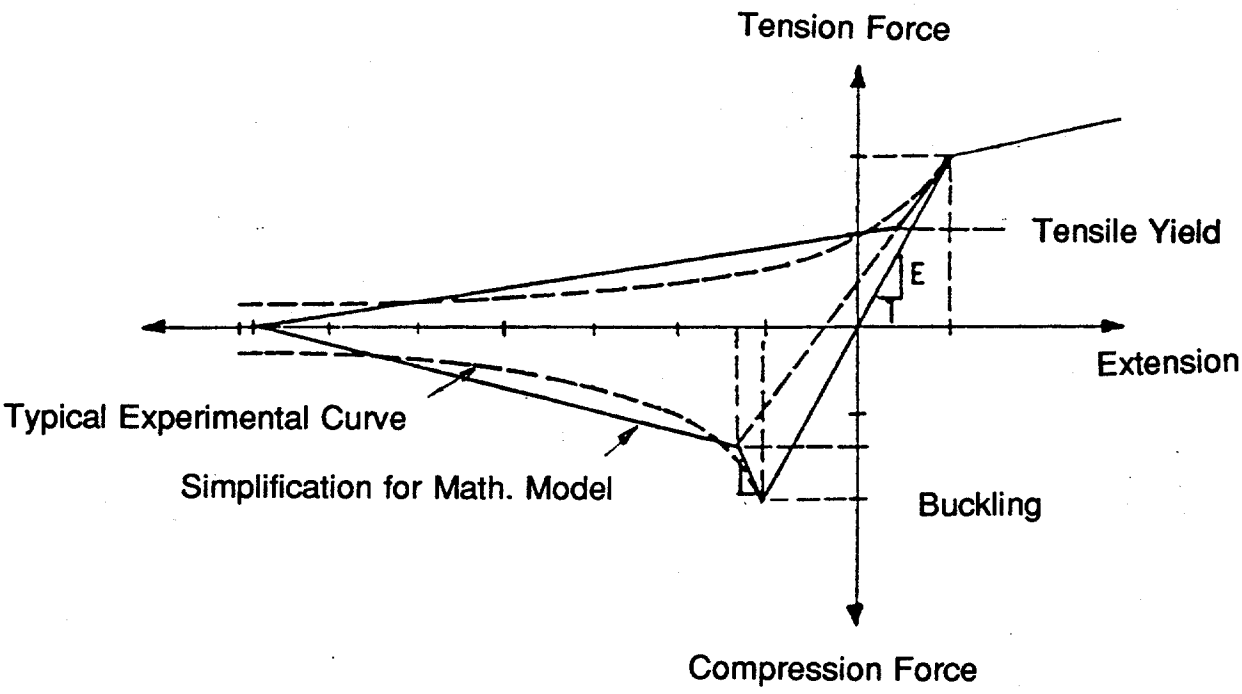

FIGURE 4-3 STRUT FORCE-DEFORMATION RELATIONSHIP

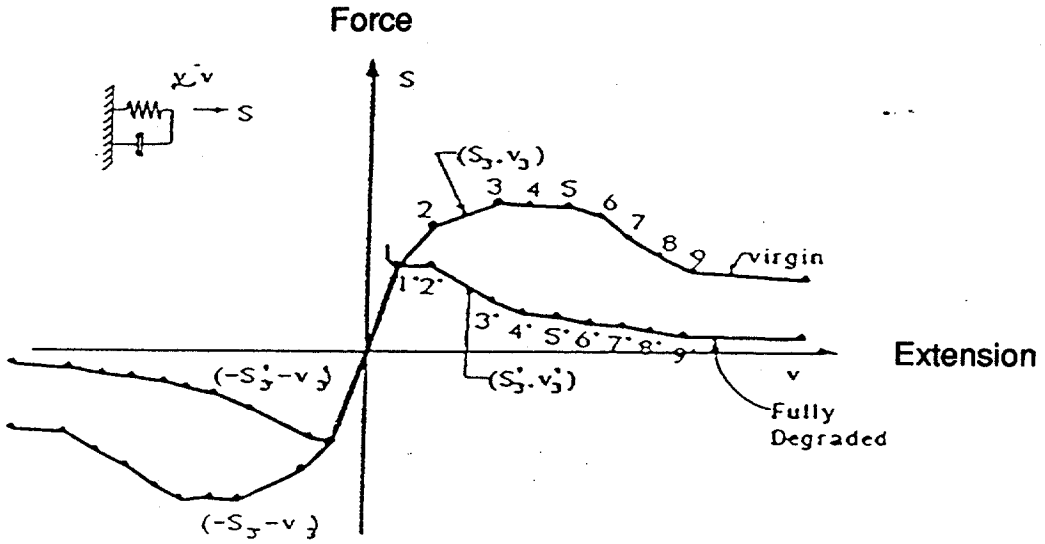

Initial Loading Curve

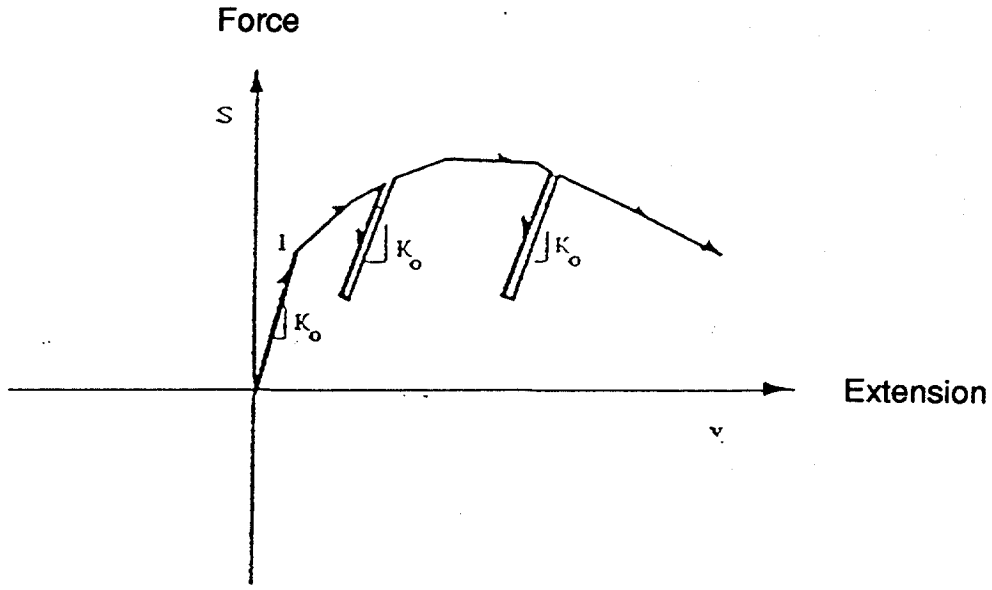

Unloading/Reloading Curve

NEAR-FIELD SOIL ELEMENT
FORCE-DEFORMATION RELATIONSHIP

FIGURE 4-4

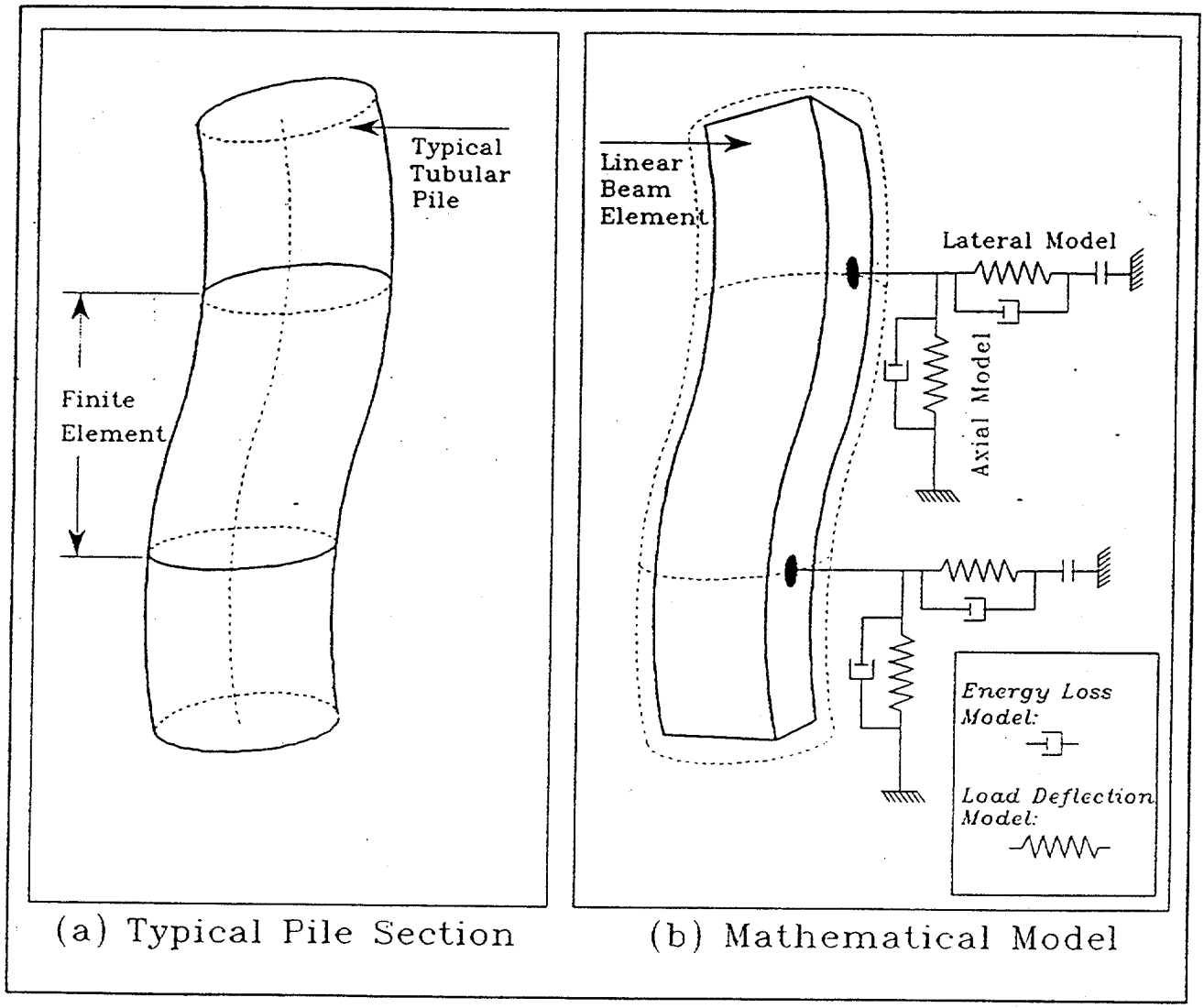

FIGURE 4-5 PILE MODELING

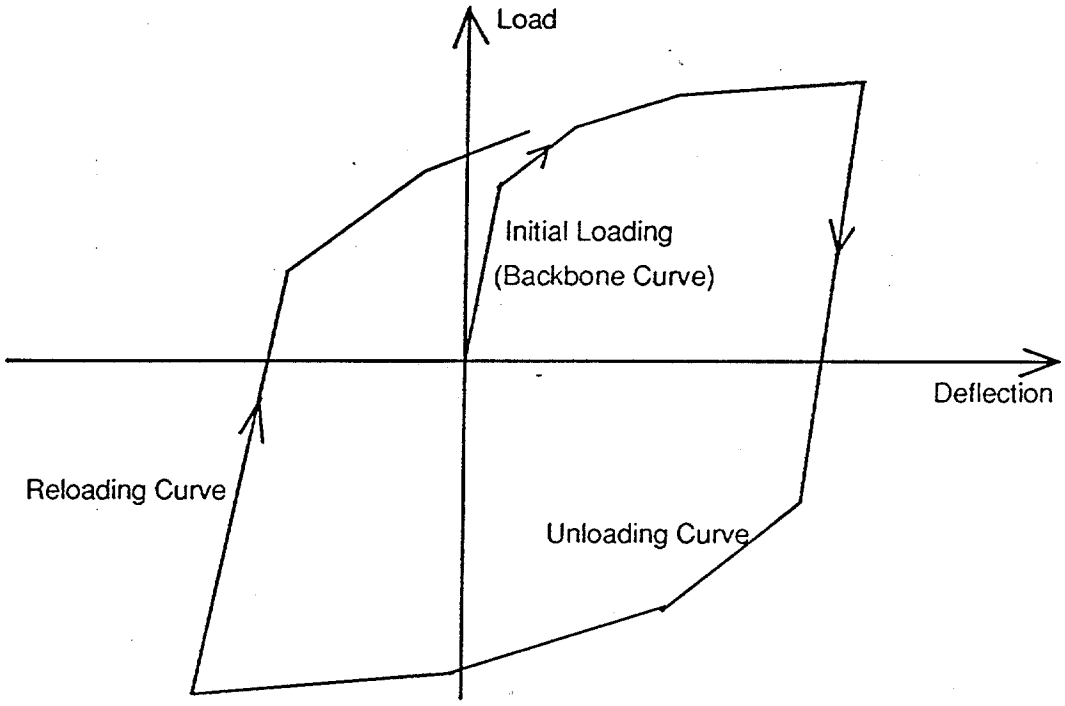

FIGURE 4-6 TYPICAL BACKBONE CURVE AND HYSTERETIC LOOPS

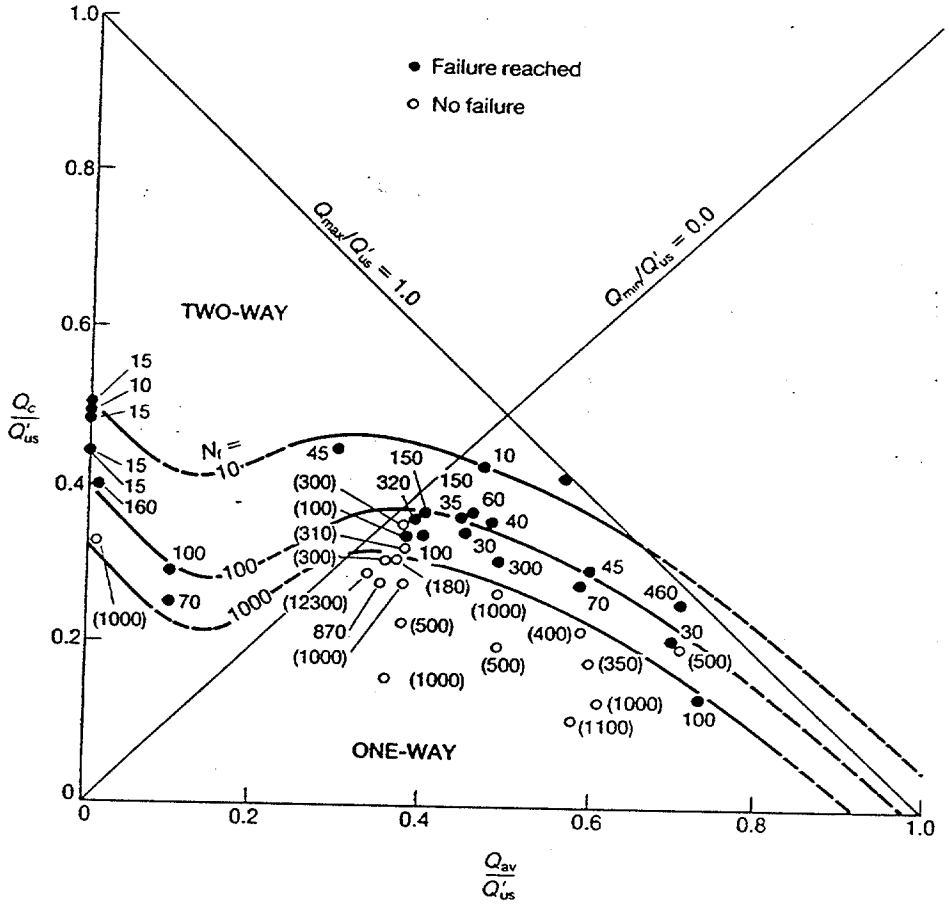

TYPICAL FAILURE INTERACTION DIAGRAM
(KARLSRUD & HAUGEN, 1985)

FIG 4-7

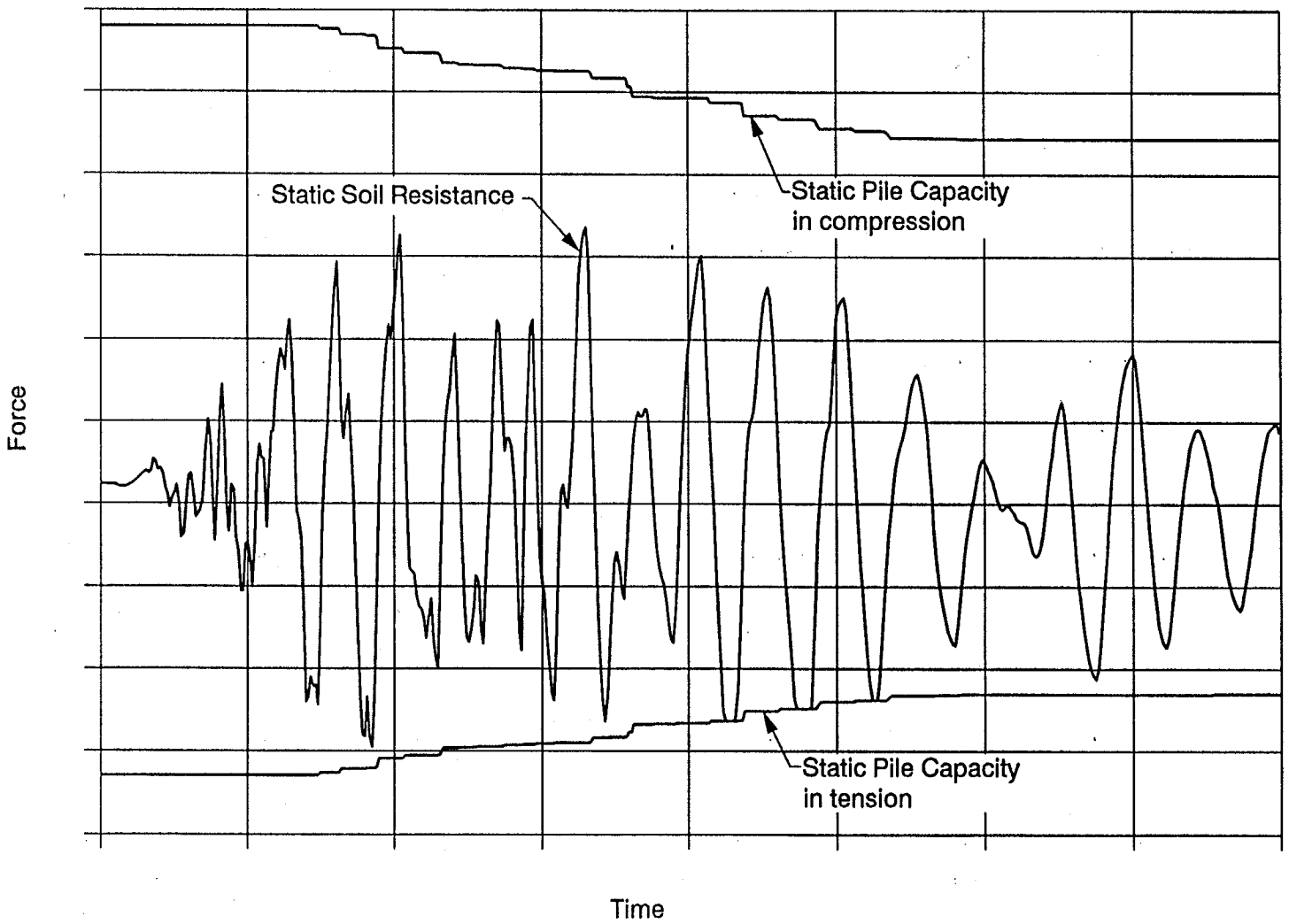

STATIC SOIL RESISTANCE VS STATIC PILE CAPACITY

FIGURE 4-8

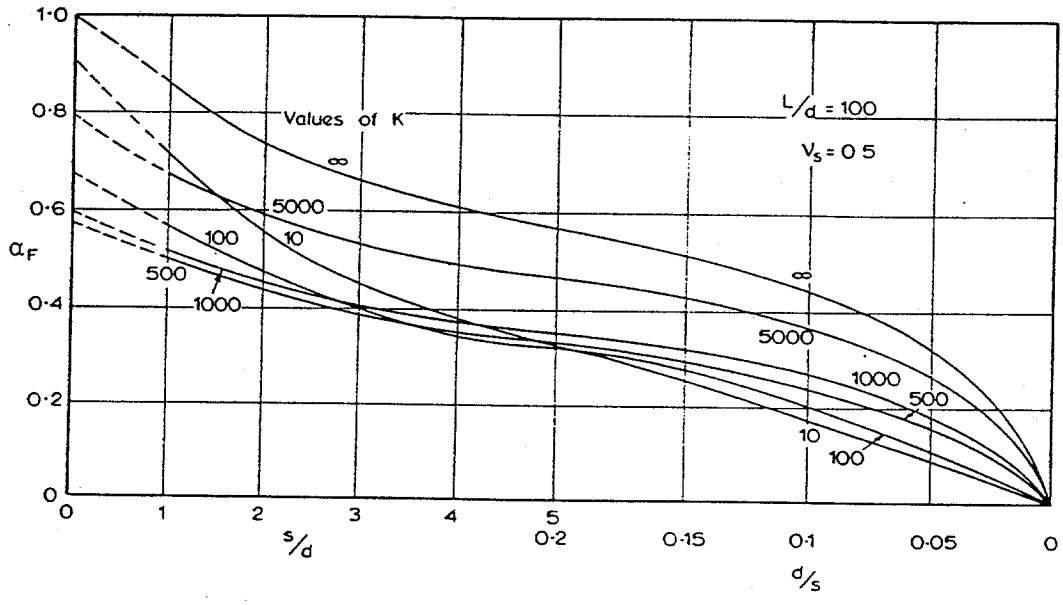

FIGURE 4-9 TYPICAL INTERACTION FACTORS (POULOS AND DAVIS, 1980)

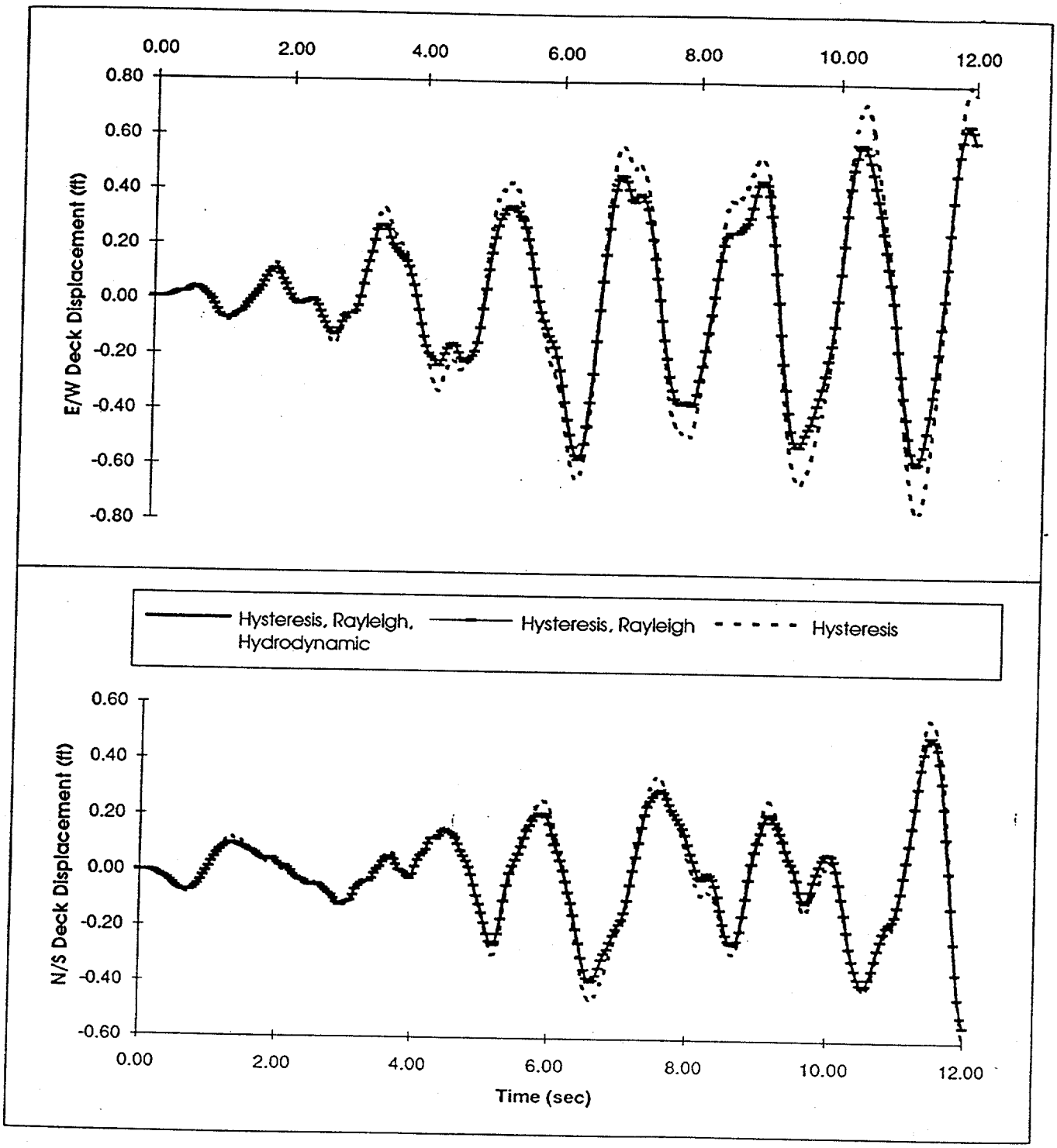

Relative Effect of Damping Sources
Ductility Level Earthquake Loading
Figure 4-10

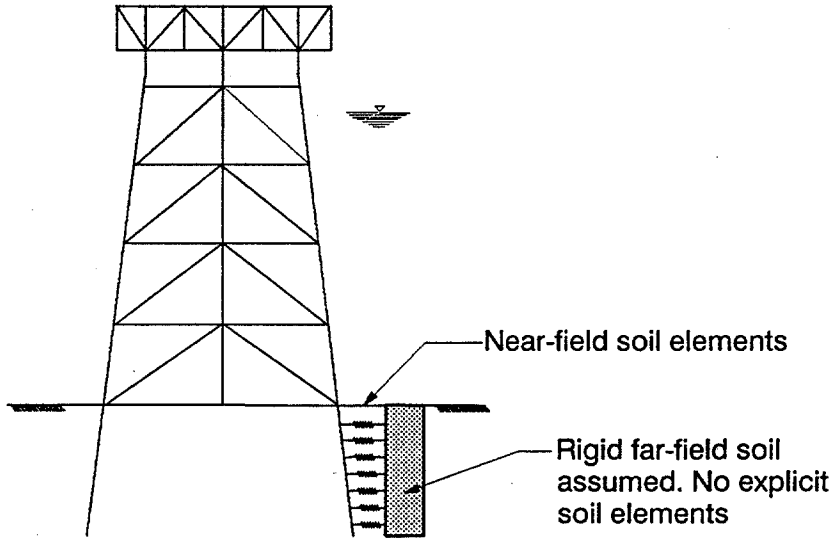

a) Near-Field Soil Elements Only

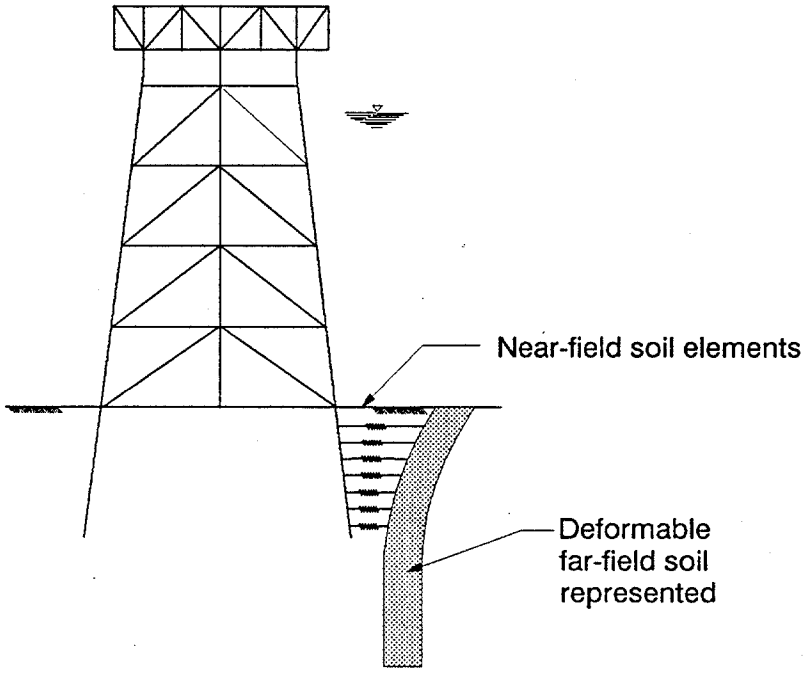

b) Near-and Far-Field Soil Elements

.044\DYNJIP\SOIL-EL

FIGURE 4-11

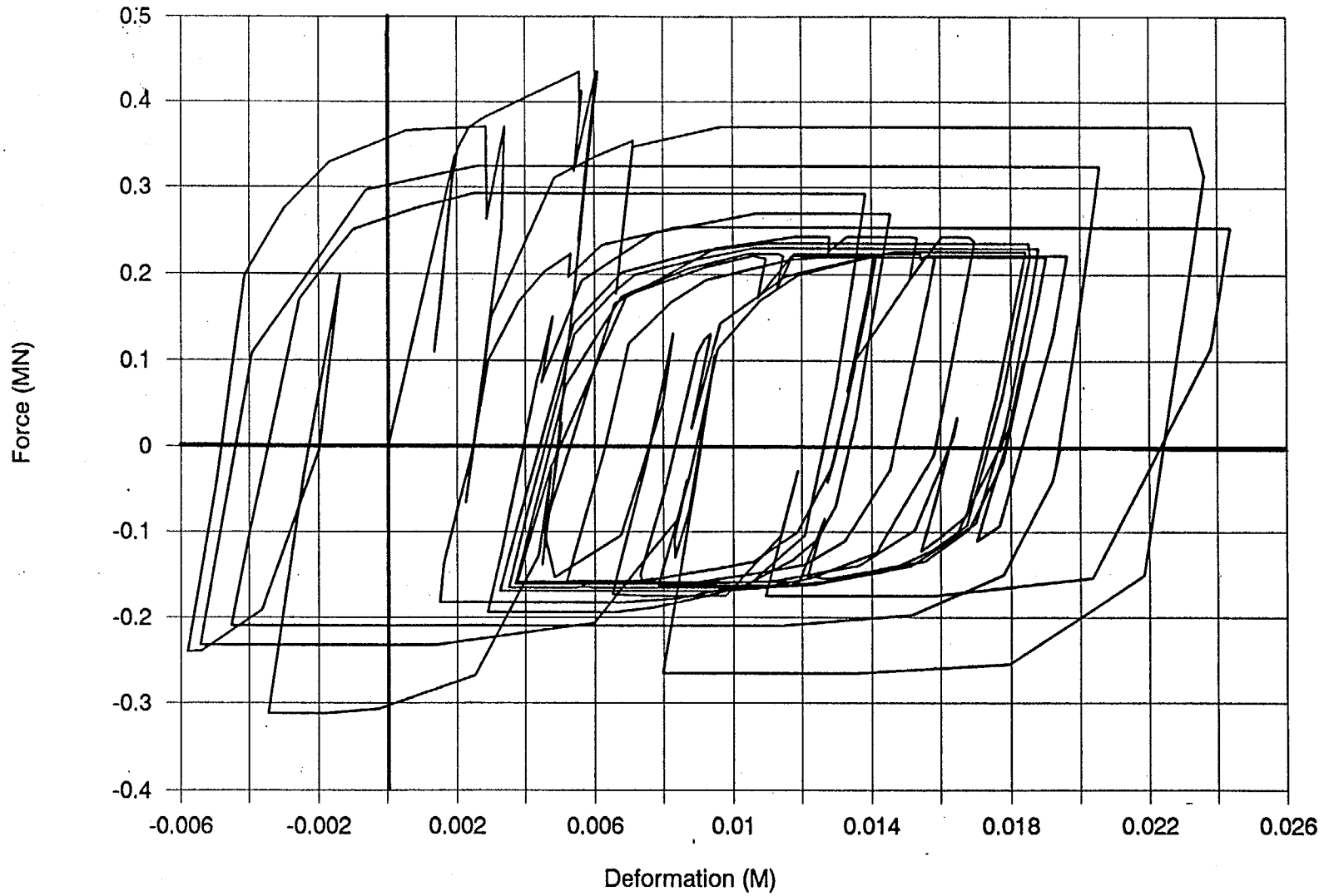

SOIL HYSTERETIC BEHAVIOR

FIGURE 4-12

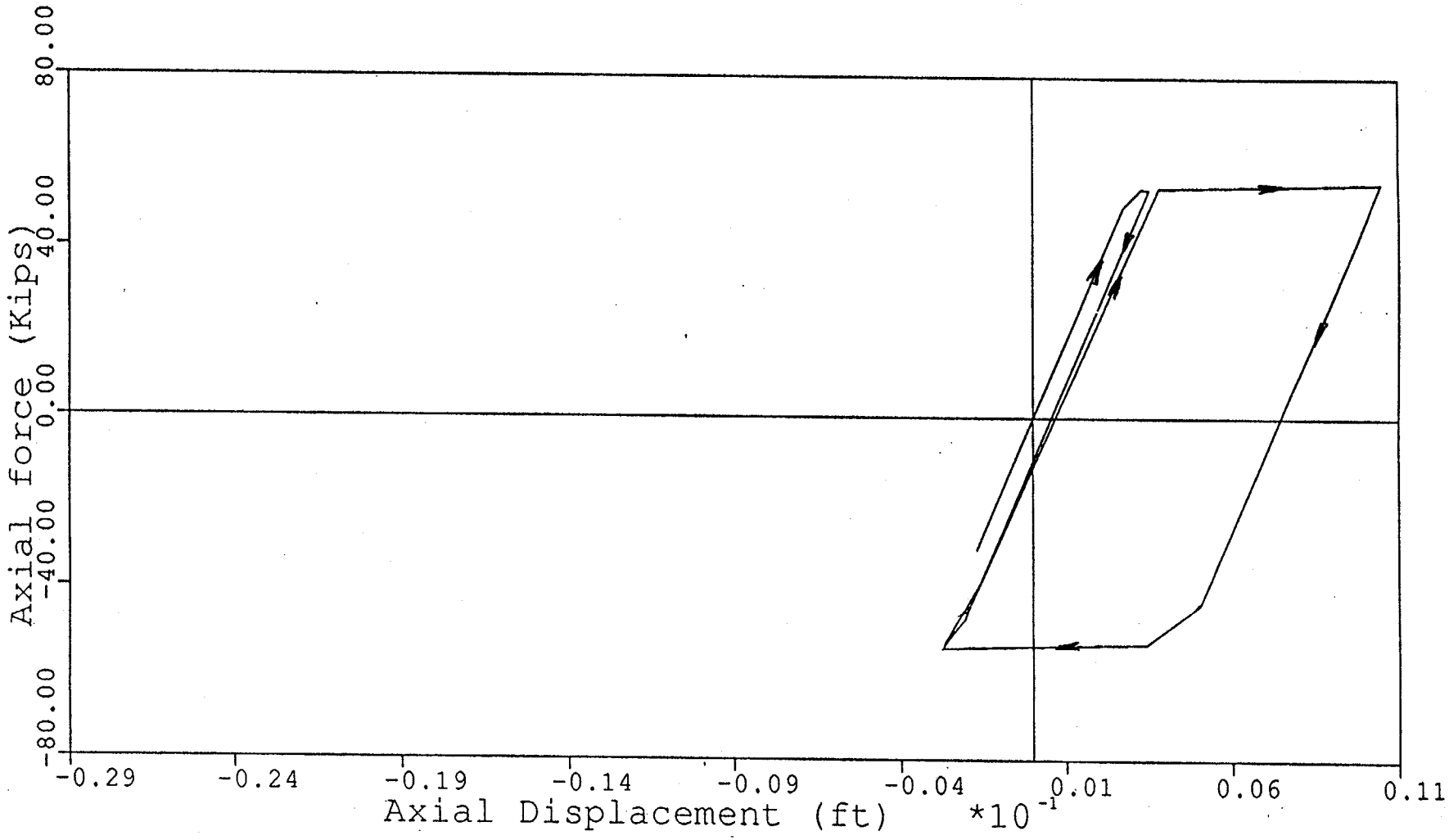

HYSTERESIS LOOPS

FIGURE 4-13

Section 5
Response Spectrum Analysis

The response spectrum method is a powerful design procedure for assessing earthquake response of structures used primarily for SLE applications. It is based on the modal superposition approach. The response in each mode is determined independently from a spectral curve giving the response of a one degree of freedom system whose period varies over a range that includes the important periods of the structure.

The analysis first starts with the design response spectrum for the site. For American waters Figure C2.3.6-2 in API RP 2A provides a recommended curve for various soil conditions. This should be read in conjunction with Section C2.3.6c which gives the effective horizontal ground acceleration with which to scale this figure.

The analyst then performs a frequency analysis of the structure being studied to determine the mode shapes and periods. This model is a linear model with soil characteristics linearized at representative strains expected to be encountered during the earthquake.

A number of modes should be computed, enough to capture virtually all of the response. Since higher modes in offshore jackets tend to have decreasing participation factors it often turns out that relatively few modes are needed, perhaps about 30 to 40 for a typical jacket. The proportion of the total mass that is accumulated by the sum of the so-called modal masses gives a good sense of whether enough modes have been included. This is discussed further in Section 5.1.1 below.

For a given direction of ground motion the member forces are determined for each mode from the mode shape and the ordinate of the response spectrum curve at the modal period. These modal responses are then combined in some appropriate way. Member forces are then found similarly for other directions and combined in an appropriate way. The combination rules for modes and directions are discussed further in Section 5.2 and 5.3 below.

5.1 DEFINITION OF GLOBAL AND LOCAL MODES

5.1.1 Modal Mass

The effective modal mass for a given ground motion direction and mode n is defined by:

$$m_n^{eff} = \frac{L_n^2}{M_n}$$

where L_n is the modal participation factor defined by:

$$L_n = <\phi_n^T> [M] \{r\}$$

$<\phi_n{}^T>$ is the row vector of the mode shape.

$[M]$ is the mass matrix of the system, whose rows and columns correspond to the nodal degrees of freedom of the system $\{v\}$.

$\{r\}$ is a row vector whose rows corresponds to the nodal degrees of freedom of the system, $\{v\}$, and which defines how the nodal degrees of freedom $\{v\}$ are related to the ground motion direction. This vector consists of 1's and 0's if the nodal degrees of freedom are all in the same coordinate directions, and one of these is the ground motion direction.

$[M_n]$ is the modal mass defined by

$$[M_n] = <\phi_n^T> [M] \{\phi\}$$

It can be shown that, summing the effective modal mass over all modes

$$\sum m_n^{eff} = <r^T> [M] \{r\}$$

the right hand side of which is simply the total mass acting in the direction of the ground motion.

If we only include a limited number of modes in the analysis, $\Sigma m_n{}^{eff}$ will be less than the total mass. Thus the sum of the effective modal masses gives us an indication of whether we have included enough modes in the solution to get the desired accuracy. Usually about 90% of the total mass should be included in the sum of the effective modal masses.

5.1.2 Local Modes

The primary objective in developing a model and determining modes and frequencies for response spectrum analysis is to capture the dominant global vibration characteristics of the

structure. The guidelines provided in API RP 2A 1993 (reference section 2.3.6c.3) suggest that at least two modes in each of the three principal directions plus significant torsional modes be defined and included in the analysis. The ratio of the sum of the modal mass to the total mass (compared by direction) can also be used as a basis of determining the number of modes needed to adequately represent global response.

Obtaining accuracy in the definition of global response will not necessarily mean that all member forces are defined accurately. In most template type platforms there will exist several individual members and assemblages of members will exhibit local modes. Local modes are those which do not affect the global response of the structure but which may add significantly to the response (i.e., deformations and forces) of individual members. The guidelines provided in API RP 2A (reference section c2.3.6c.3) suggest that "Additional modes may be required if local member effects are important. However, the dynamic response of sub-assemblages and individual members may require separate consideration."

The identification and inclusion of local modes is complicated in most cases for the following reasons;

- **Lumped Mass.** Individual member vibration modes cannot be defined explicitly within the global frequency analysis unless the mass of the member is distributed properly along its length. This requires either a program which recognizes distributed mass or a modeling strategy which includes additional nodes allocated along a member's span. Most programs used for analysis of offshore platforms will not recognize distributed mass for frequency analysis. It is often impractical to model all members with distributed nodes to capture these modes although this approach can be used for a limited number of members.

- **Number of Modes.** In most instances an adequate representation of a platform's global vibration characteristics can be defined with 30 to 50 modes. The periods of vibration associated with the significant global modes of most offshore platforms in shallow to intermediate water depths fall in the .5 to 3 second range. The relative spacing between modes (i.e., the difference in periods) becomes smaller as higher frequency modes are defined. The existence of higher global modes in the .3 to .5 second range (e.g., second and third bending modes, second vertical torsional modes, etc.) along with the local modes residing in that range makes it very difficult numerically to define all local modes which may be important.

- **Coupled Response with Global Modes.** In most instances, local modes will be very closely spaced with global modes with similar directional characteristics (e.g., the local vertical mode of a conductor support panel and the global vertical mode of the platform). In these cases the response of the local mode may have substantial

dynamic amplification since it is excited by the motions resulting from the global mode. This situation is not difficult to identify but is difficult to include within the analysis without either explicit inclusion of the local mode or conservative superposition of local and global analysis results.

Many local modes can be identified through simplified local analysis and hand calculations. Examples of areas where local modes can be important include; braces with long unsupported lengths, conductors, risers, conductor framing panels (which may be critical if significant marine growth exists), deck cantilevers, flare booms and drilling masts.

Once a local mode is determined, its response can be estimated based on the response spectra associated with its boundaries with the global system. The natural period of the member can be estimated from formulas for beams with appropriate end fixity, from the known length and mass distribution, e.g., Roark and Young, 1975. This calculation is straight forward in situations where there are few boundaries between the local and global elements (e.g., a single brace) but becomes very difficult where there are multiple boundaries which are subjected to motions which are out-of-phase. This process is also complicated by local components (e.g., conductor framing) which may exhibit multiple local modes.

A response spectrum analysis was performed on a simple two dimensional frame to demonstrate the effects and analysis of local modes. Analyses were performed to assess the added stresses resulting from the local mode of an individual single diagonal brace. The two models used to perform the analysis are shown in Figure 5-1. Each of the models includes linear beam elements with mass lumped at the primary joints. The detailed model includes a series of 10 linear beam elements to represent the lowest right-side diagonal brace. The mass for this diagonal is distributed at each of the 11 nodes (i.e., 9 more nodes than in the simplified model).

The geometry of the frame and its member sizes are provided in Figure 5-2. Also shown in this figure are the results of the eigenvalue analysis which show the significant modes for both models. These results show that the global mode periods are essentially unaffected by the inclusion of the detailed brace model. The period of the local brace mode is closely spaced to 3 global modes. The comparison of mode shapes is provided in Figures 5-3.

In this two-dimensional example, the individual brace mode will increase the in-plane bending forces. The orientation of the brace is such that end node motions both horizontally and vertically (i.e., x and z) can excite its local mode. The local mode response will therefore be effected by global modes with either horizontal or vertical components.

A three-dimensional example would include a second local mode for this brace which would result in out-of-plane motions. This mode would be very similar to the in-plane mode (the

only difference being that of rotational stiffness at the joints) and would likely act in-phase. The out-of-plane mode would be excited by end node motions resulting from the second horizontal (i.e., y) motions. The bending stresses resulting from the in-plane and out-of-plane modes would be added vectorially.

The results of the analysis are summarized in the following table.

LOCAL VIBRATION EFFECTS

Item	Lumped Mass	Distributed Mass	Difference
Deck Displacement (ft)	.9283	.9298	+.2%
Axial Force (k)	3395	3390	-0.1%
Bending Moment (k-ft)			
Lower End	1292	1598	+23%
Midspan	----	1055	----
Upper End	460	1201	+156%

The global displacements and forces as well as the axial force in the individual brace are essentially identical for both analyses. The bending moment of the brace as defined by the detailed model is approximately 150% greater than that defined by the simplified model. This increase in bending moment results in a 28% increase in maximum combined stress for this brace.

5.2 MODAL ACCELERATION METHOD

If the there are a number of modes that have periods low enough that they develop essentially no dynamic amplification (periods less than 0.04 sec in the API RP 2A curve of Figures C2.3.6-2), but they contribute significantly to the forces in one or more members it is rather inefficient, and potentially inaccurate to include all these high modes. This is because the higher modes of a large system may be inaccurately determined by the computer, and the computer takes more time to determine these higher modes than lower ones. Since modes with these frequencies experience no dynamic amplification they respond statically and their effects can therefore be determined by a static analysis using the peak ground acceleration as loading. No matter how many modes fall in this category, no modal

analysis is needed, the response from all these modes being computed exactly by one static analysis.

The response from modes with periods above these higher modes are computed by modal analysis, and combined mode by mode with the static analysis.

A problem arises however if this process is performed exactly as just described. The static analysis includes the static response of the lower modes as well as their dynamic amplification effects. So the static response of these modes has been included twice – once in the modal analysis and once in the static analysis. Therefore the response of each of the lower modes must be reduced by subtracting the static part of that response. This is a simple computation involving only quantities such as the modal participation factor L_n and the mode shape $\{\phi\}$ that have been already calculated.

5.3 MODAL COMBINATIONS

The response spectrum method computes the maximum response of each mode exactly, by scaling appropriately the value of the response spectrum ordinate at that period. However the time of occurrence of these maxima are different, so they cannot be simply added algebraically without considerable conservatism. When there are many modes and it is assumed that the times of occurrence of the maxima in each mode are randomly distributed, it can be shown that the square root of the sum of the squares (SRSS) of the individual maxima is the best estimate of the maximum with all modes included.

This can lead to significant errors when there are very few (but more than one) important modes, or when these modes are not randomly distributed.

This will occur if the modes have such low periods that they all respond statically, in which case they all have their maxima at the time when the ground acceleration is at its maximum. However this is rather trivial, since in this situation a static analysis could have been done.

A more serious condition occurs when two or more modes have closely spaced periods. In this case, the maxima in each mode may occur close together in time. Adding the responses by the SRSS process seriously underestimates the correct addition, which may be close to an algebraic sum.

Various procedures over the years have been devised to combine the responses in each modes. These have included adding the absolute sums of responses from closely-spaced modes. A widely-used procedure that bases its algorithms on random vibration theory is the Complete Quadratic Combination (CQC) method. This develops a square matrix, called the correlation matrix, of dimension equal to the number of modes in use, the elements of

which depend on the periods (and damping) of the pairs of modes corresponding to each element of the matrix. The response from all modes is found as the square root of the value found by pre- and post-multiplying this matrix with the modal responses.

At one extreme, when the modal frequencies are widely spaced, the correlation matrix is the unit matrix. In this case, it can be seen that the results are identical to the SRSS method. At the other extreme, for closely spaced modes the correlation matrix consists of 1's in all elements, which gives the same results as the absolute sum method except that the sign of the response quantities is preserved. When the responses from two closely-spaced modes are of opposite sign, the CQC method preserves this character reducing the resulting combined response. However, the absolute sum method does not account for this effect and thus can be very conservative in such situations.

Maison, Neuss and Kasai (1983) examined various modal combination rules on a regular fifteen story steel moment-resisting frame. Two situations were examined, the first with the centers of mass and stiffness coincident, the second with an offset. They compared response spectrum results using absolute sum, SRSS, CQC and another rather similar procedure described by Rosenblueth and Elorduy (1969), with time history results. For the regular building the SRSS, R&E and CQC gave results very close to time history results. For the offset case, the CQC and R&E methods were greatly superior to the SRSS combination method. Fig 5-4 compares story deflections, shears and overturning moments for the four modal combination procedures with the time history results. The CQC results are shown as *Der Kiureghian*, after the originator of this method. For this case the CQC and R&E procedures are greatly superior.

Since the computational penalty for the CQC method is small, there is no reason why this should not be used routinely in all response spectrum analyses.

5.4 DIRECTIONAL COMBINATIONS

The addition of the effects from ground motion in three perpendicular directions is now discussed. If the ground motion in each direction is assumed to arise from waves traveling in one direction then there will be clear correlation between the times of maximum response from the ground motion in each direction. In fact, ground motions are far more complex than this, and there is no correlation between motions in different orthogonal directions. For this reason the best estimate of the total response is to assume the timing of the peak response from ground motions in each direction is random and use the SRSS method to combine directional responses.

5.5 DEFINITION AND APPLICATION OF GROUND SPECTRA

Specific guidelines for the development of site seismic hazard data is provided in section c.2.3.6b of API RP 2A, 1993. These guidelines provide a generic spectrum which can be used for preliminary design and studies. However, spectra used for final design should be based on a site specific hazard analysis. Seismic hazard analysis typically involves the development of a probabilistic model which represents all of the known sources of seismic activity which can generate consequential ground motions at the site. Such a model must address the relationship between the magnitude and recurrence period of each source, the maximum magnitude of each source and the attenuation relationships which define site motions as a function of source motions. Attenuation relationships are typically derived from recorded ground motion data. It is preferable to obtain this data from recording stations with local site and seismotectonic conditions which are similar to that of the platform location.

5.6 DECK RESPONSE SPECTRA

It frequently occurs that secondary structural elements such as cranes, flare booms or drilling rigs are designed independently of the main jacket. If dynamic effects on these structures and their connections are to be considered, various possible ways exist to do this. These will be outlined and discussed.

If the details of the secondary structure are known at the time that the jacket is being analyzed, a model of the structure could be included in the main jacket model. This could be either a detailed, member-by-member model, or more likely a simplified model representing the principal mass and stiffness components. This (coupled) model is then analyzed in one piece and the forces in the structure and its connections determined in the usual way. Care must be taken of course that the modes included in the analysis include the principal modes for the secondary structure. This is the most accurate, for not only does it include the dynamics of the secondary system, but it includes its effect on the jacket motion if this is significant.

Frequently the detail of the secondary structure will not be available until after the analysis of the jacket is complete, or various options are being considered for this structure. The question then is, how can the seismic analysis of the secondary structures be made?

If the natural periods of the equipment are small relative to the dominant periods of the deck, the simplest method is to determine the peak acceleration of the deck, where the equipment is being placed, and apply this as lateral acceleration in a static analysis of the secondary structure. If the secondary structure has important periods around or greater than the dominant periods of the deck motions, (which probably include important periods of the

jacket and possibly the earthquake, see, for instance, Fig 5-5), then since dynamic amplification effects are not being considered in this process, the results are less accurate. Further, since the secondary structure was not present in the jacket analysis, interaction effects are lost.

If the dynamics of the secondary structure are important, more effort must be put into the analysis. The most rigorous method will be to develop the response spectrum of the deck itself, and use this as "ground" motion input for the secondary structure. Two ways that this can be accomplished are now described.

In the first method, a number of small spring-mass sub-systems are included in the jacket model. The lines of actions of the springs should be in directions that the response spectra are desired, probably in three orthogonal directions. In each of these directions there will be a set of such systems whose natural periods with the deck fixed vary over the possible range of important periods expected in the secondary structure. Once again, since the secondary structure was not present in the jacket analysis, interaction effects are lost.

A response spectrum analysis is carried out on the jacket with its sub-systems, and the displacement of each sub-system from all modes is found. For each sub-system, this represents the ordinate of the displacement in the desired response spectrum for the deck. The resulting response spectra in the three directions can then be used for the analysis and design of the secondary structures.

Other more sophisticated methods can be used to develop the response spectra of the deck, directly from the results of the frequency analysis of the jacket and the ground motion spectra. The frequency analysis of the jacket need not include the secondary structure, but the missing interaction effects can be included in the computation. These methods are based on random vibrations and perturbation theory, e.g. Singh, 1980. Specialized software is available to perform these analyses.

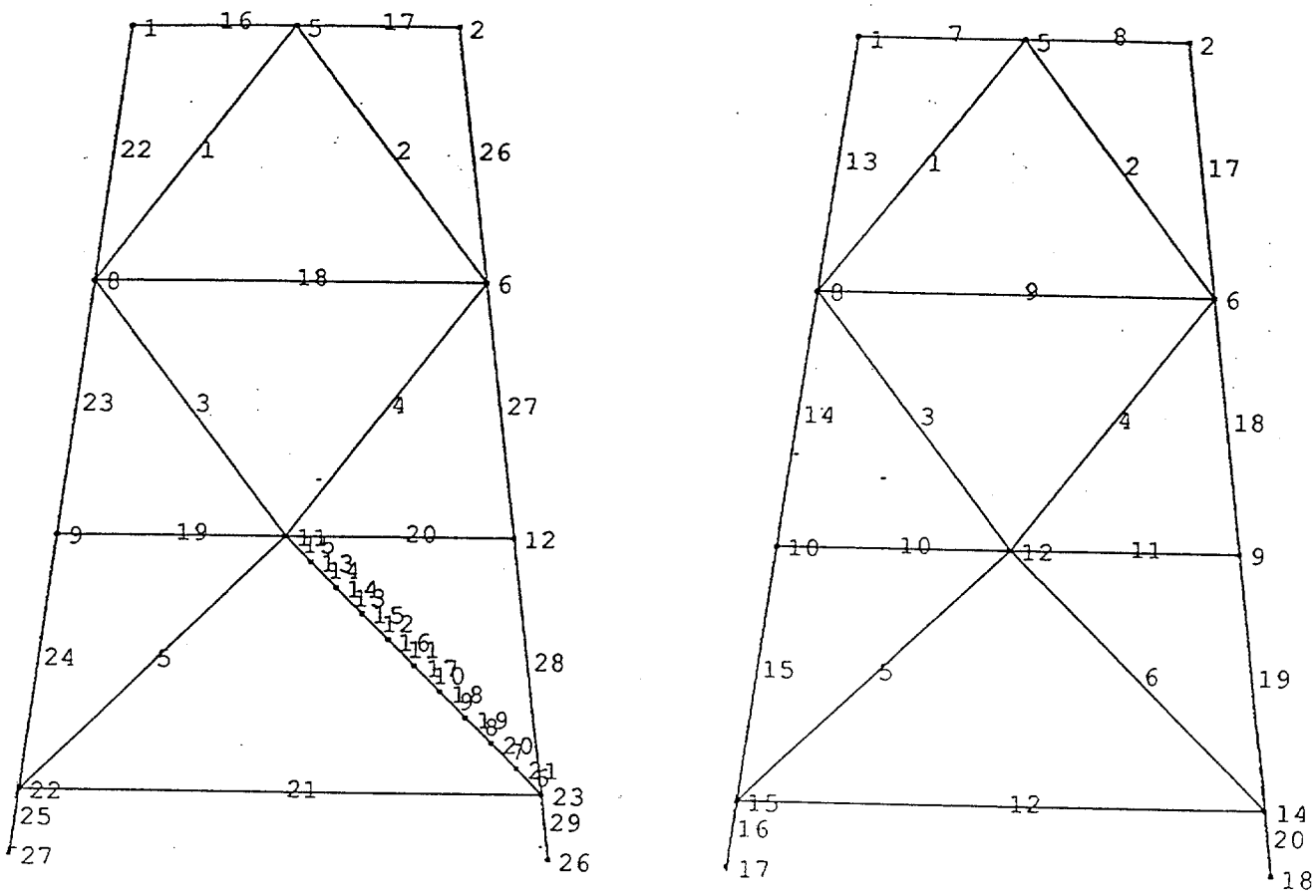

FIGURE 5-1 MODELS USED TO ASSESS LOCAL VIBRATIONS

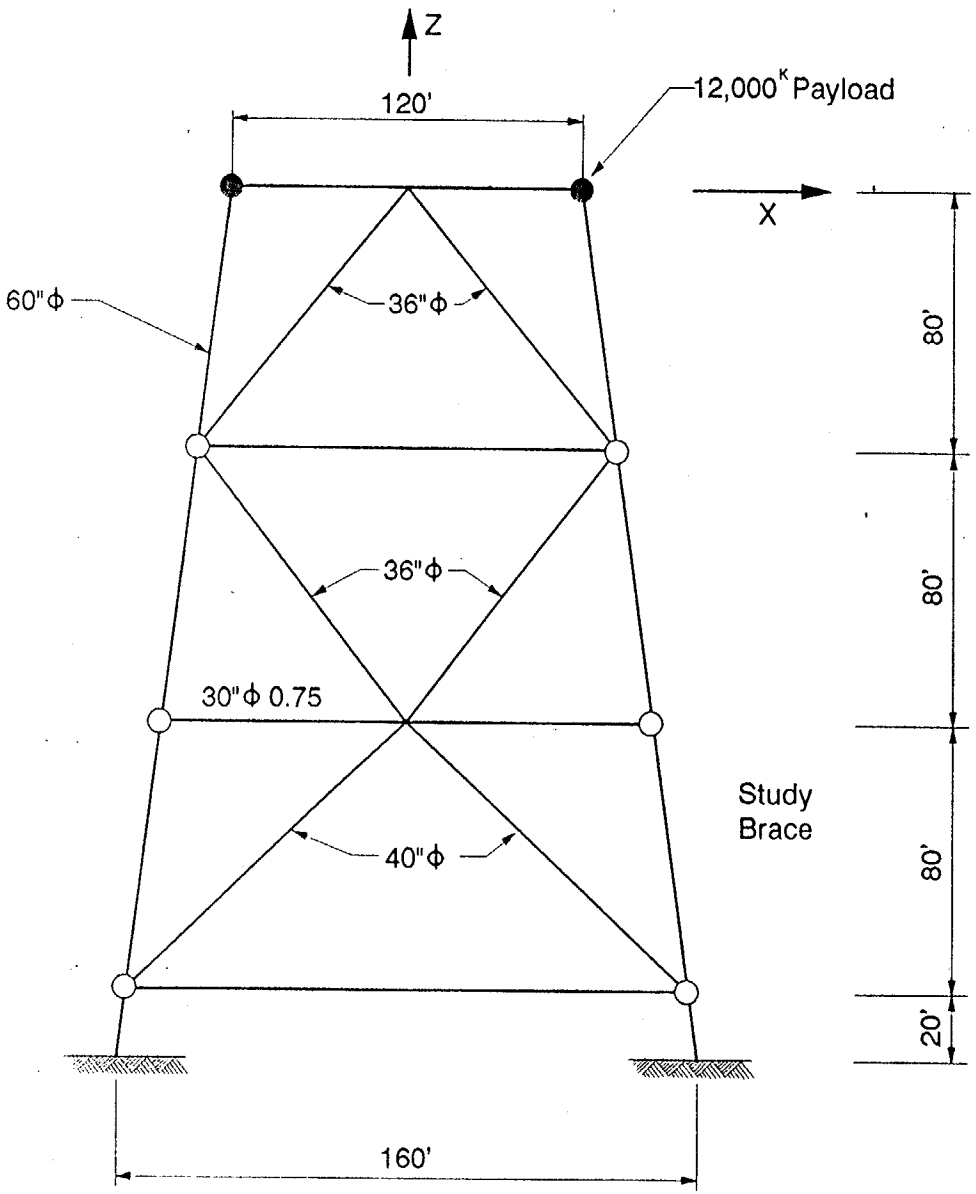

Eigenvalue Analysis Results		
Mode	Lumped	Distributed
1st Horizontal	1.62 sec.	1.62 sec.
1st Vertical	.517 sec.	.517 sec.
2nd Horizontal	.488 sec.	.507 sec.
2nd Vertical	.421 sec.	.421 sec.
Local	—	.356 sec.

Test Model Configuration

.031\CAP-JIP\FIG-X3

FIGURE 5-2

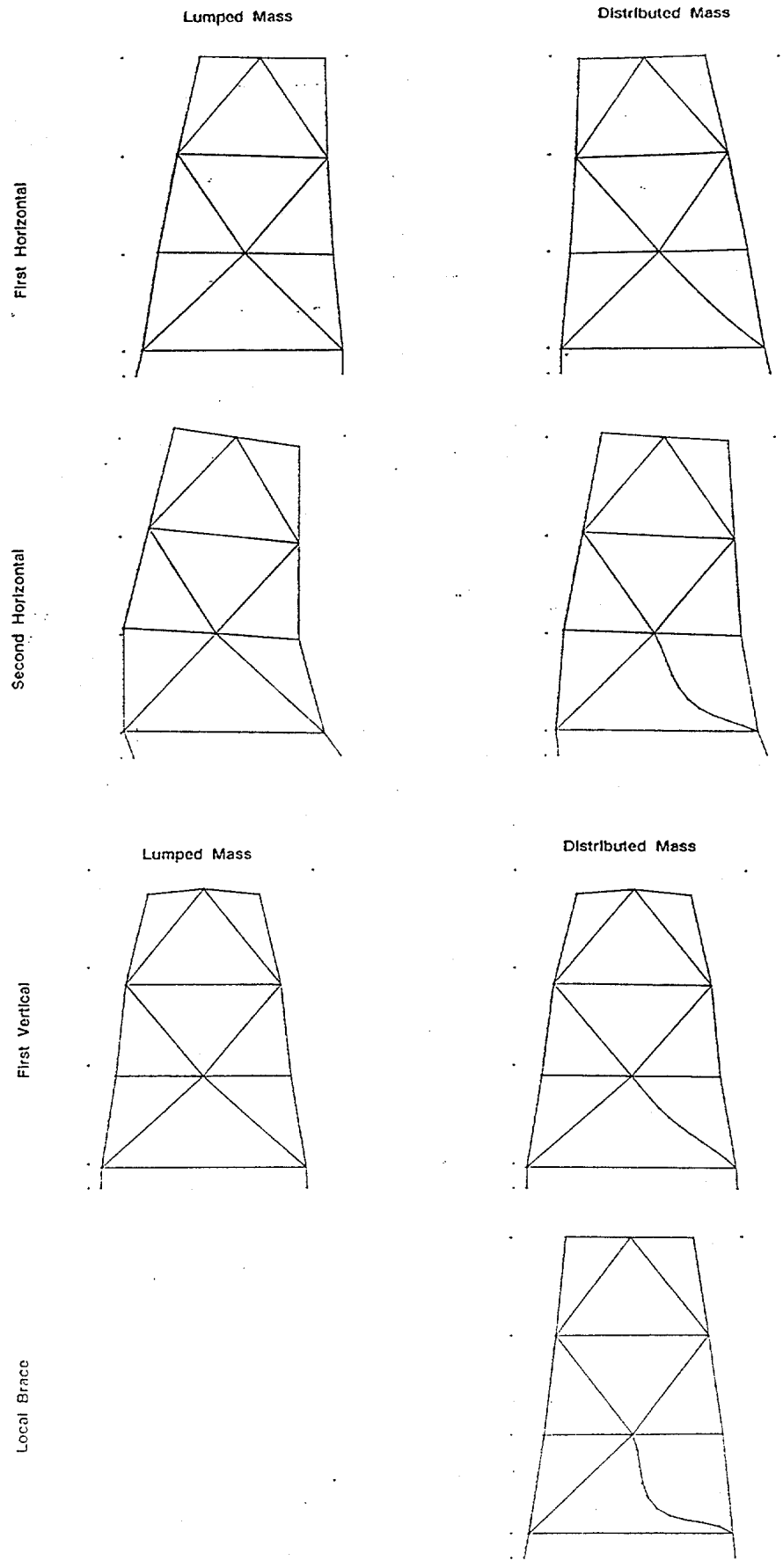

FIGURE 5-3 MODE SHAPE COMPARISONS

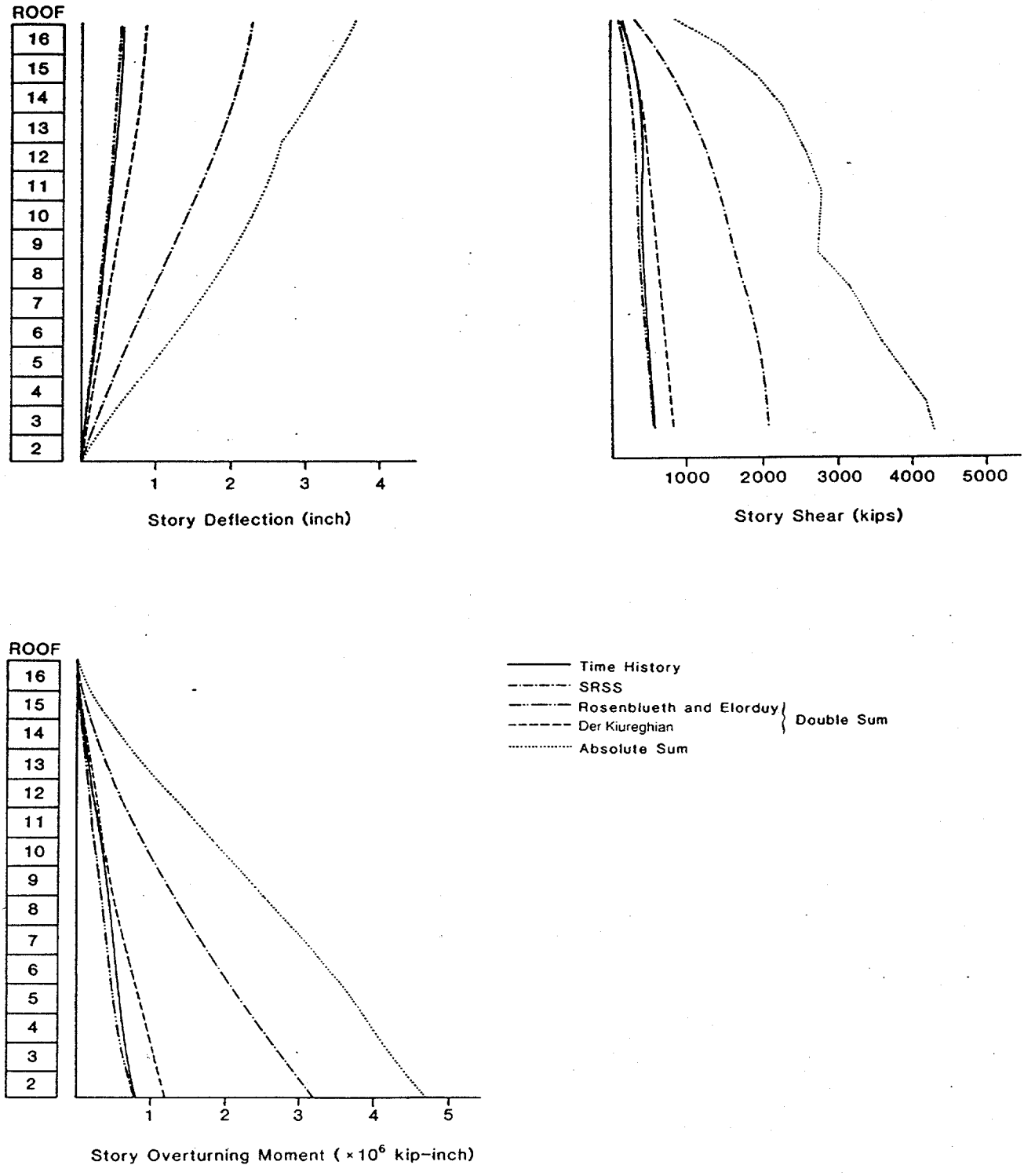

COMPARISON OF MODAL COMBINATION RULES ON BUILDING
FIGURE 5-4

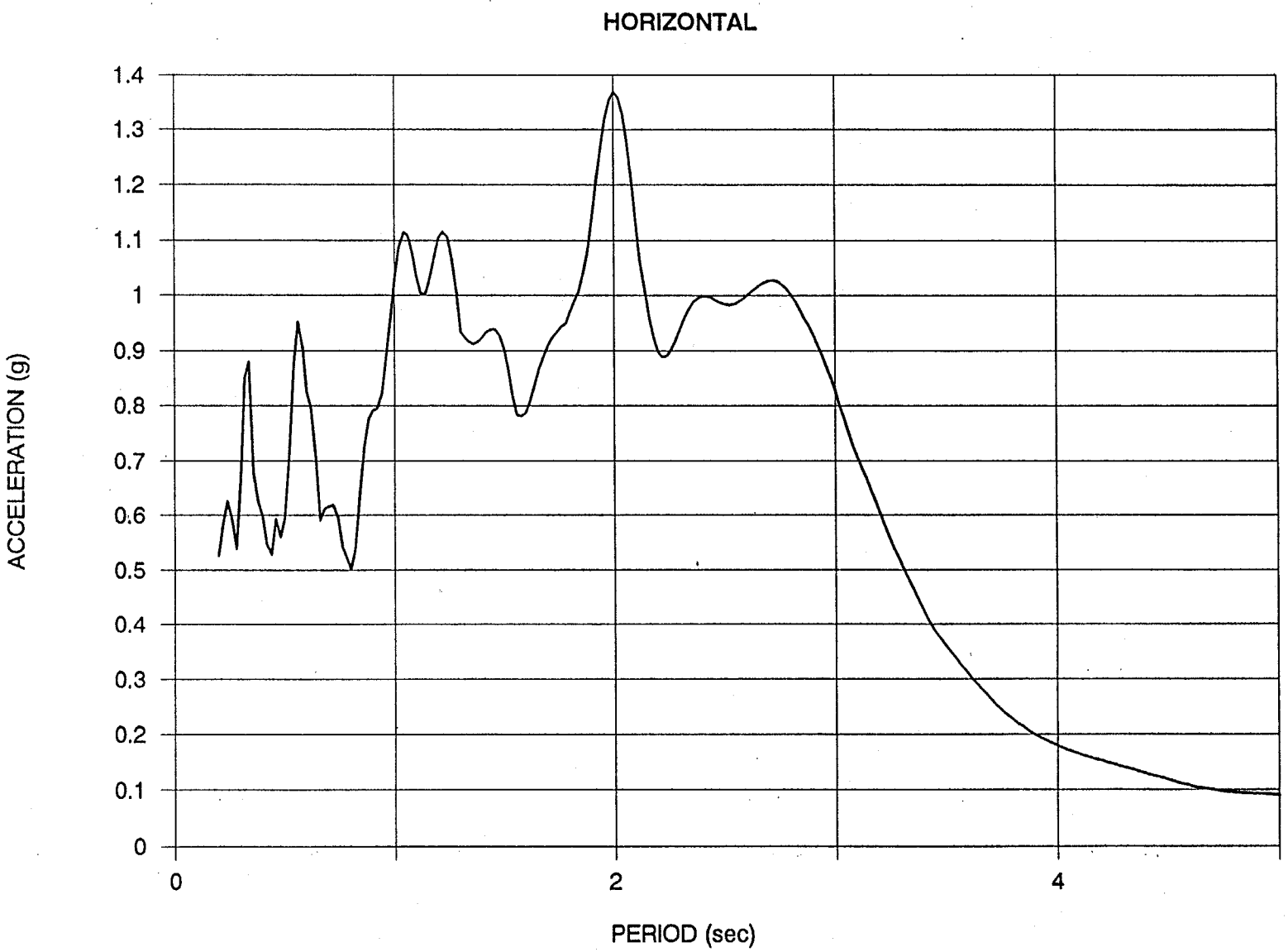

DECK FLOOR RESPONSE SPECTRUM

1971 SAN FERNANDO EARTHQUAKE
TYPICAL INTERMEDIATE DEPTH PLATFORM

FIGURE 5-5

Section 6
Static Pushover Analysis

Pushover analyses are used to define the load/deformation behavior of a structure up to and potentially beyond ultimate capacity. The analysis requires a predetermined load pattern which can be based on the results of either response spectrum or time history analysis. The results of the analysis can be used to assess the performance of the platform in terms of maximum strength or energy absorption. The API RP 2A (1993)recommends that time history analysis method be used for design under DLE condition but recognizes the benefit of more simplistic methods, such as static pushover, to complement the results of the time history analysis.

This static pushover method of analysis captures most sources of nonlinear response including local member failure and subsequent load redistribution with minimal numerical instability. The analysis involves the application of gravity loads followed by the application of a representative load pattern which is increased incremental until the point at which the platform achieves ultimate capacity. The analysis can be continued beyond ultimate capacity to assess platform ductility, however, this requires a process to reduce the applied load in balance with the reduced post-ultimate resistance. Analysis can be performed until a collapse mechanism is reached.

The results of a pushover analysis are only an approximate representation of the actual behavior of the platform under earthquake loading and are highly dependent on the loading profile. The static pushover method is a useful analytical tool in that it establishes static ultimate strength, defines failure sequence for the selected loading pattern, defines energy absorption for the selected loading pattern, defines critical or weak elements in the structure and is relatively easy to perform. Aspects of dynamic structural response such as load reversal, soil and structural cyclic degradation, change in vibration characteristics due to nonlinearity and nonlinear amplitude dependent damping, and soil and structure hysteretic behavior are not represented through static pushover analysis. Pushover analyses provide a good means of comparing alternate structural concepts in terms of ductility.

6.1 STATIC PUSHOVER TO ASSESS ENERGY

Earlier version of API RP 2A (15th edition) included a recommendation of four times the energy at SLE loading as a check for adequate ductility. Strain energy is computed by integrating the member forces with respect to the corresponding deformations, and adding for all members.

The static pushover can be used to evaluate adequate ductility as part of the DLE requirements for new design and for the assessment of existing platforms where the target earthquake resistance requires response beyond the elastic range.

The method involves the application of gravity loads and a system of vertical and lateral loads derived from the SLE response spectrum. This system of loads is scaled initially to produce forces in the structure which correspond to the forces calculated in the strength analysis. These loads are then scaled proportionately to induce yielding and buckling of platform members until the required energy absorption is obtained with the structure remaining stable. Only a minimum amount of energy absorbed by the foundation should be included in this assessment. The total foundation capacity must be shown to be greater than the DLE induced loads. Individual piles may be overloaded provided the total foundation load can be redistributed to other piles. Inelastic behavior is accounted for by modeling the post-yielding and post-buckling response of members and redistributing internal forces due to such behavior.

6.2 LOCAL ACCELERATION EFFECTS

The local inertia loads associated with the mass and added mass of a member subjected to a global acceleration produces local forces transverse to the member which reduce the critical buckling load. Since the overload analysis is intended to represent performance under dynamic conditions the effect of local accelerations must be incorporated into the development of member properties. The accelerations resulting from the strength level response spectra analyses can be used to reduce member buckling loads.

6.3 METHODS OF ASSESSMENT

Pushover analyses can be used to assess the performance under extreme earthquake loading either in terms of strength or energy absorption. Platforms which can be shown to have an ultimate strength equal to or greater than that induced by the extreme earthquake (i.e., as defined from a Response Spectrum analysis) will likely demonstrate survivability if a more accurate time history analysis is performed.

The comparison of ultimate strain energy to a reference strain energy has been used for the DLE analysis of new platforms. Earlier versions of API RP 2A (fifteenth edition) included a recommendation of four times the energy at SLE loading as a check for adequate ductility. While this same comparison can be made on existing platforms, it does not provide a simple basis to calculate failure probability. The energy demand on the platform from the extreme earthquake can be compared against the energy resistance as defined from the pushover analysis, however, this requires that a nonlinear time history analysis be performed and creates some inconsistencies in the basis for the definition of energy absorption.

An example of a static pushover analysis is provided in Figure 6-1. The load pattern for this platform was established using a design level response spectrum applied using a 1:1:.5 component scaling in the two horizontal and the vertical directions, respectively. The nodal

inertia forces resulting from this response spectrum analysis were then applied and scaled uniformly to the point at which system collapse was initiated.

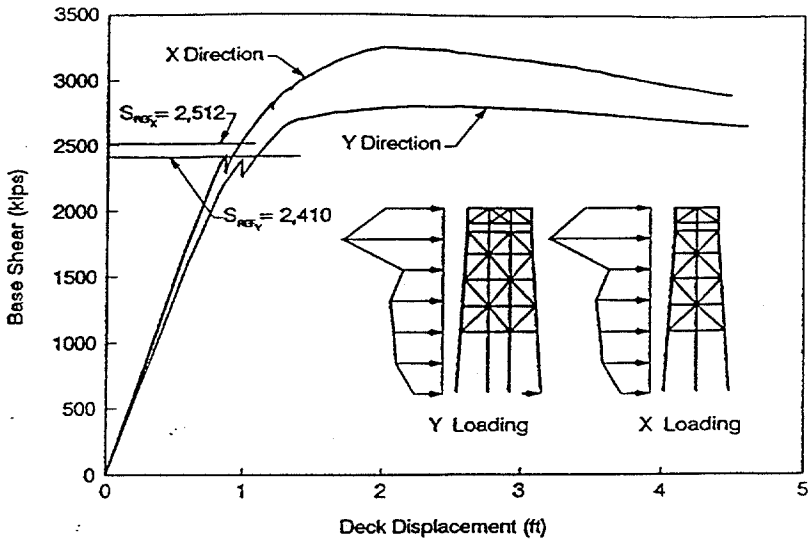

Static Pushover Analysis
Load - Deformation Response

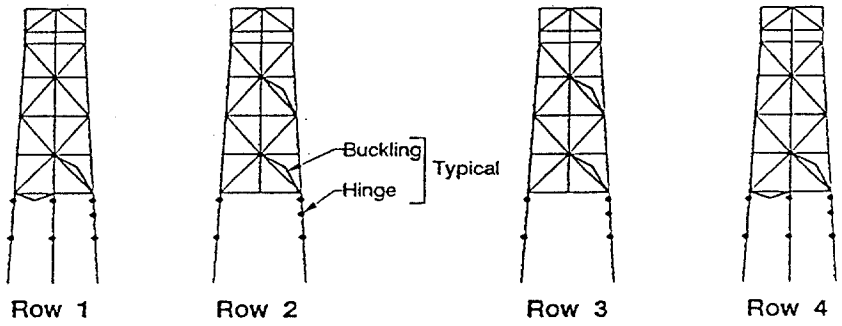

X Direction Analysis

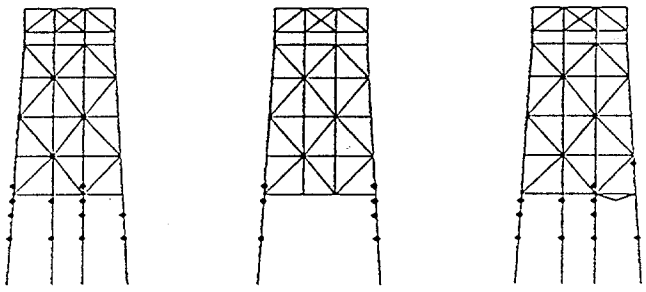

Y Direction Analysis

Static Pushover Analysis
Location of Inelastic Events

FIGURE 6-1 STATIC PUSHOVER EXAMPLE

Section 7
Time Domain Analysis

Time domain analyses are used to determine if a structure can survive a predetermined event that is characterized by a site ground motion record. These ground motion records are traditionally defined with the use of measurements from actual earthquakes that are scaled to match a site-specific uniform risk spectra. In some instances, synthetic records provide a more rigorous test of a structure owing to the greater uniformity of ground motion intensity relative to structural vibration frequency.

The strength and nonlinear load-deformation characteristics of structural elements and soils are modeled as in the static pushover analyses. In addition, time domain analyses provide bases for evaluating critical response quantities such as dynamic response, load reversal, soil and structural cyclic degradation, change in vibration characteristics due to nonlinear response, increased effective damping due to soil and structural hysteresis, explicit definition of phasing and local vibration effects.

Time history analysis methods determine the displacement and velocity of nodes in the structure (the state) at time $t + \delta t$ from those at time t. Initial conditions are specified, then the states at all future times are found by stepping forward in time, step by step. The applied loads are known during the time step δt and the mass, damping and stiffness properties of the structure are available from member properties. If the stiffness, damping and mass are constant, and the applied load is independent of the state, the new state at the end of the time step can be determined immediately from that at the start. Otherwise (e.g. yielding or buckling as a function of member stress, say) the final state depends on conditions at the start and end of the step, the process is nonlinear, and the final state at the end of the step can only be found by iteration.

There is a variety of algorithms available to step forward in time. In all of these procedures it is important to choose an appropriate time step size, relative to expected response periods, which are related to important periods of the applied loading and free vibration modes. Certain procedures are known as conditionally stable, since the time step size must be smaller than a certain critical value for a stable solution. In others, (unconditionally stable) the time step is arbitrary, the choice being only dictated by the accuracy desired, since reducing step size increases the accuracy of the solution. In linear systems of this type, the time step size should generally be of the order of 1/20th of the lowest period of the expected response. For any time step size, the response associated with shorter and shorter periods is progressively filtered out. Some computer codes are able to vary the time step size as the analysis progresses, to improve convergence characteristics of nonlinear analyses.

7.1 DEFINITION OF LOADING

Loading is defined in time history analysis from ground accelerograms which define ground acceleration as a function of time. These accelerations are integrated into the equations of motion as follows:

$$\bar{m}\ddot{x} + \bar{c}\dot{x} + \bar{k}x = -\bar{m}\ddot{x}_g(t)$$

In situations where multiple support excitation is required, such as the case when varying lateral motions are applied along the depth of the soil column, it is preferable to incorporate the variability of motions through an explicit analysis of the free field. Separate analysis of the free-field can be performed to establish displacement time histories which can be applied to the near-field, however, this is not recommended as it includes a significant numerical inaccuracy.

Specific accelerograms should be defined for each of the three orthogonal directions. Target spectra may be developed for the primary horizontal motions or specifically for horizontal and vertical motions. If a single horizontal spectrum is specified, accelerograms should be developed to match this spectrum with the appropriate relative scaling factors. The API RP2A recommends that a three dimensional analysis use a 1:1:.5 combination for the two horizontal and vertical directions, resp.

Development of explicit vertical ground spectra and the corresponding selection of accelerograms may have a significant effect on earthquake loading. Studies have shown that the frequency content of vertical and horizontal motions for most site conditions is quite different. This results in uniform hazard spectra with substantial different shape for the horizontal and vertical components. An example of such a comparison is provided in Figure 7-1. The vertical motions will tend to have relatively higher amplitude motions in the high frequency, low period, range (e.g., below .5 seconds). This is important since the vertical modes of most platforms will be within this range.

7.1.1 Scaling Methodology

The objective of selecting earthquake accelerograms is to characterize the ground motion intensity, frequency content, phasing and duration of an event based on conditions expected at the site. The target spectrum defines the amplitude of acceleration as a function of frequency. Since many records can be scaled to "match" the target spectrum, the few that are selected are chosen based on the similarity of soil and seismotectonic conditions at the platform location and the site at which the recording was taken. The API RP2A recommends that at least three sets of representative ground motion time histories be used for DLE analysis. Each record contains three orthogonal components, two horizontal and

a vertical. Each of the components of each record is scaled independently. The selection of the actual earthquake records is normally made by a seismologist, based on local site and tectonic characteristics and is not described further here.

The process of selecting representative natural records and establishing appropriate scaling factors is subjective and can be approached in several ways. API RP2A suggests the use of multiple sets of ground motions which characterize the likely envelop of ground motion intensity, frequency content, phasing and duration expected at the site. Due to the variability (i.e., peaks and valleys) inherent of natural records it is impossible to select one record which can provide an adequate test of the structure's ductility. API RP2A suggests the use of at least three set of representative earthquake ground motion time histories.

Average Velocity. This scaling method is based on achieving an average spectral velocity at the dominant frequencies (i.e., that to which the structure is most sensitive) which is equal to the target spectrum. Assuming that the target spectrum has a constant spectral velocity for periods between the dominant horizontal modes of vibration, the horizontal components should be scaled so that the average spectral velocity of each record is equal to that of the target spectrum. In addition, each record should be evaluated with respect to the fundamental vibration modes of the platform to assure that no significantly high or low spectral ordinates occur at the primary modes.

Response Spectrum Analysis. This method utilizes the results from response spectrum analysis to establish the global response (i.e., base shear and overturning) which would result from the original (i.e., unscaled) and target spectra. The ratios of base shear and overturning quantities established with each spectrum are then used to establish the amplification required to obtain similar global response. The ratios of the base shear and overturning will typically be different and thus require an averaging to obtain a single scaling factor. In this process the scaling factors are applied linearly across the complete frequency range.

7.1.2 Effect of Water Overburden on Vertical Motions

Most ground motions records which are available for use in platform time history analysis are based on terrestrial measurements of earthquakes. Under most conditions, vertical motions are dominated by P-waves which, at terrestrial sites, will tend to reflect significantly at the surface thereby increasing the amplitude of vertical motions. The amount of reflection which occurs for seafloor motions is not as significant due to the similarity in the impedance of the saturated soils and the water column. Ground motion records can be modified to assess the significance of the water column which would tend to reduce the vertical motions in the higher frequency range. The details of this modification are not

given here, as this is primarily a matter for the geotechnical or seismic engineers, rather than the design engineer.

7.2 ASSESSMENT OF COLLAPSE

Time domain analyses provide a deterministic check of a structure's ability to withstand a specified event without failure. The results of a single analysis provide a pass or fail assessment against this criteria. This is fundamentally different from pushover analyses which attempt to identify the level of loading required to fail the structure. It is likely that multiple time history analysis would be required if it is intended to define the structure's maximum resistance.

Time history analyses which assess response near failure are difficult to perform due to the numerical instabilities which occur as a result of the significant change in local and global stiffness resulting from soil softening and member failure.

There is no single criterion which can be applied to all platforms which designates structural collapse. The API recognizes global instability as the point at which deflections are large enough to cause collapse under the influence of gravity loads. An analysis can, theoretically, simulate global collapse as the structure drifts laterally with progressively larger lateral excursions, however, this is not commonly achieved.

A more practical means of evaluating the results of the time history analysis involves the examination of the individual failures which occur during the analysis and assessing the development of global and local collapse mechanisms. This process requires the analyst to identify systems with little or no remaining strength. The analyst should use the information at his disposal to locate areas which are susceptible to failure. Such information is described in the following paragraphs. In many instances this process may be performed throughout the analysis (i.e., as nonlinear events occur). If mechanisms are identified prior to the completion of the analysis it is likely that numerical instability will prevent the full completion of the analysis. If mechanisms are determined during the analysis and the full analysis is successfully completed an assessment of the residual strength of the platform should be made.

7.3 ASSESSMENT OF RESULTS

7.3.1 Global Response

The most common collapse mechanism developed within the jacket is that of loss of strength of all bents between two horizontal framing levels. This mechanism involves the failure of several diagonal braces followed by the development of plastic hinges within the legs.

Structures which conform to the API recommendations for ductile design will retain adequate load paths (e.g., X-brace framing) to prevent double hinging of the legs in all but the most extreme circumstances. Tensile failure within the X-brace is normally very ductile and limits the demand placed on the portal action of the legs. The development of collapse mechanisms for these structures requires either applied load beyond the capacity of the X-brace frame, rupture of the X-brace frame or buckling of horizontal members which carry compressive loads reacting against the tensile force of the diagonal brace that remains intact.

Specific information which is useful in the identification of a mechanism includes the following:

- An identification of each inelastic event. The location and sequence of member and, if applicable, joint failure provides a key component of the description of stability or collapse. The monitoring of the various states of a yielded member, as the load reverses, and the corresponding redistribution of load to adjacent members will describe the criticality of a particular member failure. The ability of the structure to mobilize other load paths will also become apparent with this information.

- Energy absorption as defined as a function of time. The total strain energy absorbed by the platform through the time history sequence can be used as an absolute indicator of the intensity of the earthquake. Analyses which show strain energy increasing significantly following the primary ground motions may be indicating potential instability. A comparison of the relative energy absorbed by the jacket and foundation components should show good balance. See, for example, Figure 7-3. Analyses which show a very high percentage (e.g., 75%) of the energy absorbed through the foundation may be unconservative. In these instances, it is prudent to assess the effect of upper bound soil strength with minimal degradation. Strain energy is also useful in selecting a critical earthquake record to use for subsequent iterations on an analysis.

- Deck displacements time histories. Displacements measured at some set reference point should be monitored to assess lateral drift resulting from global mechanisms. It is common to observe some lateral and vertical plastic settlement at the completion of the analysis. Continued drift observed near the completion of the analysis or the lack of decay in cyclic motion indicates the development of possible collapse mechanisms.

- Story drift. The relative displacement between horizontal framing levels can reveal the specific location of collapse mechanisms within the jacket.

7.3.2 Foundation Response

The response of the piling and surrounding soils very much controls the forces delivered to the structure. The soils adjacent to the piles (i.e., the near-field) are subject to significant degradation and can therefore contribute to global collapse.

The behavior of the near-field soils adjacent to the piles affects the response and resulting stability of the platform in several ways. The hysteretic behavior of the soils results in substantial energy absorption, which in turn increases the effective damping of the systems and tends to provide some isolation of the motions "imparted" to the platform. The plastic deformation and degradation of the soils increase the vibration periods of the primary modes of the structure, often reducing the dynamic response to the ground motions.

Platform failure modes are typically caused by the large deformation effects (i.e., p-delta) resulting from story drift and global rotations. A prominent source of platform deformation results from the plastic deformations and degradation of the soils. The dynamic resistance of the pile/soil system must be monitored closely to ensure no instability is triggered by the significant reduction in foundation resistance or plastic deformation of the foundation.

An example of a single pile load and resistance time history resulting from an extreme earthquake loading is provided in Figure 7-2 [4]. The curves shown in this figure include

- The pile head axial load
- The total soil reaction (friction and end bearing) in resistance to the pile axial load
- The instantaneous soil capacity (tensile and compressive) in resistance to pile axial load.

The third curve demonstrates the loss of axial strength due to cyclic degradation which occurs for each of the primary loading cycles for the pile. The difference between pile head axial load and total soil resistance indicates the dynamic response of the pile/soil system.

In this example, there are several cycles of loading which exceed the static strength of the pile, but the foundation has not failed. A monotonic pushover analysis would indicate pile failure at this load level. In each cycle that exceeds the existing soil resistance generates plastic deformation of the pile, load redistribution to other piles and change in load path through the jacket. Excessive plastic deformation will result in increased overturning through p-delta, which may initiate platform failure.

7.3.3 Local Vibration Effects

The use of strut elements to model the buckling behavior of the primary structural braces produces a limitation with respect to the determination of the effects of transverse local inertia forces acting along the length of the member. Typically these forces can be accounted for during a design for SLE conditions through the direct or indirect inclusion of the local vibration modes into the global response spectrum analysis.

Including local inertia forces within the design for DLE conditions can be accomplished by estimating a conservative level of peak lateral acceleration based on a modal analysis procedure, followed by the reduction in the buckling capacity of the brace which is applied throughout the time domain analysis. This method effectively assumes that the bending stresses resulting from peak local inertia forces act concurrently with the axial stresses resulting from global response. This method can lead to substantially conservative results in situations where the vibration frequencies for local and global modes are similar.

Segmented beam-column elements with distributed mass can be used to properly model both the response to global frame action (i.e., buckling) and local vibration effects (i.e., bending). The use of large deformation behavior within the segmented beam provides a fully coupled response (i.e., the current axial buckling strength is based on the current lateral deformation of the beam). In most applications it would not be practical to apply this modeling strategy to all of the braces subjected to buckling and local vibration effects.

A third solution which has been used consists of the use of parallel nonlinear strut and linear beam elements. In this analysis the linear beam is modeled to measure the deformations and bending forces resulting from the local vibration effects, but is defined so that it carries no axial load itself. The strength of the strut is not modified during the analysis to account for lateral deformations. However, the deformations and bending moments within the beam can be processed to determine the "correct" buckling capacity for the strut as a function of time. This strength history can then be compared to the actual load history to assess brace buckling. See, for instance, Figure 7-4. This comparison is then used to adjust the modeled strut capacity as required for further analysis until convergence is reached.

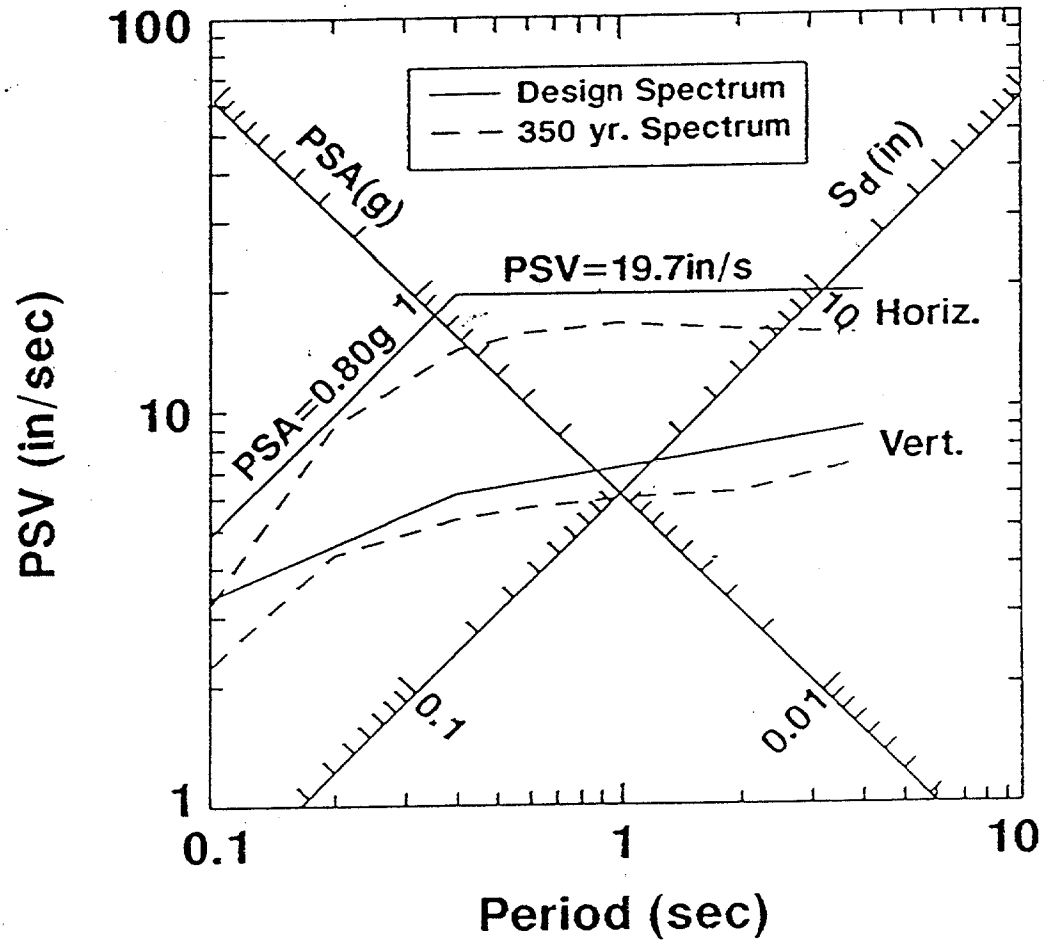

FIGURE 7-1 COMPARISON OF HORIZONTAL AND VERTICAL PSEUDO-VELOCITY RESPONSE SPECTRUM

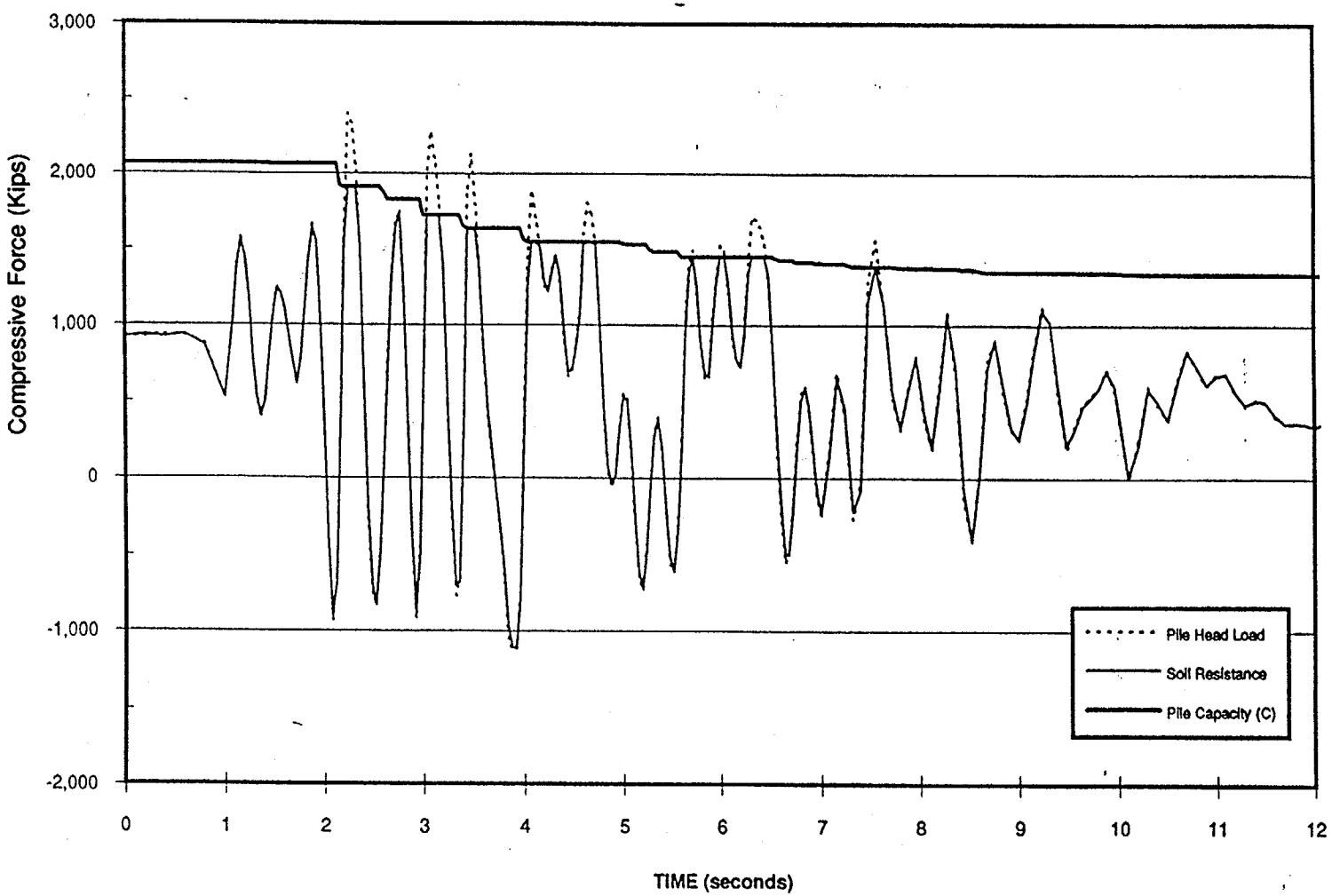

FIGURE 7-2 SINGLE PILE LOAD AND RESISTANCE TIME HISTORIES

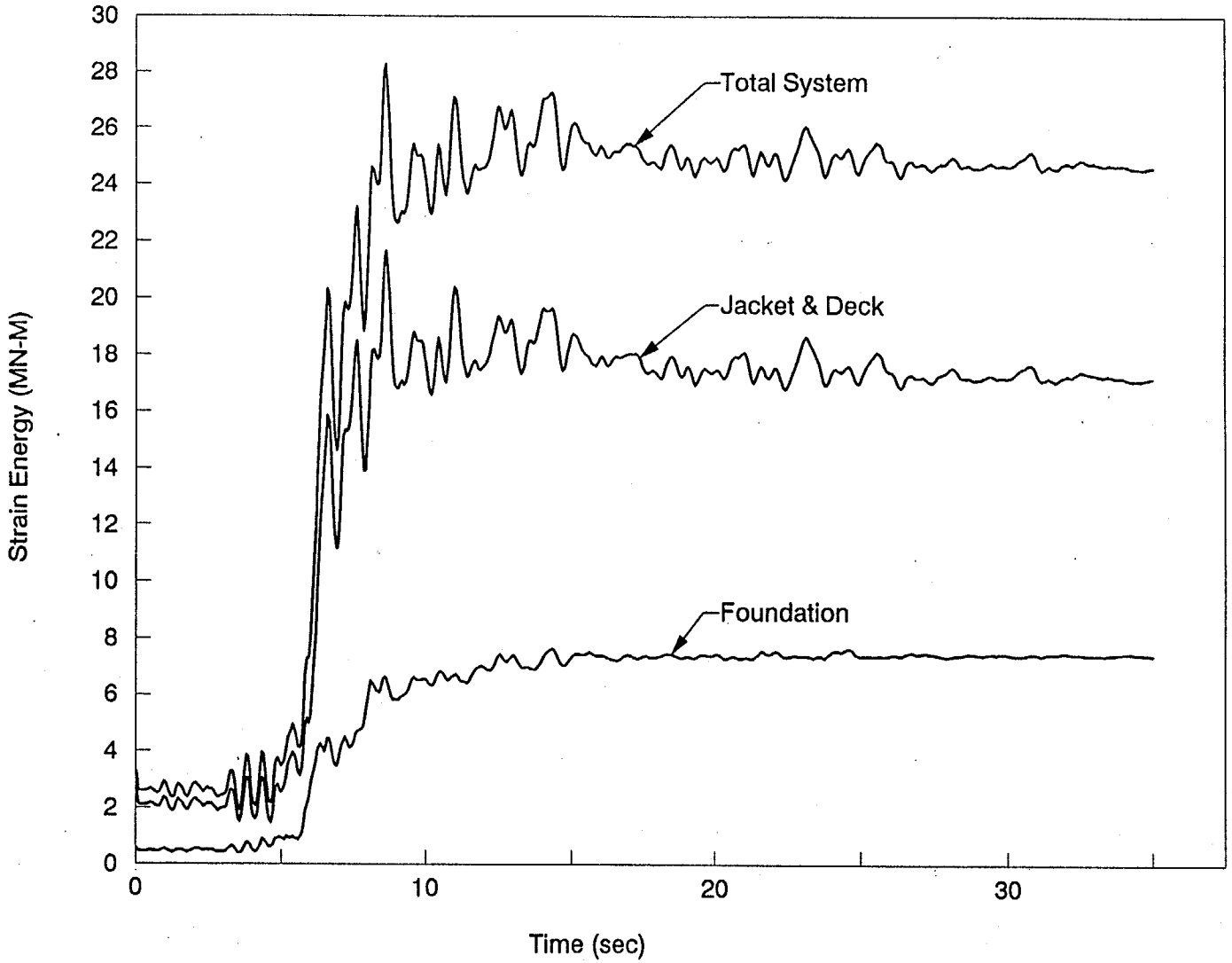

STRAIN ENERGY TIME HISTORY PLOT

FIGURE 7-3

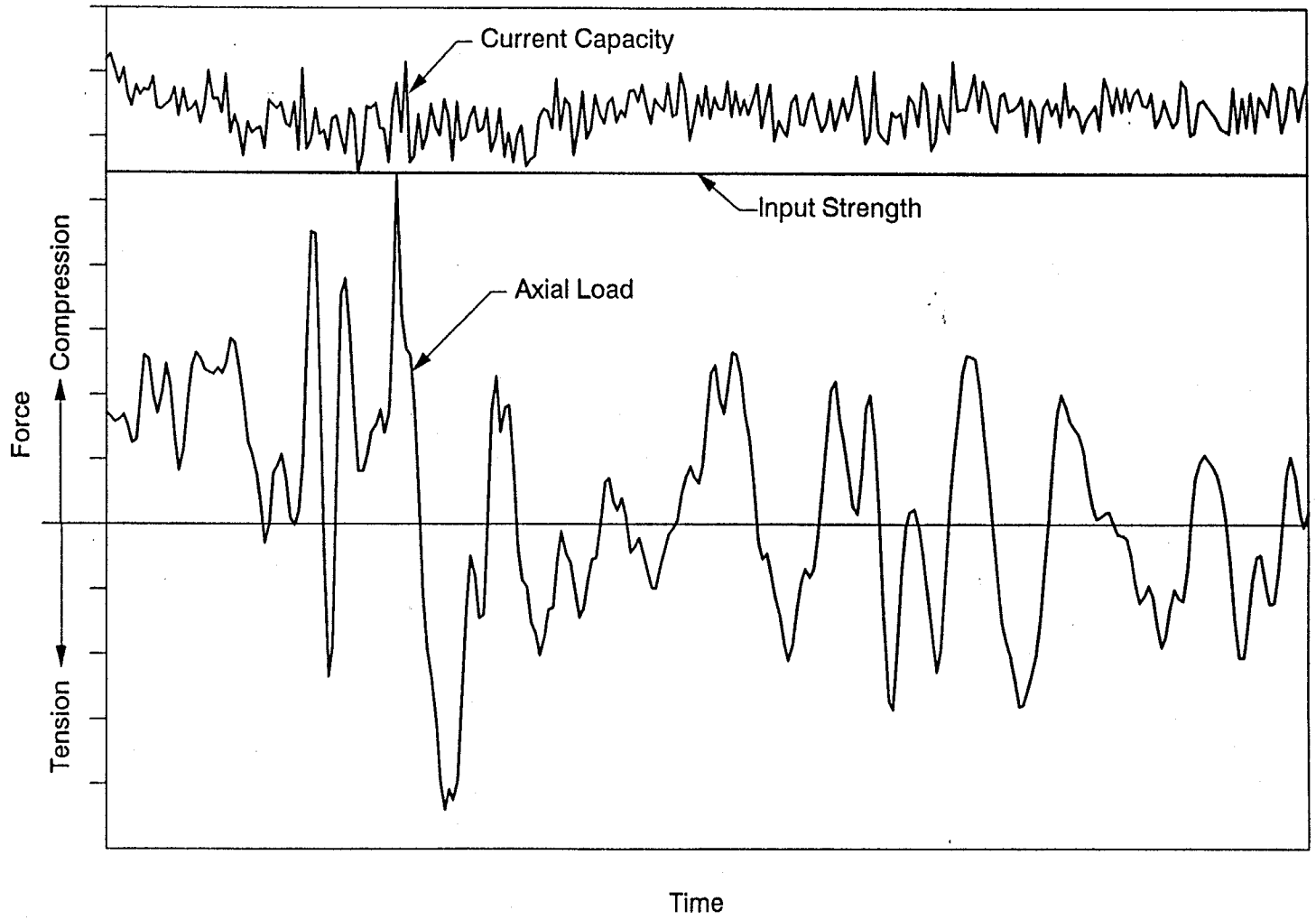

LOCAL BRACE VIBRATION RESPONSE

FIGURE 7-4

Section 8
References

The following provides a list of references by topic.

Soils

Idriss, I. M., et al. (1976), "Behavior of Soft Clays under Earthquake Loading Conditions," Paper No. OTC 2671, Proceedings of the Eighth Offshore Technology Conference, Houston, Texas.

Karlsrud, K. and Haugen, T. (1985), "Behavior of Piles in Clay Under Cyclic Axial Loading, Behavior of Offshore Structures," BOSS 85, Elsevier Science Publishers, B.V., pp. 589-600.

Kaynia, A.M., and Kausel, E. (1980), "Dynamic Behavior of Pile Groups, Conference on Numerical Methods in Offshore Piling," University of Texas, Austin, Texas, pp. 509-532.

Liam Finn, W. D., et al. (1978), "Application of Effective Stress Methods for Offshore Seismic Design in Cohesionless Seafloor Soils," Paper No. OTC 3112, Proceedings of the Tenth Offshore Technology Conference, Houston, Texas.

Matlock, H. M. and Foo, S. H. C. (1979), "Axial Analysis of Piles Using a Hysteretic and Degrading Soil Model, Numerical Methods in Offshore Piling," Institute of Civil Engineers, London.

Poulos, H.G., and Davis, E.H. (1980), Pile Foundation Analysis and Design, John Wiley & Sons.

Seed, H. B., and Idriss, I. M. (1969), "Influence of Soil Conditions on Ground Motions During Earthquakes," J. of the Soil Mechanics and Foundation Engineering Div., ASCE, V. 95, No. SM1, pp. 99-137.

Soil-Structure Interaction

Arnold, P., et al. (1977), "A Study of Soil-Pile-Structure Systems in Severe Earthquakes," Paper No. OTC 2749, Proceedings of the Ninth Offshore Technology Conference, Houston, Texas.

Kagawa, Takaaki, (1978), "Soil-Pile-Structure Interaction of Offshore Structures During an Earthquake," Paper No. OTC 3820, Proceedings of the Tenth Offshore Technology Conference, Houston, Texas.

Matlock, H., et al. (1978), "Example of Soil-Pile Coupling under Seismic Loading," Paper No. OTC 3310, Proceedings of the Tenth Offshore Technology Conference, Houston, Texas.

Matlock, H., et al. (1981), "Soil-Pile Interaction in Liquefiable Cohesionless Soils During Earthquake Loading," Proceedings, International Conference on Recent Advances in Geotechnical Earthquake Engineering and Soil Dynamics, St. Louis, Missouri, Vol. 2.

O'Neil, M.W., and Ghazzaly (1977), "Analysis of Three Dimensional Pile Groups with Nonlinear Soil Response and Pile-Soil-Pile Interaction," Paper No. OTC 2838, Proceedings of the Ninth Offshore Technology Conference, Houston, Texas.

Veletsos, A. S. and Boaz, I. B., (1979), "Effects of Soil-Structure Interaction of Seismic Response of a Steel Gravity Platform," Paper No. OTC 3404, Proceedings of the Eleventh Offshore Technology Conference, Houston, Texas.

Site Seismicity

Crouse, C. B. and Quilter, J. (1991), Seismic Hazard Analysis and Development of Design Spectra for Maui A Platform," Proceedings, Pacific Conference on Earthquake Engineering, 137-148.

Schnable, P. B., et al. (1972), "SHAKE-A Computer Program for Earthquake Response Analysis of Horizontally Layered Sites," University of California at Berkeley, Report No. EERC 72-12.

Structural Analysis and Modeling

Adelson, B. L., and Steinmetz, R. L., (1983), "A Comparison of Analytical Methods with Experimental Data for Earthquake Ductility Assessment," Paper No. 4537, Proceedings of the 15th Offshore Technology Conference, Houston, Texas.

AISC, American Institute of Steel Construction, Inc., "Manual of Steel Construction."

API (American Petroleum Institute), "Recommended Practice for Planning, Designing, and Constructing Fixed Offshore Platforms - Working Stress Design." RP2A-WSD. Twentieth Edition. July 1, 1993.

Chen, J., et al. (1989), "Measurement of Earthquake Ground Acceleration and Structural Response of a Fixed Offshore Platform," Paper No. OTC 6172, Proceedings of the 21st Offshore Technology Conference, Houston, Texas.

Craig, M. J. K. (1980), "Inelastic Earthquake Analyses of an Offshore California Platform," Paper No. OTC 3822, Proceedings of the Twelfth Offshore Technology Conference, Houston, Texas.

Craig, M. J. K. et al. (1993), "API RP 2A 20th Edition Update: Seismic Topsides Design and Assessment Guidelines," Paper No. 7156, Proceedings of the 25th Offshore Technology Conference, Houston, Texas.

Der Kiureghian, A., "A Response Spectrum Method for Random Vibrations, Report No. UCB/EERC-80/15. Earthquake Engineering Research Center, University of California, Berkeley, California, 1980.

Det norske Veritas. "Rules for the Design, Construction and Inspection of Offshore Structures, Appendix B. 1977"

Galambos, T.V., Editor, (1988), "Guide to Stability Design Criteria for Metal Structures." John Wiley & Sons.

Kamil, Hasan (1978), "Nonlinear Design of Offshore Structures under Extreme Loading Conditions," Paper No. OTC 3047, Proceedings of the Tenth Offshore Technology Conference, Houston, Texas.

Long, J. R., et al. (1989), "Seismic Evaluation of Platform Cranes," Paper No. OTC 3821, Proceedings of the 21st Offshore Technology Conference, Houston, Texas.

Mahin, S. A., et al. (1980), "Seismic Behavior of Tubular Steel Offshore Platforms," Paper No. OTC 3821, Proceedings of the Twelfth Offshore Technology Conference, Houston, Texas.

Maison, B.F., Neuss, C.F., Kasai, K., "The Comparative Performance of Seismic Response Spectrum Combination Rules in Building Analysis." Earthquake Engineering and Structural Dynamics, Vol 11, 1983, pp 623-647.

Marshall, P. W., et al. (1977), "Inelastic Dynamic Analysis of Tubular Offshore Structures," Paper No. OTC 2908, Proceedings of the Ninth Offshore Technology Conference, Houston, Texas.

Nair, D., et al. (1980), "Comparison of Spectrum and Time History Techniques in Seismic Design of Platforms," Paper No. OTC 3823, Proceedings of the Twelfth Offshore Technology Conference, Houston, Texas.

O'Rourke, M.J., and Dobry, R. (1979), "Spring and Dashpot Coefficients for Machine Foundations on Piles," Paper presented at the American Concrete Institute Meeting, Milwaukee, Wisconsin.

Penzien, J. (1975), "Seismic Analysis of Platform Structure-Foundation Systems," Paper No. OTC 3821, Proceedings of the Seventh Offshore Technology Conference, Houston, Texas.

Roarke, R.J. and Young, W.C., (1975) "Formulas for Stress and Strain". McGraw Hill Book Company.

Rosenblueth, E, Elorduy, J, "Response of Linear Systems in Certain Transient Disturbances." Proc. Fourth World Conf. on Earthquake Engineering, Santiago, Chile, 1969, A-1 pp 185-186

Singh, M. P., "Seismic Design Input for Secondary Structures," Journal of the Structural Division, ASCE, Vol 106, No ST2. Proc. Paper No. 15207, February, 1980. pp 505-517

Ueda, S. and Shiraishi, S. (1979), "Observation of Oscillation of a Deep Water Platform and the Ground During Earthquakes," Paper No. OTC 3614, Proceedings of the Eleventh Offshore Technology Conference, Houston, Texas.

Ueda, S. and Shiraishi, S. (1982), "Observation and Analysis of Earthquake Response of a Coupled Pile Offshore Platform," Paper No. OTC 4208, Proceedings of the 14th Offshore Technology Conference, Houston, Texas.

Seismic Requalification

Craig, M. J. K. et al. (1993), "Rehabilitation of a 96-Slot Platform," Paper No. 7147, Proceedings of the 25th Offshore Technology Conference, Houston, Texas.

Dolan, D. K., et al., (1992), "Seismic Reassessment of Maui A," Proceedings, 24th Annual Offshore Technology Conference, OTC 6934, Houston, Texas, May 4-7.

Dolan, D. K., et al. (1993), "Rehabilitation of a 96-Slot Platform," 25th Annual Offshore Technology Conference, OTC 7147, Houston, Texas.

Dolan, D. K. (1993), "Case Studies on Seismic Reassessment Analysis," Proceedings, International Workshop on Seismic Design and Reassessment of Offshore Structures," (To be published).

Kallaby, J., et al. (1993), "Platform Emmy Strengthening and Requalification," Paper No. OTC 7139, Proceedings of the 25th Offshore Technology Conference, Houston, Texas.

Martindale, S. G., et al. (1989), "Strength/Risk Assessment and Repair Optimization for Aging, Low-Consequence, Offshore Fixed Platforms," Paper No. OTC 5931, Proceedings of the 21st Offshore Technology Conference, Houston, Texas.

PMB Engineering Inc. (1987 through 1990), "Assessment, Inspection and Maintenance, Phases I through IV" Joint Industry Project.

Vanzini, R., et al. (1989), "Requalification of Offshore Platforms on the Basis of Inspection Results and Probabilistic Analyses," Paper No. OTC 5930, Proceedings of the 21st Offshore Technology Conference, Houston, Texas.

Visser, R. C. (1989), "A Retrospective of Platform Development in Cook Inlet, Alaska," Paper No. OTC 5929, Proceedings of the 21st Offshore Technology Conference, Houston, Texas.

Wiggins, R. A., et al. (1978), "Seismic Risk for Offshore Structures," Paper No. OTC 3113, Proceedings of the Tenth Offshore Technology Conference, Houston, Texas.

Appendix A
Seismic Risk Analysis of Jacket Structures

SEISMIC RISK ANALYSIS OF JACKET STRUCTURES

A Report to the PMB Dynamic Capacity
Joint Industry Project

C. Allin Cornell
December, 1993

1. INTRODUCTION

The objective of this report is to present a set of current methods used to evaluate seismic safety of large structures such as jacket-type offshore platforms when the specification of the safety goals is in explicit probabilistic terms. Examples of such goals are those proposed in the API-sponsored study (Ref. 1) and under current consideration by the API Requalification Committee for adoption in part or in the whole; Reference 1 suggests a limiting failure probability of 10^{-3} per year and anticipates that non-linear analyses will be used to demonstrate compliance. We shall use this number for illustration (only) in what follows where a specific number is useful for clarity.

The procedures here are predominately those designed to confirm that a safety goal is met (e.g., that the failure probability, p_f, of the structure is less than or equal to 10^{-3}), but as will be shown, they are (best) based on a procedure that estimates the p_f explicitly. Such a procedure will also be shown. It can be used when such an estimate is needed for safety confirmation and/or other for objectives such as total risk analysis (from all sources) and/or for cost-benefit analysis (Ref. 2). Equally importantly, we shall use this probability of failure estimation procedure to show the approximations, limits of application, etc., of the simpler confirmation schemes.

The focus here is on fixed-base steel jacket structures. The procedures outlined include those applied in a variety of fields (e.g., major bridges, nuclear power plants, hazardous chemical and waste facilities) where there is need for accurate seismic assessments in a probabilistic context, a context which is common to modern engineering of such facilities. Some characteristics that are common to steel jacket offshore structures, but to few of the other facilities, will be highlighted during the presentation. These include:

(1) both local and global force-deformation curves that often fall abruptly after their peaks to substantially lower levels (we'll call this "softening behavior" for short, although it should be remembered that it represents reduction in strength as well as stiffness, and that it is the negative stiffness that is uncommon in other facilities);

(2) sites that often have very soft soils and foundations that depend on deep piles, implying a soil-structure system that exhibits very "early" non-linear behavior; and

(3) first natural periods that are 1 second and longer.

In all cases the assumption is made here that the engineering response analysis (at least implicitly) considers non-linear dynamic behavior. By "implicitly" it is recognized that there are schemes that are based on "judgmental" modifications of linear dynamic analysis, on non-linear static-pushover analysis, and on (in part) analogies and experience carried over from explicit non-linear dynamic analyses of other more or less similar structural models. It is expected, however, that non-linear dynamic analyses are the "norm", and this assumption is made in most of the following discussion.

We assume that the reader is familiar with analysis practice of jackets; this is covered in depth in the companion report by Mr.

Dan Dolan. Further, we assume the reader is familiar with at least the standard output of probabilistic seismic hazard analysis (SHA), if not with the details of the conduct of such a study. Seismic hazard analysis has been reviewed recently in the 1992 MMS Workshop (Ref. 3). That output is in the form of (1) seismic hazard curves (annual probability of exceedance versus ground motion level) for ground motion measures such as peak ground acceleration (PGA) and, much more importantly, for spectral accelerations, S_a, at various frequencies, f, as well as (2) uniform hazard spectra (UHS) for various values of the annual probability of exceedance, p_e, e.g., $p_e = 1/1000$ (or, equivalently, for a mean return period = $1/p_e$). In the best modern SHA practice both median and mean estimates (as well as less-often-used fractiles) will be provided. We shall return to the question of which to use in the last section. From these results we shall be primarily interested (1) in the UHS at p_f^o (where p_f^o is the specified maximum allowable p_f, i.e., p_f^o is the safety goal, or some value closely related to it); (2) in the S_a at some reference frequency, f_o, such as the first mode frequency of the (elastic) structure and at the p_f^o level (call this S_a^o); and, to a limited degree, (3) in the slope of the S_a hazard curve near this p_f^o level.

It is convenient and common to break the seismic safety problem into three primary pieces: (1) basic seismic exposure, (2) dynamic response, and (3) capacity. Safety analysis recognizes that each piece is a complex, multidimensional problem with many issues, natural variabilities, and professional uncertainties.

Nonetheless practical analysis (be it probabilistic or deterministic) demands that the interfaces between these major elements be limited in complexity. In the limit the interface or "pinch point" between hazard and response will be just the spectral acceleration, S_a, at a reference frequency, and the interface between response and capacity will be a scalar quantity such as a member's yield force or the system's global ductility, μ. For complex non-linear multi-degree of freedom structures the necessary response input is one or more sets of ground acceleration time histories; similarly the success or failure of the system requires consideration of more than simply a comparison of the response or demand ductility, μ_R, and the capacity ductility, μ_C. Nonetheless, both practice and formal analysis normally focus on such scalar interface/pinch-point variables, as we shall do here. They permit the development of consistent procedures and deeper understanding; the discussion will, however, include practical issues beyond these scalar factors. For example, how should records be selected or constructed consistent both with a specified level, p_f^o, and with the kinds of events (magnitudes and distances) that cause the ground motions.

In the following sections we shall first outline several practical schemes for <u>confirming</u> the safety goal. Then we shall discuss how to <u>estimate</u> p_f. We shall use these results (and simplifications of them) to show both the bases and limitations of the simpler practical confirmation schemes. Finally, we shall discuss in the light of these practical and analytical results, several issues that arise in practice, such as the role of duration, choice of records, and "aleatory versus epistemic" uncertainty (i.e., randomness versus professional uncertainty). A key question that will be pursued is the role of variability in capacity and response (given the general intensity level); when can these variabilities practically be ignored, how can they be

included in the estimation and confirmation procedures (exactly or approximately). Seismic hazard analysis shows that, relatively, there is much larger variability (and uncertainty) in the basic seismic input level, justifying approximate treatment of these secondary random factors (capacity and response).

2. METHODS TO CONFIRM A SPECIFIED PROBABILISTIC SAFETY LEVEL

This section will present several practical procedures for confirming (or not) that the probability of failure, p_f, of the system is less than or equal to the specified level, p_f^o. This task can be easier than estimating the p_f directly, primarily because it can be done by making one (or more) non-linear analyses with records at a single specified level (e.g., at S_a^o, a level consistent with the "1000-year" one-second spectral acceleration). In contrast, probability estimation of a realistic non-linear system requires multiple levels of each record. While it makes sense intuitively that runs at a single level are sufficient for confirmation, it is a major purpose of Chapters 3 and 4 to confirm this and to show what adjustments might need to be made to allow for the lessor information provided by these limited runs.

2.1 Calculate and Compare p_f

The direct way to confirm that the structure's p_f is adequately low is to calculate the value and compare it with the

specified value p_f^o . Chapter 3 will demonstrate how to estimate the failure probability, both for its own sake and as basis for simpler confirmation methods. We pass first to the two most familiar confirmation methods, the uniform hazard spectrum basis and the scenario event basis.

2.2 The Uniform Hazard Spectrum Basis

2.2.1 UHS Basis: The starting point for this procedure is the entire uniform hazard spectrum (UHS) associated with the reference probability level p_f^o . (Commonly this level is the safety goal itself, e.g., 10^{-3}, and we shall generally assume that here for illustration. As we shall show below (Section 4.2), we can either lower this probability level or increase the associated UHS by a "safety or load factor" to allow for variabilities that are not explicitly addressed in this procedure.)

2.2.2 Time Histories: From here one of two methods is usually used to obtain acceleration time histories for analysis. Either,

(1) use one "artificial", "spectrum compatible" set of 3 components of accelerograms or

(2) use a suite of n real, observed record sets.

Spectrum compatible accelerograms are histories which have been modified (by one of several available methods) to produce a response spectrum within a few percent of the smooth target spectrum, here the UHS spectrum. Their advantage is that one need, in principle, run only a single non-linear analysis with this set of (three orthogonal component) accelerograms. This alternative has been used often in practice, for example in certain bridge

projects by Caltrans (California Department of Transportation), in offshore practice, and elsewhere.

The alternative involves using a suite of n sets of accelerograms (3 components per set). The records are normally selected using several criteria: (1) the spectra should be comparable to that of the UHS in shape, and, if possible, also in general level; and (2) the records, desirably, should be associated with events (magnitudes, distances, faulting type) and local geological conditions (e.g., soil depth and stiffness) comparable to those associated with the seismic threat to the site (given a ground motion of this general intensity). This last set of criteria will be discussed further below in Section 2.3. The value of n is often suggested to be in the 3 to 6 range (e.g., API RP2A, Edition 20), but our developments in Chapters 3 and 4 will permit this topic to be discussed more effectively later.

2.2.3 Scaling: Once the n sets of records are selected (under this second alternative method), a decision must be made about scaling the records. Options used include (1) conservatively scaling each record until its spectrum lies on average (over all frequencies) well above the UHS and so that most "valleys" in the spectrum lie above or near the UHS, especially in the frequency range of predominant interest; or (2) scale the records so that the (smoother) average spectrum lies near or slightly above the UHS especially in the frequency range of interest; or (3), perhaps most desirably (particularly in the context of what will follow in Chapters 3 and 4), scale each record such that each record matches the UHS at some reference frequency, f_o, to be discussed further below (Section 3.3.2). The last condition implies simply scaling all records to have S_a^o (as defined above). The second option is not completely specified; the degree of dispersion in spectral accelerations (e.g., near f_o) should, in any case, be constrained to be comparable to (or less than) that observed in nature (for

given magnitude and distance), i.e., of the order of ±60% of the mean in the 0.5 to 1 hertz range.

The first option introduces an undesirable bias. The second option (with the residual dispersion suggested) implies a double-counting; this 60% has already been explicitly included in the SHA (as what is called "attenuation law" randomness). The third option is preferred by this author for reasons that will become more clear below.

2.2.4 Comparison: As for the choice between a single spectrum-compatible record set versus multiple, real record sets, the latter would be preferable if there were no additional cost (provided the records are selected with some care). Spectrum-compatible records are, of course, virtually perfectly accurate (by design) for single degree of freedom (SDOF) linear systems; there is some evidence that they are conservative for other problems, but this issue has not yet been systematically studied to the author's knowledge. The trade-off here favors multiple records as computer power becomes cheaper, but the equation is altered somewhat in the case of "softening" structures, such as jackets, because the potentially ill-behaved nature of the numerical analysis problem (especially if the structure has many failed members and/or is near "failure") may make fully automated analysis infeasible; the manual, interactive effort may increase the analysis cost substantially for multiple records.

2.2.5 Dynamic Analyses and Decision: Given the single spectrum compatible record set or the n multiple sets, the non-linear dynamic analyses follow. In simple terms, the analyses will confirm that the structure is "safe enough" if it does not fail under this input (or suite of inputs). In practice, borderline cases will require judgment as to whether the structure failed or not. But, even if this decision is based on a simple scalar criterion, such as global ductility, there are still judgments such as whether one compares the resulting ductility response, μ_R, with the median (best estimate) capacity or with some conservative

estimate, say the 10th percentile, of the capacity in ductility terms, μ_c. (Not to mention how one judges well the best estimate and uncertainty band of such a global failure measure.) Finally, what if, of the set of n records, only some fraction lead to system non-failure? There are no written guidelines on these judgments. Based on the analysis to be presented in Chapters 3 and 4, the author suggests using a comparison between the average of the n observed responses ($\bar{\mu}_R$) and the mean capacity ($\bar{\mu}_c$). (It is proposed in what follows to make allowance elsewhere, if at all, for variability in response, given input level S_a^o, and for variability in capacity.

2.3 The Scenario Event Basis

2.3.1 Scenario Event versus UHS: This popular procedure involves defining one or more scenario events, i.e., specific magnitude-distance pairs defining design earthquakes. From each design event, representative records and/or a spectrum are developed. The advantage of this scheme is that, in contrast to the "composite" UHS spectrum, these design event spectra are consistent with identified events and therefore have "more realistic" shapes. It is also stated often that engineers "prefer" to have specific events in mind, rather than the probability-weighted results of many potential events, which the UHS represents. Further, for MDOF non-linear systems, it is correctly argued that the UHS may be conservative because it is, in effect, simultaneously driving different structural modes by different events. This is particularly evident when the site is threatened both by frequent, closer, smaller events (which may be critical for higher frequency modes or equipment) and by distant larger events (which may prove the dominant threat for longer periods). (There is some evidence this could be an issue for very long period — deep-water — structures in the Santa Barbara Channel. The conditions for the UHS conservatism to be highly important are not apparently common, however. For this "double threat" case, the

scenario event procedure works well because it can offer the option of two design events, one to reflect each case. The price paid is that one must analyze for both events and design (or confirm) with respect to both cases.

2.3.2 Basis for the Scenario Event: There are several ways used to determine what the scenario event should be, i.e., what magnitude, M, and distance, R, what rupture style, rupture length, etc. The first, most common one has been an informal, "deterministic", judgmental process based on information about fault locations, seismicity rate, fault lengths, historical seismicity, etc. Indeed, there have been many important facilities (e.g., large dams) based on this rather ill-defined Maximum Credible Earthquake (MCE) concept, without any formal probabilistic seismic hazard analysis. The two can be brought together, however, by taking the spectra and/or records that one judged to be consistent with this scenario event and re-scaling them to match the UHS in general level. Unless something like this is done there is no way to make a quantitative probability-based confirmation of the seismic safety from the deterministic MCE scenario.

The second basis for a scenario event (or events) is the informal review of the integrand from the SHA. One selects S_a^o (the spectral acceleration at the reference structural frequency associated with P_f^o the reference probability) and displays graphically the SHA integrand of the conventional SHA integral* (Ref. 4):

*More generally the analysis involves a sum of such integrals, each term in the sum representing a different seismic source, e.g., a different fault in region around the site.

$$H(S_{a_o}) = P[S_a > S_{a_o}] = \iint P[S_a > S_{a_o} | m, r] \, f_M(m) \, f_R(r) \, dmdr \qquad 2\text{-}1$$

This integrand is a function over the (m,r) plane that reflects the relative likelihood of different scenarios, (m,r), given that an event happens causing spectral acceleration greater than, say, the level S_a^o. (In general one needs also a sum of such integrands over various "sources" or faults.) A peak or mode in this surface is a logical, "most likely" scenario event: (M', R'). Usually the peak is associated with a specific source which will then establish the faulting style, etc. If there are two such modes, then a double scenario case is suggested. This procedure has been in application for over a decade: in an analysis for two Santa Barbara Channel structures, in the commercial and DOE nuclear power plant industry, and elsewhere.

The third method formalizes this last integrand basis by finding the centroid of the volume, yielding ($\bar{M}$, $\bar{R}$), which are, formally, the conditional expected (mean) magnitude and distance given an exceedance at the site of S_a^o. This procedure was apparently first proposed by McGuire (Ref. 5). The method is recommended in recent DOE criteria (Ref. 6) and in current drafts of the new Nuclear Regulatory Commission nuclear power plant criteria. Clearly the values obtained should be compared with the display of the integrand itself; in the bi-modal, double threat case, ($\bar{M}$, $\bar{R}$) may not be a rational compromise and the more informal method above may be preferred. In any case, the ground motions predicted at the site using ($\bar{M}$,$\bar{R}$) may only roughly approximate the UHS (in shape and/or level). Therefore re-scaling is again in order (see below).

2.3.3 Site Ground Motion Prediction: Given (M,R) and any other characteristics defining the scenario event, the next step is to estimate the site ground motion. The two common, and preferred (see, e.g., Ref. 7) ways to do this are: either (1) use a suite of real records in the "bin" ($M \pm \Delta M$, $R \pm \Delta R$); or (2) use conventional ground motion prediction methods (e.g., semi-empirical "attenuation laws" based on regression analysis of observed data) to find the predicted response spectrum. If the suite of records is used, it should be as large as the available catalogue of recorded ground motions permits. The (unscaled) spectra of these records are then plotted and, at each frequency, averaged and sorted to establish the mean, median, standard deviation, higher fractiles, etc., of the S_a. Either method (1) or (2) therefore yields median spectra, mean spectra, 84th percentile spectra, etc., at the site given the scenario event. One common practice (e.g., NRC and Caltrans) is the use of the 84th percentile spectrum, but this is not recommended by this author in this probabilistic safety confirmation context because the ground motion variability has already been explicitly considered in the SHA. (It is contained in the first of the three factors of the integrand of Eq. 2-1.) Therefore the median shape is recommended as current DOE criteria recommend. In either case the level should be re-scaled in this context (see below). Note that the first method (the suite of records) provides, also, a set from which a sub-set can be selected for dynamic analyses if the "n real record" option is adopted (Section 2.2.2).

2.3.4 Re-Scaling: While current practice does not often dictate this (see, however, Reference 6), it is recommended in this context that the response spectrum predicted from the scenario event be re-scaled to the UHS, at least in the frequency range of interest. Typically the UHS will not be of the same shape as the scenario spectrum, because the UHS reflects a composite of events. If there is a double scenario case, the two spectra, when re-scaled, will typically match the UHS quite well when enveloped; usually one will dominate in the higher frequencies and one in the lower. As mentioned, even if the scenario is formally derived from

the SHA integrand for S_a^o to be $(\bar{M}, \bar{R})$, experience suggests that the resulting predicted (median) response spectrum will not match the UHS in level (it is often too low). In all cases, then, the re-scaling is necessary if the resulting analysis is going to be used to confirm the seismic safety in probabilistic terms.

Now that the response spectrum for the scenario has been established, the remainder of this procedure is identical to the latter part of the previous UHS based procedure. In short, either a spectrum-compatible record or a suite of n real records is used to represent the scenario spectrum. These records are then used for the dynamic analyses and the success/failure judgment. In the double scenario case, one can either envelope the individual scenario spectra by one spectrum or carry all the way through the dynamic analyses and judgments using the two scenarios. The latter option is less conservative but more costly in dynamic analysis time.

This completes the presentation of the primary procedures and options for confirming safety. It remains to show why and when they work accurately, and how they might be adjusted to be more accurate. The reader is reminded that up to this point only the probabilistic aspects of the seismicity (as reflected in the UHS) have been explicitly considered. Lacking are the variability in the response of the real non-linear MDOF system given the value of S_a (the response of a representative linear SDOF oscillator) and the variability in capacity. These may or may not be important.

3. PRACTICAL ESTIMATION OF FAILURE PROBABILITY

3.1 General Background

This chapter will discuss the problem of directly estimating the seismic failure probability for realistic structures in computationally realistic ways. The problem is characterized by

the dominant randomness and uncertainty being in the seismic exposure portion of the problem, a situation we can exploit in several ways. It is also characterized by the major computational expense lying in the deterministic non-linear dynamic analysis of a structure of given properties subjected to a given 3-D acceleration record. This implies the need to limit the number of "calls" to such analyses. In these two respects the reliability analysis problem is not unlike the storm reliability problem for jackets, especially if one considers dynamically sensitive deep-water structures.

As discussed above, it is customary to think of arranging the problem into three basic elements: seismic exposure, dynamic response, and capacity of the system. Each element is characterized by a multitude of variables and time/space varying processes, most of which are candidates for treatment as random quantities. Practicality demands simplification; engineering accuracy and credibility pushes for more complexity. Many engineering disciplines have faced the problem. The best compromise here seems to be to limit carefully the dimension of the two interface or "pinch point" vectors that lie between the three elements. For example, between the seismic hazard and the response analysis one could consider carrying a random vector of quantities such as the general intensity level (e.g., S_a^o), the shape of the response spectrum, the duration*, and even the magnitude and distance of the "causative" event (because these influence the properties of the ground motions the structure experiences). The more such variables that are carried into the response analysis, the more time history response analyses need be run to reflect the effects of these different variables at their different combinations of levels. The answer to the difficulty lies in the

*Keeping these first three factors is directly analogous to characterizing a design sea state by level (H_s), spectral shape (T_p), and duration.

combination of (1) eliminating as explicit variables those that do not vary much (conditionally on the critical variables), (2) eliminating those variables that do not significantly effect critical response variables (or whose effect is captured sufficiently well implicitly elsewhere), and (3) randomizing over certain variables. Making these reductions in effort requires judgment based on experience with the problem at hand and/or analogous problems. In short, this problem is like any practical engineering analysis where the problem is large and the resources are limited.

In the sections below we shall describe briefly some potential tools for conducting this reliability analysis. We shall conclude by outlining a specific way of formulating the problem that reduces these pinch point variables in an effective way, producing an explicit formulation that can guide practical analysis, help consolidate usefully the results from analysis of analogous structures, and quantify the development and evaluation of still simpler procedures, such as those outlined above in Chapter 2.

3.2 Some Possible Analysis Approaches

We next address computational schemes for calculating the failure probability.

3.2.1 Conditional Monte Carlo: The application of brute force Monte Carlo is to be discouraged because we are seeking small probabilities in a problem involving large analysis costs per call. But other methods are available that exploit the characteristics of this problem. The most appropriate would appear to be conditional sampling. In its simplest form, it assumes one variable "dominates"; here it would be S_a, the spectral acceleration at a reference frequency, f_o. A suite of records (randomly sampled over variables such as M, R, duration, etc.) would be chosen, and a sample of "structures" (with sampled values of any random parameters, e.g., member capacities, soil properties, etc.) would be selected. For each record/structure pair, i=1,2,...n, a

sequence of dynamic analyses would be done at varying values of S_a until the value associated with the failure threshold was identified, S_a^o. Then the estimate of the failure probability would be

$$\hat{p}_f = \int f_{S_a}(x)\, \hat{p}_{f|s_a}(x)\, dx \qquad 3\text{-}1$$

in which $f_{S_a}(x)$ is the PDF of the reference spectral acceleration, i.e., the (absolute value of) the derivative of the hazard curve, and $\hat{p}_{f|s_a}(x)$ is the estimate of the system failure probability given that $S_a = x$. The latter function or the system "fragility curve", as it is called in the nuclear seismic PRA (probabilistic risk analysis) field, is estimated by simply n_x/n, where n_x is the number of the record/structures pairs sampled that failed at an S_a value less than or equal to x. Notice this function also plays the role of the CDF of some kind of "system capacity variable", an implicit variable that includes here the effects of both response and member capacity.

This scheme takes advantage of the availability of seismic hazard analysis results for the "exact analytical" treatment of the dominant variable. It uses Monte Carlo to deal only with the less important stochastic variables and processes ("less important" in the sense that they lead to the comparatively little dispersion in $\hat{p}_{f|s_a}$ compared to that in f_{S_a}. The scheme also uses, notice, a single "pinch point" variable, S_a, between hazard and response/capacity.

This general Monte Carlo scheme has been used successfully by De (Ref. 8) and by others to estimate the system reliability of jackets under static wave loadings. As they point out, because only a scalar variable is used to represent the load, one should use with it load characteristics representative of the near-failure levels; here that means (a sample of) spectral shapes and record durations consistent with magnitude/distance pairs likely to produce an S_a value of the failure causing level. Here that would be near where $\hat{p}_{f|s_a}(x)$ equals 0.5. In fact, FORM theory (see below) says it should be associated with the "most likely failure point", s_a^*, a value somewhat below that associated with $\hat{p}_{f|s_a}(x) = 0.5$, to a degree depending on the relative variability of S_a and the "implicit system capacity". This sample of records representative of the "failure point" S_a level, could be produced by sampling (M,R) pairs from the (normalized) integrand of the SHA integral (Eq. 2-1); this integrand is a conditional distribution on M, R given exceedance of level S_a. Since this sampling must be done before $\hat{p}_{f|s_a}(x)$ has been obtained, a reasonable value is s_a^o, the value associated with a probability near the anticipated failure probability or near the safety goal, p_f^o.

Note that because the hazard analysis is conducted numerically, we obtain from it the hazard curve, $P[S_a>x]$ at only a set of points x_1, x_2, ---. Therefore the density function $f_{s_a}(x)$ is really represented by a probability <u>mass</u> function $p_{s_a}(x_i)$

associated with the intervals or "bins" of spectral acceleration $x_i - x_{i-1}$, i=1,2,---. Extending this idea, one ambitious project (the Seismic Safety Margins Research Project conducted in the 1970s by Lawrence Livermore National Lab for the Nuclear Regulatory Commission) broadened the pinch point to two dimensions. They constructed (M,R) bins. They let SHA put weights on these bins. Then they produced multiple random samples of records, each sample representative of a different bin. Each of these samples of records was used in the dynamic analysis to construct empirical distributions on a multitude of response quantities, both structural responses and floor accelerations (input to equipment). These distributions where "convolved" with structure and equipment capacities to produce failure probabilities for each piece of equipment and each structural component (conditional always on the specific (M,R) bin being considered). These probabilities were used with the system logic (via event and fault trees) to produce (conditional) probabilities of different system responses (core damage, various release levels, etc.). Finally a sum over the bins, a two dimensional version of Eq. 3-1 in summation form, produced the probabilities of failure (e.g., of core damage). The messages are that the conditional Monte Carlo scheme need not be limited to a scalar (such as S_a), that the expensive dynamic analyses can be done with a smallish sample of records because the response variability is usually relatively small, and that these response results can be combined either by further Monte Carlo or by more formal analysis of the capacity variables.

The size, n, of the sample necessary to estimate $p_{f|s_a}(x)$ sufficiently accurately depends on the variability of S_a relative to that of this implied system capacity random variable, or in different words how flat $f_{s_a}(x)$ is in the interval where $p_{f|s_a}(x)$ rises from 0 to 1. Experience suggests sample sizes of "the order of 10" (not 100), but this will become clearer in the discussions below; it is, in effect, necessary in these circumstances to

estimate relatively well the value of x at which $p_{f|S_a}(x)$ passes through 0.5. This is in effect the median of the implicit system capacity. It is less important to estimate well the dispersion (e.g., the width of the 0.1 to 0.9 range), and still less important to estimate the tails (near 0 and near 1) of $p_{f|S_a}(x)$. Hence, small samples suffice.

It should be kept in mind that cost is dependent primarily on the number of non-linear dynamic analyses; this number is n x m, where m is the number of runs (say 3 to 5) necessary to establish the incipient failure level S_{a_i} for each record/structure sample.

The conclusion is that the number of dynamic analyses, n x m, will range from about 3 x 3 to about 8 x 5, i.e., say 10 to 50. We shall see below that experience from study of analogous systems may help to keep this number at the low end of this range.

3.2.2 First-Order Reliability Method (FORM): This method of reliability analysis deserves mention because it has been so successful in many reliability problems, including recently time-varying random process analysis of (non-linear) TLPs (Ref. 9). It is not immediately clear how we can take advantage of FORM in our seismic problem and there is little precedence for it as yet. It does help us conceptually, however, with such notions as the "most likely failure point", which helps focus attention on making sure any necessary approximations are consistent with variable levels near this point. For example, it implies that when response and capacity variability are small compared to seismic hazard variability, one should focus on mean or median estimates of response and capacity and on seismic parameters, e.g., S_a, in their tail near the probability of failure level. As response or capacity variability increases, one should be interested in levels nearer their mean plus (or minus) one standard deviation, and in

seismic hazard at levels associated with probabilities (of exceedance) somewhat larger than p_f .

3.2.3 NPP Seismic PRA Procedure: A method which has been applied in several score of seismic risk assessments for nuclear power plants in the last 15 years is based on the SHA curve for a single hazard pinch point variable (Refs. 10, 11, and 12). This variable has commonly been the PGA, because higher frequencies are of interest, but more recently it has been S_a at a single reference frequency or averaged over a frequency range of interest. The scheme uses a long sequence of random variables to express the contributions of the various uncertainties in the problem. The first is the seismic hazard related variable, S_a (or PGA). The second set is a suite of (lognormal) response-related variables, e.g., foundation effects, damping, structural stiffness, and F_μ a factor which reflects the effects of non-linear dynamic behavior. We shall come back to this important factor in the discussions below (where we call this factor $F_R(\mu)$). The final variable set reflects the capacity of structure. Each of these variables is described by (1) a "bias" factor, in effect a median value, that describes the deviation from standard design assumptions, and (2) a coefficient of variation reflecting the variability in variable*. It is very important to recognize that all these variables must be designed to operate in the same dimension, here acceleration or displacement. S_a divided by a constant $(2\pi f_o)^2$ is the peak displacement, S_d. Therefore the coefficients of variation are the same. But when non-linear relationships hold this must be considered explicitly. For example, the factor associated with damping should reflect the non-linear relationship between peak

*In fact, this coefficient of variation is strictly $\sigma_{\ell nX}$, a standard deviation of the natural log, denoted β in the PRA literature. Further it is conventional to state two β's for each variable, one reflecting (event-to-event) random variability, β_R, and one reflecting professional uncertainty (model error, etc.), β_U.

elastic displacement, S_d, and damping ratio, η, e.g., $S_d \approx c\eta^{-b}$, (with b < 1). Then if damping has a COV of x percent, the random factor reflecting the effect of damping on displacement will have a lessor COV, bx.

We shall encounter the same issue below when dealing with F_μ; it shows significantly greater non-linearity with respect to μ for softening jacket structures than for simple elastic-plastic systems or more robust shear wall or ductile moment-resisting frames.

The net result of this PRA procedure is a median "capacity" (representing the "code capacity" times the sequence of response and capacity bias factors) and a "capacity" COV (calculated as the square root of the sum of squares of the COVs of the individual factors). From this "system capacity" description, one computes the fragility curve, i.e., the conditional p_f given S_a. Then a final integration (like Eq. 3-1) produces the failure probability.

The scheme has proven practical in that properly trained, experienced engineers can estimate these bias factors and COVs for the different individual effects and combine them with available design calculations to produce relatively quickly fragility curves for the many important structures and components in a NPP. (As mentioned earlier these are inserted into a system logic model to ascertain the probabilities of severe behavior in the system.) In addition somewhat standardized values have evolved for the COVs. Given the relative variabilities, the hazard input dominates and the results are insensitive to the precise value of the net fragility COV. This scheme is also economical because non-linear dynamic analyses are <u>not</u> used. Linear elastic responses are available from the design documentation; for the ductile structures used in the plants and for the relatively conservative μ values adopted for structures (e.g., "onset of concrete damage that could cause loss of anchorage for attached equipment" at levels such as

μ=4), the F_μ values can be estimated sufficiently well from analogous results for simple elasto-plastic systems.

Unfortunately we do not have that luxury in steel jackets with their dependence on slender, buckling braces. The severe softening of these horizontal force bearing elements and the subtlety of their interaction with the non-linear foundation and the frame action of the legs and horizontals have defied easy characterization or simplified models, e.g., the lumped-mass "stick" models that are customary in, say, building analysis.

Nonetheless we can draw from this NPP PRA experience. It suggests a format for structuring the problem; it suggests the use of experience to guide the selection of COVs for the less critical response and capacity variables (rather than using simulation with sample sizes large enough to estimate them well); and it suggests that focus on a single seismic/response interface variable, S_a, is effective. Finally it shows that once developed and "de-bugged", such procedures can prove useful across an industry.

This is not to overstate the case. Even after wide experience with the method, the nuclear industry has developed a new set of "deterministic margin" procedures that can be used by a still wider set of engineers less experienced in probabilistic judgments; compared to standard "working stress" methods, these margins procedures are based on probabilistic notions, include explicit consideration of non-linear behavior, and "push" the structure beyond linear behavior and closer to its limits in order to understand better the "margin". These have evolved more recently into DOE procedures that are aimed at confirming that a probabilistic performance goal has been met (Refs. 6 and 13). These schemes are based on use of the hazard curve, linear dynamic analysis, and a set of deterministic "checking" criteria (designed by specialized committee judgments to produce a 10% chance of failure at 1.5 times the design event S_a). These judgments are based largely on experience with probabilistic fragility calculations of the type described above. It does not appear that

such a scheme is feasible for jackets because of the vagaries of their soil-brace-frame non-linear dynamics and the lessor experience with full probabilistic seismic analysis. Again, however, below we shall make use of notions developed in this NPP field, especially recent schemes to provide "correction factors" for inclusion of the secondary variabilities (response and capacity).

3.3 An Explicit Procedure

In recent years we have been working in the RMS (Reliability of Marine Structures) Program at Stanford towards a practical scheme for seismic reliability of realistic non-linear MDOF structures, especially steel jackets. The most recent publications are a theses/report by Paolo Bazzurro and me, together with two manuscripts submitted for publication to ASCE (Ref. 14 and 15). These manuscripts accompany this report and provide an in-depth support for a major portion of the procedure proposed below for practical seismic reliability assessment of steel jacket platforms. In particular one will find there the linking between the SHA and the non-linear response elements of the total problem. In what follows we shall incorporate, in addition, a probabilistic treatment of the capacity variable, C.

3.3.1 Outline of p_f Estimation:

The objective is to calculate the probability of failure as the probability that the demand exceeds the capacity. This problem can be formulated in several equivalent ways:

$$p_f = P[\mu_R \geq \mu_C] \qquad 3\text{-}2$$

$$p_f = \int P[S_a \geq F_R(\mu) \cdot S_{a_{ref}} \mid \mu_C = \mu]\, f_{\mu_C}(\mu)\, d\mu \qquad 3\text{-}3$$

$$P_f = P[S_a \geq F_R(\hat{\mu}_C) \cdot S_{a_{ref}} \cdot F_C] \qquad 3\text{-}4$$

The first equation (3-2) states that failure occurs if the system response ductility, μ_R, exceeds the capacity in ductility terms, μ_C. This implies we are using a scalar (interface) measure between response and capacity to define failure. Note that any other such measure, e.g., cumulative hysteretic energy, could also be used; ductility is our example because it is the most commonly used in practice. In the Bazzurro/Cornell references cited, we also use maximum local ductility (i.e., "most damaged member"). Other options might be "at least one mechanism forms", "a portal mechanism involving the legs forms", etc.

The second equation (3-3) uses in its "interior" the format used in the Bazzurro/Cornell papers:

$$P[S_a \geq F_R(\mu) \bullet S_{a_{ref}}] \qquad 3\text{-}5$$

This relationship, which will be discussed in detail below, provides the probability that the response ductility exceeds a specified value μ; it has, however, "transformed the problem to S_a space", a formal way of stating that the variables involved now have units spectral acceleration (or are unitless multipliers) rather than ductility (which itself happens to be unitless). Notice that Eq. 3-2, which is written directly in ductility terms, could just as easily have been written in displacement terms because both the response and capacity ductility are peak displacements (e.g., peak deck displacement) divided by some reference value, d_o, which might be associated with the onset of yielding in the steel or, more generally, the onset of significant non-linearity in the structure/foundation system. Rather than using ductility or displacement terms, Eq. 3-5 uses spectral acceleration terms.

In Eq. 3-5 S_a is, again, the seismic hazard measure in a convenient form, spectral acceleration at a reference frequency. (We shall discuss this frequency and other "reference" details further below.) $S_{a_{ref}}$ is the spectral acceleration level of the

ground motion at which the structure's peak displacement just equals the reference displacement, i.e., when $\mu_R = 1$. This reference spectral acceleration value is random; it will vary to some (usually very minor) degree from record to record (unless the structure is SDOF linear elastic up to this reference point, e.g., up to the yield displacement of the simple oscillator, when $S_{a_{ref}}$ is a deterministic quantity equal simply to $(2\pi f_o)^2 S_{d_{yield}}$).

Finally, in Eq. 3-5 $F_R(\mu)$ is the (random) multiplier or scale factor on a ground motion record, beyond level $S_{a_{ref}}$, needed to just achieve the (here) specified response ductility μ. This factor $F_R(\mu)$ (called simply F_μ in Bazzurro/Cornell) contains the effects of the significant non-linear behavior of the specific MDOF system and the particular (non-linear) damage-causing potential of a randomly chosen individual record. For example, one might expect that very long duration records would be "more effective" and hence that $F_R(\mu)$ would be smaller, i.e., it would not be necessary to scale the record so far above $S_{a_{ref}}$ in order to cause ductility μ.

We shall discuss $F_R(\mu)$ in more detail below. In short, random variables S_a and $F_R(\mu)$ in Eq. 3-5 contain the hazard information and the response information.

If we want to go further to incorporate also randomness in the capacity, we must, as Eq. 3-3 shows, (1) use Eq. 3-5 to calculate the probability that a specific μ is exceeded, (2) multiply that probability by $f_{\mu_C}(\mu)\,d\mu$, the probability that the capacity "equals" μ, and then (3) "sum" over all μ values. Thus Eq. 3-3 is a direct extension to the Bazzurro/Cornell work for incorporating capacity randomness. While explaining how to calculate p_f , Eq.

3-3 does not, however, provide the insights and computational ability we can achieve with Eq. 3-4.

This last equation has F_R evaluated at the median ductility capacity, μ_c, and introduces a random factor F_c with median 1 and coefficient of variation V_{F_c} to reflect the randomness in the ductility capacity. (As we shall see below this COV is <u>not</u>, however, directly that of the ductility capacity itself.)

The <u>combined</u> coefficient of variation (COV) of all three random variables on the right-hand-side of Eq. 3-4 is

$$V_R = COV_R \cong \sqrt{COV_{F_R}^2 + COV_{S_{a_{ref}}}^2 + COV_{F_c}^2} \qquad 3\text{-}6$$

where COV_R represents the COV of the "right-hand-side" or the (MDOF) response <u>and</u> the capacity, i.e., everything except the seismic hazard itself, which is represented by the spectral acceleration (SDOF linear response) random variable S_a and its distribution, the seismic hazard curve $H(x) = P[S_a>x]$.

To obtain a useful explicit form of the results, let us assume (as we have done in other recent seismic criteria developments, e.g., Reference 13) that the hazard curve can be approximated by the form

$$H(x) = k_0 x^{-k_1} \qquad 3\text{-}7$$

in the range of interest, which will turn out to be in the neighborhood of $H(x) = p_f$, especially somewhat "to the left" (i.e., for values of H(x) somewhat higher than p_f). Further, assume that the triplet of right-hand-side variables in Eq. 3-4 are adequately represented by lognormal distribution with median

$$\hat{R} = \hat{F}(\hat{\mu}_C) \cdot \hat{S}_{a_{ref}} \cdot 1 \qquad 3\text{-}8$$

and COV (or more precisely standard deviation of the natural log) as given in Eq. 3-6. Note $\hat{R}$ is the spectral acceleration level at which failure is "expected". Then it can be shown that

$$p_f = H(\hat{R})\, e^{1/2\,(k_1 \sigma_{lnR})^2} \cong H(\hat{R})\, e^{1/2\,(k_1 V_R)^2} \qquad 3\text{-}9$$

in which σ_{lnR} is the standard deviation of the natural log of R (the three right-hand-side variables), and V_R is its COV. (Recall for lognormal variables: $\sigma^2_{lnR} = \ln(V_R^2+1)$.) This equation, 3-9, says that the failure probability is simply the hazard function evaluated at $\hat{R}$, the median "capacity" (in S_a terms), times a factor which depends on the combined variability, V_R, in the MDOF (non-linear) response (factor) and in the ductility capacity (factor) elements, and on the local slope of the hazard curve, as measured by k_1.

The first factor, $H(\hat{R})$, is in effect the estimate of p_f "permitted" by Reference 1. It is important to understand how large the second factor might be. Table 3.1 shows a set of values of this second factor for various levels of V_R and slope k_1. The slope is also shown in terms of an equivalent and easier to estimate parameter, a_R. This slope parameter is the ratio of ground motion values (here, S_a values) necessary to change the hazard by one order of magnitude. One might find this by reading the hazard curve at 10^{-3} and at 10^{-2}, and taking the ratio of the two spectral accelerations. The relationship between a_R and k_1 is $k_1 = 1/\log a_R$. A typical value in coastal California in this probability range is $a_r = 2$, i.e., a k_1 of 3.3. Notice that for this slope parameter value the p_f is only 1.25 to 2.2 times

larger than H(R) for COVs in the 0.2 to 0.4 range. (Incidentally, Table 3.1 is calculated using the exact formula in Eq. 3-9.) Recall that the variability is in the factors F_R and F_C, and not

	Hazard Curve Slope		
	k_1	4.1	3.3	2.51
COV of R	a_R	1.75	2.0	2.5
0		1.0	1.0	1.0
0.2		1.4	1.25	1.1
0.4		3.5	2.2	1.6
0.6		13	7	3.9

Table 3.1 Values of $\exp(\frac{1}{2}k_1^2\sigma_{lnR}^2)$ the Multiplier on $H(\hat{R})$ in Eq. 3-9 for Different Values of COV of R and Hazard Curve Slope.

in response displacements or ductility capacity directly (see Section 3.3.4). Also the major response variability, namely that associated with S_a itself (i.e., the variability in the response of a reference linear SDOF system given magnitude M and distance R) is already included in the SHA, i.e., in the factor $H(\hat{R})$, via the first factor of the integrand of Eq. 2-1.

Typical values of the COV of the non-linear response factor(s) F_R (and $S_{a_{ref}}$) will be discussed below. How to estimate the COV of F_C from that in μ_C will also be discussed.

Finally, before leaving this computation section, it will be useful below to notice that the p_f in Eq. 3-9 can be associated with a particular value of the spectral acceleration, S_a, in the

hazard curve. If the factor $\exp(\frac{1}{2}k_1^2\sigma_{\ln R}^2)$ is unity, then this particular S_a value is just the median "capacity" ($\hat{R}$). If, however, the factor is larger than one (Table 3.1), then the "associated" S_a value, call it S_a*, is just

$$S_a^* = \hat{R} \cdot e^{-1/2 k_1 \sigma_{\ln R}^2} \qquad 3\text{-}10$$

	Hazard Curve Slope		
k_1	4.1	3.3	2.51
COV of R a_R	1.75	2.0	2.5
0	1.0	1.0	1.0
0.2	1.08	1.07	1.05
0.4	1.35	1.28	1.20
0.6	1.87	1.66	1.46

Table 3.2 Values of $\exp(\frac{1}{2}k_1\sigma^2_{lnR})$ the Multiplier on $\hat{R}$ in Eq. 3-10

Values of the reciprocal of this factor, i.e., values of $\exp(\frac{1}{2}k_1\sigma^2_{lnR})$, are given in Table 3.2. Notice that this result implies that one can read the hazard curve at the value of S_a^* (Eq. 3-10) to find the failure probability. This S_a^* value is, perhaps, 10 to 20% less than the median capacity, R (in spectral acceleration terms); this is the disbenefit of variability in capacity.

It further suggests that if one wants to confirm that failure probability is less than p_f^o, he needs to find the corresponding S_a value (S_a^o) from the hazard curve, and confirm that $\hat{R}$ is greater than S_a^o times $\exp(\frac{1}{2}k_1\sigma^2_{lnR})$, which is why this value is tabled in Table 3.2. Alternatively one could enter the hazard

curve at a probability less than P_f^0 by a factor $\exp(\frac{1}{2}k_1^2\sigma_{\ln R}^2)$

and find a value of S_a against which the median capacity, $\hat{R}$, would need to be compared. Clearly we can use these concepts in Chapter 4 when we suggest modifications to the methods in Chapter 2 for confirming seismic safety; the modifications correct, if necessary, for the variability of (non-linear) response and capacity factors.

3.3.2 Comments on Reference Values: The scheme above uses S_a at a reference structural frequency as the hazard/response interface variable. If the real structure were SDOF and linear up to a point of incipient yielding, then f_o would obviously be the natural frequency of this linear system, the reference displacement d_o would be the yield displacement, and the reference spectral acceleration level, $S_{a_{ref}}$, would be simply $(2\pi f_o)^2 d_o$, and $S_{a_{ref}}$ would be non-random. For realistic MDOF systems experience (Ref. 14 and 15) shows that the choices of the reference frequency and the reference displacement are not extremely critical, but common engineering judgment is useful. The objective is to choose these parameters such that there is relatively little variability (record-to-record) in the scaled S_a value (called $S_{a_{ref}}$) at which any particular record causes the reference displacement d_o. Inspection of the static pushover diagram (even for a system with soft non-linear soil) can suggest a reasonable value for d_o. If the second mode and first mode are critical, one might want to use a reference frequency between the two. See Bazzurro/Cornell for further discussion and examples. The COV of $S_{a_{ref}}$ was found there to be relatively insensitive to d_o and (with the exception of one structure/foundation system) to have a very small COV.

3.3.3 Discussion of $F_R(\mu)$: This factor captures the post-elastic behavior of the real structural system in the form of the multiplier on $S_{a_{ref}}$ necessary to scale any specific record up to where it leads to a specified non-linear response level, μ. This factor has received attention from many investigators for various structural types. In recent years at Stanford we have studied its statistical behavior. For example, for various SDOF non-linear systems (none particularly representative of softening jacket behavior), Sewell showed that $F_R(\mu)$ has mean values independent of magnitude, M, and distance, R, and a COV in the 20% range. This independence is helpful because it permits us to separate the probabilistic treatment and study of S_a (via SHA) from that of $F_R(\mu)$ (via non-linear analyses of a given structure under multiple records). The comparatively small COV implies that it takes relatively few non-linear analyses to estimate sufficiently reliably the mean or median of $F_R(\mu)$ for any given structure. For example, if the COV of $F_R(\mu)$ is 0.2, and one estimates $F_R(\mu)$ by the average of the results for only four records, the COV of the estimate is only $0.2/\sqrt{4} = 0.1$, which is effectively negligible when combined with other COVs in the problem. (In Chapter 5 we shall discuss including even this uncertainty in the analysis.) Further the randomness in $F_R(\mu)$ has been found to have some negative correlation with S_a itself (record-to-record), implying one could further reduce the effective COV of $F_R(\mu)$ to its conditional value given S_a. In fact, in Bazzurro/Cornell and in some preceding analyses we have combined the COV of $F_R(\mu)$ with that of S_a given M and R; this latter value may be 50 to 60%, implying that the COV of $F_R(\mu)$ adds very little after a square-root-of-sums-of-squares combination with the COV of S_a. We have chosen here to keep the COV of $F_R(\mu)$ separated and to treat it as shown in the equations above. (These equations are somewhat conservative given the usually observed negative correlation just mentioned.)

The computation of the mean (or median) and the COV of $F_R(\mu)$ versus μ requires multiple non-linear analyses: multiple records at

multiple scaling factors, yielding observed μ levels. Interpolation yields $F_R(\mu)$ for specified μ. But it is not necessary to study $F_R(\mu)$ in depth for every structure. We can take advantage (1) of prior studies with large sample sizes and varied simpler structural types, and (2) of prior studies on larger structures. The trends for "non-softening" non-linear SDOF systems (e.g., bi-linear and shear-wall like force-deformation diagrams) have been well studied by Sewell (Ref. 16) in 1988 and in subsequent work sponsored by NRC, CDMG, NSF, and Portland General Electric. Fig. 3.1 shows, for example, $F_R(\mu)$ vs. μ for bi-linear SDOF systems. Note the COV values. Some very preliminary, unpublished results by D. Schmucker and me are shown in Fig. 3.2 for SDOF systems with somewhat more jacket-like behavior. (The force deformation diagrams are in fact those of Marshall struts with various parameter adjustments to produce α values ranging from 1.0 to 0.1, where α is ratio of the yield force to the reduced force post-yielding ("buckling"). The figure shows average values of F_R versus μ over a suite of eight records, and the COV as well. Notice that for $\alpha = 0.5$ the $F_R(\mu)$ values are about half those for $\alpha = 1$. This is the effect of "softening". The relatively high COV values even for the "elasto-plastic" system ($\alpha = 1.0$) appear to be the result of the shallow unloading slope after buckling. Fig. 3.3 shows results from Bazzurro/Cornell for a 2-D frame model of an offshore structure, one with comparatively heavy legs (and hence high α). Note the typical COVs, 0.3 or less for μ of 4 or less. Its $F_R(\mu)$ behavior is comparable to that of an SDOF system with $\alpha = 1.0$. Fig. 3.4 shows results for a four-leg North Sea structure. Its $F_R(\mu)$ trend is more like that of SDOF system with $\alpha = 0.3$ (compare Fig. 3.2), although the COV is very small.

The robustness of $F_R(\mu)$ as an interface measure to pass from hazard, reflected in S_a, to global, MDOF, non-linear response is confirmed in studies by Sewell and by Bazzurro/Cornell, who, in studies of SDOF systems and of the 2-D MDOF system, show the virtual independence of $F_R(\mu)$ from magnitude, M, distance R, intensity level, (e.g. PGA level), and duration. These qualities make it a desirable interface parameter.

3.3.4 Discussion of the Capacity: This discussion will be limited. Measures of "failure" have been dealt with elsewhere in the JIP. Certainly little study has been made of the variability (structure-to-structure) of the ductility capacity, nor is it common to express professional uncertainty in this capacity quantitatively. Therefore we shall not put forth here any judgments as to the COV to use.

It is important to remember that in the computations above it is not ductility, per se, that enters the calculation but rather $F_R(\mu)$ and F_C, the factor (with median one) that captures the variability in the effect of variability in μ_C. For example, looking at Fig. 3.4, let us assume that this mean curve is fit sufficiently well by a power function:

$$F_R(\mu) = \mu^{b_1} \qquad 3\text{-}11$$

For example, observing that the mean of $F_R(\mu) \approx 1.8$ for $\mu \approx 3$, the value of $b_1 = \log F/\log\mu = 0.53$. We can use this result to conclude that

$$COV(F_C) \approx b_1 COV(\mu_C) \qquad 3\text{-}12$$

or 53% of the COV of μ_C in the example case.

Hence, for this example structure, if the ductility capacity had $\mu = 3$ and COV about 0.4, the value of $F_R(\mu)$ would be about 1.8, and the COV of F_R would be 0.10 (Fig. 3.4) and the COV of F_C would be $(0.43)(0.4) \approx 0.2$. The COV of $S_{a_{ref}}$ is negligible for this structure (0.03); the net COV of the "right-hand-side" is $\sqrt{0.10^2+0.20^2} = 0.22$.

4. SIMPLIFICATIONS TO THE CONFIRMATION PROCEDURES

4.1 p_f Estimation

The possible simplifications to the calculation of the failure probability follow from our discussions above. If one ignores the variability in all but the seismic hazard, then it is sufficient to simply scale several records to various levels, estimate $\hat{S}_{a_{ref}}$, estimate $\hat{F}_R(\hat{\mu}_C)$, and enter the hazard curve at a spectral acceleration equal to $\hat{S}_{a_{ref}} \cdot \hat{F}_R(\hat{\mu}_C)$ and read the failure probability.

With a rough estimate of the COV of the "right-hand-side", Eq. 3-6, one can enter Table 3.1, with this COV and with the hazard curve slope k_1 (or a_R) (near the estimated p_f) and find a "correction factor" by which to increase the p_f estimate above. Notice that a typical value might be 2.

4.2 The Uniform Hazard Spectrum and Scenario Event Bases

In these two confirmation procedures, the starting point was the reference value p_f^0, usually assumed to be the safety goal, i.e., the specified acceptable failure probability $p_{f_{spec}}$. This is a satisfactory approximation provided the product $k_1^2\sigma_{\ln R}^2$ is sufficiently small. But as shown in Chapter 3 it is, in any case,

sufficient to start the confirmation process with a reference p_f^0 equal to the safety goal times a factor $\exp[-\frac{1}{2}k_1^2\sigma_{\ln R}^2]$, e.g., a reduction factor of about 1/2 to 1/1.5 (Table 3.1) for typical values. This factor is "well within the noise" with which we can currently estimate such low probabilities of failure as 10^{-3} and can probably be ignored in most cases. For other cases the correction may be appropriate. Then, with this reduced p_f^0 value, the confirmation process will confirm (or not) that the true p_f is less than the safety goal, i.e., less than the acceptable value.

Alternatively, one can start the process with $p_f^0 = p_f$ specified as suggested in Chapter 3. But after picking out the corresponding UHS or the corresponding S_a, one should multiply these by the factor $\exp[\frac{1}{2}k_1\sigma_{\ln R}^2]$ or 1.1 to 1.2 (Table 3.2) for typical values of k_1 and $\sigma_{\ln R}^2$. Again, it is well understood that certainly hazard estimation and even, perhaps, highly non-linear response and capacity estimation are susceptible to much larger (unintentional) errors than 10 to 20%, and this increase can often be ignored. However, if the correction is made, this factor will assure that the proper safety goal has been confirmed.

It is important to note, too, that the analysis above has confirmed that a proper checking objective is the median level; note for example, in Eq. 3-4, that F_R is evaluated at the median ductility capacity μ_c. In the theoretical development, the comparison is between the spectral acceleration, S_a^o at the

reference probability P_f^0 and the "capacity" $\hat{F}_\mu(\hat{\mu}_C) \cdot \hat{S}_{a_{ref}}$. But in the confirmation practice proposed we will have an estimate instead of the (median) ductility response at S_a^o and the median ductility capacity, μ_C. But the latter pair are related to the former pair through the (implicit) function $\hat{F}_R(\mu)$. It is left to the "correction factors" discussed above to address any variability in μ (response or capacity) beyond that reflected in the hazard curve.

Note, finally, that the confirmation studies (being at only one S_a level) do not lead to an estimation of the $\hat{F}_R(\mu)$ versus μ curve or of the COV of $F_R(\hat{\mu}_C)$. But one can use the estimate of the COV of μ_R (the observed response ductilities) to estimate the COV of $F_R(\hat{\mu}_C)$ by Eq. 3-12, provided studies of analogous systems have provided an estimate of b_1.

4.3 Conclusions

The formal calculations in Chapter 3 demonstrate that the practical confirmation schemes in Chapter 2 can be used to evaluate whether a specific probabilistic safety target is met by a specific structure. These schemes compare the (median) ductility response estimated from one or more non-linear analyses at a spectral level S_a^o against the (median) ductility capacity available. We have found that in cases of relatively large COVs (in the non-linear MDOF response factor and/or in the capacity) and/or in cases of relatively steep hazard curve slopes, it is feasible to correct

either the reference probability or the spectral accelerations (by factors in Tables 3.1 or 3.2). Otherwise the confirmation schemes are unchanged; they appear to be deterministic despite dealing with the several variabilities in the problem.

5. SOME ADDITIONAL ISSUES AND COMMENTS

Some items that often are discussed in seismic safety analysis are collected here because the computational scheme above provides a good context in which to discuss them.

5.1 Duration: It is heard frequently that, beyond spectral ordinate level, duration is the next most important parameter in defining non-linear seismic behavior. Yet duration does not appear explicitly in the analysis above.

We have seen above that (linear, SDOF parameter) S_a captures the general intensity level of the earthquake motion (at a reference frequency of prime interest to the structure), and that $F_R(\mu)$ captures the "remaining" MDOF, non-linear response prediction. Duration is incorporated, implicitly in S_a to the degree that it affects linear elastic peak response. Further duration effects are implicit in $F_R(\mu)$. But as mentioned above it has been shown by Bazzurro/Cornell and by Sewell that there is virtually no systematic dependence of $F_R(\mu)$ on duration (as measured by any of the common measures), nor on magnitude and distance (which, presumably, "dictate" what the duration will be). The reasons for the insensitivity appear to have to do with the non-stationary nature of seismic ground motion.

Kennedy has shown (See Ref. 16)that the parameter that does affect $F_R(\mu)$ is the shape of the response spectrum, in particular whether the spectrum increases or decreases at frequencies somewhat less than the reference (elastic) value f_o. This shape determines whether the softening structure "encounters" stronger or weaker input intensity.

It has been found, incidentally, that cumulative damage measures such as cumulative hysteretic energy do have F_R factors that depend somewhat on duration, but there is in fact little systematic dependence of duration on magnitude and distance in the range of usual interest (i.e., there is little correlation). This is reflected in the failure of F_R for cumulative measures to depend importantly upon magnitude and distance. (Incidentally, if there is found to be a systematic dependence, it can be incorporated into the hazard analysis by using S_a/F_R rather than S_a in the SHA integral.)

These insensitivities begin to fall apart for sites at long distances from very long ruptures (very large magnitudes, $\geq$ 8, say). In this case there may be a record which is both virtually stationary and strong (above the yield-causing level) for a long interval. We have encountered this in studying effects of a potential magnitude 8 to 9 in the Cascadia subduction zone off the coast of Oregon and Washington. Alaskan sites might potentially suffer from this problem. It can be handled by maintaining the dependence of $F_R(\mu)$ on magnitude and incorporating it within the SHA, as shown by Sewell.

5.2 Professional or Epistemic Uncertainty: It is sometimes desired to keep explicitly the effects of uncertainty associated with the limited information we have about earthquakes, responses, and capacities. The analysis in Chapter 3 can be extended easily to include this. The answer is that the equation for the mean (over this uncertainty) probability failure is found (1) by replacing the "best estimate" or median hazard curve in Eq. 3-9 by the mean hazard curve, i.e., $\hat{H}(\hat{R})$ by $\overline{H}(\hat{R})$, and (2) by adding to the (random variability) $\sigma^2_{\ell nR}$ an additional uncertainty term $\sigma^2_{\ell nU}$ that reflects the epistemic (or Type II) uncertainty in the right-hand-side, R. In different words one would increase the COV of R in Eq. 3-6 by two or three additional terms reflecting this type of uncertainty in the non-linear response factor $F_R(\hat{\mu}_C)$ and the

capacity factor F_C. Remember these are uncertainties in the factors, not in the displacements or ductilities themselves; see Eq. 3-12.

An example of an epistemic uncertainty is the limited sample size (number of records) used to estimate the median of $F_R(\hat{\mu}_C)$ (or, in the confirmation procedures, the median of μ_C itself). As mentioned this uncertainty has a COV of $COV_{F_R}/\sqrt{n}$. This uncertainty can be added to the random variability giving:

$$COV_{F_{TOTAL}} = COV_{F_R}\sqrt{1+\frac{1}{n}} \qquad 5\text{-}1$$

A sample of 4 to 8 implies an increase of 11 to 6% in the COV of F_R. For the typical COVs we find for F_R (e.g., 10 to 20%), these are negligible increases.

Whether or not one wants to include epistemic uncertainty depends upon (1) how large it and the random variability are and (2) the particular decision criterion. The epistemic uncertainty may be small relative to the random variability, or together they may be negligible; as discussed above, in this case they can be ignored or, perhaps, corrected for. The decision criteria may be based (explicitly) on either the mean p_f or the median (point estimate) p_f. Any cost/benefit analysis should indeed use the mean p_f (and hence include the uncertainty, if it is significantly large). Technical criteria can and are based on medians or means, depending on the policy. The recommendations in Reference 1 are based on a median. NRC global safety goals are

explicitly means, but they may be implemented at the engineering level using median technical analyses and criteria.

5.3 Choice of Record Sets. As discussed in the previous section, the number of record sets to be used can be based, in principle, on the effect on the COV, or for any given number of record sets, the COV (and hence the confirmation criteria) can be adjusted accordingly.

As for which records, e.g., which magnitudes and distances. It is desirable to use a suite of values reflecting the SHA integrand, as described in Chapter 2. But given the discussion above about the demonstrated insensitivity of $F_R(\mu)$ to magnitude and distance, it is clear, to this author at least, that the decision is not as critical as it has been thought to be in the past.

6. REFERENCES

1. Iwan, W.D., Thiel, C.C., Housner, G.W., Cornell, C.A., "Seismic Safety Requalification of Offshore Platforms," A Report Prepared for API, May, 1992.

2. Bea, R.G. and Craig, M.J.K., "Developments in the Assessment and Requalification of Offshore Platforms," Proc. OTC, OTC 7138, Houston, TX.

3. MMS, "Seismic Design and Reassessment of Offshore Structures," Proceedings of the International Workshop, Sponsored by MMS, CSLC, CIT, USGS et al, W.D. Iwan, editor, Cal. Inst. Tech., 1992.

4. Cornell, C.A., "Engineering Seismic Risk Analysis," Bull. Seis. Soc. of Amer., Vol. 58, No. 5, October, 1968.

5. McGuire, R.K. and Shedlock, K.M., "Statistical Uncertainties in Seismic Hazard Evaluations in the United States," BSSA, Vol. 71, No. 4, pp. 1287-1308, August, 1981.

6. U. S. Dept. of Energy, "Natural Phenomena Hazards Design and Evaluation for DOE Facilities," DOE-STD-1020-92, Feb. 28, 1993 Draft, DOE, Washington, DC.

7. Nuclear Reg. Comm., "Standard Review Plan," Rev. 2, NUREG-0800, U.S. Nuclear Reg. Commission, Washington, DC, August, 1989.

8. De, R. and Cornell, C.A., "Factors in Structural System Reliability," Proc. Fourth Working Conference on Rel. and Opt. of Structural Systems, IFIP, Munich, 1992. (To be Published by Springer-Verlag, Lecture Notes in Engineering Series.)

9. Banon, H., Toro, G., Jefferys, R., De. R., "Development of Reliability-Based Global Design Equations for TLPs," Proc. 1994 Offshore Mech. and Arctic Engr. Conference, Houston, ASME, New York, NY, Feb. 1994.

10. ANS and IEEE, "PRA Procedures Guide; a Guide to the Performance of Probabilistic Risk Assessments for Nuclear Power Plants," Final Report, Vol. 2, Chapter 11, Prepared for U.S. NRC, NUREG/CR-2300, NRC, Washington, DC, 1983.

11. Cornell, C.A. and Newmark, N.M., "On the Seismic Reliability of Nuclear Power Plants, Proc. ANS Topical Meeting on Probabilistic Reactor Safety, Newport Beach, CA, May, 1978.

12. Kennedy, R.P., Cornell, C.A., Campbell, R.D., Kaplan, S., and Perla, H.F., Probabilistic Seismic Safety Study of an Existing Nuclear Power Plant, Nuclear Eng. and Design, Vol. 59, No. 2, August, 1980.

13. Bandyopadhyay, K., Cornell, C.A., Costantino, C., Kennedy, R.P., Miller, C., and Veletsos, A., Seismic Design and Evaluation Guidelines for the DOE High-Level Waste Storage Tanks and Appurtenances, Brookhaven Natl. Lab., Rept. No. BNL52361, Upton, NY, Jan., 1993.

14. Bazzurro, P. and Cornell, C.A., "Seismic Hazard Analysis for Non-Linear Structures. I: Methodology"
Submitted to ASCE for Publication, 1993.

15. Bazzurro, P. and Cornell, C.A., "Seismic Hazard Analysis for Non-Linear Structures. II: Applications"
Submitted to ASCE for Publication, 1993.

16. Sewell, R.T., "Damage Effectiveness of Earthquake Ground Motions: Characterizations Based on the Performance of Structures and Equipment," Supervisor: C.A. Cornell, Ph.D. Thesis, Dept. of Civil Engr., Stanford Univ., Jan. 1989, Stanford, CA.

[wplet2.51\SRA-jkt.doc]

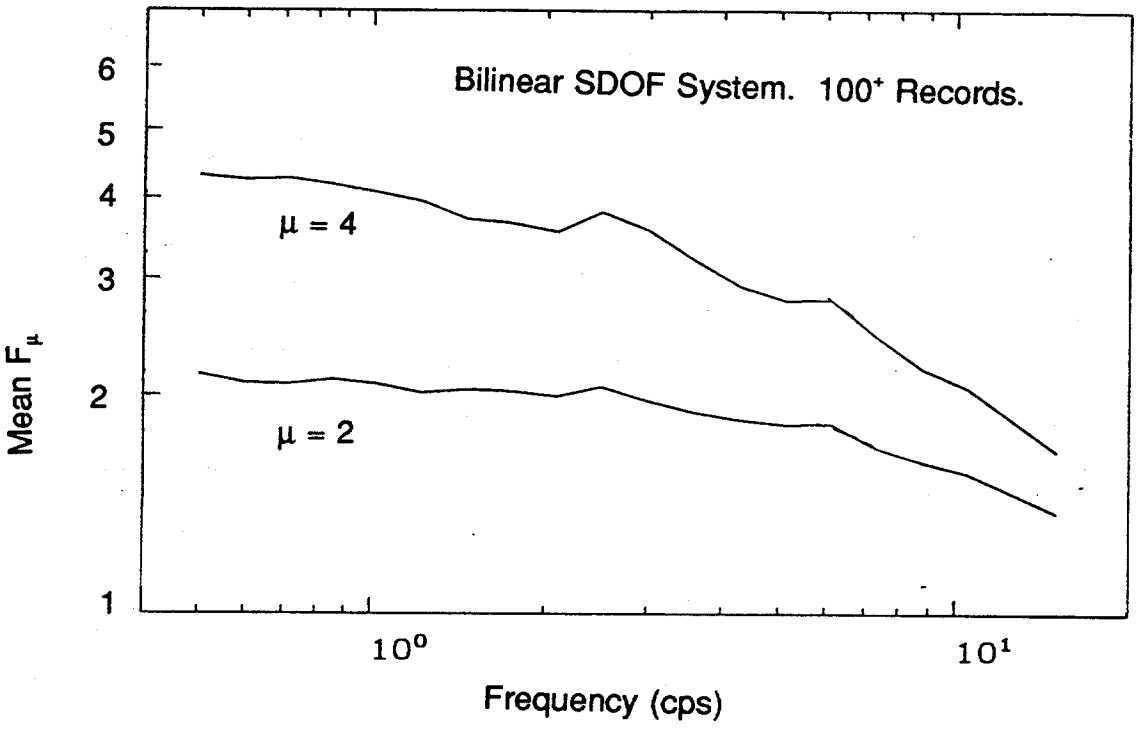

Figure 3.1 - Mean of F_μ versus Structural Frequency.

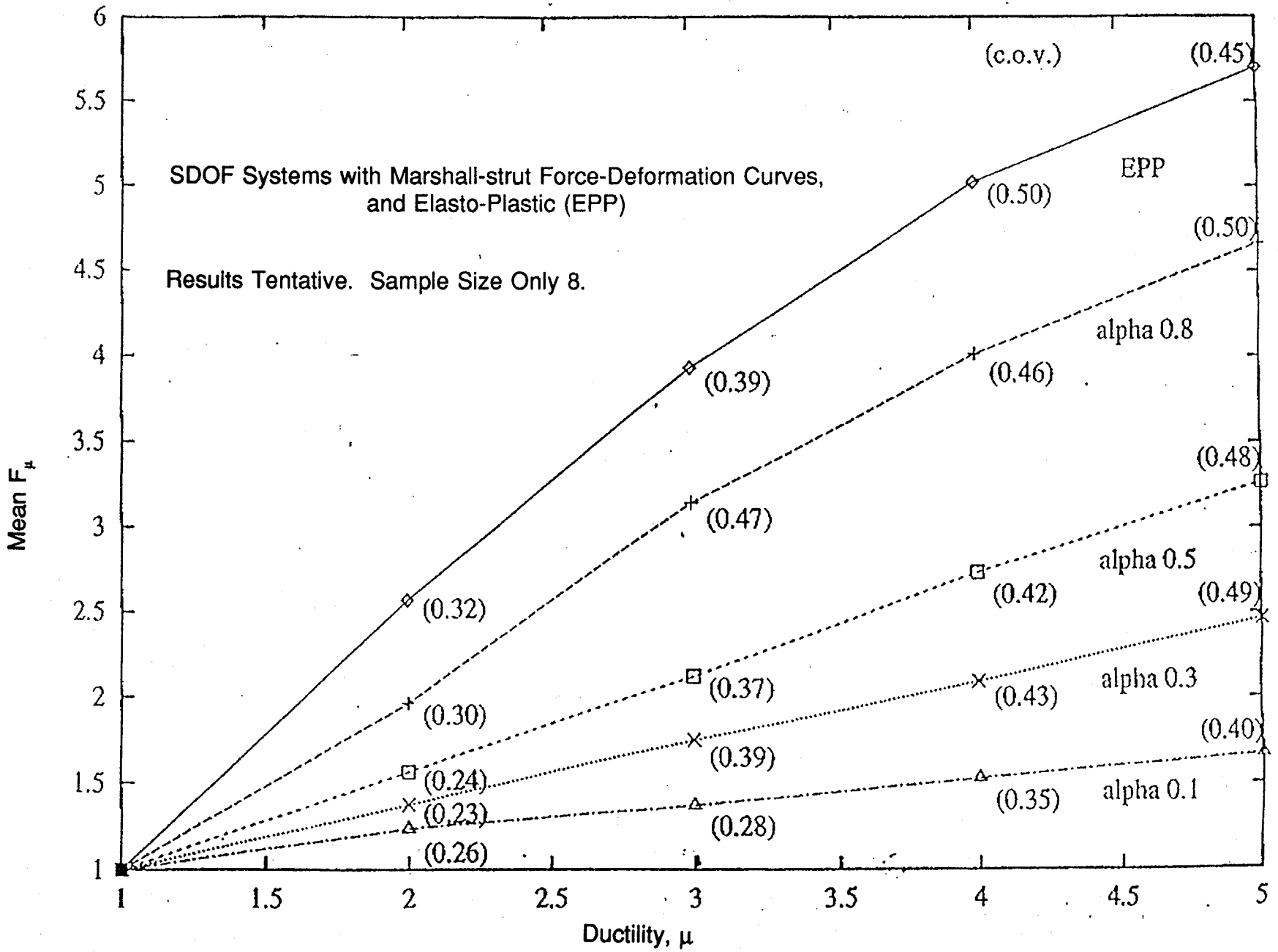

Figure 3.2 Mean F_μ versus Ductility, μ, for Various Ratios, α, of Residual Post-Buckling Strength to Buckling Strength.

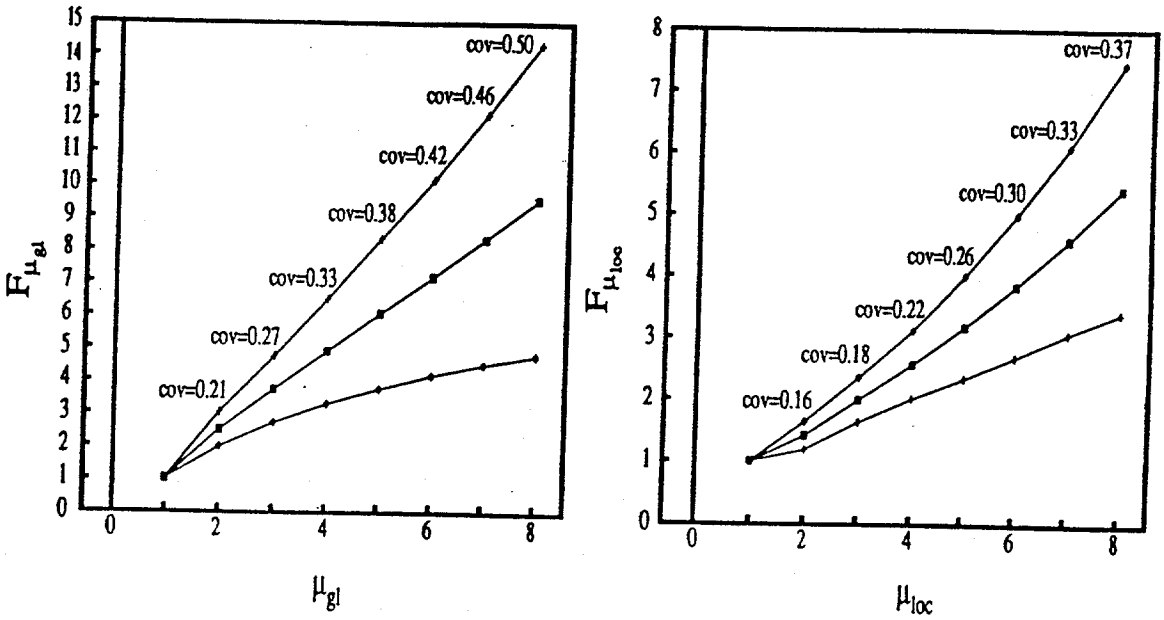

Mean and Mean ± 1 Sigma.
43 Records.

Ref: [14], Bazzurro and Cornell.

Figure 3.3 Global and Local F_μ versus Ductility, μ, for UCB Test Frame

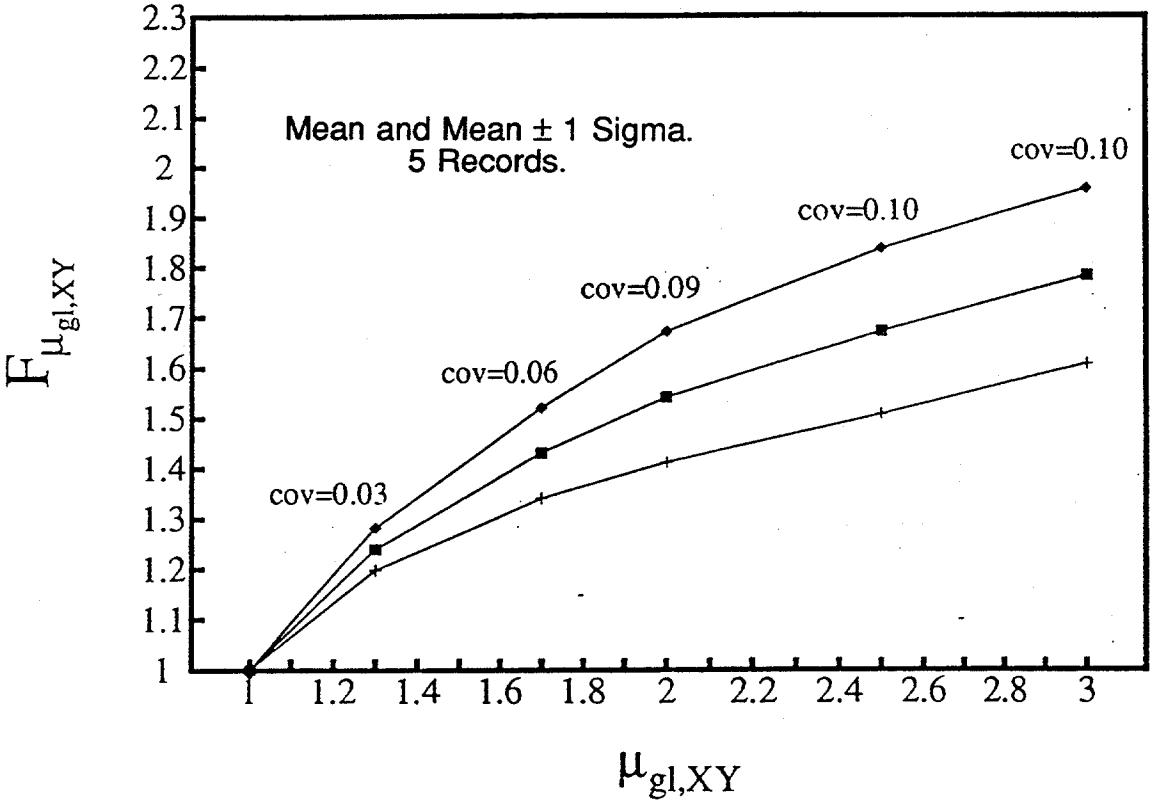

Figure 3.4 Global F_μ (i.e. Based on Deck Displacement) versus Ductility μ, for the Statpipe Riser Platform

Copies of Papers to be Published by Cornell and Bazzurro

I: Seismic Hazard Analysis of Non-Linear Structures. I: Methodology

I: Seismic Hazard Analysis of Non-Linear Structures. II: Applications

Submitted to ASCE 6/93
Minor Editorial Corrections Needed

SEISMIC HAZARD ANALYSIS OF NON-LINEAR STRUCTURES. I: METHODOLOGY

By Paolo Bazzurro [1] and C. Allin Cornell [2]

INTRODUCTION

The objective of this work is to calculate the annual probability of exceeding a specified level of a post-elastic damage in a realistic, multi-degree-of-freedom (*MDOF*), non-linear structure. This task requires coupling of conventional seismic hazard analysis (SHA) and an appropriate assessment of the sensitivity of the structure to such damage. The study of non-linear structural dynamics has a long and broad history. The objective of this paper requires that that study be done in a comparatively novel way, however, one that in fact subtly but importantly changes the perspective to one of assessing the capability of a specific ground motion record to cause a given level of post-elastic damage in the specified structure. This capability is measured here by a factor F_{DM}. This altered perspective has several important characteristics and implications.

[1]Grad. Student at Civil Eng. Dept., Stanford University, Stanford, CA 94305, on leave of absence from D'Appolonia S.p.A., Genoa, Italy

[2]Professor, Civil Eng. Dept., Stanford University, Stanford, CA 94305

First, this approach has been developed as much by ground-motion and/or attenuation analysts interested in the ground-motion/structure interface, as by structural analysts *per se.* In fact, it can be considered as the next step in the evolution of characterizing a given strong motion accelerogram by, first, traditionally, peak ground acceleration (PGA) then, later, by the peak acceleration response (S_a) of (a spectrum of) linear single-degree-of-freedom (*SDOF*) oscillators of specified properties (period and damping), and more recently by the F_{DM} factor (Kennedy *et al.*, 1984, and Sewell 1988, 1992). This factor measures the *post-elastic* damage potential of the record for a specific structural system. It will be defined carefully subsequently; it is related to the distinction between elastic and inelastic response spectra and to the R or R_w factors used in modern building and bridge codes. It is a property of each record.

In this ground motion characterization context, the behavior of F_{DM} for different non-linear SDOF systems has in recent years been studied just as PGA and S_a have, that is, (1) for dependence (in the mean) on event magnitude, M, and distance to the causative fault, R, and (2) for statistical variability event-to-event. These statistics are the attenuation laws (1) that have permitted the production of probabilistic seismic hazard analyses for PGA or S_a (i.e., a uniform hazard spectrum, UHS), and (2) that together with F_{DM} (for *SDOF* systems) have permitted recently the calculation of *non-linear* UHS (Sewell, 1988, Cornell and Sewell, 1987). These last spectra give the annual probability that a specified *SDOF* non-linear system will

suffer, say, a ductility in excess of 4. As such, they implicitly contain and display any effects such as duration, spectral shape, degree of non-stationarity, etc., that influence non-linear damage. But even non-linear UHS cannot by themselves solve probabilistic seismic safety analysis problems for realistic *MDOF* structures. Hence the next step here.

The systematic study of F_{DM} values for *SDOF* systems has revealed that as a statistical variable, F_{DM} factors have certain, somewhat unexpected, but consistently empirically observed properties that have encouraged the extension of the concepts above to realistic structures. In brief these properties are insensitivity of F_{DM} (in the mean) to M and R, and a very moderate statistical variability (relative to that of elastic spectral ordinates). Together these two properties imply (1) that only a very moderate sample size of real records (say 5) is sufficient to establish (the mean value of) F_{DM} for any given structure, and (2) that this mean is the only structure-specific value needed to calculate the probability that is the objective of this paper. It must be confirmed, of course, that these two properties continue to hold for realistic *MDOF* structures.

A primary conclusion of this work is that the important and detailed study of predicting strong ground motions, both by analysis of large numbers of empirical records and by the newer, more theoretical means (e.g., Joyner and Boore, 1988), can continue to focus on conventional elastic response spectra. Further, for realistic *MDOF* structure-specific, annual probability of damage computation, it should be sufficient for the engineer to conduct appropriate

dynamic analyses of his structure for only a few records. Together these two kinds of studies will permit calculation of the seismic hazard the structure faces in direct damage terms. This paper displays the theory and confirms the applicability. The companion paper (Bazzurro and Cornell, 1993) gives two major applications to large, highly non-linear soil-structure systems. They show that the probabilistic analysis is indeed easily implemented.

Earthquake Damage Potential

The first task consists of determining which ground-motion characteristics have a direct impact on the non-linear damage potential of an earthquake ground motion. Several studies, for example, by Riddel and Newmark (1979), Iwan (1980), Newmark and Hall (1982), Kennedy *et al.* (1984), Hadidi-Tamjed (1987), Sewell (1988), and Osteraas and Krawinkler (1990) have made valuable contributions to a better understanding of records from this perspective.

Historically, the most widely used intensity parameters have been PGA and S_a (or spectral velocity S_v). The former, a single high-frequency measure, has long been recognized to have a very poor correlation with either actual observed or theoretically computed damage in structures. The latter, S_a, is able to capture only the peak elastic response of an *SDOF* system at the frequency of vibration corresponding to the undamaged state. Damage prediction cannot be based on the linear spectrum alone, however, because

severe damage has been demonstrated to occur when structures experience one or more non-linear response cycles. When excited by a severe ground motion a structure becomes increasingly more flexible and its effective frequency of vibration decreases. For this reason, the power of the ground motion at all frequencies lower than the initial fundamental frequency of vibration is a key factor in explaining the effectiveness of a particular ground motion in causing damage (Kennedy *et al.*, 1984). If in this frequency range the acceleration response spectrum of a specified ground motion falls off sharply, then as soon as the system experiences damage and its natural frequency decreases the effectiveness of the seismic excitation drops, benefitting the structure. This phenomenon would result in a lower earthquake damage potential than a record with a spectrum that increases with decreasing frequency.

Other researchers have coupled ground-motion duration, T_D, with intensity parameters in order to improve the description of the earthquake damage potential. Intuitively, one might expect that two ground motions having, say, the same PGA but different T_D will cause different amounts of damage to the same structure. The common rationale used for substantiating this argument is that longer durations contain more cycles for damaging an already degraded structure. Sewell (1992) showed, however, that one could be led to erroneous conclusions in estimating the damage potential of a ground motion from its duration. The results of this study, based on a statistical analysis performed on *SDOF* non-linear systems by using 262 real earthquake recordings rescaled in order to yield the same peak elastic response, suggest that no

systematic and meaningful dependence has yet been found between ground-motion duration and the induced damage. (This conclusion is stronger for damage measured by peak displacement, e.g., the ductility ratio, μ, than for various cumulative damage measures.) Furthermore, the use of T_D in the SHA would be problematic in any case because it cannot be predicted with helpful accuracy. M^{c}Guire and Barnhard (1979), found that the duration of an earthquake shows a great variability (coefficient of variation of the order of 100%) which is not statistically explainable by correlation with other seismic parameters, such as M or R.

Kennedy *et al.* (1984) introduced a non-linear response factor, F_μ, to account, implicitly and empirically, for all the systematic effects of the ground motion (such as spectral shape, duration, phasing, etc.), and all aspects of the non-linear behavior of the structure (force-deformation law, $P-\Delta$ effects, etc.). The factor, F_μ, is a descriptor of the post-elastic damage of *SDOF* systems where the damage is measured in terms of the ductility ratio, μ. Consider an *SDOF* system that is brought just to incipient yield by a particular ground motion. $F_{\mu=x}$ was defined as the scale reduction factor in the structure's yield force capacity to achieve a ductility ratio equal to x. Note that $F_{\mu=1.}= 1$.

This concept was extended later by Sewell (1988) to account for damage measures, DM, different from the ductility ratio μ (for example measures of cumulative damage, such as the normalized hysteretic energy). In terms of a generic damage measure, DM, F_{DM} can also be defined in the following

alternative and equivalent form:

Definition: $F_{DM=x}$ is the amount by which an earthquake record that causes incipient yielding in a system must be scaled up to obtain a new record capable of inducing in the structure a non-linear damage level, x, associated with a specified damage measure, DM.

In the case of *SDOF* systems, the spectral reduction factor F_{DM} for $DM = \mu$ is equivalent to the well known response modification factor, R, which is defined as the ratio of the absolute maximum linear base shear to the absolute maximum non-linear base shear of a structure subjected to seismic excitation. Since this equivalence does not hold for *MDOF* systems the factor F_μ is somewhat more general and flexible than R. It follows from the previous definitions that F_{DM} assumes greater values for less damaging ground motions, and smaller values for ground motions that are particularly severe for the structure. From this perspective, F_{DM} can be considered as an *inverse measure* of the damage potential of a ground motion.

In the aforementioned study, Kennedy *et al.* showed that an empirical, analytical relationship can be found between F_μ and the average slope of the acceleration response spectrum in the range of frequencies swept by the structure during the ground shaking (the upper bound is the undamaged fundamental frequency and the lower bound is the secant-stiffness frequency of oscillation of the damaged system at the displacement corresponding to μ). Subsequent statistical analyses (Sewell, 1992) showed that calculated and analytically estimated values of F_μ for non-linear *SDOF* systems are in very

good agreement.

F_{DM} is a function both of the seismic input parameters (implicitly the magnitude, source-to-site distance, duration, etc.) and of the structural characteristics (implicitly the force-deformation law, frequencies of vibration, damping, etc.). Its functional dependence on both earthquake and structural parameters for a wide set of damage measures was studied in depth by Sewell (1988). As a random variable, F_{DM} was demonstrated (1) to be effectively statistically independent of the ground-motion parameters, such as magnitude, M, and distance, R, that come directly into play in the SHA calculations, (2) to have relatively small dispersion compared to the scatter of S_a, and (3) to have a dependence on structural frequencies that is virtually independent of the particular damage measure adopted. More recent studies have shown some magnitude dependence for unimportant, very small magnitudes (M^{c}Cann, 1989) and perhaps very large magnitudes, especially when the damage measure is a cumulative one rather than a peak displacement. The first two results outlined above are the necessary criteria, as will be clear later, to permit a simplified, direct probabilistic analysis of the annual risk of non-linear damage using an extension of the conventional SHA approach. Hence, the empirical factor F_{DM} is an effective, fully adequate measure of earthquake damage potential for non-linear *SDOF* systems.

The complex behavior of real structures, however, is not fully captured by the behavior of simple non-linear *SDOF* systems. An extension of the response factor F_{DM} to non-linear *MDOF* systems is necessary.

RESPONSE FACTOR F_{DM} FOR NON-LINEAR MDOF SYSTEMS

In the literature, several authors have investigated slightly different versions of the non-linear response factors F_{DM} for *MDOF* systems (for example, see Bertero (1986), Hwang and Hsu (1989), Inoue (1990), Nasser and Krawinkler (1991), Bazzurro and Cornell (1992)). In the following a more general version of the factor F_{DM} for real *MDOF* structures is suggested. For *MDOF* systems several F_{DM} factors can be introduced depending on the location of damage in the structure (global versus local), the type of damage (peak or cumulative), the damage measure *DM* employed (e.g., ductility ratio versus normalized hysteretic energy), and the level of damage sustained (from mild damage to rupture for local members, and from mild inelastic displacement to collapse for the global system).

Definition: for a particular non-linear *MDOF* system and a specified ground motion a particular factor $F_{DM_l=x}$ related to a damage at location l and measured by *DM*, is given by the following ratio:

$$F_{DM_l=x} = \frac{S_{a_{DM_l=x}}(f,\xi)}{S_{a_{ref}}(f,\xi)} \tag{1}$$

where:

- the subscript *ref* regards the *reference event* in the system, which is an event to be chosen (for example, incipient first yielding in the superstructure or in the soil, incipient buckling of the first brace, a specified

top-of-structure displacement in a given direction, etc.). Note, that in the conventional *SDOF* definition this event is always first yield in the structure. This definition proves insufficiently general for realistic structures. Where possible, the event should represent the transition from linear to non-linear behavior. A discussion on criteria to guide this reference event choice can be found in Bazzurro (1993). Experience to date finds that the results are insensitive to the precise choice.

- f and ξ are (approximate) estimates, respectively, of the fundamental frequency of vibration and of the damping of the system when the reference event is about to be reached. Other choices of these values might be made (see Iwan (1980) or Kennedy *et al.* (1984)) but experience suggests that the choice is not critical; the objective is to measure the strength of the ground motion in the general frequency range of interest. The "better" the choice, the less will be the COV of F_{DM} (in principle), but its value is quite low enough for this simple choice.

- $S_{a_{ref}}(f, \xi)$ is the ξ-damped spectral acceleration of the considered earthquake record for which the reference event is just reached. For three-dimensional (3D) structures this quantity should be the S_a associated with the ground-motion component applied in the horizontal direction most related to the specific choice of the adopted reference event. If the reference event cannot be clearly associated with one direction, an arithmetic mean of the spectral acceleration in the two horizontal

components can be adopted.

- $S_{a_{DM_l=x}}(f,\xi)$ is the ξ-damped spectral acceleration of the appropriately amplified ground-motion record for which the damage $DM = x$ is induced at location l. For 3D structures the same horizontal component used for the reference event case should be employed here as well.

The definition above still applies when the location l is replaced by an ensemble, $\mathbf{L} = \{l_1, \ldots, l_n\}$, of n different locations in the structure and DM is replaced by any functional form of the damage sustained in the locations considered in $\mathbf{L}$ (for example, the average or the peak damage suffered in a specified group of members, e.g., the columns). The notation will be simplified subsequently by dropping the dependence on l. Note that an alternative definition in terms of the scale reduction in the structure's yield force capacity (as discussed above in the case of *SDOF* systems) is plausible but, in general, is of no practical use for *MDOF* systems. In fact, the amount of reduction of the structure's yield force capacity is not easy to establish for all types of structures (for example, reinforced concrete buildings).

It is important to recognize that both $S_{a_{ref}}(f,\xi)$ and $S_{a_{DM=x}}(f,\xi)$ are ground-motion dependent quantities. Thus, $F_{DM=x}$ needs to be treated as a random variable. The variability of F_{DM} and its statistical dependence on earthquake parameters such as M and R have been investigated in a limited way and only for a small set of lumped-mass stick-modeled MDOF structures (Inoue, 1990). Coarsely modeled structures, neglect of foundation

effects, and the rather limited number of the applied ground-motion records, are the main shortcomings of the study. The study confirms, however, the same important statistical properties that Sewell (1988) demonstrated for *SDOF* systems: lack of important M and R dependence and limited variability record-to-record. In the present work an attempt is made to overcome the limitations: the structure model is more realistic, global and local post-elastic damage measures are examined, and a large ensemble of ground motions is used. Here the dependence of the local and global factors F_{DM} on other earthquake characteristics, such as PGA and T_D, is also examined. The structure considered for this statistical study is a jacket-type offshore platform.

F_{DM} Factors For A Jacket Offshore Platform

The structure examined is a tubular steel-braced-jacket offshore platform located in 37 meters of water in the Santa Barbara Channel in Southern California. This symmetric platform has four legs and rests on pile foundations. The piles are grouted inside the legs and extend about 64 meters into the foundation soil that is composed of two layers: a clay layer until 56.5 meters below the mudline and a sand layer underneath. The platform was designed according to API guidelines (e.g., American Petroleum Institute, 1991) to withstand wave and seismic loadings characteristic of the area in which it

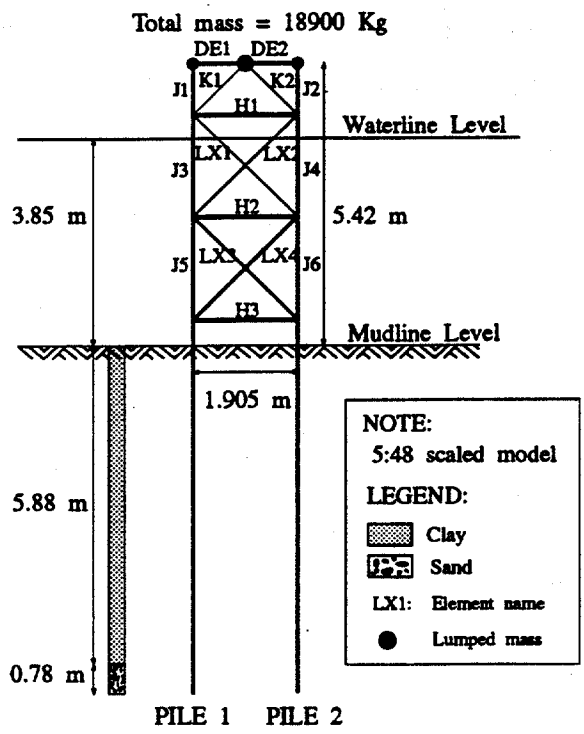

Figure 1: **UCB Frame with piles and profile of the soil foundation.**

is located. This structure is selected here because it was extensively studied by others. A two-dimensional 5:48 scale test pinned-based frame of this structure was built, thoroughly dynamically tested, and analyzed at the University of California, Berkeley (see Popov *et al.* (1985), and many relevant references cited there). This scaled structure, displayed in Figure 1 with the pile foundation, will be referred to as the "UCB Frame" in subsequent discussions. This structure and its foundation make a good test case, too, because the buckling of the braces are a particularly extreme form of non-linearity and the soil has an additional often strongly non-linear influence.

The purposes of the analyses performed on the UCB frame are multifold:

1. investigate the possible dependence of the F_{DM} factors on earthquake parameters, such as PGA, T_D and, most of all, M and R;

2. evaluate the amount of record-to-record variability in F_{DM} factors.

3. study the effect of different modeling issues (e.g., use of brace elements with different post-buckling behavior and explicit modeling of the foundations) on the F_{DM} values;

Two primary models are considered:

- the UCB Frame pinned at the base of the legs (at mudline level);

- the UCB Frame with pile a foundation (see Figure 1), which reproduces the behavior of the actual production facility prototype platform.

These 2D models, given the symmetry of the actual platform with respect to its horizontal orthogonal axes, may be considered as sufficiently representative of the actual 3D prototype for the purposes here (3D jacket models are addressed in a companion paper (Bazzurro and Cornell, 1993)). These frames are made up of tubular members; the only exceptions being the deck elements ($DE1$ and $DE2$) which are I-beams. The accurate modeling of the post-buckling behavior of the complex brace elements is critical for capturing the capacity and the realistic dynamic response of this structure. The strain-softening post-buckling behavior can be difficult to analyze numerically. To

verify the accuracy and the robustness of the F_{DM} values, two finite element computer programs with different post-buckling brace elements were used: the widely distributed program DRAIN-2D (Kanaan and Powell, 1973) and a commercial software package KARMA (ISEC Inc., 1989), considered representative of the state-of-the-art for performing non-linear dynamic analyses of offshore platforms. The post-buckling brace element available in DRAIN-2D, developed on the basis of the work done by Jain and Goel (1978), does not account for strength and stiffness degradation of the section and is only suitable for very slender members ($kL/r \geq 60$). The brace included in KARMA, instead, is a more refined element whose hysteretic post-buckling behavior can describe both slender and stocky braces; it includes strength and stiffness degradation.

Using the aforementioned computer programs, fully non-linear finite element models of the pinned UCB Frame were developed. Non-linear beam-column elements were used for modeling the legs and the piles, post-buckling elements for all the diagonal and horizontal braces (with $k = 0.5$), and linear beams for the deck. The foundation soil was described by non-linear near-field elements coupled to the piles both along the shaft and at the tip. The capacity of the soil was implemented in accordance with the API criteria (American Petroleum Institute, 1991) by specifying the lateral resistance of the soil-pile system by means of $p - y$ curves, and the axial resistance by means of $t - z$ curves. Both sets of curves were specified for virgin and degraded soil. The masses, member sizes and material properties employed are

consistent with the report UCB/EERC 82-02 (Ghanaat and Clough, 1982). The added mass and the mass of the marine growth were not included in the model. In addition to the non-linear behavior of structural members due to inelastic material properties, special attention was given to large geometric deformation effects (i.e., $P - \Delta$ effects) which may be very important for offshore structures where much of the mass is located at the deck level.

The different sets of non-linear dynamic analyses performed on the UCB Frame model made use of the seismic records included in Table 1. The horizontal component for each earthquake was randomly selected. These ground motions were chosen in order that the values of M and R were in the range of interest for well engineered structures, and the (M, R) plane was uniformly covered. The analyses were performed in the time domain using an integration time step of 0.02 seconds and a material-structural damping of 5% before yielding.

Two different non-linear response factors, F_{DM}, are considered for the UCB Frame: one to monitor the global behavior of the structure, $F_{\mu_{gl}=x}$, and another to monitor the local damage in the more critical top-panel X-braces (elements LX1 and LX2), $F_{\mu_{loc}=x}$. The damage measure adopted is the ductility ratio, μ, expressed in terms of deck lateral displacement in the global case, and in terms of axial deformation of the braces in the local case. The formal definitions of the two response factors are the following (which, note, are equivalent to the more general definition in the previous section):

- $F_{\mu_{gl}=x}$ is the amplification factor by which an earthquake motion that

Earthquake No.	Name	Station Name	Date	Comp.	R (km)	M	PGA (cm/sec^2)	T_D (sec)	Soil Type
1	Kern County, CA	Taft Lincoln school	07-21-52	EW	42	7.4	175.9	28.9	Soil
2	Imperial Valley, CA	El Centro, Sta.9	05-19-40	S90W	12	7.0	210.1	24.5	Soil
3	Kern County, CA	Caltech Athen.	07-21-52	S00E	109	7.4	-46.5	30.0	Soil
4	Lytle Creek, CA	Cal Edison, Colton	09-12-70	South	29	5.3	-40.2	10.6	Soil
5	San Fernando, CA	Palos Verdes	02-09-71	S25E	57	6.6	-40.1	55.2	Soil
6	Hollister, CA	Gilroy, Gavilan	11-28-74	S23E	10	5.2	-94.1	2.8	Soil
7	Kalapana, Hawaii	Hilo, Univ Hawaii	11-29-75	N16W	45	7.1	-169.9	56.1	Soil
8	Santa Barbara, CA	S.B. Freitas Bldg.	08-13-78	158°	10	5.7	284.7	7.7	Soil
9	Tabas, Iran	Tabas	09-16-78	Long	3	7.7	795.8	16.3	Soil
10	Imperial Valley, CA	El Centro, Arr.5	10-15-79	230°	4	6.5	367.2	9.5	Soil
11	Imp.Vly, Aftershock	El Centro, Arr.4	10-15-79	140°	11	5.0	229.6	6.4	Soil
12	Livermore, CA	Livermore, Hosp.	01-27-80	038°	15	5.5	60.6	10.7	Soil
13	Parkfield, CA	Taft Lincoln school	06-27-66	S69E	105	6.1	11.2	33.4	Soil
14	Borrego Mountain,CA	San Onofre Plant	04-09-68	N33E	122	6.6	40.0	31.3	Rock
15	Mt. Hamilton, CA	Holl. City Hall	04-24-84	271°	59	6.2	71.1	25.1	Soil
16	Imperial Valley, CA	Brawley Muni Arpt.	10-15-79	225°	9	6.5	162.2	15.0	Soil
17	Imperial Valley, CA	El Centro, Arr.10	10-15-79	050°	9	6.5	-168.2	13.1	Soil
18	San Fernando, CA	Fort Tejon, CA	02-09-71	N00E	64	6.6	-24.7	8.4	Soil
19	San Fernando, CA	Port Hueneme	02-09-71	S90W	62	6.6	-25.2	51.0	Soil
20	San Fernando, CA	Long Beach, CA	02-09-71	N21W	61	6.6	-28.4	63.8	Soil
21	San Fernando, CA	Oso Pump Plant	02-09-71	N00E	47	6.6	-85.2	7.7	Soil
22	San Fernando, CA	Tehachapi Pump Pl.	02-09-71	S00W	66	6.6	-20.8	10.4	Rock
23	Borrego Mountain,CA	El Centro, Sta.9	04-09-68	S00W	45	6.6	-127.8	49.3	Soil
24	Parkfield, CA	San Luis Obispo	06-27-66	S54W	64	6.1	11.4	20.4	Rock
25	Parkfield, CA	Temblor, CA, No.2	06-27-66	S25W	61	6.1	-340.8	4.5	Rock
26	Sitka, Alaska	Sitka Observatory	07-30-72	NORTH	45	7.7	-70.1	26.9	Rock
27	Lima, Perù	Inst. Geofisico	10-03-74	N08E	38	7.6	179.0	48.4	Soil
28	Lima, Perù	Dr. Huaco Home	10-03-74	LONG	40	7.6	192.4	44.6	Soil
29	Kern County, CA	S.Barbara Courthse	07-21-52	S48E	85	7.4	128.6	33.7	Soil
30	Lytle Creek, CA	Cedar Springs	09-12-70	S05W	13	5.3	59.4	12.4	Rock
31	Kalapana, Hawaii	Punaluu, Hawaii	11-29-75	N16W	27	7.1	-169.9	30.9	Soil
32	Long Beach, CA	L.A. Subway Trml.	03-11-33	N51W	28	6.2	95.6	24.0	Rock
33	Imp.Vly, Aftershock	Brawley Muni Arpt.	10-15-79	225°	25	5.0	-35.2	7.4	Soil
34	Santa Barbara, CA	S.Barbara Courthse	08-13-78	090°	3	5.1	-284.1	10.0	Soil
35	Lytle Creek, CA	Park Dr.,Wrightwood	09-12-70	S65E	19	5.3	139.0	3.2	Soil
36	Hollister, CA	San Juan Bautista	11-28-74	S57E	8	5.2	112.1	8.1	Soil
37	Loma Prieta, CA	Fremont	10-18-89	0°	55	7.0	-117.7	18.4	Soil
38	Loma Prieta, CA	Monterey	10-18-89	0°	49	7.0	68.52	13.3	Rock
39	Loma Prieta, CA	Santa Cruz	10-18-89	0°	16	7.0	-433.1	9.5	Rock
40	Loma Prieta, CA	Yerba Buena Island	10-18-89	90°	95	7.0	-65.8	8.3	Rock
41	Loma Prieta, CA	Palo Alto Hospital	10-18-89	212°	47	7.0	378.2	13.1	Soil
42	Loma Prieta, CA	Stanford, SLAC	10-18-89	360°	51	7.0	282.1	11.6	Rock
43	Loma Prieta, CA	SFO Airport	10-18-89	90°	79	7.0	-325.8	11.3	Soil

Table 1: **Ground-motion records used for the analyses performed on the UCB Frame. Note that T_D is the duration that brackets 90% of the ground-motion energy (Trifunac and Brady, 1975).**

causes the first incipient inelastic event in the superstructure (found to be always the buckling of either LX1 or LX2 in the top panel) has to be scaled up in order that this amplified ground motion will induce a deck lateral displacement x times larger than the lateral displacement observed when the reference buckling event occurs;

- $F_{\mu_{loc}=x}$ is defined as the amplification factor by which an earthquake that causes the first incipient inelastic event in the superstructure has to be amplified in order that this rescaled ground motion will induce a damage $\mu_{loc} = x$ in *at least* one of the two braces, LX1 or LX2.

Other local-damage-related response factors are not considered because the damage experienced by the other elements is consistently lower than the damage in the top-panel X-braces. To compute the non-linear response factors for a range of μ values, five analyses were performed for each record scaled to successively higher values. The values of $F_{\mu_{gl}}$ and $F_{\mu_{loc}}$ for any desired damage level were computed by linear interpolation.

To improve the understanding of the overall behavior of the structure during the ground shaking (in particular of the results regarding the global response factor, $F_{\mu_{gl}}$), a pseudo-static pushover analysis was carried out on both UCB Frame models by using KARMA. The pushover analysis was conducted by imposing a scaled load pattern representative of the seismic inertial loads and successively computing the corresponding equilibrium displacement configuration of the system. From the results for the pinned model

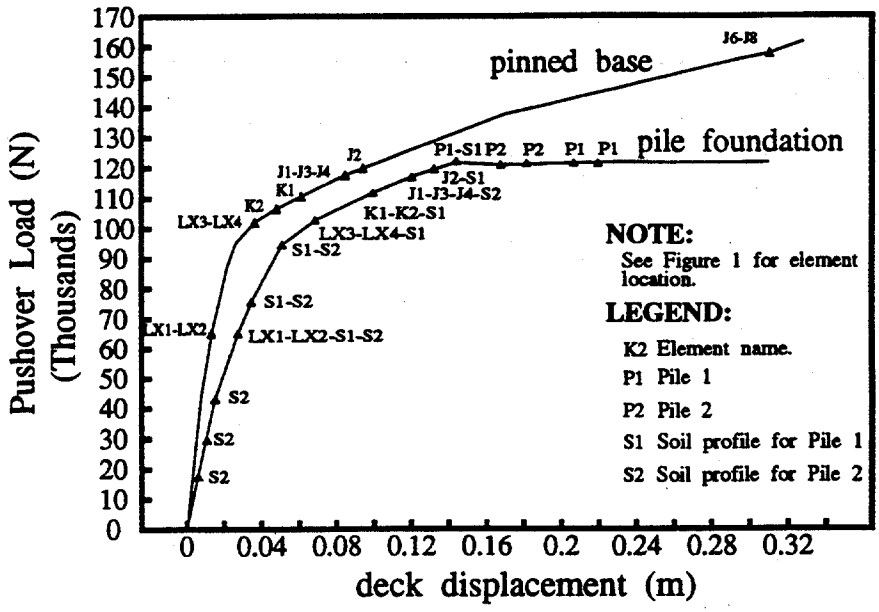

Figure 2: **Lateral pseudo-static pushover load versus deck displacement for the UCB Frame. The pattern of inelastic events leading to failure is marked on the curves.**

(Figure 2), it appears that the scaled frame responds elastically up to deck displacements of about 1.2 centimeters, at which point the X-braces in the top panel enter the post-elastic range (brace LX1 buckles and, then, LX2 yields). At deck displacements of roughly 8 centimeters, yielding begins in the legs, the structure becomes less rigid and deteriorates towards failure as a mechanism. In the pinned case, for a deck displacement on the order of 10 centimeters ($\mu_{gl} \approx 8$), the structure has already accumulated a significant amount of damage both in the vertical X- and K-braces and in the legs, and its behavior has deteriorated severely even though its total capacity (at least with regard to pseudo-static loading) has not yet been mobilized.

From Figure 2, it follows that the explicit modeling of the foundations has reduced the ultimate capacity of the structure by approximately 25%. A failure mechanism in the pile-foundation system brings the structure to collapse without allowing the full portal capacity of the legs to be achieved. The beginning of the plateau in the force-displacement curve is reached for deck displacements of approximately 14 centimeters (in the scaled frame), while the buckling of the upper-panel braces LX1 or LX2, occurs at approximately 2.5 centimeters (a value decreased to about 2 centimeters in the more refined non-linear dynamic analyses). Hence, in the case with a pile foundation, a global ductility ratio of 5 to 6 can be associated with very severe damage if not collapse. Note that this form of load-controlled static pushover analysis is not able to capture the global unloading episodes that might accompany a displacement controlled analysis.

Robustness of F_{DM} to the Use of Different Brace Elements

The effect of the use of brace elements with different post-buckling behavior on the response factors $F_{\mu_{gl}}$ and $F_{\mu_{loc}}$ for the pinned version of the UCB Frame is examined first. The values of $F_{\mu_{gl}=4}$ and $F_{\mu_{loc}=4}$ obtained by using DRAIN-2D and KARMA are presented in Figure 3 as a function of the magnitude of the first 15 ground motions used in Table 1. Note that a pair of values corresponding to DRAIN-2D and KARMA for the same ground motion are

vertically aligned. The values obtained for $F_{\mu_{gl}}$ and $F_{\mu_{loc}}$ by using the two different models are seen to be quite similar, with few exceptions. These figures suggest that in both the global and the local cases the values of the response factors coming from the KARMA model tend to be smaller than the corresponding ones obtained from the DRAIN-2D model. Thus, the structure modeled by KARMA is, on average, more susceptible to damage than the structure modeled by DRAIN-2D. This is due to the degrading nature of the post-buckling brace elements in the KARMA model which leads to larger deformations. This effect leads, on average, to larger displacements of the deck and, hence, to smaller values of the non-linear factors, F_{μ}.

The DRAIN-2D/KARMA differences on a record-by-record basis yield little difference in the critical statistics, such as average values (see Figure 4) and coefficient of variation (COV). The COV of $F_{\mu_{gl}=4}$ is, for example, equal to 0.20 in the case of DRAIN-2D and to 0.32 in the case of KARMA. In the local damage case, a COV of $F_{\mu_{loc}=4}$ equal to 0.11 by means of DRAIN-2D and to 0.15 by means of KARMA were obtained. The COV's of $F_{\mu_{gl}}$ and $F_{\mu_{loc}}$ will be addressed further below.

It is important to point out that to cause incipient buckling of at least one of the upper-panel braces, selected as the reference event, a spectral acceleration ordinate $S_{a_{ref}}(f = 0.9Hz, \xi = 5\%)$ (f is the fundamental frequency and ξ is the damping ratio of the pinned full-scaled prototype) equal to $0.31g$ is needed. Because the behavior of the system is linear elastic until the occurrence of the reference event (see Figure 2) and because the first mode is

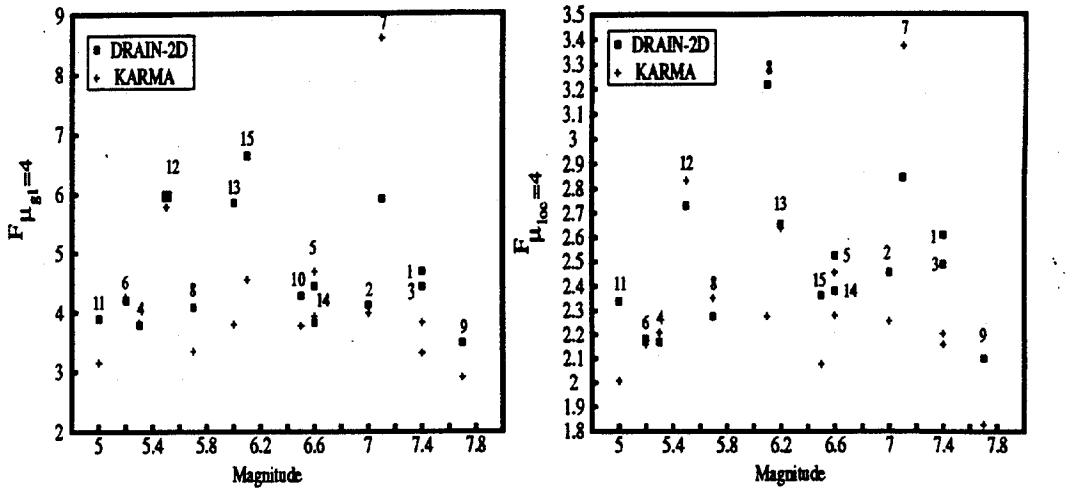

Figure 3: $F_{\mu_{gl}=4}$ and $F_{\mu_{loc}=4}$ values obtained by using DRAIN-2D and KARMA models of the pinned UCB Frame.

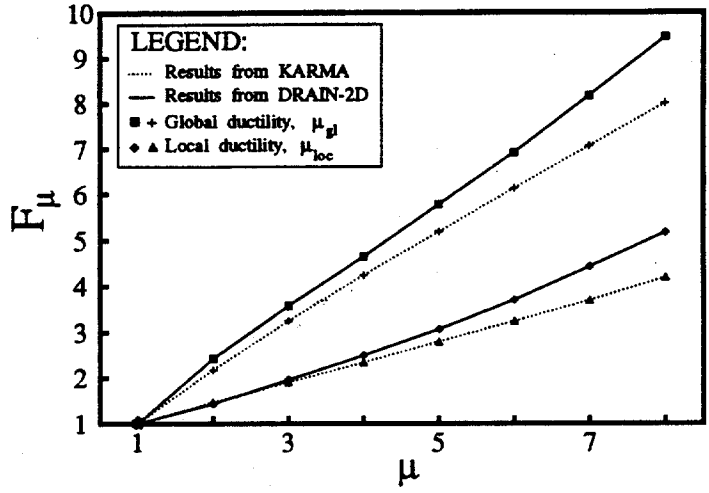

Figure 4: Mean curves of $F_{\mu_{gl}}$ and $F_{\mu_{loc}}$ obtained by using both the DRAIN-2D and the KARMA model of the pinned UCB Frame.

dominant in the response of the structure, $S_{a_{ref}}$ is virtually a constant (the COV is less than 1%). Therefore, in analyzing the DRAIN-2D results, for example, a global damage of $\mu_{gl} = 2$ is, on average, induced by a ground motion with a spectral ordinate of approximately (2.5)(0.31g)=0.78g (this can be confirmed by studying Figure 4 where the expected value of $F_{\mu_{gl}=2}$ is approximately 2.5). On the other hand, at an average spectral acceleration of only about $(1.4)(0.31) = 0.43g$ there will be a ductility of about 2 in at least one of the X-braces in the top panel.

Summarizing, the non-linear dynamic analyses performed on two models of the pinned UCB Frame show that, although some difference exists on an earthquake-by-earthquake basis, the summary statistics of the response factors (which constitute the results of practical interest) are robust to the use of brace elements with different post-buckling behavior for all the considered damage levels. Moreover the use of brace elements without degradation of the section characteristics can lead to slightly unconservative estimates of both local and global non-linear response factors.

In a supplementary study the braces in the pinned frame were replaced by simpler elasto-plastic members. DRAIN-2D analyses yielded F_μ values 10% to 15% larger for $\mu = 8$.

It can be concluded that, at least in the *MDOF* system examined here, the non-linear response factors are measures that, on average, are not greatly affected by changes in the post-buckling behavior description of brace elements in the structure, even though they may not be so stable for a given record.

Effects of Foundation Modeling on F_{DM} Values

The effect of different modeling of the foundation on the response factors $F_{\mu_{gl}}$ and $F_{\mu_{loc}}$ is investigated by means of the UCB Frame models developed by KARMA. For this study the first 15 records in Table 1 were applied both to the model with a pinned base and to that with a pile foundation. The mean curves of $F_{\mu_{gl}}$ and $F_{\mu_{loc}}$ for the pile foundation model are shown in Figure 5. Compare them to Figure 4 for the pinned case. Note that the buckling of the first brace in the piled structure, an event which is again considered as the reference event, is caused, on average, by a spectral acceleration ordinate $S_{a_{ref}}(f = 0.75Hz, \xi = 5\%)$ equal to $0.48g$. The value of 0.75Hz is the fundamental frequency of the pile-founded full-scale prototype structure. The COV of $S_{a_{ref}}$ is found to be 12% (not ≈ 0 as in the pinned case, because here the buckling of the brace occurs when the system response is already non-linear due to the foundation soil).

The first inelastic event in the soil is, of course, a plausible alternative choice for the reference event of the system. In Bazzurro (1993) it is shown that the precise choice of the reference event is not important in the present methodology. Its choice may effect $S_{a_{ref}}$ and F_{μ}, but the product of $S_{a_{ref}}$ times F_{μ} for a value of ductility that corresponds to the same level of damage (e.g., the same local ductility or the same top displacement) is independent of the choice of the reference event.

As in the pinned case, the COV's of $F_{\mu_{loc}}$ are somewhat smaller than the COV's of $F_{\mu_{gl}}$ for the entire damage range considered. For example, the COV

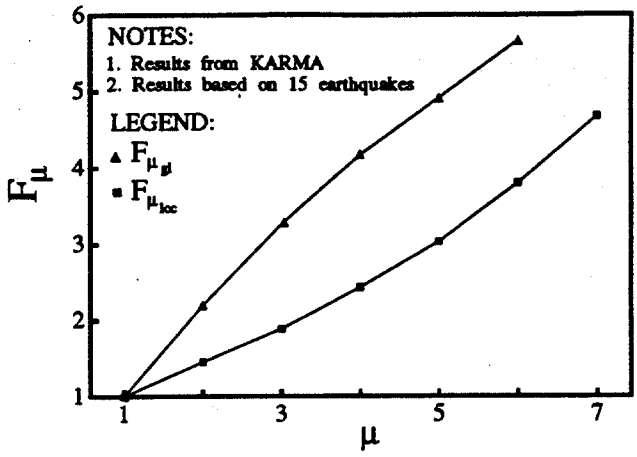

Figure 5: **Mean curves of $F_{\mu_{gl}}$ and $F_{\mu_{loc}}$ for the UCB Frame with pile foundations.**

of $F_{\mu_{gl}=4}$ is equal to 0.33 and the COV of $F_{\mu_{loc}=4}$ is 0.17. The variability of both the response factors appears to be rather limited compared to the COV in S_a, which may be in the order of 0.5 to 0.8 for this frequency range (Joyner and Boore, 1988).

The effect of the explicit modeling of the foundation on the severity of the damage induced in the upper X-brace system can be detected by comparing the summary statistics of $F_{\mu_{loc}}$. Both sets of results have been obtained by using the same computer program, the same superstructure model, and the same 15 ground-motion recordings. Not unexpectedly, the more flexible boundary conditions provided by the pile foundations benefit the superstructure and, in particular, the tendency of the upper X-brace panel to be damaged. In fact, to induce, for example, a damage of $\mu_{loc} = 7$, on average, the records must be scaled to a spectral ordinate of $(3.75)(0.31g) = 1.16g$

when the structure is pinned, and $(4.68)(0.48g) = 2.25g$ when the structure is mounted on piles. The values of $0.31g$ and $0.48g$ are the (mean) spectral acceleration levels necessary to induce the buckling of the top-panel X-braces in the respective structures, and 3.75 and 4.68 are the mean values of $F_{\mu_{loc}=7}$ in the two cases. Consider also, however, that these spectral acceleration levels necessary to cause the same prescribed amount of damage are at different frequencies: 0.9 Hz for the pinned full-scale prototype and 0.75 Hz for the full-scale prototype with pile foundation. Therefore, given that the typical shape of acceleration response spectra is such that the ordinates tend to increase with frequency in this frequency range, even if the two S_a values were the same, it is less likely that any given S_a value would be exceeded at 0.75 Hz than at 0.90 Hz. Such effects will be accounted for in the SHA to follow.

Statistical Study of the Non-linear Response Factors

Given the findings above, the investigation of the statistical behavior of behavior of F_{DM} with respect to ground-motion parameters is carried out using only the DRAIN-2D finite element model of the pinned UCB Frame. All 43 earthquake records in the data base are used for this purpose.

To examine whether $F_{\mu_{gl}=4}$ and $F_{\mu_{loc}=4}$ show any linear dependence on ground-motion parameters R, M, T_D, and PGA, two multiple linear regression analyses were performed. The data and two sets of partial regressions are displayed in Figures 6 to 9. Similar results for other damage levels do

not display any different or additional information; therefore, they are not shown here.

From Figures 6 to 9, it can be seen that $F_{\mu_{loc}=4}$ is not significantly correlated with any of the ground-motion parameters considered here, while $F_{\mu_{gl}=4}$ shows no systematic dependence on R and T_D, but exhibits a very slow *positive* (but not statistically significant) trend with respect to M and PGA. Intuitively one might have expected a *negative* trend in F_{DM} with respect to one or more of these variables. The coefficient of multiple determination, that refers to the amount of variability of the dependent variable (here, $F_{\mu_{gl}=4}$ or $F_{\mu_{loc}=4}$) explained by all four independent variables (here R, M, T_D and PGA) in a multiple linear regression, is found in both cases to be less than 5%. An overall F-test, performed on the null hypothesis that the four regression coefficients are all equal to zero, showed that the null hypothesis may be accepted at a significance level of 5%.

This lack of dependence of the mean of F_{DM} upon magnitude and distance not only re-confirms Sewell's (1988) results for *SDOF* systems, but also it will facilitate greatly the practical application of the probability analysis. This will be demonstrated below.

These results also seem to confirm that, as in the case of *SDOF* structures (Sewell, 1992), the ductility-based non-linear response factors F_μ for *MDOF* structures do not show any systematic dependence on the duration of the ground motion. This lack of dependence appears to hold not only for global-damage-based factors but also for the response factor employed to

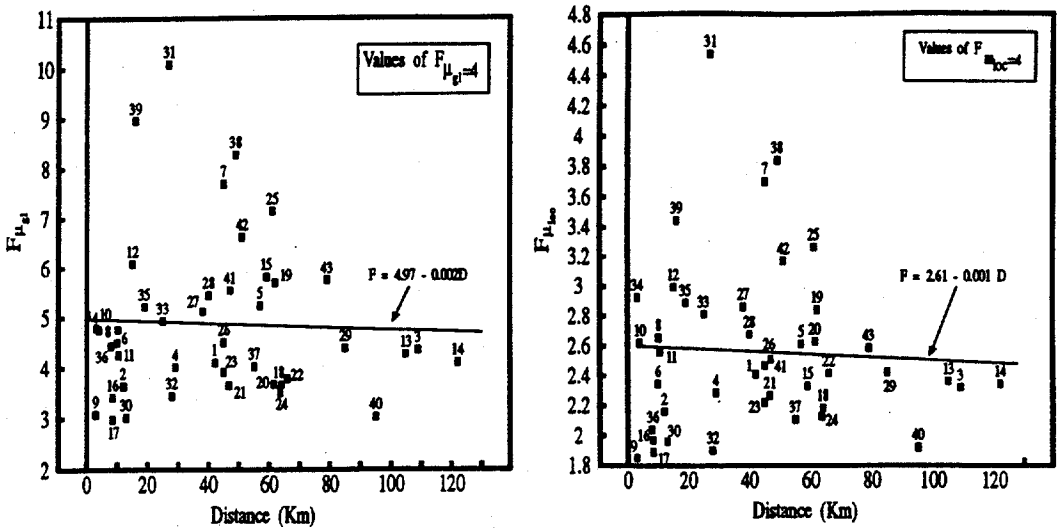

Figure 6: **Partial linear regressions of $F_{\mu_{gl}=4}$ and $F_{\mu_{loc}=4}$ on R based on 43 earthquakes for the pinned UCB Frame.**

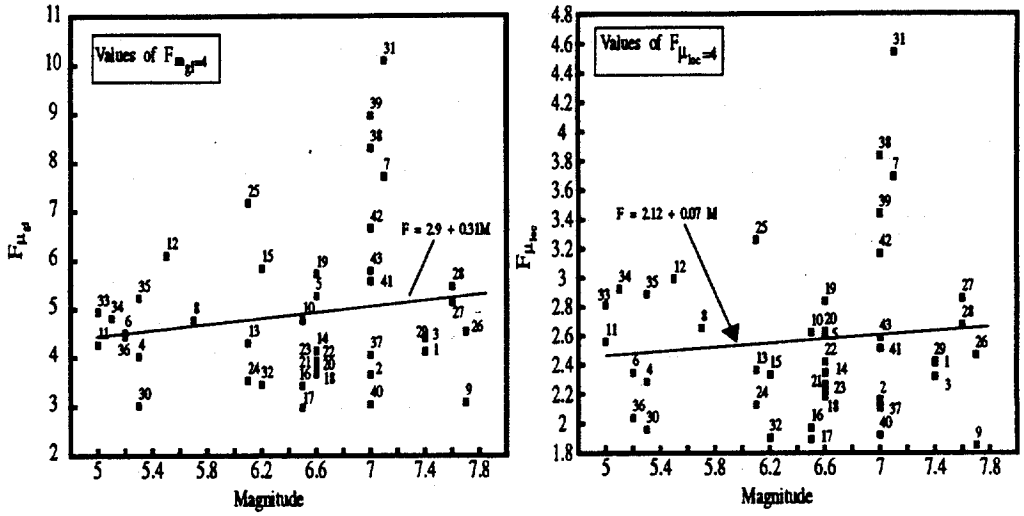

Figure 7: **Partial linear regression of $F_{\mu_{gl}=4}$ and $F_{\mu_{loc}=4}$ on M based on 43 earthquakes for the pinned UCB Frame.**

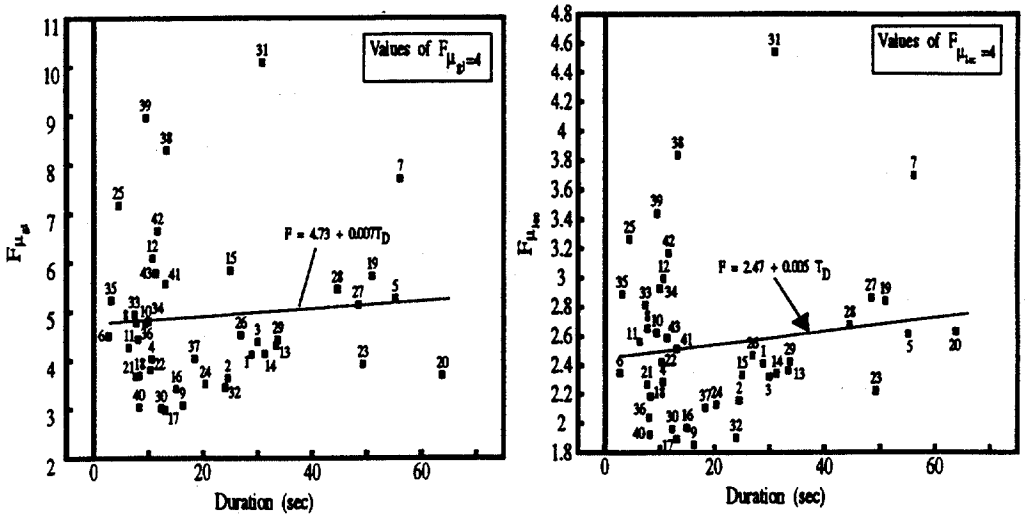

Figure 8: **Partial linear regression of $F_{\mu_{gl}=4}$ and $F_{\mu_{loc}=4}$ on duration, T_D, based on 43 earthquakes for the pinned UCB Frame.**

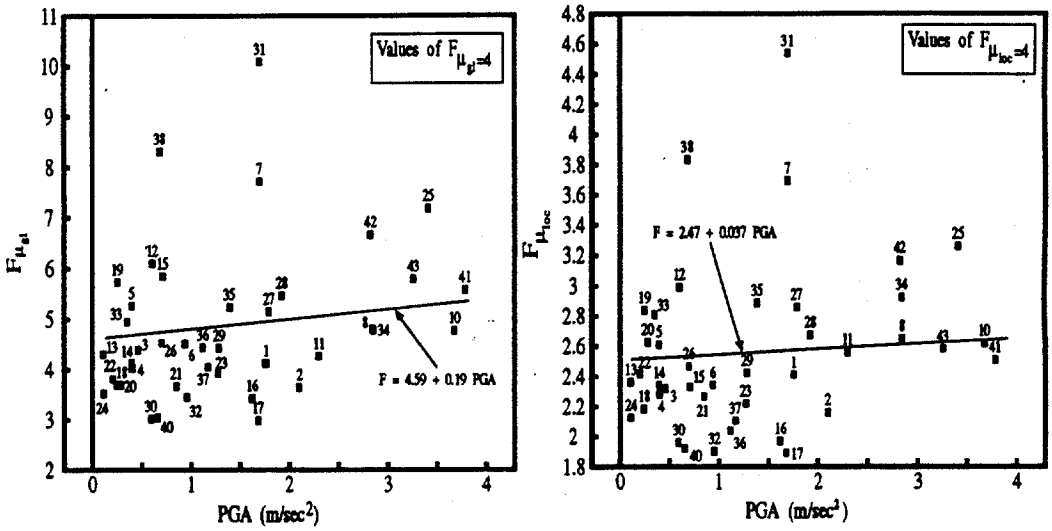

Figure 9: **Partial regression of $F_{\mu_{gl}=4}$ and $F_{\mu_{loc}=4}$ on PGA based on 43 earthquakes for the pinned UCB Frame.**

describe local damage in structural elements. Therefore, even in the *MDOF* case, *the ground-motion duration seems not to play an important role in the characterization of the damage potential of an earthquake.* This conclusion applies when ductility is the damage measure; it has not been confirmed for measures such as cumulative hysteretic energy. In any case any effect of duration on linear damage that might exist is included implicitly in the value of F_{DM}.

To show the connection between the shape of the earthquake response spectrum and the corresponding damage potential measured (inversely) by the non-linear response factors, let us consider, for example, the values of $F_{\mu_{gl}=4}$ displayed in Figure 6 to Figure 9. It is evident that ground motions that are very effective in damaging this particular structure (for example, Loma Prieta, Yerba Buena Island, record No. 40 in Table 1, that yields a value of $F_{\mu_{gl}=4} \approx 3$) are included in the data base together with comparatively ineffective ones (for instance, Kalapana Hawaii, Punaluu, record No. 31 in Table 1, that shows a value of $F_{\mu_{gl}=4} \approx 10$). The difference in the damage potential of these two ground motions with regard to the pinned UCB Frame is evident from the corresponding acceleration response spectra presented in Figure 10. In a range of frequencies slightly lower than the fundamental frequency of the undamaged pinned prototype platform (0.9 Hz), the Yerba Buena spectrum has much more power than the Kalapana spectrum; a bump may be seen in that frequency range in the Yerba Buena acceleration response spectrum, while in the case of Kalapana the accelera-

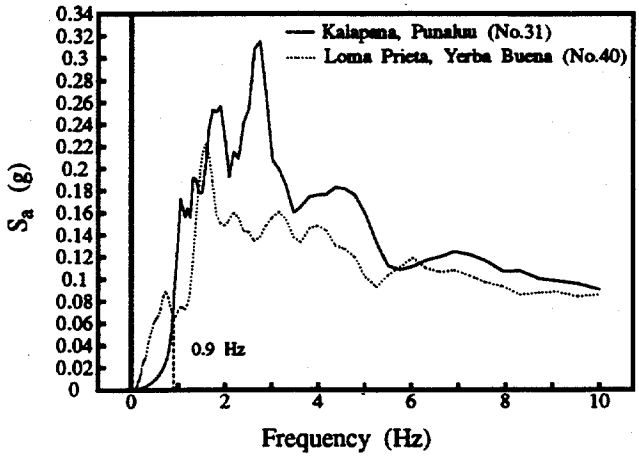

Figure 10: **Acceleration response spectra of Loma Prieta, California, Yerba Buena Station, and of Kalapana, Hawaii, Punaluu Station records.**

tion ordinates in the same range decrease very quickly. This marked local difference in shape of the response spectrum and in damage potential is adequately captured by the corresponding $F_{\mu_{gl}}$ values.

Finally, the summary statistics of $F_{\mu_{gl}}$ and $F_{\mu_{loc}}$ corresponding to damage levels ranging from $\mu = 1$ (beginning of the post-elastic response) to $\mu = 8$ (severe global and local damage) computed for the pinned UCB Frame by using an ensemble of 43 ground-motions are displayed in Figure 11. These statistics consist of the mean value curve, the mean $\pm\sigma$ curves, and the COV for each damage level mentioned above.

It can be observed that for this particular structure, despite its buckling braces, the mean value $F_{\mu_{gl}}$ is approximately equal to the value of μ_{gl}, which implies that the platform possesses an important reserve of capacity beyond

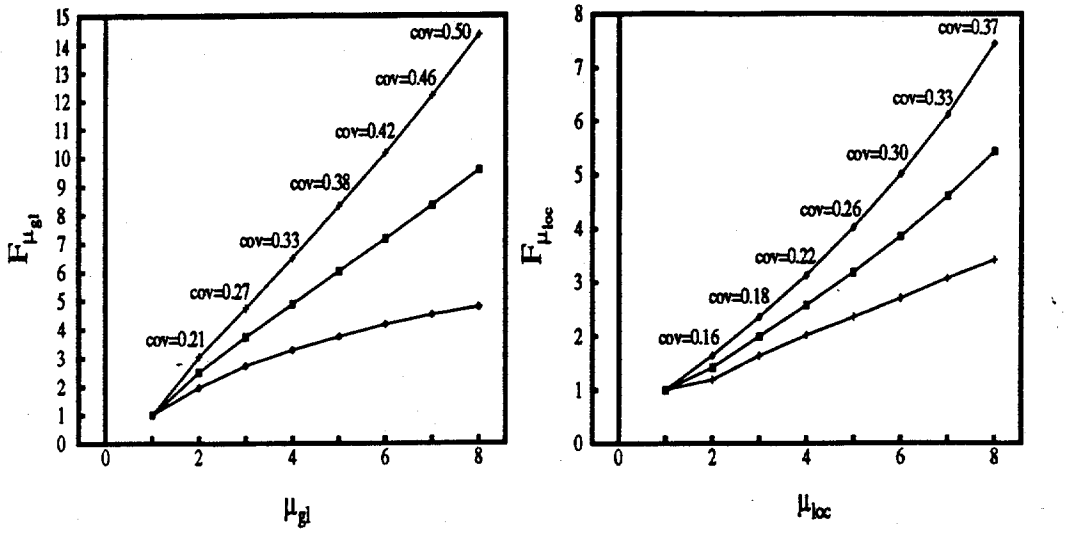

Figure 11: **Summary statistics of $F_{\mu_{gl}}$ and of $F_{\mu_{loc}}$ obtained by applying 43 earthquakes to the pinned UCB Frame.**

the occurrence of the first inelastic event. This near equality is typical of elasto-plastic *SDOF* systems in this frequency range (Sewell, 1988). The companion paper (Bazzurro and Cornell, 1993) shows that not all realistic structures are this robust. Note that for the UCB Frame it takes, on average, a ground motion approximately 5 times stronger than that capable of causing the buckling of one of the upper X-braces to cause severe damage to the structure (e.g., a damage level $\mu_{gl} = 4$). Since a ground motion with a spectral acceleration ordinate, $S_{a_{ref}}$, (at the fundamental frequency and damping ratio of this structure) equal to $0.31g$ is needed to induce the buckling mentioned above, it appears that, on average, a motion with an extremely unlikely (elastic) spectral acceleration ordinate of $1.5g$ is required to bring this pinned structure to collapse. At this same ground motion,

however, the local brace damage will be extremely severe ($\mu \approx 8$).

From Figure 11 the COV's of $F_{\mu_{loc}}$ are seen to be smaller than the COV's of $F_{\mu_{gl}}$ for the entire damage range considered. These COV levels are, recall, not large relative to that of the spectral acceleration (given a specific magnitude and distance). Because the total variability, as will be made clear later, is computed by an SRSS operation and because the COV(S_a) is on the order of 0.7 in this frequency range, even a COV(F_{DM}) equal to 0.5, which is the largest value encountered in this study (Figure 11), induces an increase in the global variability of approximately only 20%.

Important consequences of the relatively limited dispersion of both nonlinear response factors, $F_{\mu_{gl}}$ and $F_{\mu_{loc}}$, and of their lack of dependence on M and R, are the following:

1. the expected value $E[F_{DM}|m,r]$, where m and r are two generic realizations of the random variables M and R, for any response factors F_{DM} of interest and for any considered damage level may be approximated by the simple (unconditional) expected value, namely by $E[F_{DM}]$;

2. the unconditional expected value, $E[F_{DM}]$, may be adequately estimated by means of a very limited number of ground-motion excitations, making the use of this procedure practical for real applications.

Because of resource constraints in real applications, the expected values of the response factors F_{DM} cannot be found by using a large number of earthquakes, as was done here for the pinned UCB Frame. Therefore, it be-

comes important to establish what kind of approximation in the calculation of the expected values is introduced by the use of only a few ground motions. This problem is addressed in Bazzurro (1993) where it is shown that the uncertainty associated with the estimate of $E[F_{DM}]$ can be reduced to negligible values (again relative to the uncertainty of S_a) by using a sample size of 5-7 ground motions. In general the COV of the estimator of the mean is the COV of F_{DM} divided by the square root of the sample size.

GENERALIZED SEISMIC HAZARD ANALYSIS METHODOLOGY

The methodology that is presented here for the direct calculation of the seismic risk of post-elastic damage in real structures is a direct extension of the conventional SHA (e.g., Cornell, 1968, Der Kiureghian and Ang, 1975) and maintains the same mathematical framework. Computationally, the evaluation of the annual probability, $\lambda_{DM_l>x}$, of exceedance of a level, x, of a post-elastic damage, DM, at location l in the structure involves the summation, over seismic sources that pose a threat to the site, of the following integrals:

$$\lambda_{DM_l>x} = \sum_{i=1}^{N} \nu_i \left\{ \int \int P[DM_l > x|m,r] f_{M,R}(m,r) dm dr \right\}_i \qquad (2)$$

where:

- N is the number of the nearby seismic sources;

- ν_i is the annual mean rate of occurrence of earthquakes generated by source i with magnitudes greater than some specified lower bound;
- $P[DM_l > x|m,r]$ is the conditional probability that at location l a damage DM exceeds level x due to an earthquake of magnitude m with epicenter in source i at distance r from the site;
- $f_{M,R}(m,r)$ is the joint probability density function of magnitude, M, and distance, R, for source i.

Based on Equation 1, the new factor, the conditional probability inside the integrand, can be explicitly written in terms of the three random variables S_a, $S_{a_{ref}}$, and $F_{DM_l=x}$ as follows:

$$P[DM_l > x|m,r] = P[S_a(f,\xi) > S_{a_{ref}}(f,\xi)F_{DM_l=x}|m,r] \qquad (3)$$

As discussed above, empirical evidence shows that the non-linear response factor, $F_{DM_l=x}$ is probabilistically dominated by S_a and that it is not dependent on M and R in the magnitude range of interest. The same observation holds also for $S_{a_{ref}}(f,\xi)$ in the case of first-mode-dominated structures, whereas it may show a mild dependence on M and somewhat bigger COV's for structures whose responses receive significant contributions from higher modes (e.g., Inoue and Cornell, 1991).

When both random variables can be considered at least approximately independent of M and R, the problem can be solved very simply by (1) replacing $F_{DM=x}$ and $S_{a_{ref}}(f,\xi)$ by their (unconditional) medians and (2)

inflating somewhat the original variability intrinsic in S_a in order to account for the (comparatively small) variability in $F_{DM=x}$ and $S_{a_{ref}}(f,\xi)$. Therefore, the seismic damage risk can be approximately evaluated by integrating Equation 2 after the following substitution has been made:

$$P[DM_l > x|m,r] \approx P\left[\frac{S_a(f,\xi)}{\varepsilon_{S_{a_{ref}}}\varepsilon_{F_{DM=x}}} > \hat{S}_{a_{ref}}\,\hat{F}_{DM_l=x}\middle| m,r\right] \qquad (4)$$

- $S_a(f,\xi)$ is the (random) spectral acceleration of an event. Its median, $\hat{S}_a$, and COV versus m and r are well studied in standard attenuation law studies (e.g., Joyner and Boore, 1988).

- $\varepsilon_{S_{a_{ref}}}$ and $\varepsilon_{F_{DM_l=x}}$ are random variables with a unit medians and standard deviations of their (natural) logarithms, $\sigma_{\ln\varepsilon}$, equal to those of $S_{a_{ref}}(f,\xi)$ and $F_{DM=x}$, respectively. Assuming lognormality, $\sigma^2_{\ln X} = \ln\left(COV^2(X)+1\right) \approx COV(X)$ (for COV(X) less than about 0.3).

- $\hat{F}_{DM_l=x}$, which is the median of $F_{DM_l=x}$, is equal to $E[F_{DM_l=x}]$ $\exp(-0.5\sigma^2_{\ln F_{DM=x}}) \approx E[F_{DM_l=x}]$ for COV($F_{DM=x}$) less than about 0.3. The median $\hat{S}_{a_{ref}}$ is similarly defined. Given the relatively small variability, the medians $\hat{F}_{DM_l=x}$ and $\hat{S}_{a_{ref}}$ can be estimated from the means of very few earthquake records (say 5) appropriately scaled to several levels of intensity.

To estimate the total variability of the quotient, $Z = (S_a/\varepsilon_{S_{a_{ref}}}\varepsilon_{F_{DM=x}})$, note that $\ln Z = \ln\left(S_a/\varepsilon_{S_{a_{ref}}}\varepsilon_{F_{DM=x}}\right) = \ln S_a - \ln\varepsilon_{S_{a_{ref}}} - \ln\varepsilon_{F_{DM=x}}$. Hence (assuming lack of correlation among the logarithms):

$$\sigma^2_{\ln Z} = \sigma^2_{\ln S_a} + \sigma^2_{\ln \varepsilon_{S_{a_{ref}}}} + \sigma^2_{\ln \varepsilon_{F_{DM=x}}} \tag{5}$$

It is important to point out that, while $\ln S_a$ has been found to be uncorrelated with $\ln \varepsilon_{S_{a_{ref}}}$ and $\ln \varepsilon_{F_{DM=x}}$ (Sewell, 1988), the latter two random variables are somewhat negatively correlated (see, Inoue (1990), and Bazzurro (1993)). Therefore, it is conservative to compute the total variability by means of Equation 5 assuming independence of the three random variables. Since this operation involves an SRSS combination of the σ^2's of the logarithms and because normally $\mathrm{COV}(S_a) \gg \mathrm{COV}(F_{DM=x}) \gg \mathrm{COV}(S_{a_{ref}})$, the additional dispersion introduced in the problem by $S_{a_{ref}}$ and F_{DM} may often be neglected. (Note that one might also include a factor $\sqrt{1+(1/n)}$ amplifying the COV's of F_{DM} and $S_{a_{ref}}$ to allow for the statistical uncertainty associated with using a limited number, n, of ground motions to estimate the means of F_{DM} and $S_{a_{ref}}$.) The probability distribution of $Z = S_a(f,\xi)/(\varepsilon_{S_{a_{ref}}}\varepsilon_{F_{DM=x}})$ must, in principle, be inferred from the data. Routinely, one can assume, however, that the distribution of this ratio is not very much different from the distribution of S_a alone (i.e., lognormal) again because the COV of S_a is dominant in the problem. Therefore, to apply the procedure just outlined for evaluating the annual probability of post-elastic seismic damage, conventional SHA software packages can be used without any modification, except, perhaps, to increase somewhat the input COV values. From a seismic hazard curve for $S_a(f,\xi)$ the hazard curves for all damage measures can be simply obtained.

In the cases when $S_{a_{ref}}$ cannot be assumed independent of M, a condition which can produce a large marginal COV of $S_{a_{ref}}$, the mild trend of $\hat{S}_{a_{ref}}$ (or $E[\ln S_{a_{ref}}]$) on M and the COV($S_{a_{ref}}$) may need to be evaluated by using more ground motions. To do so a few additional records (say other 5) appropriately scaled to *only one* level of intensity (at or near that of the reference event) can be used. These runs are usually linear; only a limited additional effort is implied. Ground motions from relatively widely spaced magnitudes can be considered in this operation in order to improve the slope fit. Practically a satisfactory fit is needed only for the magnitude range that contributes importantly to the hazard. Finally, hazard computation in this non-independent case requires a minor modification of only the attenuation law subroutine of conventional software.

Examples of hazard calculations are presented in the companion paper (Bazzurro and Cornell, 1993) where the the annual seismic risks of damage for two real, complex offshore jacket platforms are computed. It should be noted that Cornell and Sewell (1987) and Sewell (1988) introduced for non-linear *SDOF* systems an analysis similar to that above, including allowance for any systematic dependence of the mean of F_{DM} on M and R. Inoue (1990) and Inoue and Cornell (1991) extended the analysis to *MDOF* linear and simple non-linear *MDOF* systems, using a somewhat less general formulation. The factor C in the latter references is, within a constant, $S_{a_{ref}}$ here. The scheme there was found to be insufficient for certain complex structures.

Conclusions

In this study the conventional SHA methodology has been generalized to estimate directly the seismic risk of post-elastic damage in real structures. The procedure makes use of the non-linear-response-based factor F_{DM} which has been proved to be an appropriate measure of the damage potential of ground motions on non-linear multi-degree-of-freedom (*MDOF*) structures. The non-linear factor F_{DM} has been shown to be suitable for describing any kind of damage in a structure. F_{DM} factors can be introduced that depend on the location of damage in the structure (global versus local), the type of damage (peak or cumulative), the damage measure *DM* employed (e.g., ductility ratio versus normalized hysteretic energy), and the level of damage sustained (from mild damage to rupture for local members, and from mild inelastic displacement to collapse for the global system). It has been confirmed for a realistic (2D) model of an actual jacket-type offshore platform, by using a large sample of observed earthquakes chosen for their representativeness of a wide range of magnitudes and distances, that the critical statistics, $E[F_{DM}|m,r]$ and the coefficient of variation of F_{DM}, meet the necessary criteria to permit an efficient, simplified probabilistic analysis. Those criteria are: (1) there is no significant functional dependence of $E[F_{DM}|m,r]$ on magnitude, m, and distance, r; and (2) the coefficients of variation are relatively small, e.g. typically less than 30 or 40%, compared to the 50 to 80% coefficient of variation of S_a, given m and r. These two criteria ensure

that the $E[F_{DM}]$ can be estimated with sufficient accuracy by a very modest number of non-linear dynamic analyses of the *MDOF* structure.

These results were confirmed for a broad range of ductility levels and for both a global and a local damage measure. The lack of dependence of F_{DM} on other ground-motion parameters, such as peak ground acceleration and duration, has also been shown. For the example structure the mean of the non-linear factor F_{DM} was found to be robust to structural modeling issues, such as the use of brace elements with different post-buckling behavior. This mean of F_{DM} was also found effective in describing the different styles of post-elastic behavior of the structure produced by different characterizations of the foundation.

The less critical random variable $S_{a_{ref}}$ can often be treated as a constant. Dependence on M and R, if any, can be easily established with sufficient accuracy.

The methodology is practical, when incorporated in a SHA context, to evaluate directly the seismic risk of any level of post-elastic damage even in highly non-linear, realistic three-dimensional *MDOF* structures. Further applications of this methodology are illustrated in the following companion paper (Bazzurro and Cornell, 1993). Given the several kinds and degrees of material and geometric nonlinearities in these examples, it can be concluded that the method can apply as well (or better) to a variety of simpler structural types and materials, such as buildings and overpasses. It is important to recognize that the practical effectiveness of the method derives

directly from the coupling of the ground motion attenuation and non-linear structural analysis; the method exploits the comparatively broad statistical variability in S_a (given m and r) to limit the costly non-linear dynamic analyses.

ACKNOWLEDGEMENTS

The authors would like to acknowledge the kind contribution of computational support by Dr. J. Gidwani of ISEC, Inc., San Francisco, CA, and the financial support of the industrial contributors of Stanford's Reliability of Marine Structures Program (Amoco, Bureau Veritas, Chevron, Conoco, Det Norske Veritas Research, Elf Aquitaine, Exxon, Mobil, Norsk Hydro, Saga, Shell, Statoil, and Texaco). The fellowship support provided first by D'Appolonia S.p.A., Italy, and later by the Dr. R. P. Kennedy/EQE Gift Fund to the Department of Civil Engineering, Stanford University, is also gratefully acknowledged.

APPENDIX I. REFERENCES

American Petroleum Institute (1991). *API Recommended Practice for Planning, Designing and Constructing Fixed Offshore Platforms*, API RP 2A,

19^{th} Edition, Washington, DC.

Bazzurro, P. (1993). *Seismic Hazard Analysis of Nonlinear Structures with Application to Jacket-type Offshore Platforms* Engineer's Degree Dissertation, Dept. of Civil Engineering, Stanford University, CA.

Bazzurro, P., and C. A. Cornell (1992). "Seismic Risk: Non-linear MDOF Structures", *Proc. of* 10^{th} *World Conference of Earthquake Engineering*, Vol. 1 , pp. 563-568, Madrid.

Bazzurro, P., and C. A. Cornell (1993). "Seismic Hazard Analysis of Non-linear Structures. II: Applications", Submitted to *Journal of Structural Engineering*, ASCE.

Bertero, V. V. (1986). *Lessons Learned from Recent Earthquakes and Research and Implications for Earthquake-Resistant Design of Building Structures in United States*, Report No. UCB/EERC 86-03, Earthquake Engineering Research Center, University of California, Berkeley, CA.

Cornell, C. A. (1968). "Engineering Seismic Risk Analysis", *Bulletin of the Seismological Society of America*, Vol. 58, No. 5, pp. 1583-1606.

Cornell, C. A., and R. T. Sewell (1987). "Non-linear-behavior Intensity Measures in Seismic Hazard Analysis", *Proc. of the International Seminar on Seismic Zonation*, Guangzhou, China, December.

Der Kiureghian, A., and A.H.S. Ang (1975). *A Line Source Model for Seismic Risk Analysis.* Technical Report UILU-ENG-75-2023, University of Illinois, IL.

Ghanaat, Y., and R. W. Clough (1982). *Shaking Table Tests of a Tubular Frame Model*, Report No. UCB/EERC 82-02, Earthquake Engineering Research Center, University of California, Berkeley, CA.

Hadidi-Tamjed, H. (1987). *Statistical Response of Inelastic SDOF Systems Subjected to Earthquakes*, Ph.D. Dissertation, Dept. of Civil Engineering, Stanford University, CA.

Hwang, H., and J. W. Hsu (1991). *A Study of Reliability-based Criteria for Seismic Design of Reinforced Concrete Frame Buildings*, National Center for Earthquake Engineering Research (NCEER), Report No. NCEER-91-0023, Buffalo, NY.

Inoue, T. (1990). *Seismic Hazard Analysis of Multi-degree-of-freedom Structures*, Report No. RMS-8, Department of Civil Engineering, Stanford University, Stanford, CA.

Inoue, T., and C. A. Cornell (1991). "Seismic Hazard Analysis of MDOF Structures", *Proc. of ICASP*, Mexico City.

ISEC Inc. (1989). *KARMA Computer Program, Documentation*, Vols. I-V by ISEC Inc. , San Francisco, CA.

Iwan, W. D. (1980). "Estimating Inelastic Response Spectra from Elastic Spectra", *Earthquake Engineering and Structural Dynamics*, Vol. 8, pp. 375-399.

Jain, A. K., and S. C. Goel (1978). *Hysteresis Models for Steel Members Subjected to Cyclic Buckling or Cyclic End-moments and Buckling*, Report No. UMEE 78R6, Dept. of Civil Engineering, University of Michigan, MI.

Joyner, W. B., and D. M. Boore (1988). "Measurement, Characterization, and Prediction of Strong Ground Motion", *Proc. of Earthquake Engineering and Soil Dynamics II*, Geotechnical Division, ASCE, Park City, Utah, June 27-30.

Kanaan, A. E., and G. H. Powell (1973). *General Purpose Computer Program for Inelastic Dynamic Response of Plane Structures*, Report No. EERC 73-6, Earthquake Engineering Research Center, University of California, Berkeley, CA.

Kennedy, R. P., Short, S. A., Mertz, K. L., Tokarz, F. J., Idriss, I. M., Power, M. S., and K. Sadigh (1984). *Engineering Characterization of Ground Motion - Task I: Effects of Characteristics of Free-field Motion on Structural Response*, NUREG/CR-3805, Vol. 1, U. S. Nuclear Regulatory Commission.

M^{c}Cann, M. W., and J. W. Reed (1989). *Lower Bound Magnitude for Probabilistic Seismic Hazard Assessment*, Rept. NP-6496, Electric Power Research Institute, Palo Alto, CA.

M^{c}Guire, R. K., and T. P. Barnhard (1979). *Four Definitions of Strong Motion Duration: Their Predictability and Utility for Seismic Hazard Analysis*, Open-File Rept. 79-1515. United States Geological Survey (USGS), Dept. of the Interior.

Nasser, A. A., and H. Krawinkler (1991). *Seismic demands for SDOF and MDOF Systems*, John A. Blume Earthquake Engineering Center, Report No. 95, Department of Civil Engineering, Stanford University, CA.

Newmark, N. M., and W. J. Hall (1982). *Earthquake Spectra and Design*, Engineering Monographs on Earthquake Criteria, Structural Design, and Strong Ground Motions, Earthquake Engineering Research Institute (EERI).

Osteraas, J. D., and H. Krawinkler (1990). *Strength and Ductility Considerations in Seismic Design*, John A. Blume Earthquake Engineering Center, Report No. 90, Department of Civil Engineering, Stanford University, CA.

Popov, E. P., Mahin, S. A., and R. W. Clough (1985). "Inelastic Response of Tubular Steel Offshore Towers", *Journal of Structural Engineering*, ASCE, Vol. 111, No. 10.

Riddel R., and N. M. Newmark (1979). *Statistical Analysis of the Response on Nonlinear Systems Subjected to Earthquakes*, Technical Rept. SRS 468, Dept. of Civil Engineering, University of Illinois, Urbana.

Sewell, R. T. (1988). *Damage Effectiveness of Earthquake Ground Motion: Characterizations Based on the Performance of Structures and Equipment*, Ph.D. Dissertation, Dept. of Civil Engineering, Stanford University, CA.

Sewell, R. T. (1992). "Effects of Duration on Structural Response Factors and on Ground-Motion Damageability", *Proc. of SMIP'92*, edited by M. J. Huang, Div. of Mines and Geology, Calif. Dept. of Conservation, Sacramento, CA, May 21.

Submitted to ASCE
Minor Editorial Corrections Needed

The first case is the Rajah Wellhead offshore Kalimantan, operated by Unocal.

SEISMIC HAZARD ANALYSIS OF NON-LINEAR STRUCTURES. II: APPLICATIONS

By Paolo Bazzurro [1] and C. Allin Cornell [2]

INTRODUCTION

In the previous companion paper (Bazzurro and Cornell, 1993) a methodology for the direct computation of the seismic risk of post-elastic damage in non-linear multi-degree-of-freedom (*MDOF*) structures has been developed. This methodology makes use of the response factor F_{DM} to characterize the damage potential of a ground motion. This paper presents, with the aid of two examples, the detailed procedure for the computation of such a non-linear response factor for real structures modelled as three-dimensional (3D), fully non-linear *MDOF* systems. The seismic hazard curves of post-elastic damage for these two structures are also presented. These examples deal with a wide range of different problematic issues that can be encountered in practical applications. As case studies, two steel jacket-type offshore platforms are considered:

[1]Grad. Student at Civil Eng. Dept., Stanford University, Stanford, CA 94305, on leave of absence from D'Appolonia S.p.A., Genoa, Italy

[2]Professor, Civil Eng. Dept., Stanford University, Stanford, CA 94305

- [redacted] Wellhead, located immediately offshore [redacted]
- Statoil's Riser 16/11S, located in the North Sea on the Norwegian continental shelf.

These large 3D structures and their foundations are challenging examples because they display an array of types of non-linearities: steel and soil material non-linearity as well as softening geometric non-linearity, both locally (buckling braces) and globally ($P - \Delta$ effect). The application of this methodology to large, complex structures is made practical by the relatively few non-linear dynamic analyses necessary to evaluate the mean values of F_{DM} and $S_{a_{ref}}$ (Bazzurro and Cornell, 1993). Improved software and computational efficiency has brought such analyses within the same accessibility and the same cost range as former linear dynamic analyses.

Offshore Platform [redacted] Wellhead

[redacted] Wellhead (Figure 1) is a typical jacket-type platform operating in 45 meters of water. It has a rectangular base and four legs. The piles are driven to a depth of 107 meters below the mudline and grouted inside the legs. The distance between the lower side of the deck and the mean water level is about 14 meters. Both the superstructure and the piles are made up of steel tubular members. The uppermost soil layer is a soft clay, whose resistance characteristics are very poor. The structural characteristics of the

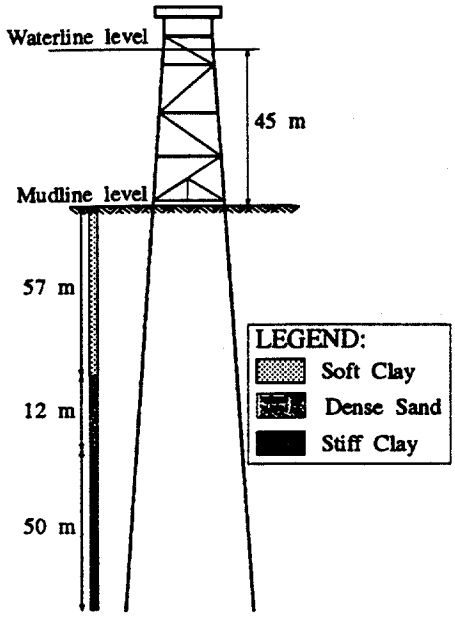

Figure 1: **Schematic view of the [redacted] Wellhead Platform with foundation soil profile (figure not to scale).**

platform, and the relevant information about loads and masses are consistent with the report Unocal 91-21 (Unocal Corporation, 1991).

Numerical Analyses and Finite Element Model

Modal analysis, pseudo-static pushover analysis, and non-linear dynamic analyses were performed on a finite element model developed by means of the computer program KARMA (ISEC Inc., 1989). The model includes 451 nodes, at which the structural masses are lumped, 644 elements and 2010 degrees of freedom. Legs and piles were modelled by large-displacement inelastic beam-column elements with distributed plasticity, diagonal braces

were modelled by large-displacement post-buckling elements with degradation of both strength and stiffness of the section. Linear beams were used for the the deck and non-linear near-field elements were used for the soil. In particular, the foundation soil was modelled by defining a set of three orthogonal springs (two lateral and one axial) at fixed elevations along the shaft of the pile. The pile-soil deformation was related to the soil resistance in both the lateral and the axial directions by specifying, respectively, lateral, p-y, and vertical, t-z, force-deformation curves. These curves, for both virgin and degraded soil, were available as result of a geotechnical investigation at the site.

The non-linear dynamic analyses were performed in the time domain, by direct integration of the equations of motion. The time step was 0.02 seconds and the value of the damping before yielding was 5% of critical. The non-linear post-elastic behavior of the elements explicitly accounts for the structural damping after material yielding. Earthquake (inertia) loads, dead load of the structure and equipment located on the deck, live loads present on the deck during oil production, and buoyancy loads on the submerged members were included in the non-linear dynamic analyses. The actions of other environmental loads, resulting from wind, wave and current, were not included. Drag forces acting on the submerged members of the jacket, due to the motion induced by the earthquake, were also neglected.

Given (Bazzurro and Cornell, 1993) (1) that the variability shown by the random variables F_{DM} and $S_{a_{ref}}$ is small relative to the variability of

S_a and (2) that there is an apparent lack of dependence between F_{DM} and $S_{a_{ref}}$, and magnitude, M, and source-to-site distance, R, only a few ground motions (usually 5 to 7) are needed to estimate the medians of F_{DM} and of $S_{a_{ref}}$ with sufficient accuracy. Nonetheless, the real earthquakes should be selected to describe the type of events that are expected to contribute to the threat to the site. In this case to evaluate the medians of F_{DM} and $S_{a_{ref}}$ the five earthquakes in Table 1 were adopted. These magnitude and distance pairs were selected to describe the seismicity of the area around the Rajah Platform site. Beyond using records only from "soil" sites, no modifications were made for the specific local site conditions.

Earthquake		Station Name	Date	Dist.	Magn.	Soil
No.	Name			(km)		Type
1	San Fernando, CA	Wheeler Ridge	02-09-71	82	6.6	Soil
2	Long Beach, CA	Vernon CMD Bldg.	03-11-33	22	6.2	Soil
3	Borrego Mountain,CA	Cal Edison, Colton	04-09-68	130	6.6	Soil
4	Kern County, CA	Caltech Athenaeum	07-21-52	109	7.4	Soil
5	Loma Prieta, CA	Olema, Ranger Sta.	10-18-89	136	7.0	Soil

Table 1: **Characteristics of the ground motions included in the database.**

Pushover analyses include all the loads listed above (except the seismic loads) plus a system of seismic-like static forces that are applied incrementally

to the structure until failure.

Results of the Analyses

Modal Analysis

Results from a modal analysis showed that, for small strains, [redacted] fundamental period is approximately 1.8 seconds and corresponds to a bending mode shape in the X direction (X, Y, and Z are, respectively, the two horizontal orthogonal directions and the vertical direction of the structure).

Pseudo-static Lateral Pushover Analysis

The purposes of lateral pushover analysis are multifold. The results of the pushover analysis not only improve the understanding of the structure's global performance, but also give valuable information regarding the choice of the significant inelastic event to be used as reference point in the calculation of the non-linear response factors, F_{DM}. A pushover analysis may also identify the sequence of yielding in elements of the structure that leads to the collapse. But, because the seismic-type of load in this analysis is applied pseudo-statically, any conclusions drawn from the pushover analysis must be confirmed by the results of non-linear dynamic analyses performed by applying real earthquake recordings.

The incremental pattern of loads was applied simultaneously in all three directions and the pushover loads displayed in the following results repre-

sent the directional components of the total load applied. The analysis was performed by using a controlled load procedure. The corresponding displacement is consistent with equilibrium of the structure at each applied load level. (For seismic loads, a displacement-controlled static pushover analysis may be preferred to a load-controlled pushover analysis).

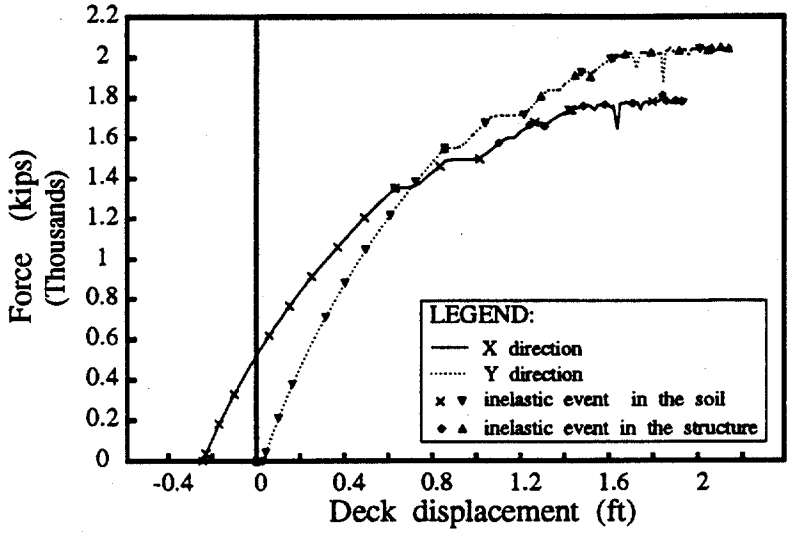

Figure 2: **Pushover load versus deck displacement in the horizontal directions, X and Y, for the [redacted] Wellhead Platform.**

The pushover load versus deck displacements in the X and Y directions are presented in Figure 2. Due to the poor strength and stiffness of the uppermost clayey layer, the platform subjected to the action of only the asymmetric static vertical deck and self-weight loads deviates from the upright position and leans towards the negative X-direction (0.25 ft) before the lateral loads are applied. Initially, under the action of the lateral loads all

the inelastic events occur only in the soil and the platform tilts virtually as a rigid body while remaining elastic. The first inelastic event in the structural frame occurs for loads of approximately 75% of the total lateral capacity of the structure, when the deck displacements are on the order of 0.85-0.90 ft (measured relative to the initial configuration) in both the X and the Y directions. When this first inelastic frame event occurs the foundation soil has already yielded in several places. The inelastic events in the structure are concentrated in the piles below mudline. Moreover, the platform is weaker in the X direction, as appears from the difference in the maximum lateral capacity between the two directions.

The results of pushover analysis suggest that the collapse mechanism for the [redacted] Wellhead Platform under seismic loadings is governed by the failure of the soil-pile foundation system mainly in the X direction. Note that, despite the presence throughout the entire height of the jacket of a bracing pattern made up of single diagonals, a pattern which currently is not a recommended practice for platforms located in seismic areas (American Petroleum Institute, 1991), the braces do not play an important role in the failure mechanism of this structure under seismic excitation.

The response to lateral loads of the entire system (structure and foundation soil) becomes strongly non-linear for very small deck displacement values, when the structure itself is everywhere very far from reaching the peak elastic capacity. Thus, selecting the first inelastic event in the structural frame as the reference event for the calculation of the non-linear response

F_{DM} would not be appropriate. This is because the damage of the foundation soil that occurs before the frame enters the post-elastic regime could not be monitored by the so-defined F_{DM} factors. To have a more general understanding of the damage experienced by the system in earlier stages, a maximum semi-amplitude of the oscillations of the deck, in at least one of the two orthogonal directions X and Y, of 0.25 ft from the initial configuration of the system (e.g., the configuration determined by action of the static vertical loads only), was taken as the reference event. This choice of the reference event was used in the following computation of the F_{DM} factors. In Bazzurro (1993) it is shown that the hazard curves for the post-elastic damage are insensitive to the choice of the reference event.

Preliminary non-linear dynamic analyses revealed that, because the X direction is more flexible and weaker than the Y direction and because the structure is initially leaning in the negative X direction, the platform responds to seismic excitations by progressively increasing its deviation from the vertical position towards the negative X direction (see Figure 3). Therefore, the reference event is realized when oscillations of the deck attain values of -0.50 ft in net displacement in the X direction.

Non-linear Dynamic Analyses

The results of the pushover analysis and of the preliminary dynamic analyses have shown that the foundation stability is critical for the global seismic performance of this platform. Consider, in fact, the time history of the deck

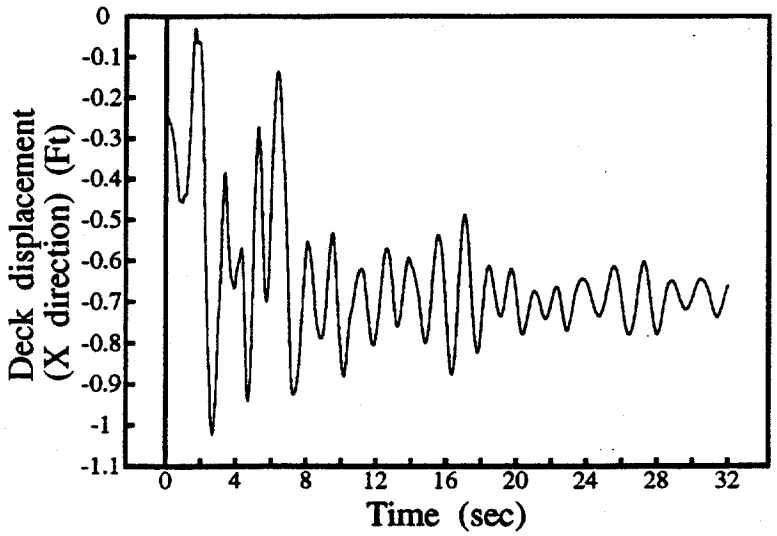

Figure 3: **Deck displacement response to the Long Beach earthquake (03-11-33) scaled up by a factor of 2.4. Analogous displacement patterns were observed for all five ground motions applied to the platform.**

displacement in the X direction, displayed in Figure 3. Note that although the deck at the end of the ground shaking attains a permanent displacement of -0.7 ft, the platform remains elastic both in the superstructure and in the piles. The permanent displacement is entirely due to the yielding of the foundation soil. These irrecoverable displacements, when caused by intense earthquakes, can impair the platform's overall stability. It is important to note that for a level of ground motion such that the peak response of the system is just at the previously selected reference threshold, the permanent displacement in the X direction at the end of the ground motion is, on average

(based on the five adopted ground motions), equal to -0.38 ft. The COV observed was only 3%.

In light of all the preceding observations, three non-linear response factors, F_{DM}, are considered in the case of the [redacted] Wellhead Platform: two for describing the global performance and one for monitoring the local damage in the piles. The overall post-elastic damage of the platform is measured by the global ductility ratio, μ_{gl}, based on deck displacement. The situation is more complicated in the case of the local damage that occurs only in the piles at a considerable depth below the mudline (about 40 meters). Piles behave as non-linear beam-column elements whose response is governed by a set of multi-linear relationships that include axial force-displacement, in-plane and out-of-plane moment-rotation, and torque-twist behavior. In these elements a four-dimensional interaction surface controls the inelastic response, and this fact makes it difficult to postulate a compound damage measure. In this particular case, though, since the damage occurs mainly in a pile at a large depth below the mudline, the axial force is dominant over bending and torque moments. Therefore, the usual ductility ratio μ_{loc}, based on the axial deformation of the element, is a reasonably accurate measure of the peak damage sustained by the piles.

Following Bazzurro and Cornell (1993), the three non-linear response factors are defined as follows:

1. $F_{\mu_{disp,X=m}}$ is defined as the ratio $S_{\mu_{disp,X=m}}(f = 0.55Hz, \xi = 5\%)/S_{a_{ref}}(f = 0.55Hz, \xi = 5\%)$, where the numerator represents the spec-

tral acceleration necessary to induce a maximum oscillation amplitude of the deck in the X direction m times greater than the semi-amplitude of the reference event displacement (0.25 ft);

2. $F_{\mu_{off,X=m}}$ is the ratio $S_{\mu_{off,X=m}}(f = 0.55\ Hz, \xi = 5\%)/S_{a_{ref}}(f = 0.55\ Hz, \xi = 5\%)$, where the numerator represents the spectral acceleration necessary to obtain a deck displacement permanent offset in the X direction m times greater than the offset displacement associated with the reference event. (This was very close to 0.38 ft for all records.);

3. $F_{\mu_{loc}=m}$ is the ratio $S_{\mu_{loc}=m}(f = 0.55\ Hz, \xi = 5\%)/S_{a_{ref}}(f = 0.55\ Hz, \xi = 5\%)$, where the numerator represents the spectral acceleration necessary to induce a damage μ_{loc} equal to m in at least one of the piles.

In the definitions above, the denominator is the spectral acceleration ordinate needed to reach the specified reference event, 0.25 ft deck displacement in the X direction. This quantity is a random variable. The average value and the coefficient of variation (COV) of $S_{a_{ref}}(f = 0.55\ Hz, \xi = 5\%)$ are:

$$\overline{S}_{a_{ref}} = 0.06g; \quad COV(S_{a_{ref}}) = 0.28$$

It has to be pointed out, however, that the sample size (5 earthquakes) is too small to give an estimate of the true COV. Note that, since the dynamic response of this platform receives significant contributions from several modes, the $COV(S_{a_{ref}})$ is somewhat larger than for other structures previously analyzed. According to Bazzurro and Cornell (1993), in this cases $S_{a_{ref}}$ may

show a mild dependence on M. The values attained by $S_{a_{ref}}$ for the five adopted records (0.04, 0.07, 0.06, 0.07, and 0.05g, respectively, for the five records in the order in which they appear in Table 1), however, showed no visible dependence on M. Therefore, no additional analyses with other records were performed to further investigate this issue.

In light of the previous definitions and of the results of the pseudo-static pushover analyses (Figure 2), a very severe damage and possibly the collapse of the structure can be associated to deck displacements in the X direction of approximately 1.25 ft. Such a displacement corresponds to $\mu_{disp,X}$ values of approximately 5.0.

The results for the three non-linear response factors adopted to monitor the damage in [redacted] Wellhead Platform are presented in terms of summary statistics. These statistics include the average value curve, $\pm\sigma$ curves, and the coefficients of variation for each damage level considered (see Figure 4 to Figure 6).

From these results it follows that the collapse of the structure ($\mu_{disp,X} = 5$) occurs, on average, at $F_{\mu_{disp,X}=5}$ values of about 8. This ratio $F/\mu > 1$ is not commonly encountered. It implies a more robust system than, say, simple elasto-plastic oscillators where $F \approx \mu$ in this frequency range (Sewell, 1988). This benefit is apparently the effect of the soft, non-linear foundation. Structural collapse is associated with spectral acceleration values of approximately 0.48g (this value can be computed by multiplying the spectral acceleration value at the reference point, 0.06g, by 8, the sample

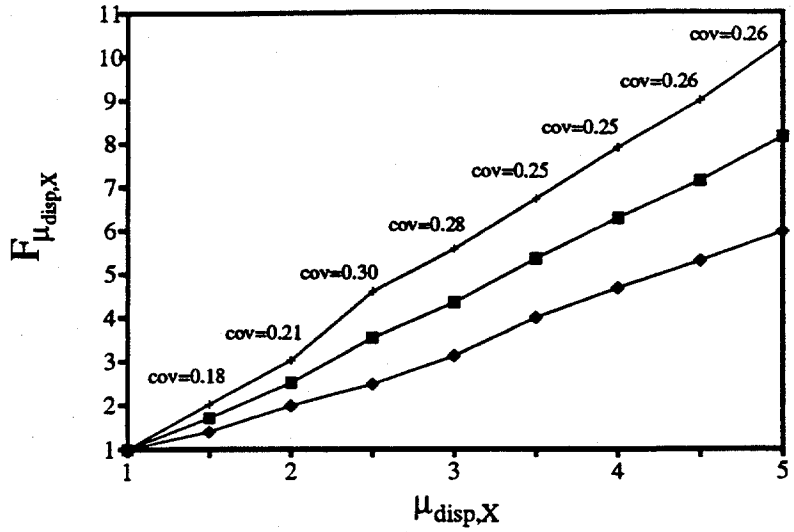

Figure 4: **Summary statistics of $F_{\mu_{disp,X}}$ (the reference lateral deck displacement is 0.25 ft) for the [redacted] Wellhead Platform.**

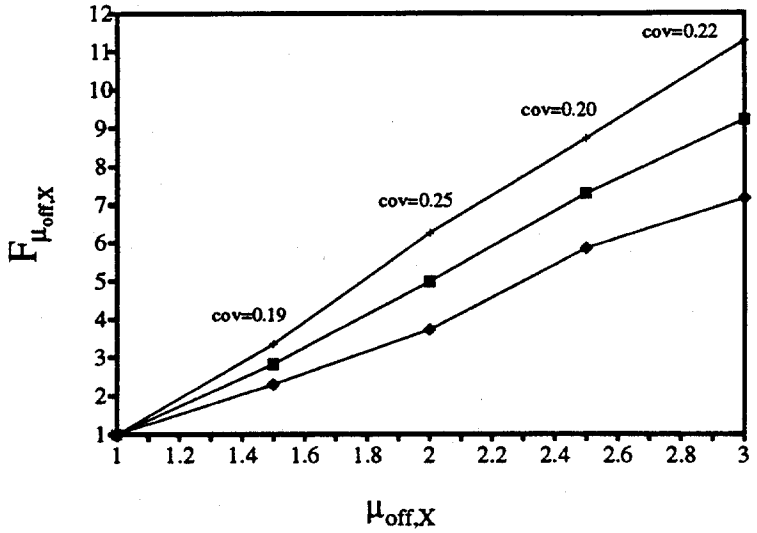

Figure 5: **Summary statistics of $F_{\mu_{off,X}}$ for the [redacted] Wellhead Platform. For $\mu_{off,X} = 1$, the permanent offset displacement of the deck is about 0.38 ft.**

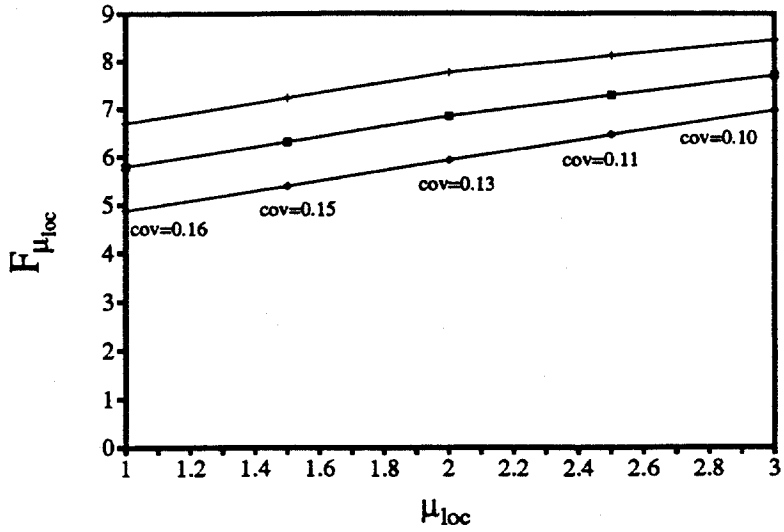

Figure 6: **Summary statistics of $F_{\mu_{loc}}$ for the [redacted] Wellhead Platform. There is no local damage ($\mu_{loc} > 1$) until the ground motion is several times that necessary to cause the reference level top displacement.**

average of $F_{\mu_{disp,X=5}}$). Moreover, one needs, on average, a ground motion having $S_a(f = 0.55\ Hz, \xi = 5\%) \geq 0.38g$ to cause any inelastic damage ($\mu_{loc} > 1$) in the structure (which occurs in the piles). From Figure 6 note that, in accordance with the results of the pushover analyses (Figure 2), the platform has very little capacity left once yielding begins in the piles. In fact, if one considers $F_{\mu_{loc}=3}$ as referring to collapse (at this point the analysis solution becomes unstable), on average it takes only a 25% increase in the strength of the earthquake that induces incipient yielding in the piles to cause failure of the system ($F_{\mu_{loc}=3}/F_{\mu_{loc}=1} = 7.5/5.9 \approx 1.25$). An earthquake

with spectral acceleration $S_a(f = 0.55\ Hz, \xi = 5\%) = 0.38g$, which causes incipient yield in the steel of the structure, also induces peak displacements in the X direction of (on average) 0.95 ft from the initial configuration, and a permanent residual deck displacement in the X direction at the end of the ground shaking of -0.83 ft from the upright position. These numbers are found by entering Figures 4 and 5 at the F_μ value of $F_{\mu_{loc}=1} = 5.9$ and reading, respectively, the values of $\mu_{disp,X}$ and $\mu_{off,X}$.

Finally, the COV's of all the non-linear response factors are only 0.1 to 0.3, which are small compared to the COV's of the spectral acceleration ordinates arising from the attenuation laws. This is true over the entire damage range up to and including collapse of the structure. The small sample size (5), of course, is not large enough by itself to confirm an estimate of the COV in any one case, but the pattern is consistent. Further the values are in agreement with the experience base associated with many other structural models.

These results will be used in the next section, where, as an application of the proposed methodology, the direct evaluation of the seismic risk of post-elastic damage in the Rajah Wellhead Platform is carried out.

Seismic Damage Risk for the [redacted] Wellhead Platform

In this section the seismic damage risk for the jacket [redacted] Wellhead Platform is evaluated by using the methodology presented in a companion paper (Bazzurro and Cornell, 1993). The platform is located in in the Makassar Strait, east of Kalimantan, Indonesia (see Figure 7).

Figure 7: **Location of the [redacted] Wellhead Platform site and seismic zones.**

The study of the tectonic features of the region and the spatial occurrence of historical earthquakes has not yet provided sufficient information for identifying with confidence active faults nearby (say within 100km)(Dames & Moore, 1981, and Risk Engineering, Inc. (REI), 1992). The evidence of the historical data, however, suggested the partition of the region into the three large seismic zones shown in Figure 7. Within each zone the seismicity was considered relatively uniform and future occurrence of earthquakes was described by a single probability distribution. Seismic events were modelled to occur as single points of energy release at a random location. The earthquake magnitude distribution adopted for the seismic zones in this study is the doubly truncated exponential distribution.

The analysis of the earthquake catalogs for the region under consider-

Seismic Zone	Historical m_{max}	Adopted m_{max}	Adopted m_{min}	Hypocentral depth (km)	Activity rate ν_i	Richter b-value
1	8.5	9.0	5.0	20	18	1.00
2	6.5	8.5	5.0	20	0.48	0.68
3	7.0	8.5	5.0	20	2.4	0.74

Table 2: **Seismicity parameters adopted in the SHA of the [redacted] Wellhead Platform (m_{max} and m_{min} are, respectively, the upper and lower bound of the magnitude, M).**

ation led to the definition of the seismic parameters in Table 2 (Risk Engineering, Inc. (REI), 1992). The equation used to estimate the spectral acceleration (for a frequency of 0.55Hz and a damping ratio of 5%) at the site is the attenuation law developed by Campbell (1990). This equation applies specifically to soil sites. No other provisions were made, however, for possible amplification of the input motions due to the extremely soft soil conditions at the Rajah Wellhead Platform site.

According to the methodology presented in Bazzurro and Cornell (1993) (Equation 5), the variability in the spectral acceleration S_a needs to be increased in order to account for the variability in both $S_{a_{ref}}$ and F_{DM} (here the three response factors $F_{\mu_{disp,X}}$, $F_{\mu_{off,X}}$, and $F_{\mu_{loc}}$). Conservatively, the COV's of $S_{a_{ref}}$ and of the response factors were taken equal to 0.3. The high negative correlation existing between $S_{a_{ref}}$ and each of the three response

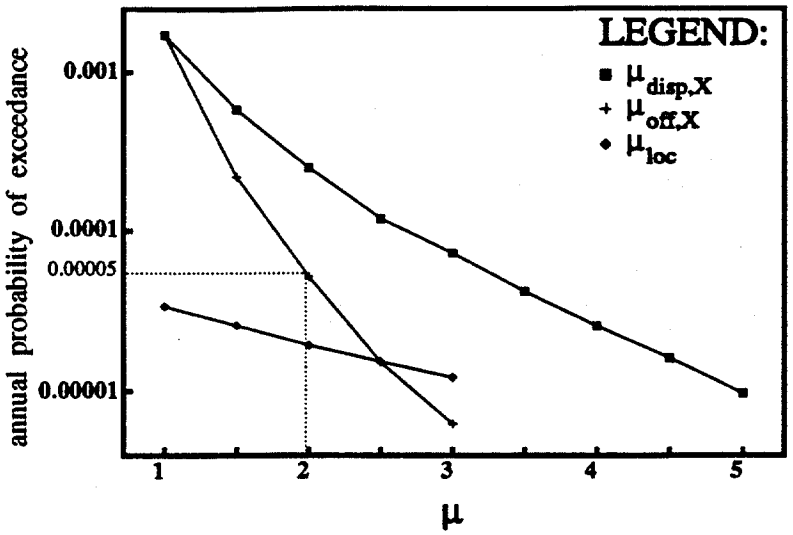

Figure 8: **Seismic hazard curves obtained for the three kinds of post-elastic damage considered critical in the [redacted] Wellhead Platform.**

factors F_μ (Bazzurro, 1993) was only (conservatively) partially accounted for. Hence the standard deviation values of $\ln S_a(0.5\ Hz, \xi = 5\%)$ suggested by Campbell (e.g., 0.591 for magnitude $m < 6.2$ and 0.496 for magnitude $m \geq 6.2$) are augmented to 0.68 for $m < 6.2$ and to 0.60 for $m \geq 6.2$. Campbell's COV values were unusually low ones; nonetheless even the conservative assumptions used here increased these standard values by only 20% or less.

The computer program EQRISK (M^{c}Guire, 1976) was used for the seismic hazard computations. The seismic hazard curves corresponding to the ductility values associated with the maximum deck displacement in the X direction (measured by $\mu_{disp,X}$), the residual permanent deck displacement in the X direction (measured by $\mu_{off,X}$), and the structural damage in the piles (measured in terms of μ_{loc}) are displayed in Figure 8. From this figure

it follows that, for example, the annual probability that the structure may experience a final permanent displacement of 0.75 ft or more in the X direction (corresponding to $\mu_{off,X} \approx 2$) is approximately 5.0×10^{-4}. Moreover, the collapse of the Rajah Wellhead Platform, which is an event that requires the values of the ductility ratios equal to or higher than any reported in previous subsection, has an annual probability of occurrence that is less than 1.0×10^{-5}.

Finally it is interesting to note that almost 70% of the total seismic risk is due to the contribution of the background seismicity zone (Zone 2) alone (see Figure 7), where the [redacted] Wellhead Platform is located, while the remaining part of the hazard is mostly due to the contribution of Zone 1.

Offshore Platform Riser 16/11S

Riser 16/11S is one of the two riser platforms that are parts of the Statpipe transportation system for gas from the Statfjord field via Kårstøin the North Sea. The platform is a framed structure with squared base and four legs, operating in 70 meters of water. Each leg has four skirt piles with diameter of 1.8 meters fastened to the platform by a grouted connection in the pile sleeves. The piles extend about 76 meters into the foundation soil. The distance between the mean water level and the base of the deck is approximately 24 meters. A schematic lateral view of the jacket platform, in which the four piles per leg are represented by a single pile, and of the soil profile is depicted

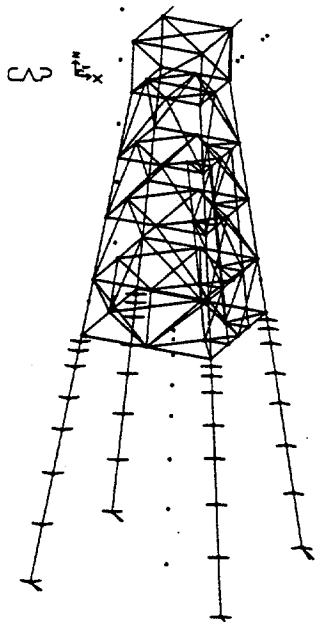

Figure 10: **Finite element model of the Riser 16/11S Platform with pile foundation.**

Numerical Analyses and Finite Element Model

The modal analysis, the pseudo-static pushover analyses, and the non-linear dynamic analyses for the calculation of the mean of F_{DM} were performed on a finite element model (Figure 10) developed by means of the SeaStar computer program (PMB Engineering, 1991). For computational purposes, the group of four piles per leg was replaced by a single pile having the same lateral capacity of the group. The model is composed of 116 nodes and 315 elements making up 582 degrees of freedom. Masses were lumped at the nodes.

The superstructure and the foundation piles were modelled by inelastic

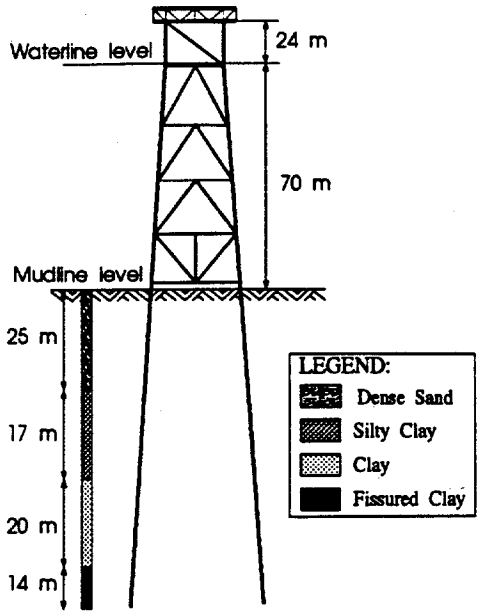

Figure 9: **Schematic view of Riser 16/11S Platform with foundation and soil profile (figure not to scale).**

in Figure 9. In particular, notice that the uppermost layer is made up of a very dense sand (internal friction angle $\phi = 38°$).

All the structural elements in the platform are steel tubular members, with the exception of the deck floor. The structure was designed according to NPD regulations (Norwegian Petroleum Directorate, 1977) and verified according to N-SD-001 specifications (Statoil, 1985). Element dimensions, material characteristics, soil profile and related geotechnical parameters as well as loads and masses are all consistent with the report DNV 83-0838 (Det Norske Veritas, 1983).

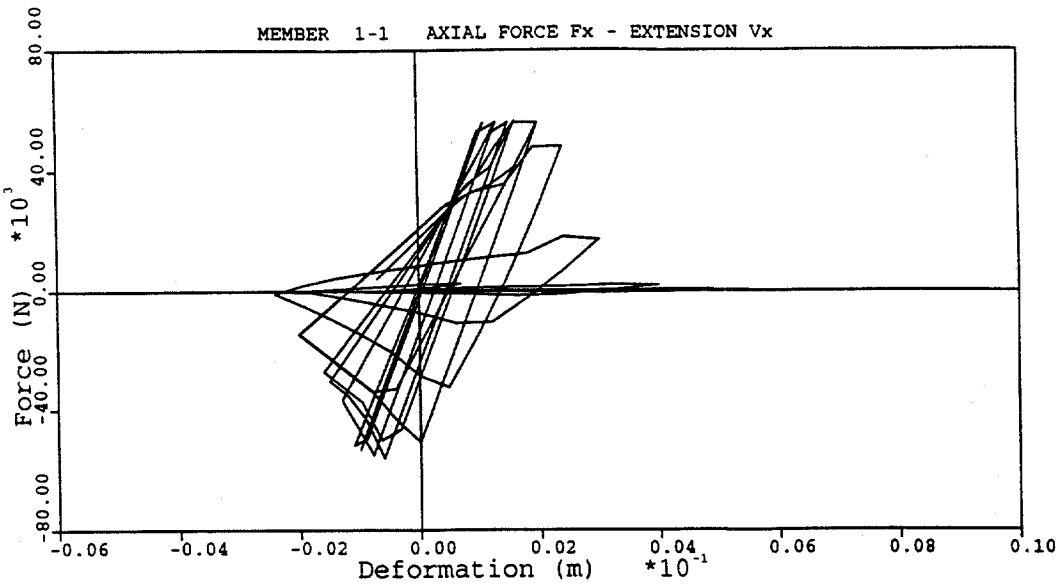

Figure 11: **Typical hysteretic sequence of cycles in a Marshall Strut.**

beam-column elements, except (1) for the horizontal and vertical diagonal braces for which post-buckling Marshall Strut (Marshall *et al.*, 1977) elements were used, and (2) for the deck that was modelled by linear beam elements. In the beam-column elements, force-moment interactions in defining yield were taken into account and yielding may take place only in concentrated plastic hinges at the ends. The post-buckling behavior of a brace is displayed in Figure 11, in which a typical series of hysteretic loops exhibited by a Marshall Strut is presented. Notice the degradation in both strength and stiffness of the section when the damage of the element increases. In the analyses, an effective length factor, k, of 0.5 was used to compute the corresponding axial capacity in compression. Possible joint failures were not considered.

The foundation soil was modelled using near-field soil elements: at each

elevation along the piles (13 nodes are located along each pile, more closely spaced in the upper part), three orthogonal springs were employed—two to describe the lateral stiffness of the underlying pile and soil and one to represent the friction between the pile shaft and the soil. The piles were also supported at the tip by an end-bearing spring. The lateral pile-soil deformation was related to the soil resistance by specifying soil resistance deflection curves (p-y curves) for both virgin and degraded soil, according to API regulations (American Petroleum Institute, 1991). The axial behavior of the soil-pile system was described by axial frictional t-z curves which were assumed to be bilinear. Hypothetical loss of contact between the soil and the piles close to the mudline level was neglected because of the excellent resistance of the sand layer. The soil elements employed dissipate energy by radiation. All the elements used in the model explicitly account for geometric non-linear effects ($P - \Delta$ effects).

The non-linear dynamic analyses of the Riser 16/11S were carried out by a direct integration procedure in the time domain using a time step of 0.02 seconds. The material and structural damping before yielding was set equal to 5% of the critical by means of the Rayleigh formulation. This value was also intended to model the energy dissipation due to fluid-structure interaction. The material and structural damping after material yielding was taken into account directly by utilizing the non-linear hysteretic elements described above.

The actions of the following loads were included in the non-linear dynamic

analyses of the Riser 16/11S Platform: seismic loads (all three components), dead load of the structure and equipment located on the deck, live loads on the deck, and buoyancy forces acting on the submerged elements of the jacket.

To compute the means of F_{DM} and of $S_{a_{ref}}$ for the Riser 16/11S Platform, five earthquake records were selected (see Table 1). These events are not particularly representative of the seismicity of the Norwegian area but they are appropriate for illustrating the methodology and comparing results with the previous structure. Other loads, such as those due to wind, wave, and current, were not considered in the analyses. Drag forces, acting on the submerged elements (because of the relative motion of the structure with respect to the water particles) were not treated explicitly.

The pseudo-static pushover analyses included all the loads listed before with the exception of seismic loads which were substituted by a system of static lateral forces (having a profile characteristic of the seismic inertial effects) that were gradually incremented until failure of the structure results.

Results of the Analyses

Modal Analysis

A preliminary modal analysis (whose results are based on the initial tangent stiffness) showed that the fundamental period of the structure with pile foundations is equal to 1.8 seconds. The first two mode shapes correspond

to bending modes in the two horizontal, orthogonal directions, X and Y, at approximately the same frequency (0.55Hz).

Pseudo-static Non-linear Lateral Pushover Analysis

Two pushover analyses for this platform were carried out by specifying incremental loads separately in the X and in the Y direction. Inertial loads due to an earthquake component in the vertical direction, Z, were not included. The analyses were performed using a lateral controlled displacement procedure. The increment in the displacement between two successive steps measured at key nodes in the structure is forced to be below a given threshold value. The load carried was established to be consistent with the equilibrium of the structure at each displacement level. The results of these analyses, consisting of curves showing total applied load versus deck deformation, are reported in in Figure 12.

The collapse mechanisms start with the buckling of one of the vertical-plane diagonal braces that connect the lower side of the deck to the first level of horizontal braces (see Figure 13). After the buckling of one of those braces, the adjacent elements receive the redistributed load and, in sequence, reach their yielding points. When the part of the structure below the deck level has entered the plastic regime, a mechanism develops with a consequent large drop-off in the capacity of the structure to withstand lateral loads. At that point, the structure may be considered to have collapsed.

Notice in Figure 12 that the first inelastic event in these analyses occurs

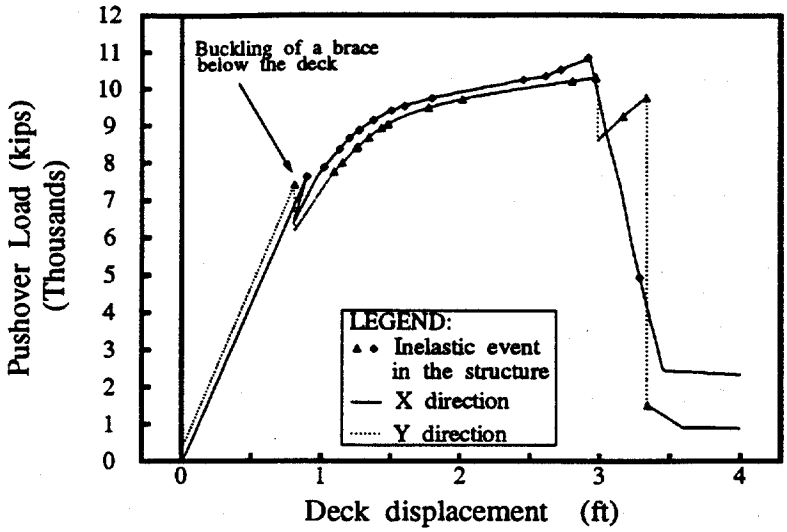

Figure 12: **Pushover load versus deck displacement in the X and in the Y direction for Riser 16/11S Platform.**

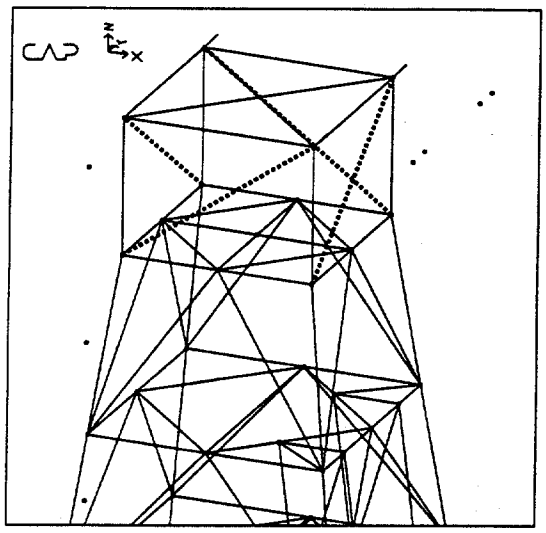

Figure 13: **Location of the four single-diagonal braces (dotted lines) that initiate the failure path of the Riser 16/11S Platform under seismic loading.**

in the superstructure while the foundation soil is still in the unyielded elastic regime. This fact is due to the very good resistance properties of the sand layer close to the mudline level. The buckling of one of the diagonal braces described above occurs for deck displacements of approximately 0.85 ft in either of the two orthogonal directions X and Y. Preliminary non-linear dynamic analyses with actual earthquake recordings have confirmed these findings. Since the platform is almost symmetrical and the four diagonal braces are identical, during a seismic excitation the brace that buckles first is typically determined by which of the two directions, X or Y, receives the stronger of the two horizontal components of the ground motion.

The buckling of at least one of these braces (and the corresponding lateral deck displacement at which it occurs) is adopted here as the reference event for the computation of F_{DM}. This Riser 16/11S Platform behaves linearly up to that point. Its analysis is therefore more representative than the Rajah Platform of many other structures to which the method might be applied (e.g., building frames with fixed bases).

Non-linear Dynamic Analyses

The results of the pushover and preliminary dynamic analyses showed that not only the beginning of the collapse mechanism starts with the buckling of one of the four diagonal braces in Figure 13, but also the greatest amount of damage sustained by the elements of the structure is concentrated in the same diagonal braces below the deck. Hence, a total of three non-linear

damage response factors are examined for the Riser 16/11S Platform: one measuring its global post-elastic deformation, and two measuring the damage accumulated in the aforementioned diagonal braces. The overall performance is given by the global ductility ratio, μ_{gl}, expressed in terms of the deck lateral displacement. The local damage is measured both (1) by a local ductility ratio, μ_{loc}, related to the maximum axial deformation of the most damaged (largest μ_{loc}) of the group of four braces, and (2) by a local ductility ratio $\mu_{loc,en}$, that monitors the total energy dissipated by the most damaged (largest $\mu_{loc,en}$) of the same four elements during the hysteretic cycles. The local ductility ratio, $\mu_{loc,en}$, based on energy dissipation is defined for a post-buckling Marshall Strut as follows (Marshall *et al.*, 1977):

$$\mu_{loc,en} = \frac{E_h}{P_y \Delta_y} + 1 \tag{1}$$

in which E_h is the cumulative energy dissipated during the hysteretic loops, while P_y and Δ_y represent, respectively, the tensile load and the elongation in the element at yielding. Note that for a hypothetical elastic-perfectly-plastic system subjected to monotonic loading, $\mu_{loc,en}$ degenerates to the conventional definition of the ductility ratio, μ.

The three non-linear response factors are defined as follows:

1. $F_{\mu_{gl,XY}=m}$ is the magnification factor by which a ground motion, that causes the occurrence of the reference event, has to be scaled up to induce a global ductility ratio $\mu_{gl,XY} = m$ measured in terms of the deck displacement in *at least one* of the two directions X and Y.

2. $F_{\mu_{loc}=m}$ is the magnification factor by which a ground motion, that causes the occurrence of the reference event, has to be scaled up to induce a local ductility ratio $\mu_{loc} = m$ in *at least one* of the four diagonal braces below the deck (see Figure 13).

3. $F_{\mu_{loc,en}=m}$ is the magnification factor by which a ground motion, that causes the occurrence of the reference event, has to be scaled up to induce a local energy ductility ratio $\mu_{loc,en} = m$ in *at least one* of the four diagonal braces below the deck (see Figure 13).

Given the previous definitions and the results of the pushover analyses (Figure 12), the collapse of the structure can be associated to a deck displacement (in the X or Y direction) of approximately 3.0 ft which corresponds to a $\mu_{gl,XY}$ value of 3.0 to 3.5.

The spectral acceleration, at the fundamental frequency and damping ratio of the system, required to cause the reference event (e.g., the incipient buckling of at least one of the four diagonal braces below the deck) is the random variable $S_{a_{ref}}$. The mean value and the COV of $S_{a_{ref}}(0.55Hz, \xi = 5\%)$ evaluated using the five earthquakes listed in Table 1 are the following:

$$\overline{S}_{a_{ref}} = 0.36g; \;\; COV(S_{a_{ref}}) = 0.03$$

The sample by itself is too small to estimate this COV with precision, but the value is consistent with results from other structures that are first mode dominated and (unlike the Rajah Platform example) linear up to the refer-

ence event (e.g., Inoue and Cornell, 1991). Further when combined with the other variability measures this COV is negligible.

The results of the analyses relevant to the non-linear response factors selected to describe both the overall and the local damage of the Riser 16/11S Platform consist of the estimated average value curve, $\pm\sigma$ curves, and the coefficients of variation for each damage level considered. The sample size should be sufficient to estimate the mean value to within about $\pm 5\%$, given the coefficients of variation observed. These summary statistics are presented in Figure 14 to Figure 16.

It follows from these figures that the collapse of the structure, corresponding to a ductility value of $\mu_{gl,XY} = 3$ induced by a ground motion having $S_{a_{ref}}(f = 0.55\ Hz, \xi = 5\%) = 0.36g$, on average would occur for $S_a(f = 0.55\ Hz, \xi = 5\%) = (1.77)(0.36g) = 0.64g$ (Figure 14 yields $\overline{F}_{\mu_{gl,XY}=3} = 1.77$). This F value for a global μ of 3 is substantially less than that observed for the UCB Frame (pinned or piled) (Bazzurro and Cornell, 1993), for the [redacted] Platform (with its soil-pile dominated non-linear behavior) or for other structures (e.g., Inoue, 1990; Sewell, 1988). Not only is the slope of the $\overline{F} - \mu$ curve small (compared to the one-to-one value characteristic of robust structures in this frequency range), but also the curvature is concave downward. Similar results were observed in a parallel analysis of the same structure with a pinned base (Bazzurro, 1993). These phenomena suggest a pattern in such softening systems. Bea (1992) has observed somewhat similar patterns in softening single-degree-of-freedom models.

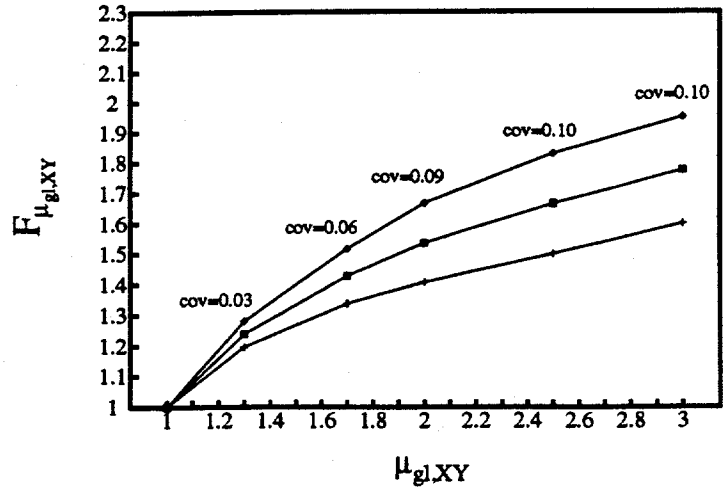

Figure 14: **Summary statistics of the global performance measure $F_{\mu_{gl,XY}}$ for the Riser 16/11S Platform.**

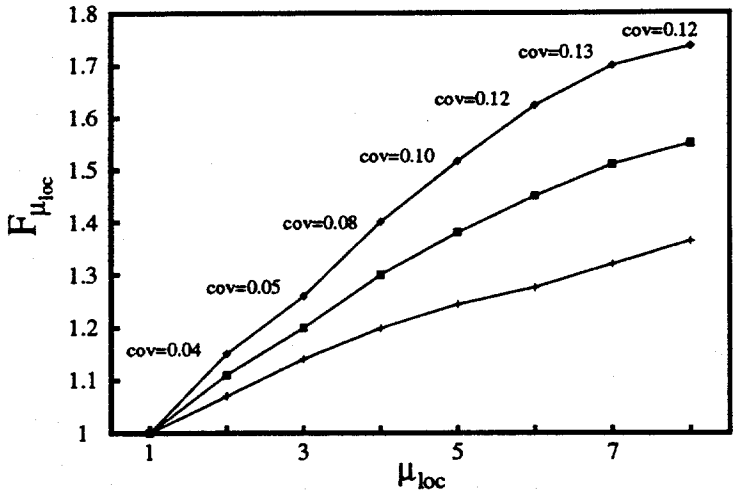

Figure 15: **Summary statistics of the peak local damage measure $F_{\mu_{loc}}$ for the Riser 16/11S Platform.**

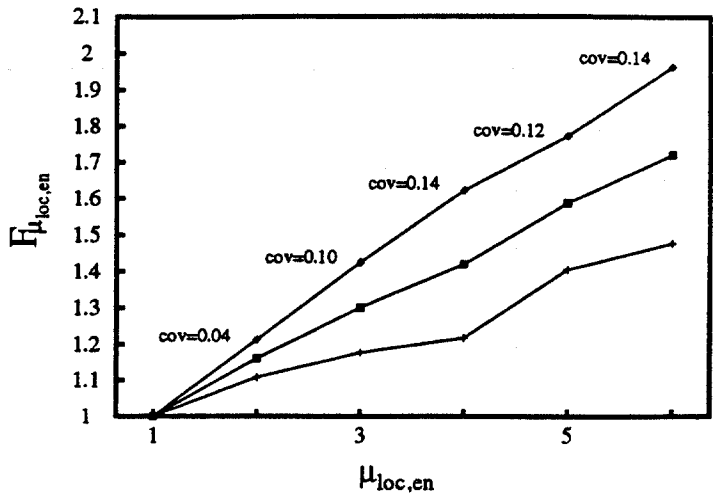

Figure 16: **Summary statistics of the cumulative local damage measure $F_{\mu_{loc,en}}$ for the Riser 16/11S Platform.**

A severe local damage of $\mu_{loc} = 8$ in at least one of the four diagonal braces under consideration, is induced on average by an earthquake having approximately a spectral acceleration of $S_a(f = 0.55\ Hz, \xi = 5\%) = 0.56g$, less than that required to produce a global ductility $\mu_{gl,XY}$ of 3. A severe cumulative local damage of $\mu_{loc,en} = 6$ in at least one of the four diagonal braces, is induced on average by an earthquake ground motion with $S_a(f = 0.70\ Hz, \xi = 5\%) = 0.61g$. Note that the typical behavior of these buckled braces (unlike the more general pattern in Figure 11) does not involve multiple large hysteretic loops because the yield level in tension is seldom reached.

The coefficients of variation for all the damage measures are small (about $10 - 20\%$) in the entire range of damage levels considered here. Again,

although the individual sample size is small, the consistency level-to-level, and measure-to-measure, with other structural models, suggests strongly that these values are quite accurate for this structure.

Seismic Damage Risk in Riser 16/11S Platform

The seismic damage risk for the Riser 16/11S Platform was evaluated by adopting the same seismic parameters used in the SHA of [redacted] Platform. This was done for comparison purposes (note that the two structures have the same fundamental period and damping). The parameters in Table 2 and the same attenuation law (Campbell, 1990) were used. This seismicity is, of course, in no way representative the structure's actual site in the Norway.

To increase the variability of S_a due to the scatter in F_{DM} and $S_{a_{ref}}$, a COV of 0.3 and 0.15 was respectively assumed for the latter quantities. These are conservative values for this structure. Negative correlation between F_{DM} and $S_{a_{ref}}$ was also conservatively neglected. The same SHA computer package, EQRISK, was employed.

The seismic hazard curves for the global damage monitored by $F_{\mu_{gl,XY}}$ (expressed in terms of the larger deck displacement in the two horizontal directions), and for the maximum local damage in the piles, gauged by both $F_{\mu_{loc}}$ and $F_{\mu_{loc,en}}$, are displayed in Figure 17. Note that for comparable levels of μ the risk grows more rapidly for global than for local damage. The annual probability of failure of the structure, which can be associated with lateral deck displacement on the order of 3 ft or more (e.g., about $\mu_{gl,XY} \geq 3$), is

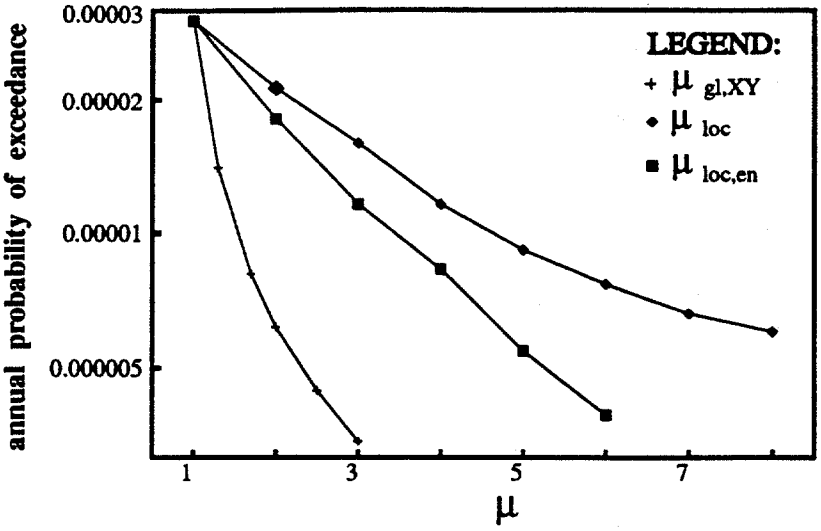

Figure 17: **Seismic hazard curves obtained for the three kinds of post-elastic damage considered critical in the Riser 16/11S Platform.**

lower than 5×10^{-6}.

CONCLUSIONS

In this paper the methodology of Bazzurro and Cornell (1993) has been applied for the direct computation of the seismic risk of post-elastic damage to two large, 3D jacket offshore platforms: Unocal's [redacted] Wellhead and Statoil's Riser 16/11S. The methodology allowed the evaluation of the seismic hazard curves for both global and local types of damage which are considered critical for these structures. The methodology, also tested in the previous companion paper on a 2D-modeled structure by means of a large ensemble

of ground motions, is proven to be applicable to realistic cases and practical to implement.

ACKNOWLEDGEMENTS

The authors would like to thank Unocal and Statoil for volunteering the use of their structures, and to acknowledge the support by ISEC, Inc., San Francisco, CA, and by PMB Engineering, San Francisco, CA. The use of their computer programs has been essential for obtaining the results included in this work. The financial support of the industrial contributors of Stanford's Reliability of Marine Structures Program (Amoco, Bureau Veritas, Chevron, Conoco, Det Norske Veritas Research, Elf Aquitaine, Exxon, Mobil, Norsk Hydro, Saga, Shell, Statoil and Texaco), of D'Appolonia S.p.A., Italy, and of the Dr. R. P. Kennedy/EQE Gift Fund to the Department of Civil Engineering, Stanford University, is also gratefully acknowledged.

APPENDIX I. REFERENCES

American Petroleum Institute (1991). *API Recommended Practice for Planning, Designing and Constructing Fixed Offshore Platforms*, API RP 2A, 19^{th} Edition.

Bazzurro, P. (1993). *Seismic Hazard Analysis of Nonlinear Structures with Application to Jacket-type Offshore Platforms* Engineer's Degree Disser-

tation, Dept. of Civil Engineering, Stanford University, CA.

Bazzurro, P., and C. A. Cornell (1993). "Seismic Hazard Analysis of Non-linear Structures. I: Methodology", Submitted to *Journal of Structural Engineering*, ASCE.

Bea, R. G. (1992). "Seismic Design and Requalification Methodologies for Offshore Platforms", *Proc. of International Workshop on Seismic Design and Requalification of Offshore Structures*, Cal. Inst. of Tech., Pasadena, CA, December 7-9.

Campbell, K. W. (1990). *Empirical Prediction of Near-source Soil and Soft Rock Ground Motions for the Diablo Canyon Power Plant Site, San Luis Obispo, CA*, Report prepared for Lawrence Livermore National Laboratories, Dames & Moore, Job No. 10805-476-166.

Dames & Moore (1981). *Seismic Risk and Site Response Study, Offshore* [redacted] Report prepared for Union Oil Company, Job No. 00111-214-02.

Det Norske Veritas (1983). *Statpipe Development Project, Independent In-place Static Analysis of Riser Platform 16/11 S*, DNV Industrial Offshore Division Report No. 83-0838, Volume 1.

Inoue, T. (1990). *Seismic Hazard Analysis of Multi-degree-of-freedom Structures*, Report No. RMS-8, Department of Civil Engineering, Stanford University, Stanford, CA.

Inoue, T., and C. A. Cornell (1991). "Seismic Hazard Analysis of MDOF Structures", *Proc. of ICASP*, Mexico City.

ISEC Inc. (1989). *KARMA Computer Program, Documentation*, Vols. I-V by ISEC Inc. , San Francisco, CA.

M^{c}Guire, R. K. (1976). *EQRISK, Fortran Computer Program for Seismic Risk Analysis*, Open File Report 76-67, USGS, Denver, CO, USA.

Marshall, P. W., Gates, W. E., and S. Anagnostopoulos (1977). "Inelastic Dynamic Analysis of Tubular Offshore Structures", *Proc. of Offshore Technology Conference*, Houston, TX, May 2-5, OTC Paper No. 2908, pp. 235-246.

Norwegian Petroleum Directorate (1977). *Regulations for the Structural Design of Fixed Structures on the Norwegian Continental Shelf*, Oslo, Norway.

PMB Engineering (1991). *SeaStar Computer Program, Documentation*, Vols. I-IV by PMB Engineering, San Francisco, CA.

Risk Engineering, Inc. (REI) (1992). *Seismic Hazard Analysis for the Offshore Kalimantan Sites, Indonesia*, Report prepared for Unocal Science & Technology Division, March 27.

Sewell, R. T. (1988). *Damage Effectiveness of Earthquake Ground Motion: Characterizations Based on the Performance of Structures and Equipment*, Ph.D. Dissertation, Dept. of Civil Engineering, Stanford University, CA.

Statoil (1985). *Structural Design Specification for Offshore Installations*, Design Specification N-SD-001, rev. 1, Stavanger, Norway.

Unocal Corporation (1991). *Static In-place Analyses of* [redacted] *Wellhead Platform (11 conductors)*, Report No. 91-21 by W. B. Lamport, Project No. 660-63202.

Earthquake		Station Name	Date	Dist.	Magn.	Soil
No.	Name			(km)		Type
1	San Fernando, CA	Wheeler Ridge	02-09-71	82	6.6	Soil
2	Long Beach, CA	Vernon CMD Bldg.	03-11-33	22	6.2	Soil
3	Borrego Mountain,CA	Cal Edison, Colton	04-09-68	130	6.6	Soil
4	Kern County, CA	Caltech Athenaeum	07-21-52	109	7.4	Soil
5	Loma Prieta, CA	Olema, Ranger Sta.	10-18-89	136	7.0	Soil

Seismic Zone	Historical m_{max}	Adopted m_{max}	Adopted m_{min}	Hypocentral depth (km)	Activity rate ν_i	Richter b-value
1	8.5	9.0	5.0	20	18	1.00
2	6.5	8.5	5.0	20	0.48	0.68
3	7.0	8.5	5.0	20	2.4	0.74

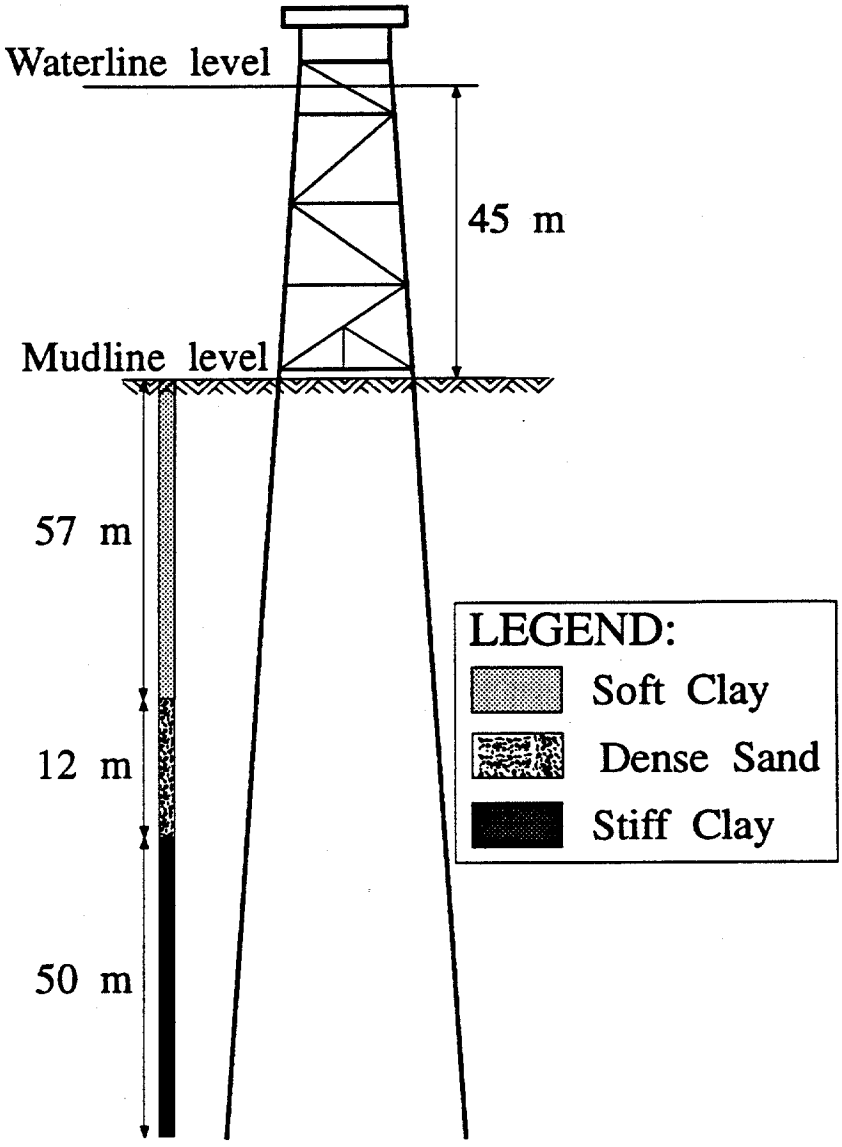
Waterline level
45 m
Mudline level
57 m
12 m
50 m
LEGEND:
Soft Clay
Dense Sand
Stiff Clay

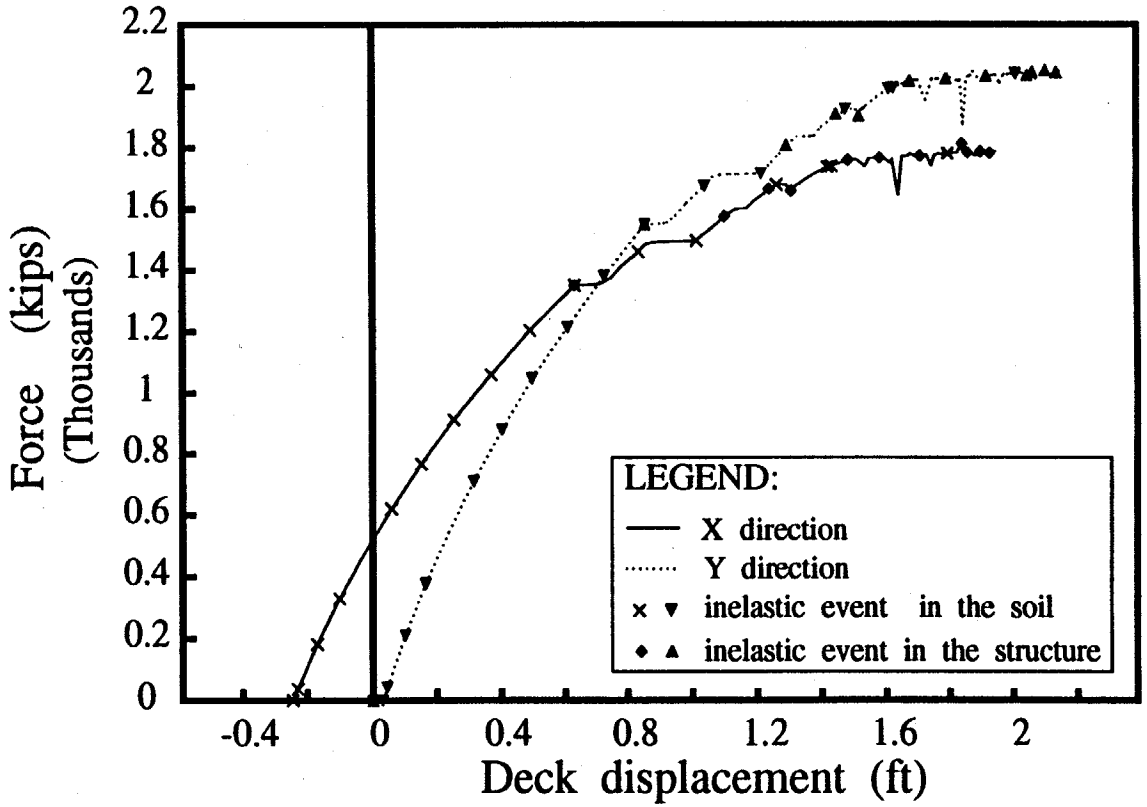
Force (kips)
(Thousands)
2.2
2
1.8
1.6
1.4
1.2
1
0.8
0.6
0.4
0.2
0
-0.4
0
0.4
0.8
1.2
1.6
2
Deck displacement (ft)
LEGEND:
X direction
Y direction
inelastic event in the soil
inelastic event in the structure

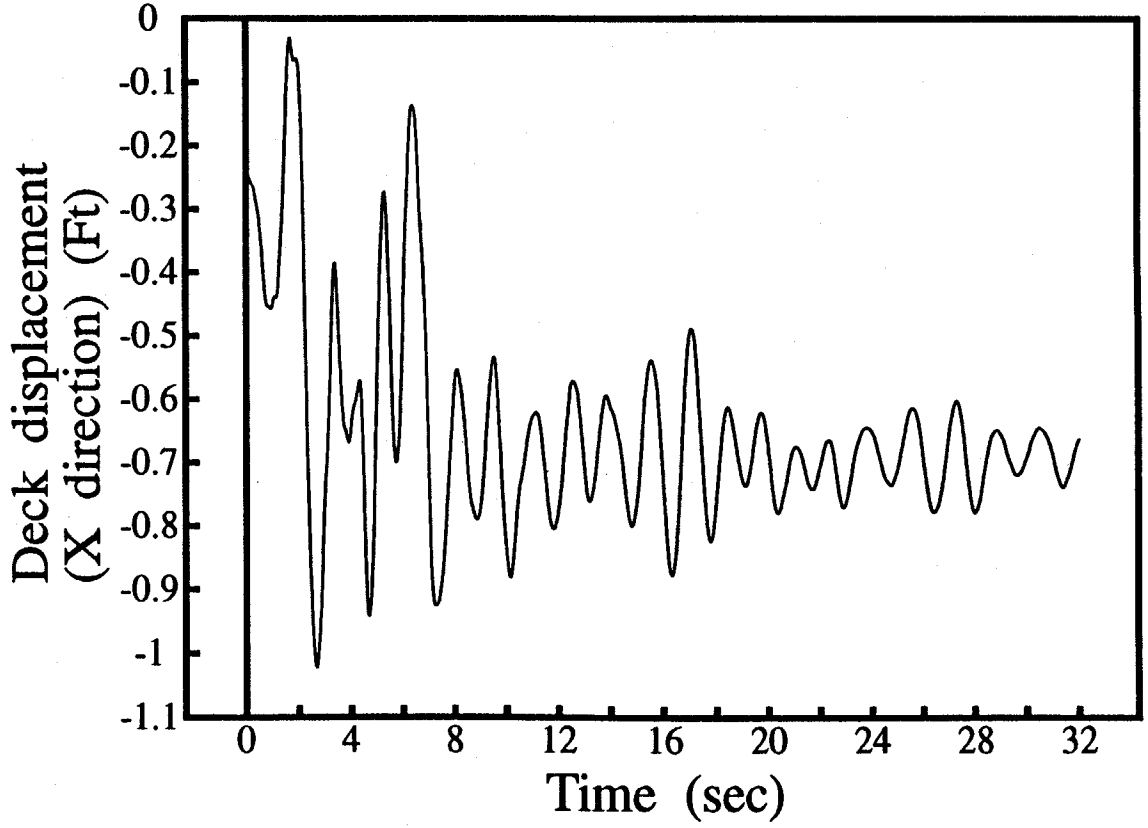
Deck displacement
(X direction) (Ft)
0
-0.1
-0.2
-0.3
-0.4
-0.5
-0.6
-0.7
-0.8
-0.9
-1
-1.1
0
4
8
12
16
20
24
28
32
Time (sec)

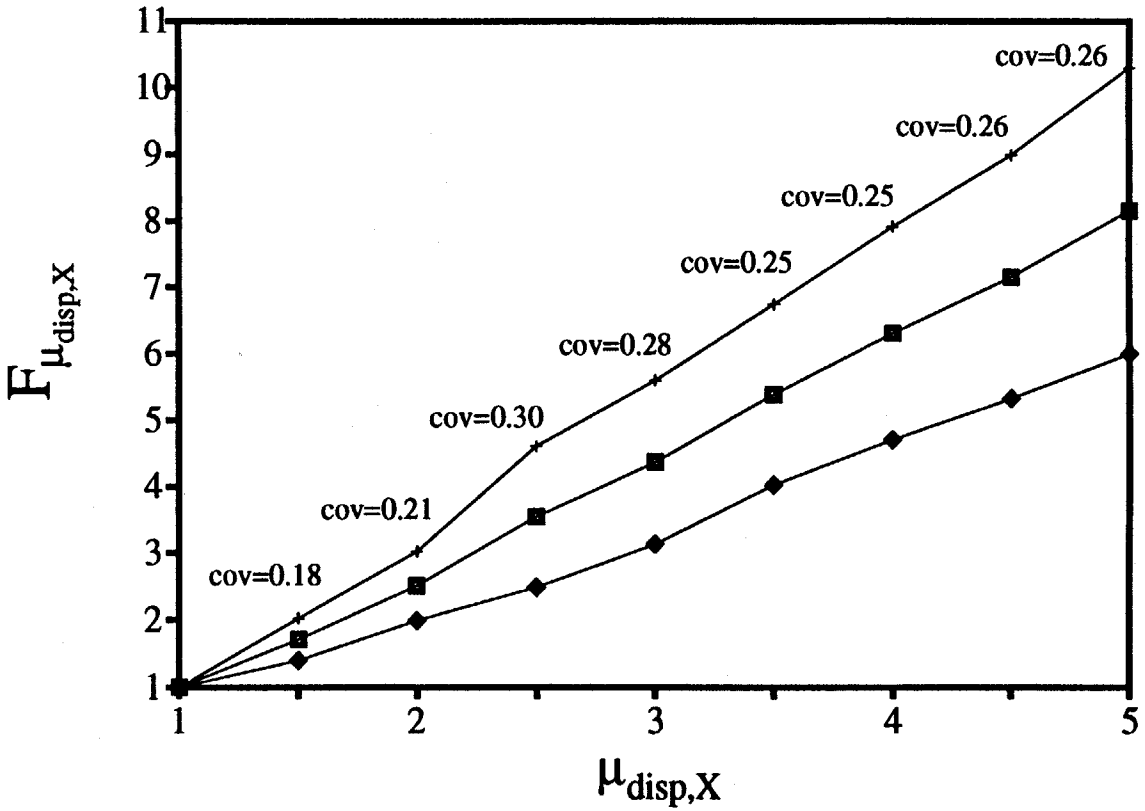
11
10
9
8
7
6
5
4
3
2
1
1
2
3
4
5
$F_{\mu_{disp,X}}$
$\mu_{disp,X}$
cov=0.26
cov=0.26
cov=0.25
cov=0.25
cov=0.28
cov=0.30
cov=0.21
cov=0.18

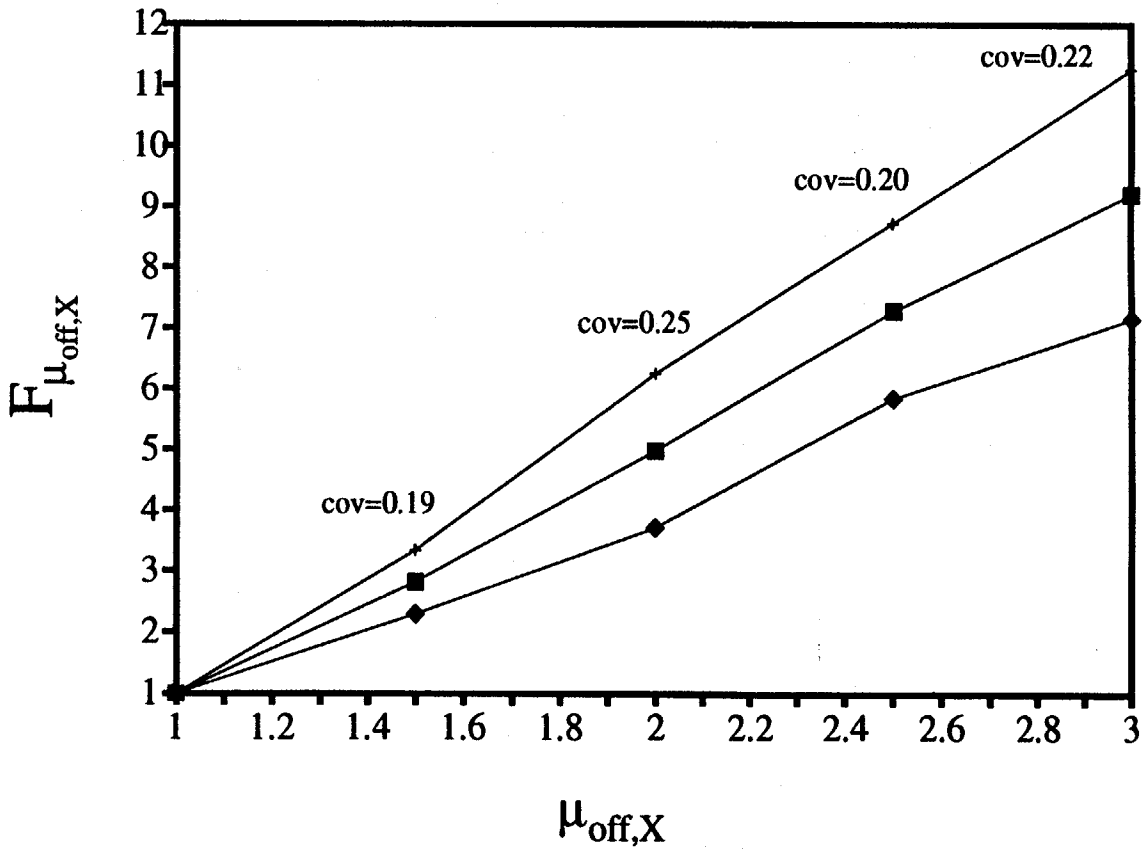
12
11
10
9
8
7
6
5
4
3
2
1
1
1.2
1.4
1.6
1.8
2
2.2
2.4
2.6
2.8
3
cov=0.22
cov=0.20
cov=0.25
cov=0.19
$F_{\mu_{off,X}}$
$\mu_{off,X}$

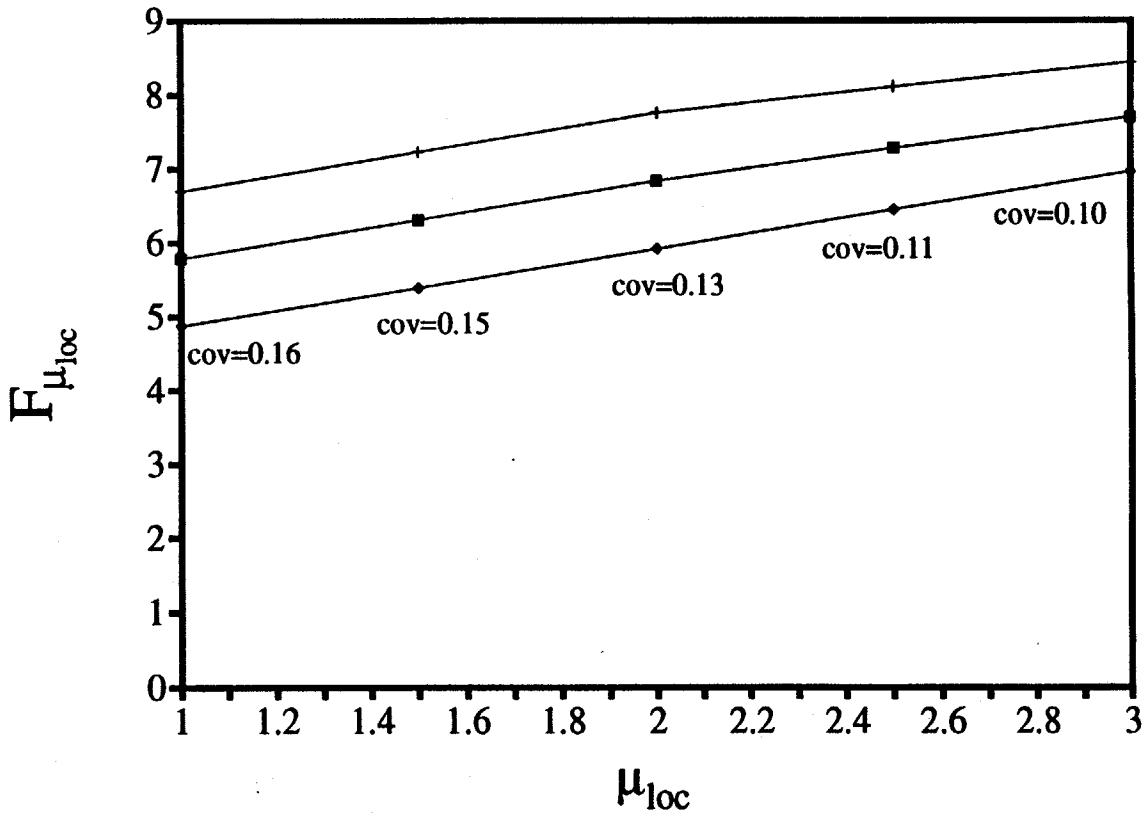
9
8
7
6
5
4
3
2
1
0
1
1.2
1.4
1.6
1.8
2
2.2
2.4
2.6
2.8
3
$F_{\mu_{loc}}$
μ_{loc}
cov=0.16
cov=0.15
cov=0.13
cov=0.11
cov=0.10

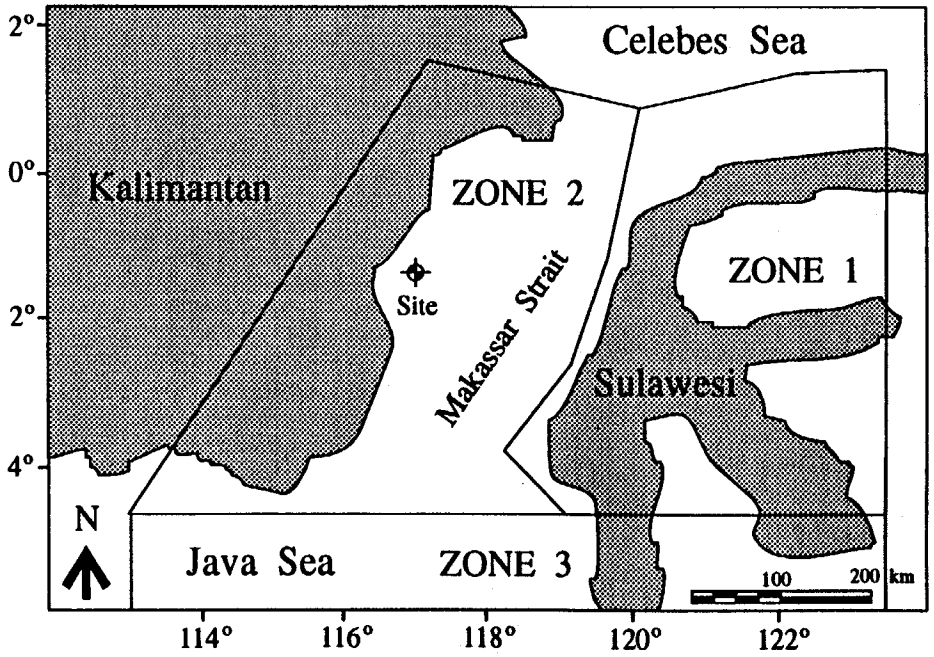
2°
0°
2°
4°
Celebes Sea
Kalimantan
ZONE 2
Site
Makassar Strait
ZONE 1
Sulawesi
N
Java Sea
ZONE 3
100
200 km
114°
116°
118°
120°
122°

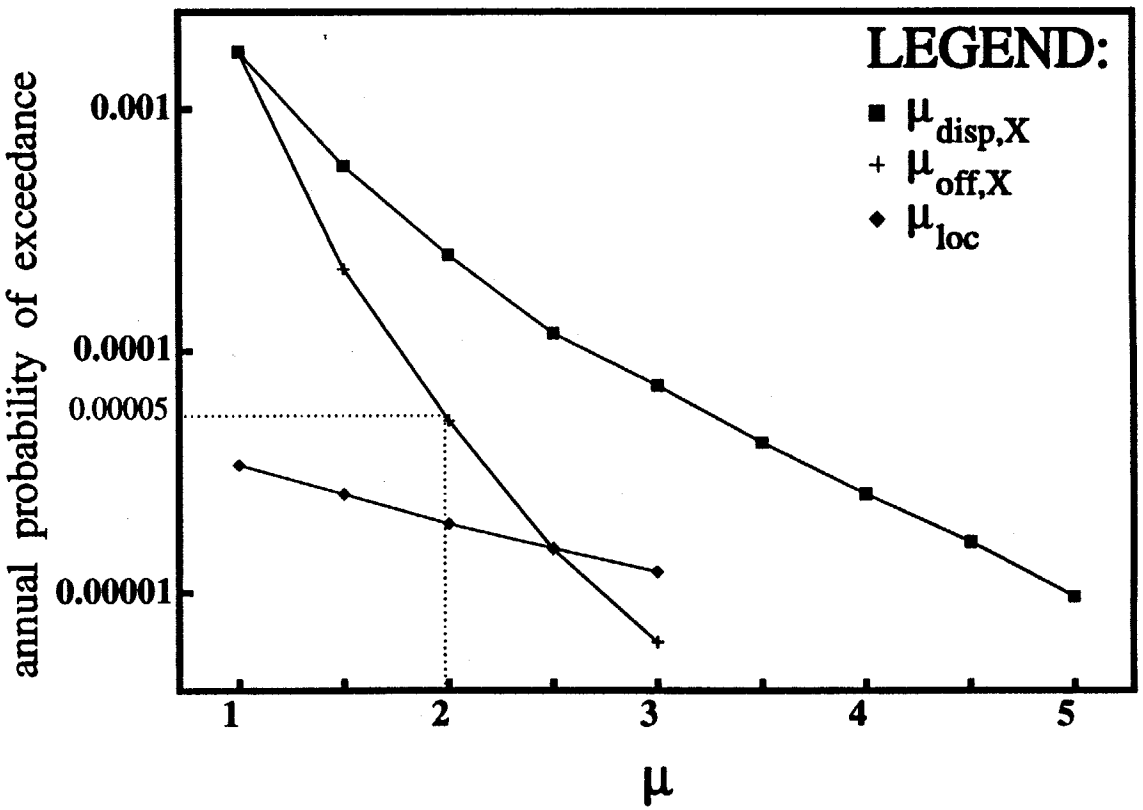
LEGEND:
$\mu_{disp,X}$
$\mu_{off,X}$
μ_{loc}
annual probability of exceedance
0.001
0.0001
0.00005
0.00001
1
2
3
4
5
μ

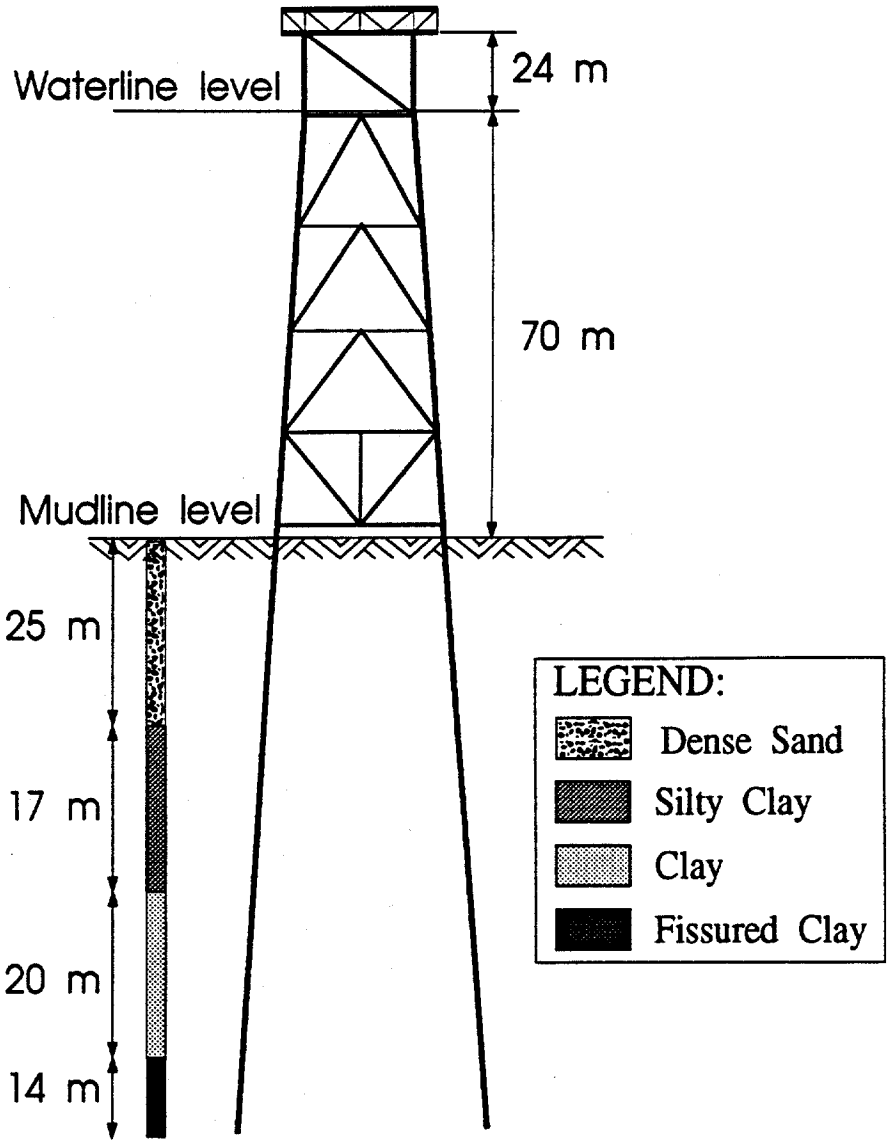
Waterline level
24 m
70 m
Mudline level
25 m
17 m
20 m
14 m
LEGEND:
Dense Sand
Silty Clay
Clay
Fissured Clay

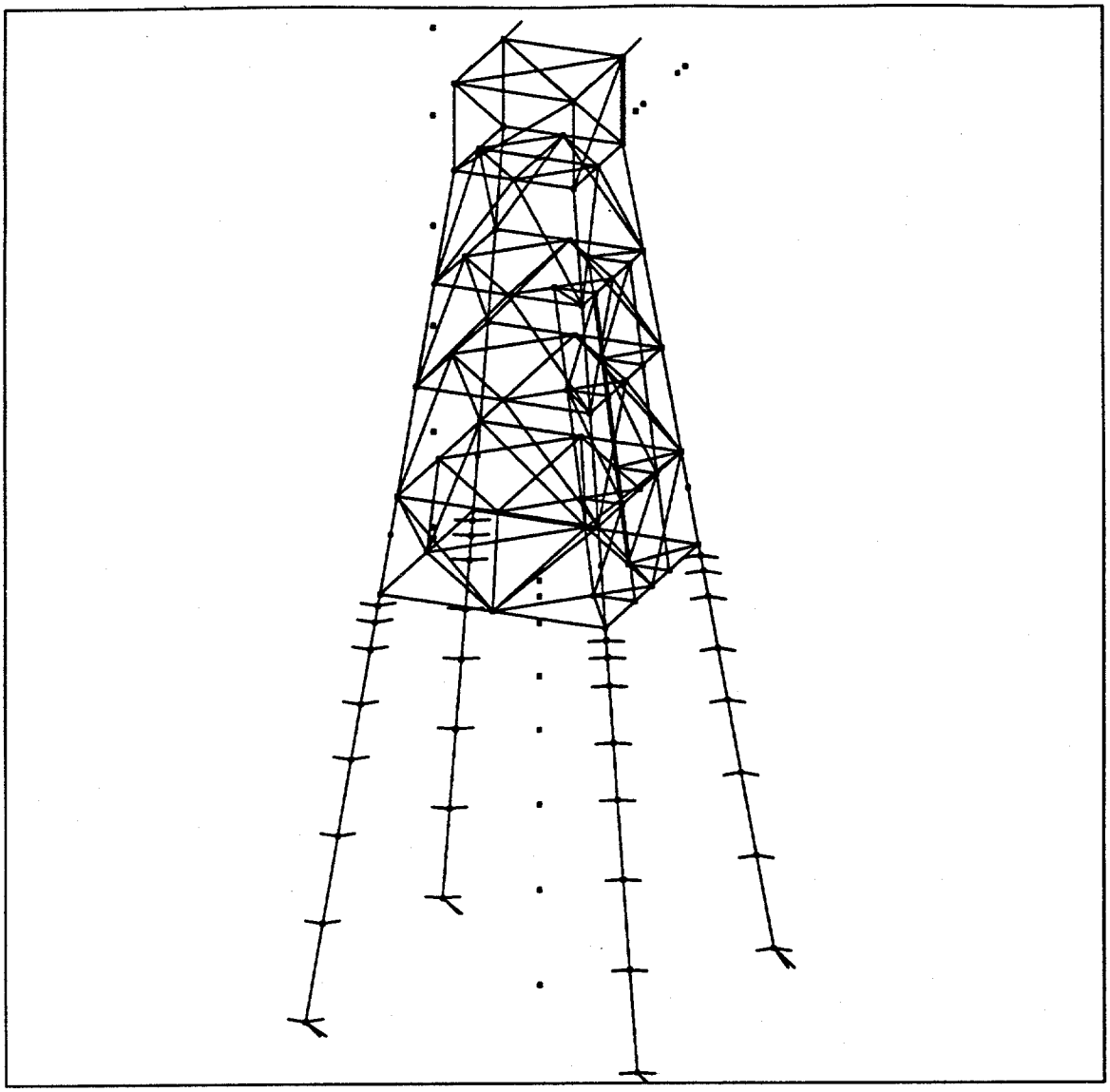

CAP

Riser 16/11 S (model with foundations)

Project: statpipe Model: full Version: 2

STANFORD UNIVERSITY RMS PROGRAM

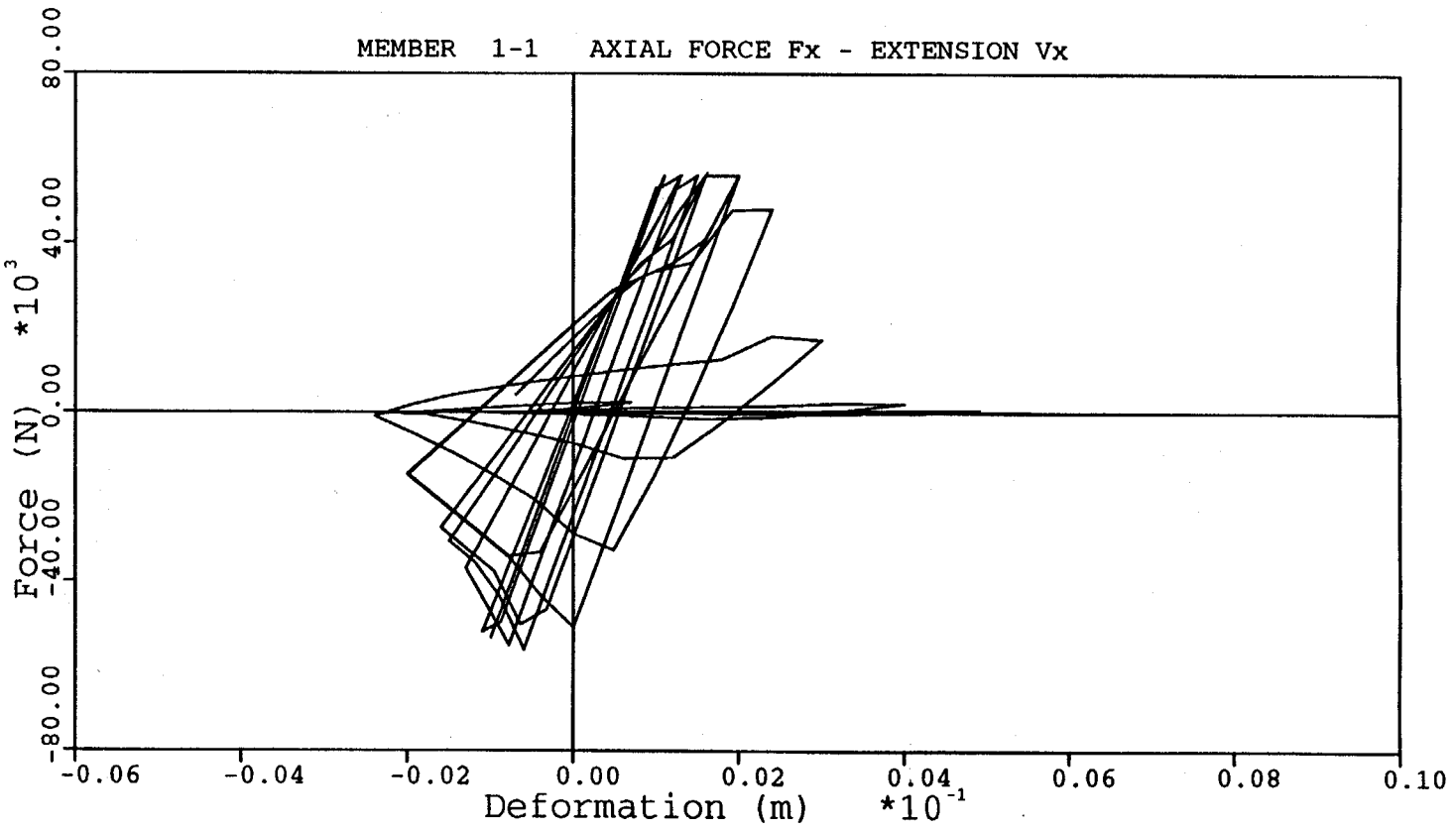

Marshall Strut

SeaStar Element No.8

DATE - 11/02/92 SEAPOST Version 3.10 TIME - 16:03:23

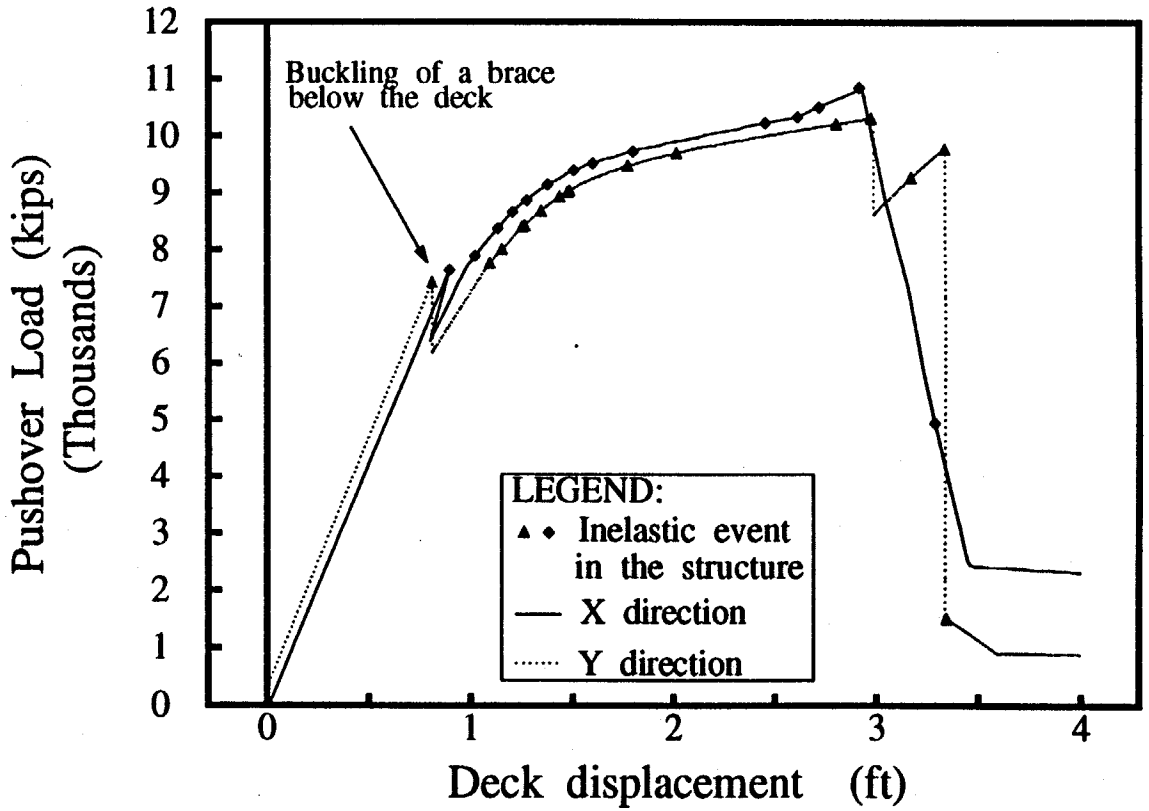
Buckling of a brace
below the deck
LEGEND:
Inelastic event
in the structure
X direction
Y direction
Pushover Load (kips)
(Thousands)
Deck displacement (ft)
0
1
2
3
4
5
6
7
8
9
10
11
12

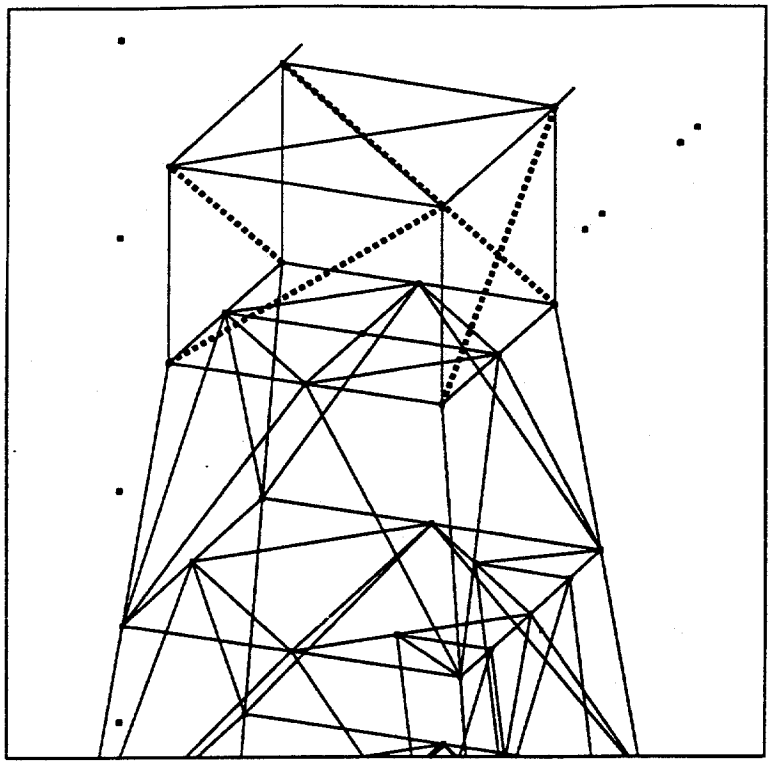

CAP

Project: statpipe Model: full Version: 2

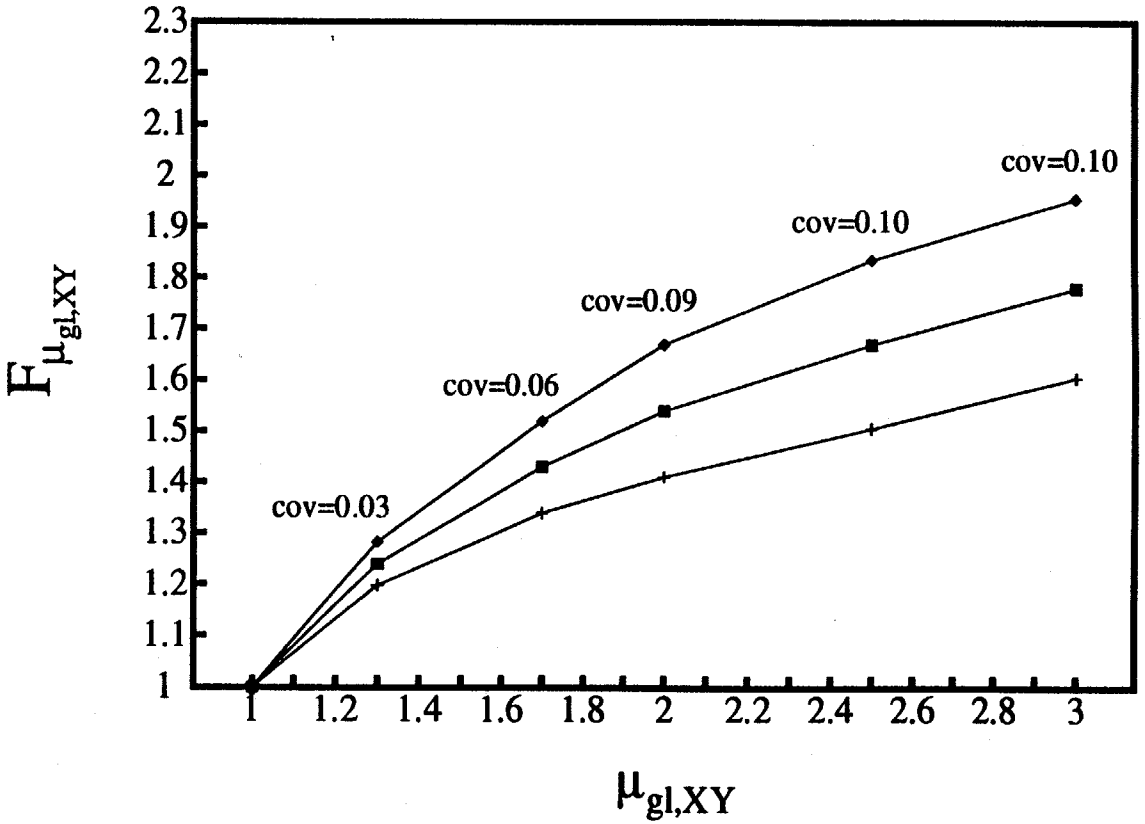
2.3
2.2
2.1
2
1.9
1.8
1.7
1.6
1.5
1.4
1.3
1.2
1.1
1
1
1.2
1.4
1.6
1.8
2
2.2
2.4
2.6
2.8
3
cov=0.10
cov=0.10
cov=0.09
cov=0.06
cov=0.03
$F_{\mu_{gl,XY}}$
$\mu_{gl,XY}$

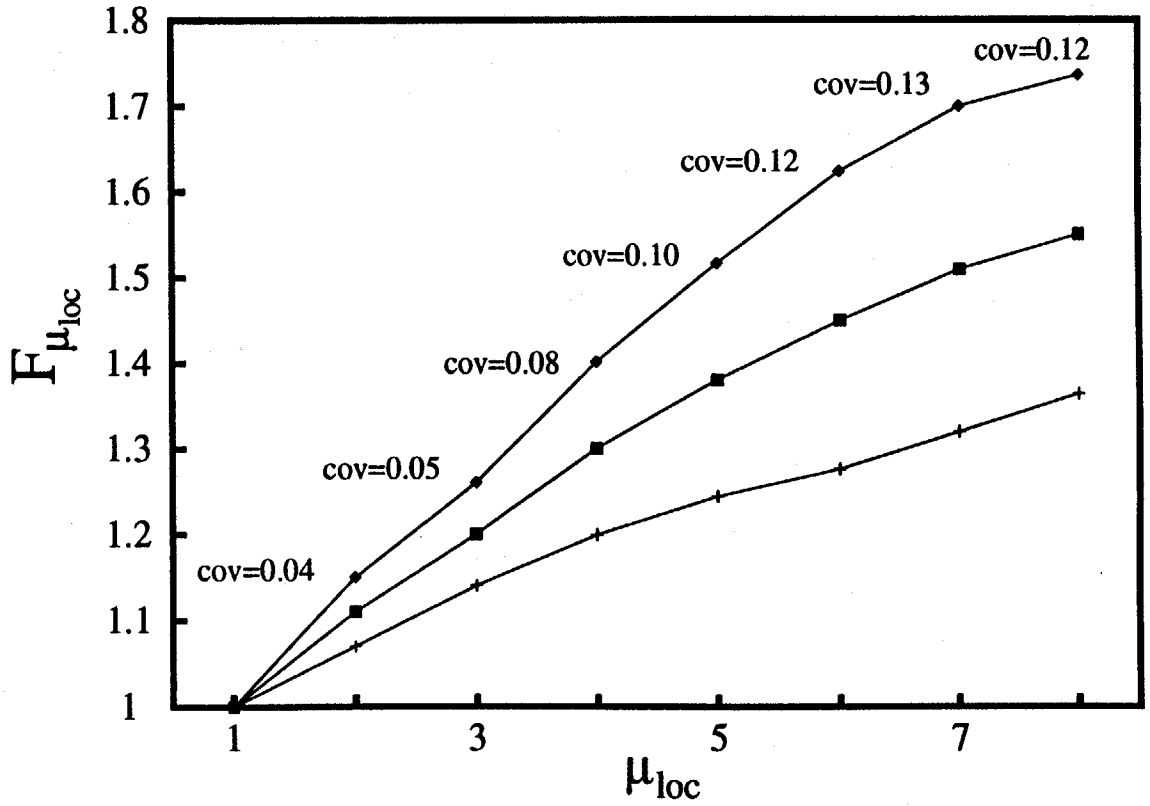
1.8
1.7
1.6
1.5
1.4
1.3
1.2
1.1
1
$F_{\mu_{loc}}$
1
3
5
7
μ_{loc}
cov=0.12
cov=0.13
cov=0.12
cov=0.10
cov=0.08
cov=0.05
cov=0.04

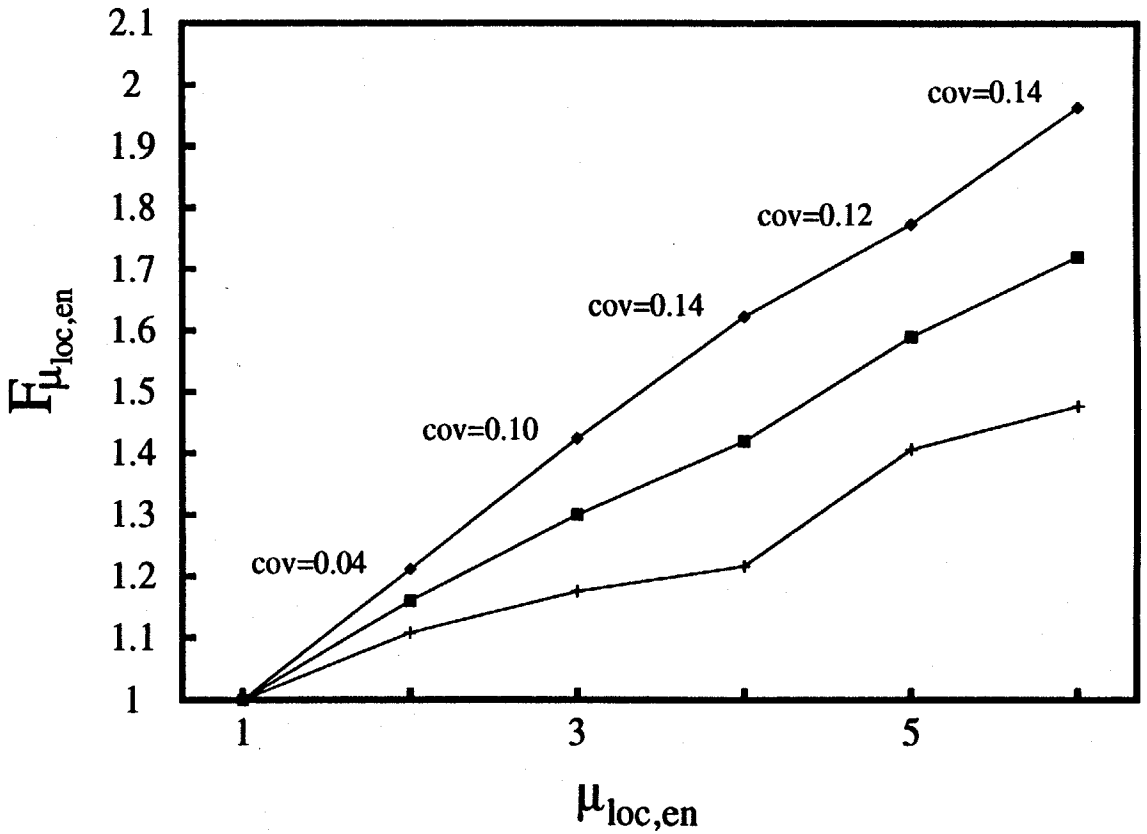
2.1
2
1.9
1.8
1.7
1.6
1.5
1.4
1.3
1.2
1.1
1
1
3
5
$F_{\mu_{loc,en}}$
$\mu_{loc,en}$
cov=0.14
cov=0.12
cov=0.14
cov=0.10
cov=0.04

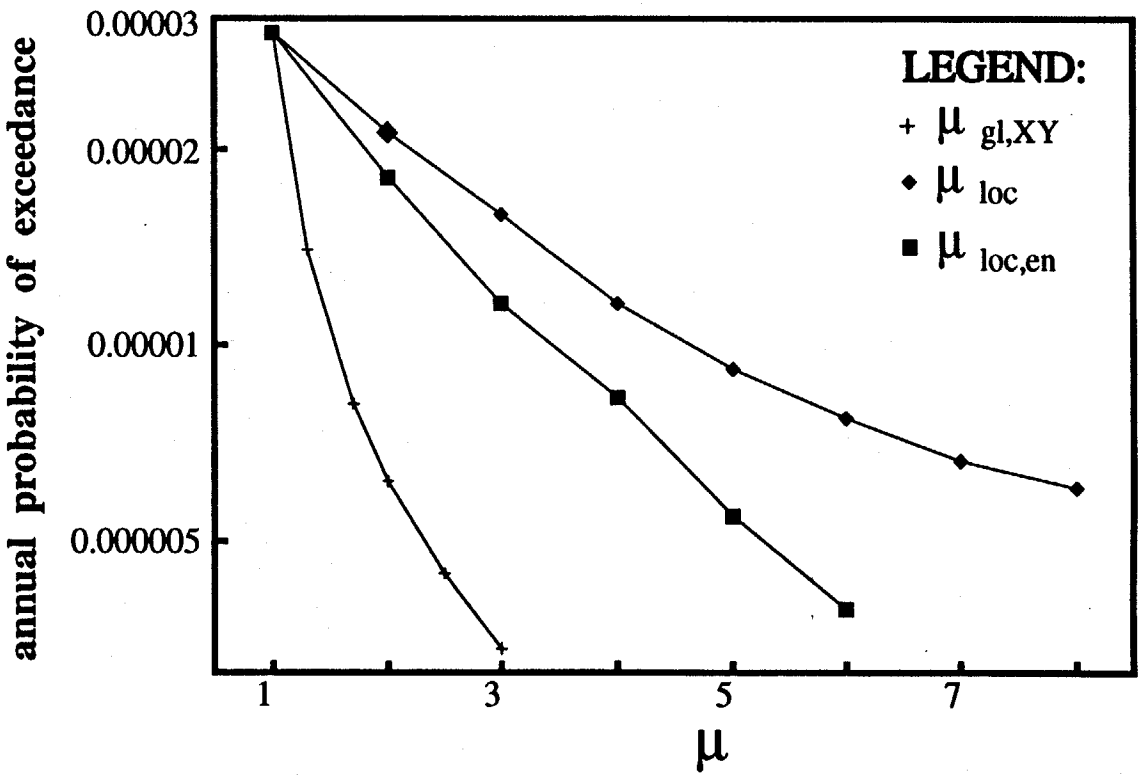
annual probability of exceedance
0.00003
0.00002
0.00001
0.000005
1
3
5
7
μ
LEGEND:
μ gl,XY
μ loc
μ loc,en